

Karlsruhe Institute of Technology (KIT)



Battery Technical Center (BATEC)
Institute of Electrical Engineering (ETI)
Karlsruhe Institute of Technology (KIT)

Waterloo Institute for Sustainable Energy (WISE)
University of Waterloo (UW)

**A comprehensive techno-economic methodological
approach for Off grid and decentralized Hybrid
Renewable Electricity Systems (OHRES)**

Based on contrastive case studies in Canada and Sub-Saharan Africa

To obtain the academic degree of **DOCTOR OF ENGINEERING**
”DOKTORS DER INGENIEURWISSENSCHAFTEN (Dr.-Ing.)”
from KIT-faculty of Electrical Engineering and Information Technology
Karlsruhe Institute of Technology (KIT)

**accepted
DISSERTATION**

Author : M.Sc. Mohamed Mamdouh M. Elkadragy
1st Supervisor : Prof. Dr. Marc Hiller Karlsruhe Institute of Technology (KIT)
2nd Supervisor : Prof. Dr. Jatin Nathwani University of Waterloo (UW)
Date of Oral Exam: 28.05.2021

"THE ULTIMATE THANKS TO ALLAH (ALMIGHTY) WHO PROVIDED ME THE STRENGTH AND OPPORTUNITY FOR COMPLETING THIS WORK,,

Acknowledgements

For my wife "Mariam" and our kids "Omar", "Habiba" & "Abd-Allah", for my parents, brother and family who were and will always be the backbone of any achievement in my life.

Thanks to the international collaborative teams in different countries and continents, whom without their remarkable contributions, this work would have never been complete. Due to the big number of these international team members, please excuse if any names were unintentionally not mentioned.

Special thanks for the efforts of my supervisors Prof. Dr. Marc Hiller and Prof. Dr. Jatin Nathwani who did invest time and effort in making this work complete. Special thanks to Prof. Dr. Joachim Knebel the main supporter and initiator of this work, and thanks to all members of the AE4H global initiative. Thanks to my scientific advisors, who did add a lot to the scope of this work. Specially Dr. Hans Holtorf who did provide his scientific knowledge and most importantly full support during the very hard personal times along the period of this work.

Thanks to all the colleagues from different institutes and facilities at KIT who did add value to this work: Dr. Manuel Baumann, Dr. Marcel Weil, Prof. Dr. Armin Grunwald, Nico, Laura, Vanessa, Alex, Michael, Thorsten, Nina, and special thanks to the working team: Uwe, Wolfgang, Siegfried who did have major contributions to this work.

Thanks to the working team from the University of Waterloo, Canada, and the WISE team who did play a major role in this work. Special thanks to Ambika Opal for her remarkable efforts until the last minute of this study, thanks to Nigel Moore for his early support and efforts.

Thanks to the tremendous efforts of George and Marg for enabling our case study in Canada.

Thanks for the tremendous efforts of the whole working team in Uganda from Sufraa Worldwide, specially Khaled, Marwa, Hag. Ismail, Josephine, Ismaily, and Entanby. Big thanks to the incredible team of students I did have the honor to work with, and supervised during the period of this work: Mughees, Ahmed, Mert, and Mohammad. In the end, a very special thanks to Dr. Rageb Alsergany, who has been since more than 10 years the main motivation for taking such a scientific step.

Abstract

This study aims to contribute to the global vision on ending energy poverty through increasing electrical energy access levels. Off grid and decentralized Hybrid Renewable Electricity Systems (OHRES) play a promising role in providing sustainable energy to people around the globe with no access to electricity. However, the diversity of global geographies, lack of performance analysis standardization, and modeling limitations hinder the scalability of OHRES. The study is carried out under the "Global Change Initiative - Affordable Energy for Humanity (AE4H)", which was established in 2015 by the University of Waterloo and Karlsruhe Institute for Technology as a platform for research and development of innovative energy technologies to drive large-scale adoption of economically feasible solutions intended to reach every global citizen.

The comprehensive methodological approach used in this study aims to understand the technical and economic factors affecting the feasibility, sustainability, and reliability of OHRES along the value chain, to increase the level of understanding, acceptance, and deployment of such systems on a global level. This comprehensive approach is based on four main building blocks: The first building block of our study is the on-ground OHRES deployment in the case-study locations in Canada and Uganda, along with techno-economic analysis and system sizing for each case study. The second building block is the development and optimization of the Hybrid off grid and decentralized systems Techno-Economic Model (HOTEM). HOTEM was developed to be used as OHRES sizing and techno-economic assessment tool. The development of HOTEM is based on the on-ground experience gained from the deployment of OHRES in our selected case studies, which allows HOTEM to be a practical tool, reflecting market needs. The third building block is the development of the off grid and decentralized systems data analysis platform (OSDAP), which is a platform for remote monitoring of OHRES. The OSDAP platform includes several functionalities such as: dynamic data visualization, performance analysis and artificial neural network based Solar irradiance forecasting. The fourth building block of our study is the lessons learned regarding major technical, economical, managerial, and modeling factors for off grid and decentralized hybrid systems, which can be utilized for both scientific research and commercial purposes.

The methodological approach presented in this study aims to address specific challenges related to off grid and decentralized hybrid electricity systems that are not properly covered in existing literature. Applied research involving not only theoretical assessment but also practical contrastive case studies and on-ground work, using such a comprehensive methodological approach along the value chain from system development to deployment and operation & monitoring is highly unique and valuable. This study therefore provides a role in filling an existing knowledge gap in the off grid and decentralized systems techno-economic context.

Contents

List of abbreviations	IV
List of figures	XI
List of tables	XI
1 Introduction, study scope, contribution and structure	1
1.1 Introduction	1
1.2 Study overview, context and overall objectives	3
1.3 Study contribution and relation to off-grid and decentralized electricity systems research context	8
1.3.1 Study related work and literature	8
1.3.2 Study contribution and relation to research context	11
1.4 Scientific publications based on the scope of the presented study	13
1.5 Thesis structure	14
2 Case studies and Off-grid and decentralized Hybrid Electricity System (OHRES) structure overview	16
2.1 Case studies overview, selection and load demands	16
2.1.1 Case Studies overview and selection criteria	16
2.1.2 Case studies load profile and energy demand	19
2.2 Off-grid and decentralized hybrid electricity systems (OHRES) technical overview	25
2.2.1 System design criteria and objectives	25
2.2.2 Off-grid and decentralized Hybrid Renewable Electricity Systems (OHRES) layout	26
2.2.3 System Voltage level selection using multi-criteria evaluation methodology	29
3 OHRES Techno-economic analysis and system size optimization	33
3.1 OHRES techno-economic analysis and system sizing	33
3.1.1 OHRES design layout scenarios	34
3.1.2 Hybrid battery storage modelling in HOMER	35
3.2 Canada Case-study hybrid system techno-economic analysis and sizing	38
3.2.1 Canada case study techno-economic modelling and assessment results	42
3.2.2 Canada case-study techno-economic re-assessment using measured renewable resources data	50
3.3 Uganda case-study hybrid system techno-economic assessment and system size optimization	55

3.4	OHRES Hybrid Battery Storage (HBS) techno-economic assessment . .	62
4	OHRES hardware functionality and optimization, dynamic testing, and on site commissioning	68
4.1	OHRES System remote Monitoring and Weather Station (SMWS), and hardware aspects	68
4.1.1	System operation data set	71
4.1.2	OHRES integrated components measurements and controller . .	74
4.1.3	Renewable resources and weather Data set	75
4.1.4	Remote monitoring and primary data transmission	75
4.2	System operation and safety developed functionalities	83
4.2.1	System operational developed functionalities	83
4.2.2	Other important integrated functionalities	86
4.3	System dynamic testing and functionality optimization	88
4.3.1	System dynamic operation testing and functionality optimization	89
4.4	OHRES on-site installation and commissioning	95
4.5	Canada case study OHRES installation and commissioning	98
4.5.1	Canada hybrid system logistics handling	98
4.5.2	OHRES hot-running test and full commission for the Canada Case study	101
4.5.3	On-site installation and commissioning failures and experience highlights	104
4.6	Uganda case study on-site installation and commissioning	108
4.6.1	Installation and commissioning of weather station in its final location	111
4.7	Highlight on the major differences experienced between the case studies in Canada and Uganda	113
5	HOTEM: Hybrid off-grid and decentralized system Techno-Economic model	116
5.1	HOTEM structure and development methodology	117
5.1.1	PV modeling	119
5.1.2	Wind turbine	124
5.1.3	Battery storage system	125
5.1.4	Generator	134
5.1.5	Inverter	137
5.1.6	Load profiling and random variability	137
5.1.7	Economic modelling	140
5.2	HOTEM optimization targets and power dispatch strategy	142
5.2.1	Cost of electricity	142
5.2.2	Loss of power supply probability	143
5.2.3	Renewable Factor	143
5.2.4	Power dispatch strategies	144
5.2.5	C-DEEPSO optimization model overview	145
5.3	HOTEM case study description and system sizing results	147
5.4	HOTEM Benchmarking	154

6	Off-grid and decentralized System Data Analysis Platform (OSDAP)	157
6.1	OSDAP data handling and visualization development	158
6.1.1	OSDAP objectives	158
6.1.2	OSDAP data handling and visualization	159
6.1.3	Data preparation and visualization Graphical User Interface (GUI)	162
6.1.4	Hybrid system testing	164
6.1.5	Canada case-study system testing and data handling	166
6.2	OSDAP Performance Analysis and Solar Irradiance Forecasting	171
6.2.1	Performance Analysis Tool Development Methodology	171
6.2.2	Solar Irradiance Forecasting Methodology	174
6.2.3	OHRES Performance Analysis Results	181
6.2.4	Solar Irradiance Forecasting Results	188
7	Final remarks, conclusion and outlook	196
7.1	Highlight on major lessons learned and key consideration factors for off grid and decentralized systems	196
7.2	Conclusion and outlook	201
	References	204
	Appendix A	214
	Appendix B	220

List of Abbreviations

AC	Alternating Current
ACL	Average Connected Loads
AE4H	Affordable Energy for Humanity
ANN	Artificial Neural Network
AGM	Absorbent Glass Mat
BMS	Battery Management System
C-DEEPSO	Canonical Differential Evolutionary Particle Swarm Optimization
CCGX	Color Control GX
COE	Cost of Electricity
CFV	Cost Future Value
DC	Direct Current
DOD	Depth Of Discharge
DHI	Diffuse Horizontal Irradiance
GHI	Global Horizontal Irradiance
HBESS	Hybrid Battery Energy Storage System
HESS	Hybrid Energy Storage System
HOMER	Hybrid Optimization of Multiple Energy Resources
HOTEM	Hybrid off grid and decentralized systems Techno-Economic Model
KBM	Kinetic Battery Model
LCOE	Levelized Cost of Energy
Li-ion	Lithium Ion
LiFePO₄	Lithium Iron Phosphate
LSTM	Long-Short Term Memory
LPSP	Loss of Power Supply Probability
MPPT	Maximum Power Point Trackers
MLRA	Multi-Layer Remote Access
NPC	Net Present Cost
NPV	Net Present Value

OSDAP	off grid and decentralized hybrid Systems Data Analysis Platform
OHRES	Off grid and decentralized Hybrid Renewable Electricity System
O&M	Operation and Maintenance
PV	Photovoltaic
POA	Plane of Array Irradiance
GHI	Global Horizontal Irradiance
GUI	Graphical User Interface
RE	Renewable Energy
SMWS	System remote Monitoring and Weather Station
SOC	State of Charge
TCL	Total Connected Loads
WACC	Weighted Average cost of Capital
WT	Wind Turbine

List of Figures

1.1	Population served by off-grid renewable energy solutions globally. . . .	4
1.2	OHRES value-chain techno-economic related phases and stages.	6
1.3	OHRES Comprehensive Techno-economic analysis and optimization approach	7
2.1	Case-studies latest taken photos in Canada and Uganda	19
2.2	Canada case study - 24h total connected loads (TCL) and Average Connected Loads (ACL) profiles	20
2.3	Uganda case study - 24h estimated load profile during week days (Monday - Friday) and weekend	22
2.4	OHRES technical design main objective	26
2.5	Off-grid Hybrid Renewable Electricity System (OHRES) layout.	27
2.6	OHRES DC voltage level - Quantitative assessment results (Published [1]).	30
3.1	OHRES technical design layout scenarios	35
3.2	Capacity curve for the hybrid battery model in HOMER	37
3.3	Lifetime curve for the hybrid battery model in HOMER.	38
3.4	Canada case-study hybrid system modelling scheme in HOMER	39
3.5	Sensitivity analysis: Effect of the PV azimuth and orientation on the COE for Canada case study hybrid system	44
3.6	Sensitivity analysis: Effect of capacity shortage changes on the COE for Canada case study hybrid system	45
3.7	Sensitivity analysis: Effect of AC load average energy changes on the COE for Canada case study hybrid system	45
3.8	Canada case study sensitivity analysis: effect of changing the nominal discount rate and the fuel price on the hybrid system architecture optimization	47
3.9	Canada case study Winning system architecture	48
3.10	Base case modelling system architecture for canada case study	50
3.11	Canada case study re-assessment winning system architecture	52
3.12	Canada case study re-assessment sensitivity analysis: effect of changing the nominal discount rate and the fuel price on the hybrid system architecture optimization	54
3.13	Uganda case-study hybrid system modelling scheme in HOMER	55
3.14	Uganda case study sensitivity analysis: effect of changing the nominal discount rate and the fuel price on the hybrid system architecture optimization	61
3.15	Uganda case study Winning system architecture	62
3.16	Dynamic financial assessment for OHRES storage systems	63

4.1	OHRES system cabinet hardware and SMWS in-door components . . .	69
4.2	Weather station sensors and out-door components as provided	70
4.3	OHRES System remote Monitoring and Weather Station(SMWS) data sets.	71
4.4	OHRES electrical and sensors measurement positions single line diagram layout.	73
4.5	CCGX selected views from the OHRES operation in Canada case-study household	74
4.6	Off-grid and decentralzied Systems Data Analysis Platform (OSDAP) general layout	77
4.7	SMWS monitoring and data-logging online platform	78
4.8	SMWS monitoring and data-logging Victron Energy online platform. . .	78
4.9	Multi-Layer Remote Access (MLRA) Model for OHRES.	79
4.10	OHRES operation and protection layers	83
4.11	Battery storage system disconnect breaker and DC dump load controller. .	86
4.12	PV disconnect controller breakers.	86
4.13	Electrical circuit diagram - Connection of the MPPT and PV disconnect controller breakers	87
4.14	OHRES test bench diagram.	89
4.15	Canada case study system last transportation phase	99
4.16	Different packing steps for the li-ion batteries for air shipment.	100
4.17	Canada case study hybrid system outdoor installations.	101
4.18	Canada case study hybrid system indoor installations and commissioning. .	102
4.19	Canada case online monitoring portal - Weather station data monitoring. .	103
4.20	Canada case online monitoring portal - AC related measurements example. .	103
4.21	Canada case indoor and outdoor OHRES installations summary.	105
4.22	Electrical circuit diagram - Off-grid Hybrid Renewable Electricity System (OHRES) electrical main components	106
4.23	Defected lead-acid battery during Canada hybrid system logistics process. .	107
4.24	Weather station and remote data acquisition commissioning and hot-running test in Uganda, Jinja.	110
4.25	Data monitoring and analysis portal for remote SMWS	111
4.26	Uganda case study - weather station installation and commissioning in its final location at Sofraa school.	112
4.27	Uganda case study - weather station part of the local capacity building activities.	113
5.1	Second building block of OHRES Comprehensive Techno-economic analysis and optimization approach - HOTEM.	116
5.2	HOTEM layout and sub-models structure.	118
5.3	Flowchart of modeling POA irradiance from measured GHI [2].	120
5.4	Solar irradiance Transposition model for the calculation of POA from GHI.	122
5.5	Solar beam (direct), sky-diffuse, and ground-reflected radiation on an inclined planar surface [3].	123
5.6	Idealized battery model overview.	125

5.7	Kinetic battery model representation.	126
5.8	KBM modelling and the peukert's effect for a lead-acid battery results compared to the manufacturer datasheet for our OHRES selected case-studies lead-acid battery (Hoppecke SUN Power VR M 6-250).	129
5.9	Different required parameters for the voltage model	130
5.10	Effect of temperature on a Lead-acid OPzV battery lifetime.	132
5.11	Hybrid Battery Energy Storage System (HBESS) simplified architecture and adapted configuration in HOTE M.	133
5.12	Hybrid battery storage dispatch algorithm.	135
5.13	HBESS Modelling results - OHRES simulation Complete year time period	136
5.14	HBESS Modelling results - OHRES simulation Week time period . . .	136
5.15	HBESS Modelling results - OHRES simulation Multi days time period .	136
5.16	Load profile of the first week of the year without variability.	138
5.17	Load profile of the first week of the year with 20% Day-to-Day variability.	139
5.18	Load profile of the first week of the year with 15% Ts-t-Ts variability. .	139
5.19	Load profile of the first week of the year with 20% Day-to-Day and 15% Ts-t-ts variability.	140
5.20	Power dispatch strategies in HOTE M.	144
5.21	C-DEEPSO algorithm flowchart.	146
5.22	24- hour load profile by a house under study.	148
5.23	Hourly load with variability used for model input.	148
5.24	Hourly solar irradiance and wind speed served as model inputs.	149
5.25	Configuration of hybrid off-grid system under case study.	151
5.26	Hybrid system generation and load dynamics.	152
5.27	PV and Wind power generation.	153
5.28	Total annual generation shares: wind, solar, battery, surplus.	154
5.29	HOMER off-grid system configuration for benchmarking.	155
6.1	Third building block of OHRES Comprehensive Techno-economic analysis and optimization approach - OSDAP.	157
6.2	OSDAP data handling and visualization Structural chart.	160
6.3	Offgrid Systems Data Analysis Platform Inputs and Analysis flow paths.	161
6.4	Offgrid Systems Data Analysis Platform close view on Raw data handling.	161
6.5	Offgrid Systems Data Analysis Platform System selected data visualization and analysis.	162
6.6	OSDAP data prepration and visualization GUI.	163
6.7	GUI: Display example of interactive plot embedded inside Canvas. . . .	164
6.8	OHRES testing scenarios.	166
6.9	Canada Case Study (Colgate's Household): Developed Load Profile. . .	167
6.10	24H Running test South orientation - 45° tilt angle.	169
6.11	24H Running test East West orientation - 45° tilt angle.	170
6.12	The Off-grid and Decentralized Systems Data Analysis Platform (OS-DAP).	172
6.13	Operation flow diagram of solar irradiance forecasting models.	176
6.14	Color-map depicting correlation between features of HelioClim-3 dataset.	177
6.15	Sliding window effect for 24-hour ahead predictions.	178

6.16	Sliding window effect for one-hour ahead prediction.	178
6.17	Nominal PV energy yield vs measured PV energy yield between 20.08.2019 and 30.09.2019.	182
6.18	Nominal power vs measured PV DC power outputs on two days.	183
6.19	Solar irradiance versus PV array DC output power per watt peak on two days.	183
6.20	Solar irradiance versus PV array DC power output on two days.	184
6.21	Battery voltage between 01.09.2019 and 30.09.2019	184
6.22	PV DC power, generator AC power and AC load 1 between 01.09.2019 and 30.09.2019.	185
6.23	Battery voltage between 16.09.2019 and 24.09.2019.	185
6.24	Comparison of sensor measured individual battery currents and CCGX derived battery bank current.	186
6.25	Training and validation loss graph of 24-hour ahead irradiance forecast- ing model.	189
6.26	24-hour ahead irradiance predictions between 20.08.2006 and 25.08.2006.	190
6.27	24-hour ahead irradiance predictions between 09.11.2006 and 14.11.2006.	191
6.28	Training and validation loss graph of one-hour ahead irradiance fore- casting model.	192
6.29	One-hour ahead irradiance predictions between 10.06.2019 and 26.06.2019.	193
6.30	Comparison of good and poor predictions in June 2019.	193
6.31	One-hour ahead irradiance predictions between 10.09.2019 and 27.06.2019.	194
6.32	Regression analysis of the model on measured weather data and HelioClim- 3 Archive weather data	195

List of Tables

2.1	Case-studies selection criteria (Published in [1]).	17
2.2	Contrastive case-studies overview in Canada and Uganda (Published in [1]).	18
2.3	Canada case study type of loads and its power consumption	21
2.4	Uganda case study type of loads and its power consumption	23
2.5	Decision making matrix for OHRES DC voltage level selection(published [1])	30
3.1	OHRES different system design layout scenarios	36
3.2	Developed hybrid battery storage model parameters used in HOMER .	37
3.3	Canada case study techno-economic modelling and assessment sensitivity analysis parameters	43
3.4	Canada case study techno-economic modelling and sensitivity analysis system architectures components	46
3.5	Canada case study techno-economic modelling and assessment sensitivity analysis parameters	49
3.6	Major differences between the two data sets for the Canada case study in the annual averages	51
3.7	Canada case study re-assessment sensitivity analysis system architecture components	51
3.8	Uganda case study techno-economic modelling and assessment sensitivity analysis parameters	59
3.9	Uganda case study techno-economic assessment results - system architecture components	59
3.10	Uganda case study selected variables for the winning system architecture techno-economic evaluation	60
3.11	Hybrid battery storage techno-economic assessment general assumptions	65
3.12	Case-specific assumptions related to storage technical aspects	66
3.13	Case-specific assumptions for battery configuration, initial cost and lifetime	67
4.1	OHRES sensor details for the voltage and current at selected measurement points	72
4.2	Renewable resources and weather data-set measurement sensors technical criteria	76
4.3	OHRES remote monitoring and control architecture	82
4.4	OHRES test bench used hardware components technical summary . . .	91
5.1	Perez model coefficients for irradiance (Author’s publication [5]).	124
5.2	Default values for voltage model parameters used in HITEM (Supervised work [6]).	131

5.3	Symbols used in the model algorithm (Supervised work [6]).	134
5.4	Modelling input parameters based on manufacturer data (Author's publication [5], and supervised work [7]).	150
5.5	HOTEM Simulation Results (Author's publication [5], and supervised work [7]).	151
5.6	Annual energy production of each hybrid component (Author's publication [5]).	153
5.7	Simulation comparison between HOMER and HOTEM (Author's publication [5]).	155
5.8	Comparison of results from HOMER and HOTEM (Author's publication [5]).	156
6.1	Measured parameters from OHRES (Author's publication [8], and supervised work [10]).	173
6.2	Derived performance parameters suggested by IEC 61724 [9] standards (Author's publication [8], , and supervised work [10]).	174
6.3	24-hour ahead irradiance forecasting model structure (Author's publication [8], and supervised work [10]).	179
6.4	One-hour ahead irradiance forecasting model structure (Author's publication [8], and supervised work [10]).	180
6.5	OHRES performance parameters (Author's publication [8], and supervised work [10]).	188
7.1	Studies and activities supervision during thesis and study period . . .	221

1 Introduction, study scope, contribution and structure

1.1 Introduction

The presented study is carried out under the "Global Change Initiative - Affordable Energy for Humanity (AE4H)[11]", which was established by the University of Waterloo and Karlsruhe Institute for Technology as a platform for research and development of innovative energy technologies to drive large-scale adoption of low-cost solutions intended to reach every global citizen. The primary goal of the AE4H initiative is to support the scientific, technological, social and policy innovations that can rapidly bring affordable and clean energy solutions to markets with emphasis on the development of human capacity requirements of countries with the greatest need.

Energy access is a lever for human development. Tremendous progress in global electricity access has been achieved over the last decade. The number of people without energy access dropped for the first time below 1 billion people in 2017, however still there are 860 million people without electricity access in 2018 [12] [13]. Access to affordable and clean energy underpins 12 of the 17 UN Sustainable Development Goals for improved quality of life across the globe. Energy poverty is not only a trap that steals from its victims' productive time, but it is a silent killer – there are approximately 4 million deaths annually from indoor air pollution due to traditional sources of fuel – exceeding the toll of malaria, TB and AIDS combined [14]. Delivering an universal energy access will require a radical increase in the affordability of clean energy that is environmentally sustainable and will require energy access to be at the center of meeting sustainable development challenges of the 21st century as described within the UN Sustainable Development Goals (UN SDG's) framework [15]. 'Energy Access' remains a powerful multiplier of the UN Sustainable Development Goals (SDGs) [12].

A global, action-oriented program driven by a sense of urgency to help find and proliferate solutions to the energy challenges of the developing world with the following objectives is necessary:

1. Enhance economic development opportunities and reduce global poverty
2. Improve the quality of life by proliferating technological innovation and best practices from around the world adapted to local needs
3. Sustainably reduce present and future greenhouse gas emissions

⁰Part of the content of this chapter is based on and from the author's published work in Elkadragy et. al [5] [8].

4. Train the next generation of leaders, change agents and provide support to entrepreneurs that is integral to the growth of the energy access sector

The study aims to participate in the global vision on ending energy poverty through increasing electrical energy access levels. The methodological approach presented in this study, aiming to address specific challenges related to off-grid and decentralized systems is not properly covered in existing literature to our knowledge. Especially applied research involving not only theoretical assessment but also practical contrastive case-study on-ground work using such a comprehensive methodological approach along the value chain from system development to deployment and operation & monitoring as described in the upcoming chapters. This study contributes to filling an existing knowledge gap in the off-grid and decentralized systems techno-economic context.

The comprehensive and wide methodological approach used in this study aims to understand the technical and economic factors affecting the feasibility, sustainability, and reliability of Off grid and decentralized Hybrid Renewable Electricity System (OHRES) along the value chain, in order to increase the level of understanding, acceptance, and deployment of such systems on a global level. The comprehensive methodological approach used contains all related techno-economic aspects of the OHRES along the different phases from development, deployment, operation and monitoring. This comprehensive approach is based on four main building blocks:

1. On-ground deployment of OHRES in selected case-study locations within Canada and Uganda.
2. HOTEM, A hybrid renewable electricity system techno-economic feasibility analysis and system sizing tool (developed in the scope of the presented study).
3. OSDAP, (Off-grid and decentralized systems Data Analysis Platform) is a comprehensive tool (developed in the scope of the presented study) for OHRES data analysis, performance monitoring, and renewable energy resources forecasting using artificial neural networks (solar irradiance).
4. Major lessons learned and key consideration factors based on the on-ground field experience in the selected case studies.

This study presents off-grid and decentralized hybrid renewable electricity systems (OHRES) design, installation and commissioning, modelling and techno-economic analysis, system sizing, system monitoring, and data analysis applications, which are practiced in our case studies.

The first building block of our study is the OHRES deployment in the selected case-study locations in Canada and Uganda. Related information to each case study were presented, along with the techno-economic analysis and system sizing for each case study. The study also covered the OHRES design overview, including an integrated 48V DC Hybrid lead-acid & Lithium-ion Battery Storage System (HBSS), system monitoring, and data analysis applications which are practiced in our case studies. The OHRES system's remote Monitoring and Weather Station (SMWS), including the allocation of remote monitoring devices, as well as system monitoring infrastructure, are described explicitly.

The second building block of our study is the development and optimization of the Hybrid Off-grid and decentralized systems Techno-Economic Model (HOTEM). HOTEM has been developed to be utilized as OHRES sizing and techno-economic assessment tool. The model can perform feasibility analysis for electrical energy production in order to obtain the best configuration and sizing of the hybrid system at the off-grid or decentralized location. The model was developed on the basis of a previous hybrid system model; however, major enhancements and optimizations were done in order to make HOTEM a functional, usable and reliable tool for the targeted application.

The third building block focuses on the development, working principals, methodology, and functionality of the Off-grid and decentralized systems data analysis platform (OSDAP) as a platform for remote monitoring of OHRES. The OSDAP tool will increase data and knowledge within the global energy access context, helping scale the future development of hybrid off-grid and decentralized energy systems around the world. The OSDAP platform includes several functionalities such as: dynamic data visualization, performance analysis and artificial neural network based solar irradiance forecasting.

The fourth building block of our study was the lessons learned and key contribution factors for off grid and decentralized hybrid systems, where major technical, economical, managerial and modeling factors were presented that can be utilized for both scientific research and practical business.

The following chapters will cover the four building blocks of the presented study in details.

1.2 Study overview, context and overall objectives

The so described developed and developing economies (based on the UN definition) faces two side of the electricity access challenge. The first side is communities without electricity access at all and this challenge is mostly related to developing countries. 600 million people of the global 850 million without electricity access are located in sub-Saharan Africa [13] [16]. The second side is communities with conventional unsustainable electricity access resources. Even in a 100% access rated countries for access to electricity [16]. There are still a few remote communities left with the need for dependency on conventional generators to satisfy the electricity demand needs, as they are not connected to the main grid. A solid example can be experienced within the area where the case study covered in our study scope is located in Canada, which is covered in more detail in a later section. In Canada, it is estimated to have 279 remote communities without an electrical grid connection, where 239 of these communities rely on conventional fuel as diesel for electricity and oil for heating [17] [14].

Off-grid and decentralized renewable-based electricity systems play a promising role in overcoming the two sides of the sustainable electrical energy access challenge. In 2015 it is reported that an estimated more than 100 million people or almost 26 million households are depending on off-grid renewable energy systems. The majority of these households (20 million) are served through Solar Home Systems (SHS), others through renewable-based mini-grids (5 million), and small wind turbines (0.8 million) [18]. This

number increase to 133 million people in 2016, with 100 million people using solar lights (less than 11 watts), 24 million people using SHS (more than 11 watts) and at least 9 million people connected to mini-grid [19]. Figure 1.1 illustrate the development of population served by off-grid renewable energy solution globally from 207 to 2016.

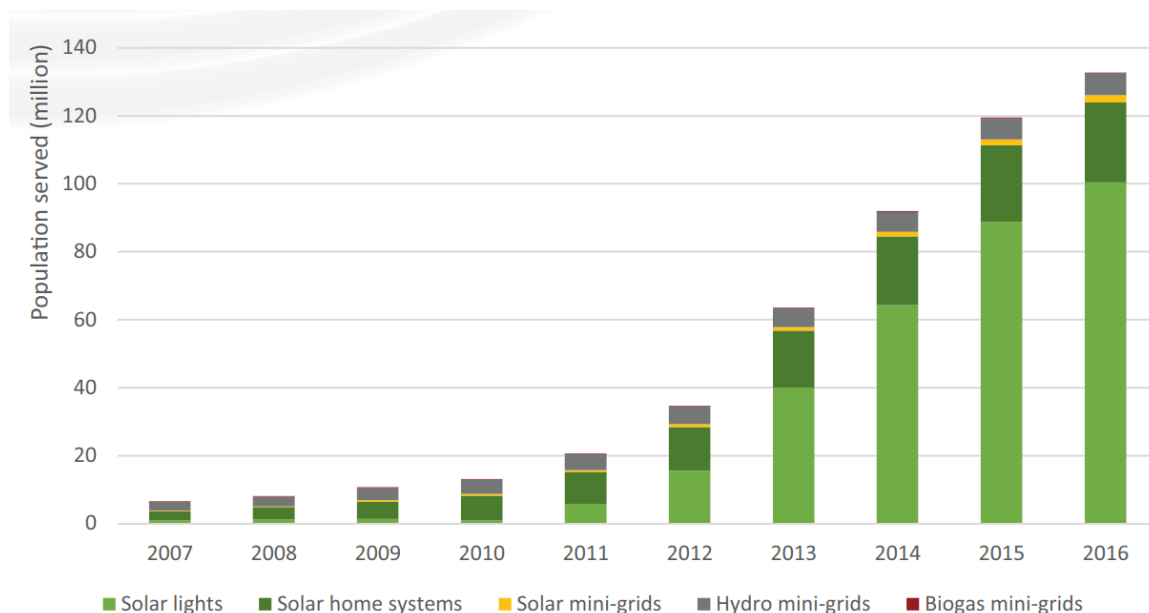


Figure 1.1: Population served by off-grid renewable energy solutions globally.
Figure reference: Source [19]

Besides the existing off-grid renewable energy systems market, on short to medium term this market has the expectation for growth especially in rural and island areas, through:

1. The hybridization concept of existing Genset (e.g. diesel, Gasoline, Propane) though utilizing renewable energy resources like solar PV, wind, biomass, and small hydro-power.
2. The replacement of diesel generators with off-grid renewable-based systems.

Hybrid Renewable Electricity Systems (HRES) represents a potentially feasible and reliable solution for providing electrical energy based on the highest possible utilization for renewable resources available for both grid-tied and decentralized off-grid applications.

Study scope and scientific methodological aspects

There are major challenges and methodological improvements needed to realize the market needs. Which some of them highlighted here based on both what is provided in [18], in addition to the experience and lessons-learned in our study scope in recent years:

- The off-grid renewable energy system's global definition criteria is very broad, including design aspects, applications, and technologies. This has a reflection on lacking standardization and incoherent and inconsistent definitions in the off-grid renewable energy field.
- There is often no distinction between installed capacities and operating capacities related to off-grid applications on national energy statistics.
- Data available on off-grid systems scope and extent is limited, and data sources across countries are scarce and inconsistent.
- Comparing data across different off-grid renewable energy systems across the world is difficult, as there is a variety of indicators used to evaluate off-grid systems.
- Even the collected data from academic and research institutions on off-grid systems for performance and/or effectiveness of its deployment evaluation are not consistent, as they are case study specific and often cover particular application or geographic area and time frame.
- The system technical design and economical aspects are very much location and case-specific based, which can have a tremendous variation not only from country to country but from a neighborhood or even one user to another within the same area.
- There is a scarcity in the available tools addressing the techno-economic analysis and system sizing for off-grid and decentralized systems. So the engineering and techno-economic assessment process of such systems are based on very simple calculations which end –in most of the cases- in a system oversizing and poor economical feasibility. Or using a paid tool which is for the end-user a black-box where a lot of the optimization, and model operational functionalities are not shared due to know-how protection. which could be an expensive, and complicated option as well for some of the end-users and stockholders in the off-grid and decentralized systems context.

Important to mention that many other challenges exist in this context varying from environmental, political, social, technical and economic perspectives [20], but they cannot be listed and addressed in sufficient depth within the scope of our study.

Our methodological approach aims to overcome some of the available challenges related to off-grid and decentralized systems, consists of two main parts:

First part: Comparative techno-economic analysis based on contrastive case-study

Addressing the techno-economic aspects related to OHRES is our focus within the context of this study. Understanding the technical and economic factors affecting the feasibility, sustainability, and reliability of OHRES along the value chain is necessary to increase the level of understanding, acceptance and deployment of such systems on

a global level. These techno-economic aspects go from one stage to the next along the OHRES implementation value chain and can be summarized as the following stages as shown in figure 1.2.

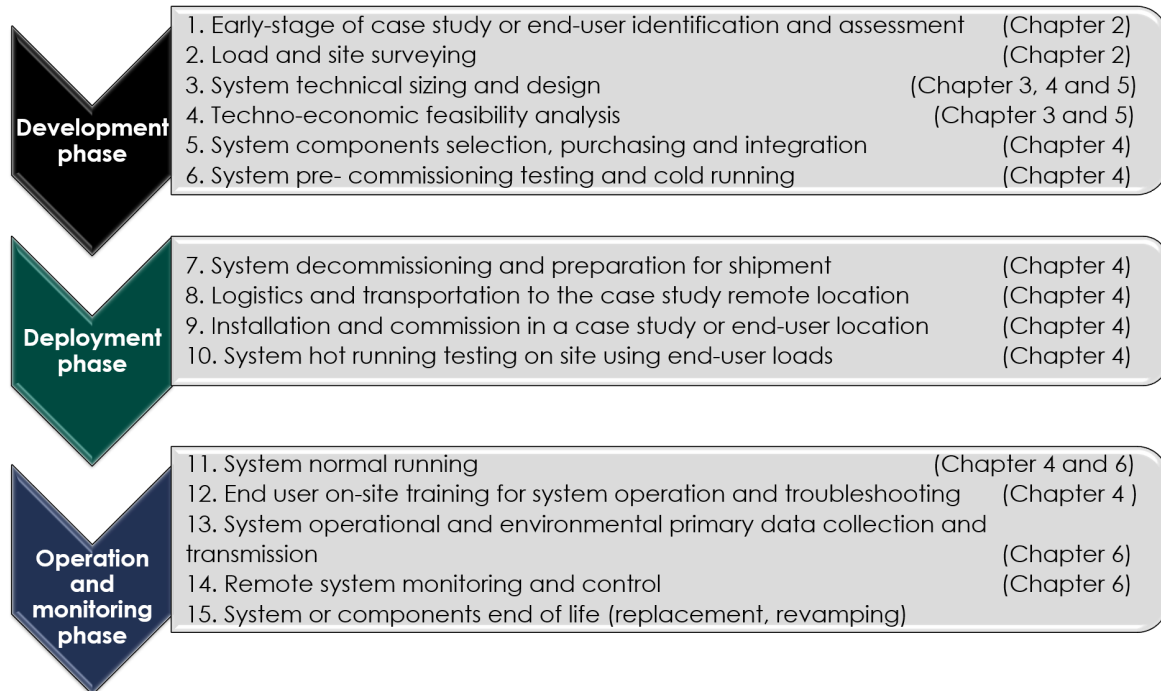


Figure 1.2: OHRES value-chain techno-economic related phases and stages.
Figure reference: Author's illustration.

Our methodology includes addressing these techno-economic aspects in contrastive case studies, in two extremely different locations and case study end-user natures within remote areas in Sub-Saharan Africa (Uganda) and Canada (Nemaiah Valley, British Columbia). More information regarding the case studies is discussed further in the next chapters. As mentioned earlier one of the methodological enhancement aspects needed for off-grid renewable energy systems was that the data provided by research institutions are not consistent as they are case study specific and often cover the particular application or geographic area. The methodological approach of have two wide contrastive case studies is tackling this aspect, leads to a wider understanding of the techno-economic challenges and influencing factors not only in these two locations but in a much wider scale of OHRES system users globally.

Second part: A comprehensive methodological approach for off-grid and decentralized hybrid systems including four main building blocks

The second major aspect of our study methodology is the comprehensive approach we are using surrounding all related techno-economic aspects of the OHRES along the different phases from development, deployment to operation and monitoring. This comprehensive approach is based on four main building blocks as shown in figure 1.3. These building blocks come in a certain order, based on the flow of the system different phases as following:

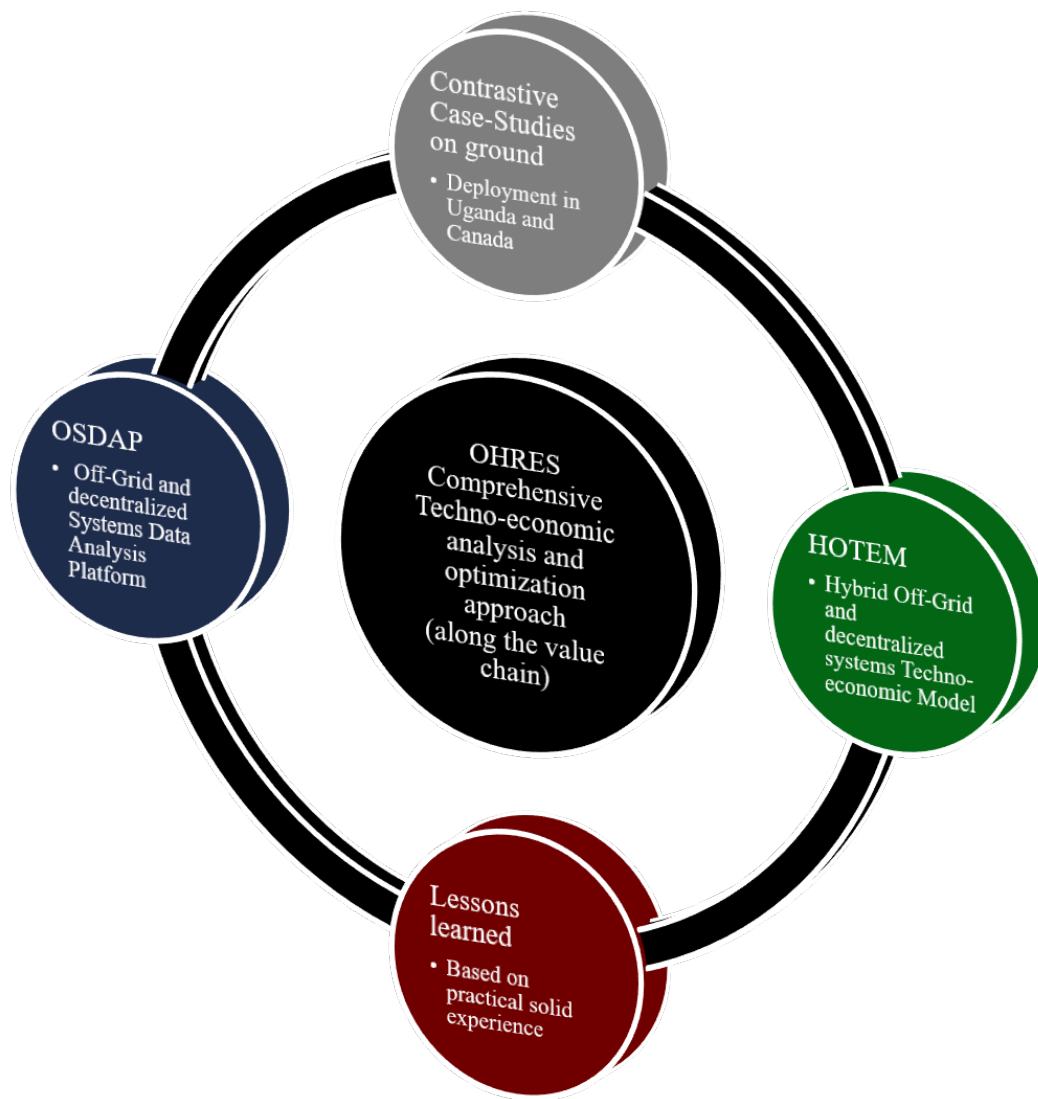


Figure 1.3: OHRES Comprehensive Techno-economic analysis and optimization approach

Figure reference: Author's illustration, published in [5].

1. HOTEM (Hybrid Off-grid and decentralized systems Techno-Economic Model)
A hybrid renewable electricity system techno-economic feasibility analysis and system sizing developed tool.
2. On-ground deployment of OHRES in selected case-study locations within Canada and Uganda.

Including a globally functional System remote Monitoring and weather station (SMWS) as described in detail in [1]. Since August 2019, our first OHRES system is already in operation in Canada (George household) case study including fully functional SMWS. In addition, the first system component part (Weather station) installed in Uganda (Sofraa School) case study including the weather station. The recent updates regarding the case studies can be found in [21]. This is providing primary system operation and renewable resources & weather data

from the selected locations.

3. OSDAP (Off-grid and decentralized systems Data Analysis Platform)

OSDAP is a comprehensive developed tool for OHRES data analysis, performance monitoring and renewable energy resources forecasting. The current ready developed version of OSDAP 2.0 includes the following functionality:

- a) Dynamic visualization for system operation and renewable resources & weather data.
- b) Performance analysis using selected performance indicators for the off-grid hybrid system overall, and for specific components.
- c) Irradiance forecasting for 24-hours and 1-hour ahead period based on machine learning algorithms (Artificial Neural Networks).

With such functionalities, OSDAP is providing a useful and understandable meaning to the primary data collected from the OHRES. Besides, other utilization cases for its functionalities on the user level which can have a positive impact on the off-grid system technical utilization, sustainability, and economic feasibility.

4. Lessons-learned within the techno-economic scope of the current work.

Based on the on-ground field experience in such a contrastive work context, especially with the exposure to the different phases of the OHRES from development to operation important lessons learned are generated. Such learned lessons represent a defined To-do and not To-do pathway for a global vision of wide deployment of similar OHRES from a techno-economic perspective.

1.3 Study contribution and relation to off-grid and decentralized electricity systems research context

1.3.1 Study related work and literature

There have been remarkable research and development efforts in the context of renewable energy based hybrid electricity systems techno-economic analysis and optimization. This work has been covered from many different perspectives such as: the utilization of renewable and non-renewable energy-based resources in hybrid systems, the integration of different energy storage technologies into hybrid systems, the techno-economic modeling tools development for the assessment of the economic feasibility of hybrid systems, development of sizing tools for hybrid systems components sizing optimization, the development and enhancement of optimization algorithms for the sizing and assessment of the system, and other development and optimization related objectives.

It is important to mention that major parts of this work are based on applied research activities, and practical experience. However, in the context of our presented study, some of the existing research efforts and previously done studies are utilized.

The off grid and decentralized hybrid renewable electricity systems storage systems development and the utilization and combination of hybrid storage technologies into these systems were previously covered in different studies. The study presented in [22] addressed the “Optimization of an off-grid hybrid PV–Wind–Diesel system with different battery technologies using genetic algorithm”. The study targeted the modeling and optimization of an off grid and decentralized hybrid electricity system, including battery storage and diesel genset. The three battery storage technologies included in the study were: lead-acid, li-ion, and vanadium redox flow. Six different scenarios for the system configuration were investigated and compared for selected sites in Germany and Syria. The optimization results showed that the scenario using the vanadium redox flow battery with the genset had the minimum Levelized Cost of Electricity (LCOE).

In [23] two stand-alone PV-storage hybrid systems were developed for a rural household. One system included a conventional battery storage system, and the second used a hybrid energy storage system based on battery & supercapacitor. The simulation results gained through applying different control strategies was that the hybrid battery & supercapacitor storage system prolonged the battery lifespan by decreasing the stress on it by reducing the peak battery current by 8.6%, preventing the battery from deep discharge and improving the battery’s average SOC by 0.34%.

The study presented in [24] included a cost-benefit trade-off analysis between a hybrid battery storage system (HBSS) including Lead-acid & Li-ion batteries, as compared to pure lead-acid battery storage for an electrical vehicle. Experimental results showed that although the HBSS had a higher cost, it was 23% more efficient than the pure lead-acid battery storage.

The optimal sizing of two grid-connected hybrid storage systems was presented in [25]. The investigated hybrid storage systems were: 1) Hybrid lead-acid & Li-ion battery storage system, 2) Lead-acid + Li-ion + power to heat (PtH). The optimization goal was to maximize profitability in the primary control reserve market. The system power dispatch control algorithm was also discussed, based on the preferable state of energy level for each technology. In the optimization results of the second hybrid storage system, the Li-ion battery was eliminated, as the lead-acid + PtH hybrid storage was found to be more profitable than the Li-ion and Lead-acid hybrid battery storage system. In [26] hybrid lead-acid & Li-ion battery storage behavior was investigated for an off-grid system used for a clinic in Africa. Simulation results generated from a developed model were validated against on-site measurement.

Four different Hybrid Energy Storage Systems (HESS) were addressed in [27] for a decentralized PV system in terms of the coupling architecture, energy management, and power flow control. The HESS’ presented were: power to heat + battery, power to heat + battery + hydrogen, super-capacitor + battery, and battery + battery. The study distinguished power and energy-oriented storage, into “high power” storage dedicated to cover high power demand, transients, and load fluctuations and another “high energy” storage with low self-discharge and lower cost per installed energy characteristics. A hybrid solar PV and HESS system in Germany was presented as a reference case to discuss the different approaches for power decomposition in the system. The study concluded that HESS represents a promising storage architecture that can support the renewable energy transition.

Studies [28], and [29] represent a very solid base for the optimization algorithm (C-DEEPSO) used in our techno-economic analysis and system sizing tool (HOTEM). In [28], C-DEEPSO is tested and suggested as one of the most useful and promising methods in designing the hybrid metaheuristic, by using a case study of the optimal control and management environment of reactive energy production sources by the wind power plant. The work published in [30] focused on evaluating five different battery technologies and their impact on hybrid systems design, using the approach of combining optimization algorithm C-DEEPSO with a decision-making methodology. The optimization goals were the maximization of the available renewable energy resources, and the minimization of the LCOE and the Loss of Power Supply Probability (LPSP). The study also included a case study in Germany for applying the developed methodology, and lithium-ion (Li-ion) battery storage technology was considered the optimal technological selection.

The study of Perera et al. [31] presented a combined method for hybrid systems design, using a multi-objective optimization with a multi-criterion decision making (MCDM) method. The optimization objectives used are to minimize the LCOE, dumped renewable energy, loss of power supply, and fuel consumption. Also, the approach was implemented in a case study, reflecting the practicality of the presented work.

In our developed Off-grid and decentralized system Data Analysis Platform (OS-DAP), Solar forecasting modeling related research efforts are utilized within our study as well. Solar forecasting models with various time horizons are available in the literature. Some studies predict solar radiation as short as 10 minutes ahead, whereas some studies predict solar irradiance one or multiple days ahead. Chow et. al. [32] developed an artificial neural network (ANN) model using a multilayer perceptron (MLP) technique which makes 10 minutes ahead predictions in real-time. After training the model, they tested their model for 10 minutes ahead and 20 minutes ahead cases by using test samples. During model testing, features from the test samples were entered into the model to derive predictions. Then the predictions are compared with the actual data. Test results show that (t+10) prediction model's correlation coefficients are within 0.8934, lower limit of the 95% confidence interval, and 0.9862, upper limit of the 95% confidence interval .

Mellit et. al. [33] used an MLP model which takes three input features: day of the year, mean solar irradiation and mean temperature for day T. The model yields 24-hour irradiance prediction of the next day (T+1) with hourly data resolution. Based on their test results, correlation coefficients of the test set range between 98-99% for sunny days and 94-96% for cloudy days. They also used error metrics such as root mean squared error (RMSE) and mean bias error (MBE) for evaluating the model. Given the test results of eight selected samples, four sunny days and four cloudy days, RMSE values range between 13.14% and 85.76%.

Qing X. and Niu Y. [34] developed an hourly day-ahead solar irradiance forecasting model using Long-Short Term Memory (LSTM) method. Their input dataset includes data features such as month, day of the month, temperature, dew point, humidity, visibility, wind speed and weather type. They test four different algorithms which are Persistence, LR, BPNN, and LSTM. After running the models with different al-

gorithms, their training RMSE (W/m^2) values are NA, 200.991, 133.1408, 199.3744, respectively. Models yield testing RMSE values of 177.031, 195.875, 105.2845, 122.7174, respectively .

Solar irradiation data have an important role in solar energy research and operation management of solar energy powered systems. Having advanced knowledge of solar radiation ahead of time increases the operation optimization of both grid-connected and off-grid systems [35]. In 2017, C. Voyant et. al. [36] reviewed five main journals of solar energy prediction (*Solar Energy, Energy, Applied Energy, Renewable Energy, Energy Conversion and Management*). They found out that 79% of artificial intelligence methods used for solar irradiance forecasting are based on artificial neural networks (ANN) . There are different ANN methods used for solar irradiance forecasting purpose. Studies [37, 38, 34] present solar irradiance forecasting models which take temporal weather data as inputs and compare performance of different ANN methods in terms of root-mean square error. Their results are in favour of the LSTM method. Therefore, we implemented the LSTM method for our solar irradiance forecasting application in OSDAP.

Beside the mentioned related work and literature review, each building block of our study included its relevant further literature due to the diverse variety of literature used in our work scope.

1.3.2 Study contribution and relation to research context

This study provides major contributions to off-grid and decentralized hybrid renewable energy systems research and commercial business areas. It is the first study to consider covering a wide and comprehensive approach for OHRES, including all related techno-economic aspects, system implementation phases, and deployment in both developing and developed economies.

Another major contribution is that the presented study plays a role in bridging the gap between theoretical academic research and the practical business side related to market experience and needs. This is done through sharing practical experiences and lessons learned gathered from on-ground research activities located in both developing and developed countries. Moreover, developing the required tools to be used along the off-grid and decentralized systems value chain required tools for system monitoring and data analysis. Such developed tools are candidates with a high potential to be open source tools, which can be utilized to enhance the quality, economics, and performance of OHRES systems, and have a direct positive reflection on such systems' global deployment and credibility.

Including scientific, theoretical and market practical sides are highly necessary in the challenging context of solving the global problem of energy access and overcoming its complex challenges. Covering only the theoretical and scientific side will lead to the creation of optimized solutions and outcomes from a scientific perspective only, which are detached from the real market challenges and needs, which is not possible to be clearly understood without practicing it on the ground. This detachment leads to the creation of a wave of inapplicable solutions with the intention of overcoming the main challenge of ending global energy poverty. There are many reasons for the inappli-

cability of the proposed solutions in that case. For example, the solutions proposed could be very optimized and clear from the scientific perspective, but on the other hand very complex to use, or represent unnecessary very detailed outcomes from the market perspective.

From the other side, the market and business-related experiences are very valuable as they deal with the real existing problems and current demanding challenges on the ground. However, in most of the cases, this experience is part of protected internal knowhow of the market-acting entities such as companies, which cannot be shared freely. This keeps most of such knowledge and its accumulation inaccessible to the research and scientific communities who share the same interest and potential to develop further practical solutions. Another aspect is that business-oriented entities such as companies lack, in most cases, the capacity to investigate and develop new innovative approaches especially in a competitive and risky market like the remote energy market. There are many reasons that can vary from one entity to another, but two common reasons are:

1. Business-oriented entities such as companies have a very high orientation toward profitability, which is necessary for the business sustainability needs of such entities. This creates a different perspective of risk preserving toward exploring new and innovative approaches, rather than the research and scientific perspective.
2. A lack of required resources whether financial, capacity, or other resources required for being involved in developing and testing innovative approaches that do not have a credible record of operation, rather than relying on the state-of-the-art commercially available solutions.

This makes studies that cover both scientific theoretical and market practical aspects, and bridge the gap between both sides as the presented study very unique and valuable for both the scientific and business communities, but these studies also face challenges regarding high risks. These high-risk challenges are related to the applied nature side of such studies nature, more than the theoretical side. Some solid examples of such challenges and risks based on our applied research methodology explained before in section 1.2 are listed below, however, more sources of risks can also be experienced and were also identified within the scope and course of our applied study nature:

- The international projects handling nature, where activities are not taking place only in a controlled research environment as a laboratory but rather in such study nature the research labs are on the ground deployed projects and case studies.
- Another source of high risk that within the scope of our study the on-ground activities and case studies are not located in a local or near within borders, but rather on cross borders international locations in multi-continent and different geographical, environmental, technical and social aspects.
- Finding the right local partners in such international work nature is also very challenging, especially partners who can support applied research projects and case studies as most local partners, in that case, have an interest in business-related

activities where there are a clear business opportunity and the economical benefit behind it, rather than being involved in applied research activities where the benefits gained can be more indirect compared to the business-related activities.

- Having a comprehensive 360 Degree methodological approach as the one used in this study and illustrated before in figure 1.3, is challenging as it required covering both theoretical and practical aspects besides being able to create a clear link between both aspects to utilize the experience and benefits gained from each side and use it in filling the gaps the other side has. An example of that is using the experience and knowledge gained from our on-ground case study as a base for the two software tools developed within the scope of this study.
- In such applied and practical research nature it is mandatory that the working team and especially the team coordinator has a good level of understanding of the theoretical and scientific aspects, besides having a good level of practical experience in handling the applied and practical side of the study scope by himself, and also manage the whole study and project scope beside coordinating other team members. Such work nature could be challenging for the scientific community as it requires building upon previous work and practical life experience which is mostly gained in the industry and business work environments.
- Handling the full project lifecycle along the value chain of systems, software and hardware development to logistics, implantation, installation, and commissioning as explained before in figure 1.2 in our study is also a source of very high risk within a research study due to the limitation of both financial and human resources available in most cases, compared to a commercial entity handling a full project lifecycle where more resources as positioned before the project starting point to fulfill the project needs.

This study incorporates a unique study methodology that includes theoretical assessment, on-the-ground case studies, and the development of software tools and resources. To our knowledge, similar scientific methodological approaches as used in this study as explained before in details in section 1.2 are not currently covered in the literature. An applied research perspective involving not only theoretical assessment but also practical contrastive case-study on-ground work is unique. Using such a comprehensive methodological approach from system development to deployment and operation & monitoring is truly unique. This study thus provides a role in filling an existing knowledge gap in the off-grid and decentralized systems techno-economic context.

1.4 Scientific publications based on the scope of the presented study

The Appendix includes a detailed list of several publications, presentation, scientific conferences, talks, research related activities, and international roles and lectures that were conducted within the scope of this study and represents major input for the thesis

work presented. In addition included also in the Appendix a table of several master thesis studies and internships which were supervised during the study conducting period. These research activities represented very important input to the following mentioned publications and the thesis work presented.

1.5 Thesis structure

The presented study consists of seven chapters. Chapter 1 provides an introduction for the study, and describes the details related to the study scope and methodology. It also provides the study contribution and relation to the off-grid and decentralized systems research context. This chapter also includes a list of selected scientific publications, which have been published during the work period of this study.

Chapter 2 is the first part related to the first building block of our methodological approach, covering the case studies and the OHRES structure overview. This chapter includes two main sections. The first section covers the case studies overview, selection criteria and related technical information. The second section covers the general technical aspects of OHRES.

Chapter 3 is the second part related to the first building block of the study. This chapter covers the OHRES techno-economic assessment and system sizing in both Canada and Uganda case studies. The chapter includes four sections: The first section covers the OHRES techno-economic analysis and system sizing. Section 2 covers the Canada case study hybrid system techno-economic analysis and sizing. Section 3 covers the Uganda case study hybrid system techno-economic analysis and sizing. Section 4 highlights a techno-economic assessment for the hybrid battery storage system used in the hybrid off-grid system.

Chapter 4 is the third and last part related to the first building block of the study. This chapter covers the OHRES hardware aspects and functionality optimization, as well as the system dynamic testing and on site commissioning activities in both case studies in Canada and Uganda. This chapter includes seven sections: The first section covers the OHRES System remote Monitoring and Weather Station (SMWS) and hardware aspects. Section 2 addresses the hybrid system operation and safety developed functionalities. Section 3 covers the hybrid system dynamic testing and functionality optimization. Section 4 describes the OHRES on-site installation and commissioning. Section 5 describes the Canada case study OHRES installation and commissioning. Section 6 covers the Uganda case study on-site installation and commissioning. Section 7 focuses on highlighting the major differences experienced between the case studies in Canada and Uganda.

Chapter 5 covers all details related to the second building block of our study, which is related to off-grid and decentralized systems techno-economic modeling and sizing tool development. This chapter will cover in detail the Hybrid off-grid and decentralized system Techno-Economic model (HOTEM) structure and development. The chapter

includes four sections: section 1 covers HOTEM structure and development methodology. Section 2 address HOTEM optimization targets and power dispatch strategy. Section 3 covers a case study description where HOTEM is used for system sizing, and the modelling results. Section 4 presents a benchmarking for HOTEM against a commercially used tool for off-grid and decentralized hybrid systems techno-economic analysis and system sizing.

Chapter 6 covers the third building block which is related to the Off-grid and decentralized System Data Analysis Platform (OSDAP). This chapter includes two sections: section 1 address OSDAP data handling and visualization development. Section 2 covers the hybrid system performance analysis and solar irradiance forecasting functionalities in OSDAP.

Chapter 7 is the last chapter of the presented study providing important final remarks, as well as the conclusion and outlook. It includes two sections: section 1 presents the major lessons learned and key considerations for off grid and decentralized systems, which have been gathered along this study from practical on-ground activities in Canada and Uganda. Section 2 represents the conclusion and outlook for the study.

2 Case studies and Off-grid and decentralized Hybrid Electricity System (OHRES) structure overview

The first building block of the study comprehensive methodological approach presented before in figure 1.3 is covered in the chapters 2, 3, and 4.

Chapter 2 is the first part related to this building block, covering the case studies related information beside the OHRES structure overview.

Chapter 2 addresses the first two stages of the hybrid systems development phase presented before in figure 1.2. This chapter includes two main section. The first section covers the case studies overview, selection criteria and related technical information. Second section covers the general technical aspects of OHRES.

Part of the content of this chapter is based on, and from the author's published work in Elkadragy et. al [1] [5] [8].

2.1 Case studies overview, selection and load demands

2.1.1 Case Studies overview and selection criteria

Our methodology includes addressing the techno-economic aspects in contrastive case studies, in two extremely different locations and case study end-user natures within remote areas in Sub-Saharan Africa (Uganda) and Canada (Nemaiah Valley, British Columbia). A brief overview of the selected case studies given in table 2.2 [1]. Figure 2.1 [21] shows the two case study locations based on photos taken during the different site visits and work on site done recently.

The selection of the contrastive case-studies is done based on the detailed criteria described in table 2.1. The distinction between developing and developed economies is based on the United Nations definition [45].

The selected case studies in Uganda and Canada have different environmental and user contexts, but the similarity in the load and energy demand levels. This allows the use of a similar range of OHRES components in both locations with some variations in installed capacities of renewable energy generation resources as solar PV and small wind based on the available environmental resources differences in both locations. However, the core parts of the system design components are still similar in both cases as shown in detail in [1].

Table 2.1: Case-studies selection criteria (Published in [1]).

Selection criteria / category for contrastive case-studies	Developed country	Developing country
Local partner or end customer related	<p>Local partner has already a good understanding of renewable energy off-grid systems (Having already social acceptance and motivation for implementing an off-grid system)</p>	<p>Local partner has already a basic understanding of renewable energy off-grid systems (Social acceptance to be build up with the partner based on such basic understanding)</p>
	<p>Good (but not a must) to have a local partner with previously installed off-grid system (To represent how the system can perform based on previously experienced user)</p>	<p>Preferable to have a local partner with no previously installed off-grid system (To represent how the system can perform in an environment which lacks previous experience)</p>
	<p>Ownership and full control of the facility where the system will be installed should be represented in both case-studies (In order to limit external critical risks on the short and medium term of the project for the purpose of use changes for the location or need to de-commission the system due to uncertainties in ownership)</p>	
	<p>Availability of very good communication channel (Critical criteria which will minimize the risk of project sustainability and also increase the efficiency of system implementation, maintenance and operation of the project life-cycle)</p>	
	Location selection	<p>Case-studies must be in a clearly defined developed vs developing economies (In order to analyze the effect of economic and basic political influences on off-grid sectors)</p>
Techno-economic aspects	<p>Remote locations with no access to the grid or very high electricity tariffs. Preferably to be a part of the remote community (Will support the economic feasibility of the off-grid system and project sustainability aspects)</p>	
	<p>Both case-studies will depend on Hybrid off-grid systems consisting of solar PV and mini-wind (if feasibility) and electrical energy storage (Hybrid Battery storage) as a main source for electrical energy (Having similarity in the renewable energy resources used and system layout, which is needed for the comparative analysis)</p>	
	<p>Case-studies should be within the same energy consumption [kWh] tier, based on [39] of the World Bank recommended framework (System design and sizing will not differ much between the case-studies, which support the objective of doing a comparative analysis)</p>	

Table 2.2: Contrastive case-studies overview in Canada and Uganda (Published in [1]).

Case-study	Canada Case study (George Colgate's Household)	Uganda Case study (Sofraa School)
Category	Developed country	Developing country
Location	George Colgate Household in Nemaiah Valley, British Columbia (BC), Canada (figure 2.1b).	Sofraa school Wakisi, Jinja, Uganda (figure 2.1a).
Access to Electricity	Nearly 100 % of the Canadian population has access to electricity [16]. However, Canada has 239 remote communities that are not connected to the main grid and depend on diesel generators to satisfy electricity demand and could benefit from off-grid renewable energy.	Approximately 22 % of the Ugandan population has access to electricity [16]. Uganda has one of the lowest electrification rates in Africa and comparably high electrical energy tariff, despite being one of the poorest countries in Africa [40]. Rural Population 83.6 % from the total Population.
Renewable resources: Solar irradiance availability	The Nemaiah Valley receives an approximated solar irradiance between 1,660 kWh / m ² and 1,960 kWh / m ² per year [41].	Most of the Ugandan territory receives a solar irradiance between 1,825 kWh / m ² and 2,500 kWh / m ² per year [42].
Supporting programs overview	Public and private sectors are working together in British Columbia to provide free energy efficiency guidance, installation of energy saving products and tailored home energy assessment by professional contractors for low income households [43].	The Ugandan government is supporting the implementation of solar applications in the country by creating national support plans including financing mechanisms for consumers and system operators, duty exemptions for certain off-grid components, and stating quality standards [44][40].
Case-study End-Use application	Residential application Private household owner.	Residential application School building with no electricity and water access.
Level of experiences regarding off-grid renewable electricity	Running on an off-grid system (need to be upgraded due to load demands), experienced user.	No previous access to electricity, lack of previous experience.
Status of OHRES system deployment	The first OHRES was completely installed and commissioned in the house remote location. The household is running on the newly installed hybrid system since August 2019.	First system part which is the weather station including the remote data logging and transfer functionality is installed in its final location in the Sofraa school building and running since March 2019.



(a) Uganda (Sofraa school) case-study with the weather station installation on the school's roof-top (photo taken after Weather Station and remote communication system installation on March 2018)



(b) Canada (George colgate houshold) Case-study, with the PV and SMWS as outdoor parts of the OHRES commissioned components (photo taken after OHRES system complete commissioning on Aug 2019)

Figure 2.1: Case-studies latest taken photos in Canada and Uganda
Figure reference: Author's figure, published in [8], and [21]

The methodological approach of have two wide contrastive case studies is tackling this aspect, leads to a wider understanding of the techno-economic challenges and influencing factors not only in these two locations but in a much wider scale of OHRES system users globally. The most recent updates regarding the deployment of our systems and our study can be found in the study web-page [21].

2.1.2 Case studies load profile and energy demand

The load profile is the backbone of OHRES sizing, component selection, design, and techno-economic assessment. That is why a detailed load survey is the first important early step that needs to be taken with the site survey. Based on the nature of the case study and the end-user experience, the outcome quality of the load survey depends highly on the answers to the following questions:

1. Does the end-user have previous experience with living on off-grid and decentralized systems?
2. Is there available historical load power measured data?
3. Does the end-user have a historical load behavior on a daily and weekly basis?

The answers to these three questions highly affect the accuracy of the generated load-profile from the load-survey. In many cases remote communities and off-grid systems do not have enough data available so proper estimations and assumptions have to be done together with the end-user for overcoming this load profile shaping challenge.

One of the strengths we have in this study scope is that we covered both contrastive cases in terms of generating a load profile, and used different methodologies depending

on the case-study conditions to overcome the challenges we faced in the load surveying process as described in the next sections.

Canada Case-study load profile

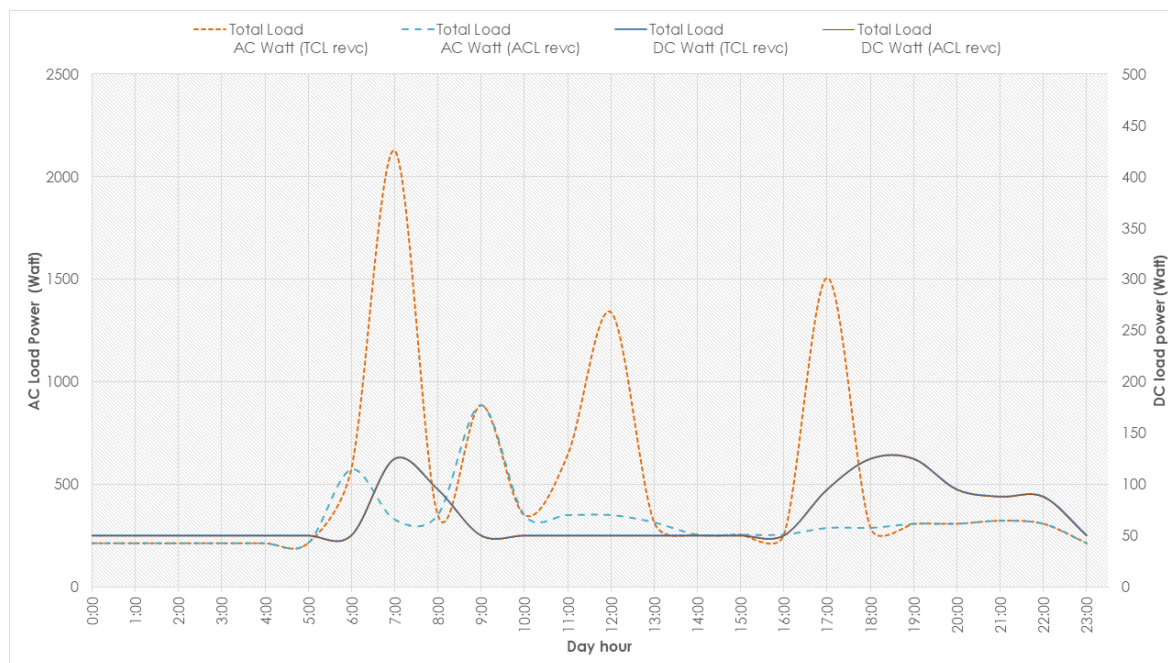


Figure 2.2: Canada case study - 24h total connected loads (TCL) and Average Connected Loads (ACL) profiles

Figure reference: Author's illustration.

The Canada case-study load profile has less uncertainty in its estimation compared to the Uganda case-study load profile. This is due to two main reasons: 1) The fact that the end-user (the house-hold owner) has lived off-grid already for many years, and has had detailed measurements done for the power consumption of the different load types used in the house. 2) The estimation of the user behavior and daily load using routines to build a 24 hour and weekly load profiles is more easily determined, as the end user has already lived with these loads for years. Building this load profile did not require a site visit due to the high-quality available load information and data, and the end-user's previous experience with off-grid systems. This is contrary to the Uganda case study conditions where there is no living history on the loads used, and the end-user does not have any experience with using off-grid systems and their load behavior.

The load survey for the Canada case study has shown that there is a variety of AC and DC loads used in the household. These loads and their power consumption are all described in table 2.3. The AC loads are represented by the washing machine, freezer, hairdryer, blender, computers, printer, TV, microwave oven, vacuum cleaner, and radio. The DC loads are mainly lighting, with a much lower share of the total load demand than the share of the AC loads.

Table 2.3: Canada case study type of loads and its power consumption

Item	Type of DC/AC	load	Power (Watt)	Number of appliances used	Total demand (Watt)
Blender	AC-120V		360	1	360
Clothes Washer	AC-120V		292	1	292
Dishwasher	AC-120V		536	1	536
Freezer	AC-120V		85	1	85
Hair Dryer	AC-120V		1800	1	1800
Inverter-no load	AC-120V		12	1	12
Lamp-Basement	DC-12V		15	4	60
Lamp-Bedrm	DC-12V		8	1	8
Lamp-Bedrm	AC-120V		15	1	15
Lamp-desk	AC-120V		14	1	14
Lamp-Kitchen	DC-12V		15	2	30
Lamp-Liv Rm	DC-12V		15	1	15
Lamp-Liv Rm	AC-120V		20	1	20
Laptop-1	AC-120V		36	1	19
Laptop-2	AC-120V		36	1	19
Microwave Oven	AC-120V		1220	1	1220
Phone	DC-12V		20	1	20
Printer-printing	AC-120V		19	1	19
Printer-standby	AC-120V		1	1	1
Refridgerator	AC-120V		115	1	115
Serius Radio	AC-120V		42	1	42
TV	AC-120V		75	1	75
Vacuum Cleaner	AC-120V		990	1	990
Xplornet converter	AC-120V		23	1	23
SMWS Monitoring and Weather station	DC-24/12V		30	1	30

Building a complete 24 hour load profile is one of the important milestones needed for system sizing and design. An hourly load survey template was developed and filled with the case-study end-user (the household owner), to build a detailed hourly load profile. This load survey resulted in two load profiles. One is the Average Connected Loads (ACL), representing the average of the daily use of loads that normally take place during most days of the week. The other is the Total Connected Loads (TCL) that normally take place during few days of the week, which represents the maximum estimated behavior of load connection that needs to be taken into consideration for the hybrid system components sizing.

Figure 2.2 shows both the ACL and TCL load profiles for both AC and DC loads. As can be seen, there is a variation between the ACL and TCL for the AC loads as they represent most of the high power demanding loads. However, for the DC loads, there is no difference between the ACL and TCL profiles. The maximum AC load power registered from the load survey in the TCL load profile is 2128 watts, however, the possibility of achieving even higher load powers for a loads transition period is taken into consideration for component selection (especially the main load inverter), as well as any de-rating effects due to operating temperature and conditions.

Uganda Case-study load profile

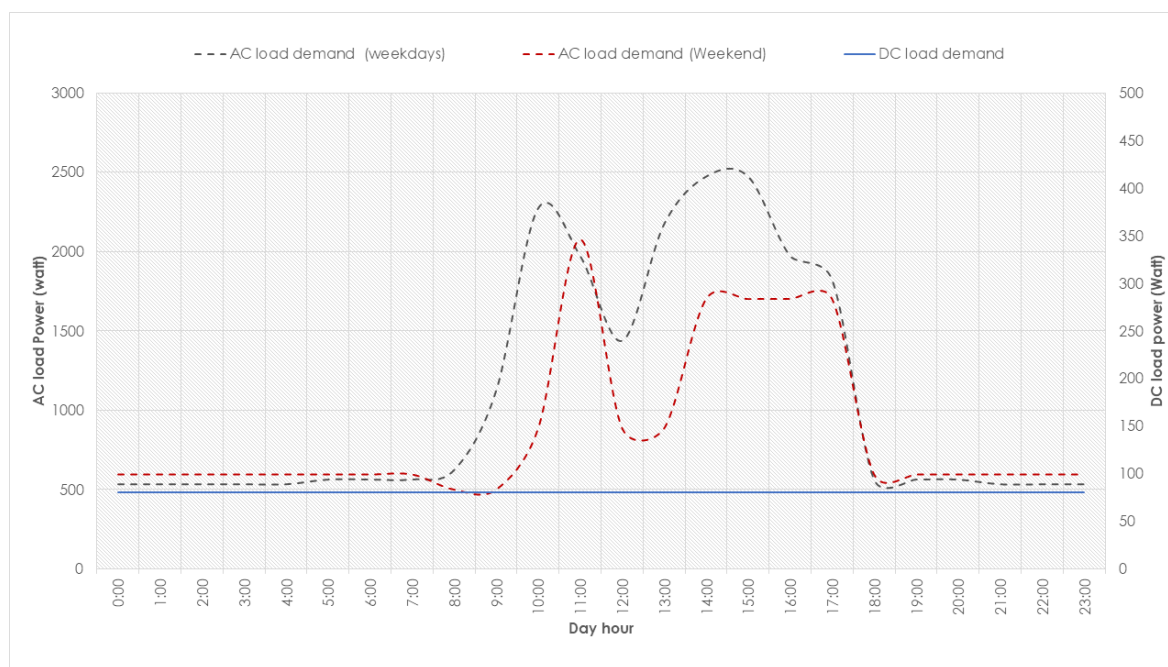


Figure 2.3: Uganda case study - 24h estimated load profile during week days (Monday - Friday) and weekend

Figure reference: Author's illustration.

The definition of the load profile for the Uganda case study is more challenging than for the Canada case study. This is due to three main reasons: 1) the lack of previous experience for the end-user (the Sofraa school) of living on off-grid systems or using any source of electrical energy. The school is fully un-electrified and the main dependency

Table 2.4: Uganda case study type of loads and its power consumption

Item	Type of load DC/AC	Power (Watt)	Number of appliances used	Total demand (Watt)
Lamp	AC-220V	5	82	410
Computer	AC-220V	40	30	1200
Printer	AC-220V	500	1	500
Projector / TV	AC-220V	300	2	600
Standing Fan	AC-220V	30	5	150
SMWS and System self consumption	DC-24/12V	80	1	80
Water pump	AC-220V	1200	1	1200
Mobile charges	AC-220V	220	1	220

is on natural resources (such as sunlight for lighting for example). 2) Due to point 1, there is no historical data available or measurements for load power consumption. This makes it difficult to build an accurate list of loads with their relative power consumption, which is a main step in the load surveying process. 3) As there are no electrical loads used before, there is no defined load usage pattern along the day or the week. This also makes it challenging to build highly accurate 24 hour and weekly load profiles, which is the backbone of the hybrid system sizing and techno-economic assessment.

It is important to mention in this stage that such a challenging load surveying process is not only limited to this specific case study, but is also the case in most remote areas and communities without electrical energy access. This challenge is critical to the success of global energy access goals and needs to be addressed in an early stage as it has a major influence on the system design and techno-economic feasibility on long-term and sustainability of energy delivery.

The methodology used to overcome such a challenging load surveying process for the Uganda case-study was based on four main pillars:

1. Custom design of a detailed hourly based load surveying template
2. Avoid completing the load survey process through remote communication (even if that could be an available option).
3. No assumptions related to the load profile behavior that do not involve the end-user.
4. Prepare for an early on-ground site visit for the case-study location.

Based on this methodology the load surveying process was the main part of the first on-ground site visit done for the school remote location in Wakisi - Jinja, Uganda.

Together with the school and our local technical partner the load distribution and survey was carried out in the school location, to make sure that the assumptions and load patterns estimation are the best possible, representing what can be expected in reality when the school is electrified and in operation. This turned out to be one of the very important lessons learned. What we experienced during the site visit and the process of having the load surveying done on-ground dramatically affected the approach we had beforehand not only for the load profile but for the whole system design aspects as well. Based on our experiences, we have seen that one of the common sources of errors is to depend only on remote communication or online methods for gathering case study or application-related data for remote areas specifically in developing economies.

Based on the on-ground site survey done during our first case study site visit, we have gathered a list of the appliances expected to be used in the Uganda case study school and its related power consumption (based on what is mentioned in each appliance's datasheet). Table 2.4 shows the types of loads used, with their corresponding powers. Most of the loads are AC loads, and this is due to the product's availability in the local market as for lighting lamps for example where DC lighting bulbs are rarely available in the local market.

An hourly load surveying template and estimation of the load's usage were done together directly with the end user in the school location. The load survey resulted in having a 24 hours load profile with hourly average loads value. Higher load curve resolution such as having a one-minute average load value is not applicable due to lack of data. Besides, it is not required for our system sizing and analysis process. Due to the nature of the school's operations, the load profiles differ in the Uganda case study between weekdays and weekends. A minimum amount of passive load management was agreed upon with the end-user, such as using the heavy uncritical loads such as the water pump during noon hours. Besides the pump operation management, it was also agreed to avoid using other heavy loads such as projector/TV and printers during the same operating hours as the water pump. These passive load management actions are done to have maximum utilization of the renewable resource availability (solar energy) and avoid deep discharge of the batteries which would have a positive reflection on its lifetime.

These load management restrictions were planned to be taken into consideration in the system design hardware components as well by adding interlocks for load activation based on the agreed load profile and management characteristics.

The weekday and weekend load curves are shown in figure 2.3 The peak load reaches 2475 watts for the AC load during weekdays and 2075 watts during the weekend. The DC loads do not change during the day or even on weekdays, as they mainly represent the system monitoring and weather station internal consumption DC power which is in operation 24 hours. For the system components' selection, especially the main load inverter sizing, peak values are taken into consideration. In addition, higher required load demand transient values, which might take place for a shorter period than 1 hour, as well as the de-rating effects due to operating temperature and conditions.

2.2 Off-grid and decentralized hybrid electricity systems (OHRES) technical overview

2.2.1 System design criteria and objectives

A major challenge in the design of an off-grid system is the high level of variety such systems are exposed to due to the fact that each off-grid location can be unique and represents its own requirements which can vary from another off-grid location in the same country. In practice even this variation can be experienced on lower geographical levels within the same remote community. Such location based requirements are combined with the lack of standardization in such field, which result in the need of a custom made solution for each off-grid project.

Due to the above mentioned challenges, it is hard to select a major criteria for the system design which can fulfill the needs of all off-grid electrical energy supply problems. However, we have taken into consideration that the criteria of the system design have a major influence on related aspects of the final solution developed and provided to the consumer, especially the technical and economical related ones. As we are targeting a major objective of ending energy poverty through Off-grid solutions, our OHRES has to balance between five main major objectives as represented in figure 2.4:

- The system has to represent economic feasibility over its lifetime. This doesn't require by default having the lowest system initial cost, rather than ensuring the reliability and sustainability of the system performance and value stream income along the system lifetime.
- From the technical side, the system should be user friendly due to the targeted segment of developing economies end-users. This feature has to be validated with local case-study tests in target locations to ensure the common understanding of the user needs and knowledge level.
- Simple system architecture is a key for system reliability and robustness as it will have a major reflection on the complexity level of the system operation and maintenance (O & M) activities. Especially in off-grid locations where a highly complicated O & M activity is economically totally not feasible due to many factors which vary from one off-grid location to another even within the same country. Most of these conditions vary even on lower geographical levels as mentioned before. System architecture level of complexity will also have a major influence on one of the challenging aspects of off-grid systems which is logistics and system handling for remote areas. System logistics could be an under-estimated aspect in theoretical evaluations for off-grid electrical systems, this is due to the lack of practical experience in most of the research work done in this area so far. In practice logistics play a major role in the system deployment feasibility, and represents a main influencing factor on the off-grid systems economics.
- The other side of having a simple architecture system is taking into consideration the increase of system reliability and robustness. Such aspect is taken into

account to ensure the sustainability of the system performance on long-term perspective, which will have a major influence on the system economics. In addition, building the trust between the end-consumers and the OHRES is elementary in developing country markets. Such trust is highly needed in order to boost the deployment of off-grid solutions in such markets where there is a high demand for these solutions.

- Safety is an non-negotiable criteria for a system design, especially for electrical energy systems. Our system is taking such aspect into high consideration by paying high attention to the safety related aspects on both components and system level.

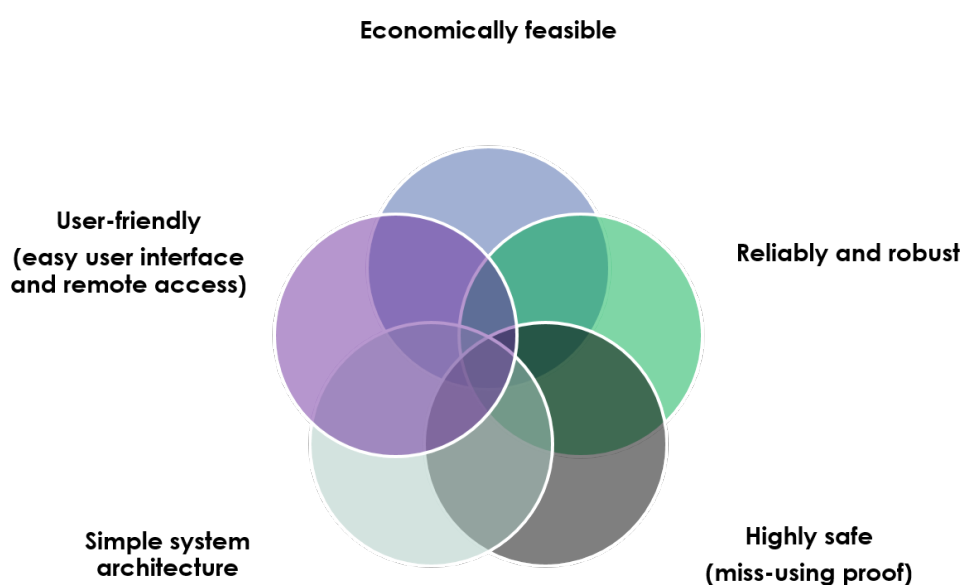


Figure 2.4: OHRES technical design main objective
Figure reference: Author’s illustration, published in [1].

2.2.2 Off-grid and decentralized Hybrid Renewable Electricity Systems (OHRES) layout

Our study focuses on Off-grid and decentralized Hybrid Renewable Electricity Systems (OHRES) aiming to participate in the global vision on ending energy poverty through increasing electrical energy access levels. OHRES (Off-grid and decentralized Hybrid Renewable Electricity Systems) allows the utilization of the location-based available renewable energy resources. It enables the integration of both fluctuating renewables (as Solar PV and Wind), and non-fluctuating renewable (as Biomass and small hydro-power) beside conventional electrical generation resources (as Diesel genets) into combined system design to reach the best possible economically feasible solution for electrical supply.

A hybrid electricity system in the context of this study is a system providing electrical energy to serve certain AC and DC loads based on six main interconnected system building blocks, falling under the following five main categories (as shown in figure 2.5):

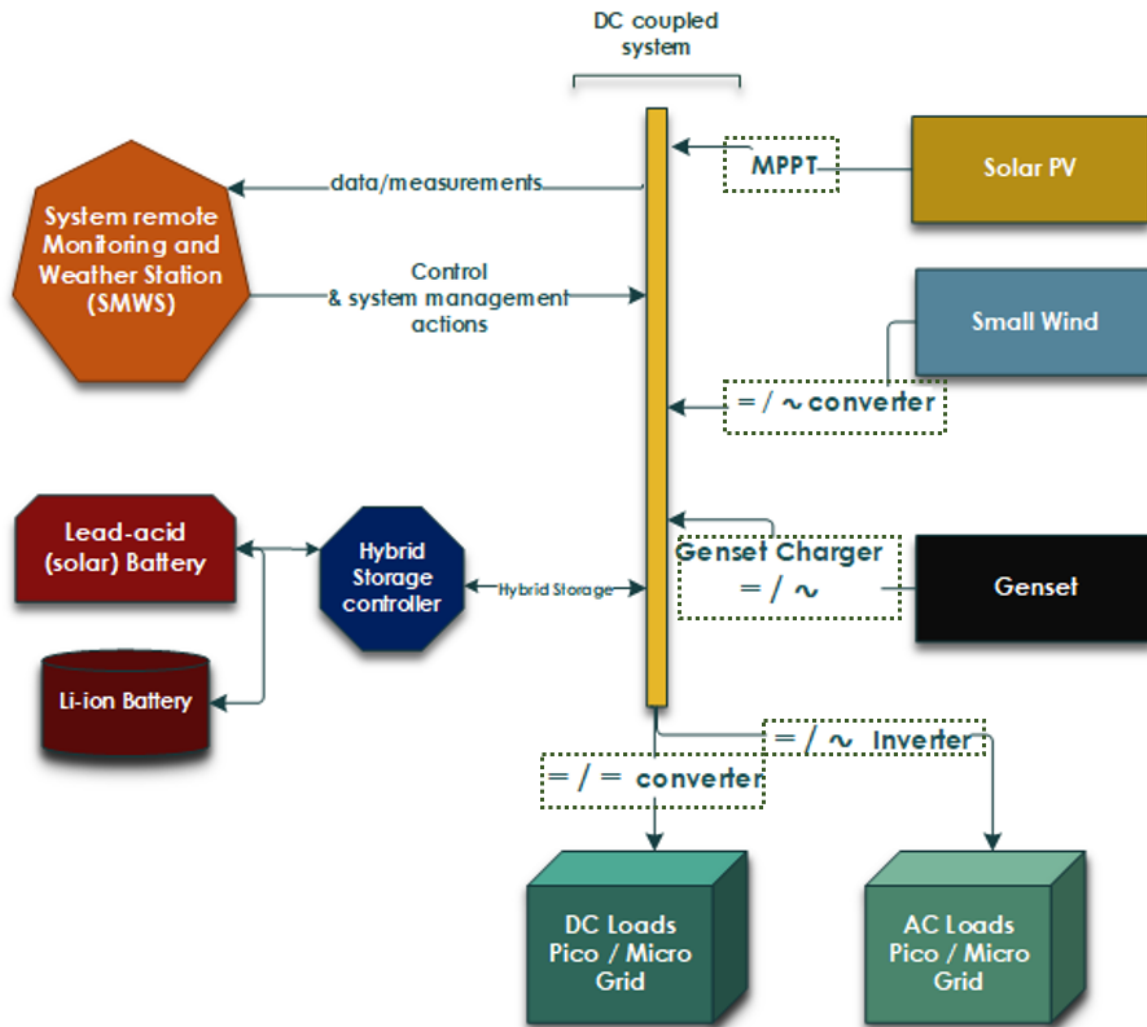


Figure 2.5: Off-grid Hybrid Renewable Electricity System (OHRES) layout.

Figure reference: Author's illustration, published in [1], [46], and [47].

1. Renewable energy resources, including mainly two renewable electrical energy sources:
 - a) Solar Photovoltaic (PV)
 - b) Wind Turbine (Small turbine in the range of 500 to 1.5 kW)
2. Non-Renewable energy resources, including one conventional electrical energy source:
 - a) Generator (Gasoline, or Dual-Fuel (gasoline and Propane) based Genset)

3. Energy storage, including a Hybrid Battery Storage System (HBSS) based on two main battery types:
 - a) Lead-acid AGM (absorbent glass mat) Solar Battery (Hoppecke SUN Power VR M 6-250 [48])
 - b) Lithium-ion LiFePO₄ (lithium iron phosphate) battery (BOS LE300 [49])
4. Electrical Loads, including two main load types:
 - a) AC loads
 - b) DC loads
5. System Monitoring and Weather Station (SMWS), including two main sets of monitoring and measurement parameters as shown in figures 4.1 and 4.2:
 - a) Renewable resources and weather measurement parameters including
 - i. Solar irradiance 1: Global Horizontal Irradiance (GHI)
 - ii. Solar irradiance 2: Plane of Array (POA)
 - iii. Wind speed (on 12 meters Hub height)
 - iv. Wind Direction (on 12 meters Hub height)
 - v. Ambient Temperature
 - vi. Relative Humidity
 - b) System operation monitoring parameters, which are mainly voltage and current measurements in selected positions for the following system parts
 - i. Solar PV
 - ii. Small wind turbine
 - iii. Genset
 - iv. Battery Storage (HBSS)
 - v. ACout 1: Main AC loads
 - vi. ACout 2: Excess of Electricity AC loads
 - vii. DC load: Main DC loads
 - viii. DC load: Excess of Electricity DC loads

All these system building blocks are interconnected through a 48V DC bus, which represents the backbone of the system components.

In the presented system structure, the lead-acid battery represents the highest portion of the storage capacity over the lithium-ion storage capacity. The lead-acid battery is responsible for covering the energy demand of the based loads and the daily energy use and loads spread over a long time period. On the other hand, lithium-ion storage is responsible for the load peaks that require fast responding time and high power. During the charging process, the battery management system (BMS) makes sure that the lead-acid gets fully charged first before the li-ion starts its charging routine. While discharging, the opposite process happens, the li-ion battery gets discharged first in

case it can cover the load power requirements then the lead-acid get discharged. In case of a high load power consumption, both batteries participate to supply the load requirements. The utilization of the main advantages of these two battery storage technologies and sizing them properly to cover a certain load curve demands for a decentralized off-grid residential application support overcoming the limitations of using each battery type alone, and represents very promising techno-economic benefits for OHRES.

2.2.3 System Voltage level selection using multi-criteria evaluation methodology

The evaluation is done with a focus on the system size fitting with our case-studies energy demands as clarified before in the corresponding section. The methodology used is a decision matrix where each of the system voltage levels is quantitatively evaluated against all of the nine selected factors of the evaluation criteria. The decision matrix includes two main sections. First the evaluation criteria section, where different evaluation factors are listed and a weight is given to each of these factors based on its importance to our system design on a scale from 1 (least important) to 10 (highly important). The second section is the system DC voltage levels selected to be evaluated, in the shown case there are four voltage levels 12V, 24V, 48V and 110V DC. Each of the voltage levels is evaluated against all of the evaluation criteria factors, and evaluation points are used from a scale from 1 (lowest) to 5 (Highest) based on the fulfillment of the evaluated voltage level to the evaluation factor.

Table 2.5 and figure 2.6 summarizes the quantitative assessment of system DC voltage level using decision matrix analysis.

Evaluation criteria and evaluated voltage levels selection

The selection of the evaluation criteria factors and the voltage levels to be evaluated is done based on various off-grid field experts recommendations collected through direct interviews for project-based practical experiences. Beyond these recommendations, only the 110V DC voltage level was included in the evaluation. The reason is that this voltage level is for some of our tested Li-ion battery modules which can have good potential to be used as a battery storage solution within an OHRES, and need to be investigated. The evaluation points are quantified taking into consideration the current off-grid market actualities. A total quantitative score is collected for each of the evaluated voltage levels, and the system which gains the highest score represents the one matches most of the evaluation criteria. The details of the evaluation are included in table 2.5. The 9 criteria aspects included in the voltage level evaluation are:

1. The reduction of system losses, which represents the potential of overall loss reduction in the system and is directly related to the need for using less current for higher voltages to fulfill certain system operation power demands as for battery charge and discharge), or fulfilling load power requirements. 2) Using Cheaper Cables with a small cross-section The electrical cable cross-section is sized based on the current flow planned in it. To fulfill certain power demands, the lower

Table 2.5: Decision making matrix for OHRES DC voltage level selection(published [1])

Evaluated system level DC voltages	12V DC		24V DC		48V DC		110V DC		
	Evaluation factor Weight 1-10 (a)	Evaluation points 1-5 (b)	Quantitative score (a*b)	Evaluation points 1-5	Quantitative score	Evaluation points 1-5	Quantitative score	Evaluation points 1-5	Quantitative score
Evaluation factor weighting criteria scale	1 = Least important 10 = Highly important								
Evaluation points criteria scale	1 = Lowest value 5 = Highest value								
Evaluation Criteria									
Reduction of system losses	10	1.5	15	3	30	4	40	5	50
Using of cheaper cables with small cross section	5	1	5	3	15	4	20	5	25
Validity of price competitive system components specially MPPT and inverters	8	2.5	20	5	40	5	40	0	0
Off-grid components can handle more power in the same product category	10	1.5	15	3	30	5	50	5	50
Availability of a range of commercial off-grid component in the voltage range	10	5	50	5	50	4	40	0	0
DC loads (speciality lighting) availability in the market	4	5	20	5	20	2.5	10	0	0
Compatibility with the currently used DC loads (specially lighting) in the off-grid applications	4	5	20	5	20	2.5	10		0
Compatibility with commonly used commercial available li-ion storage systems	9	2	18	2	18	5	45	5	45
Can take advantage of future trend of development for the storage market	6	2.5	15	2.5	15	4	24	5	30
Evaluation score			178		238		279		200

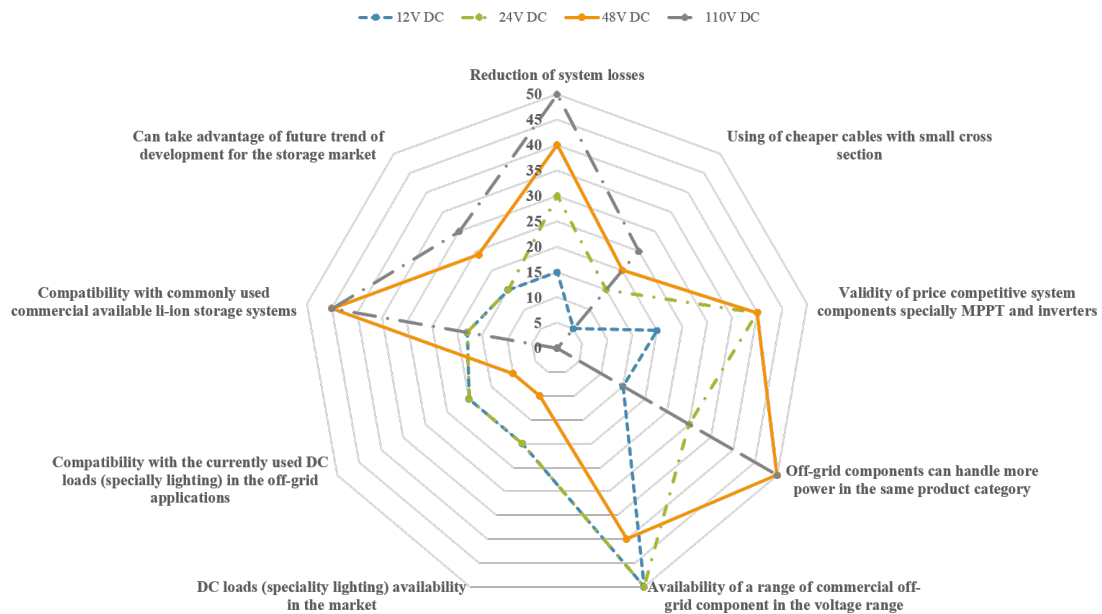


Figure 2.6: OHRES DC voltage level - Quantitative assessment results (Published [1]).

the voltage range used the higher the current range needed to pass through the cable to fulfill the power requirement. Using high voltage ranges will result in reducing the current needed to flow in the cable, which leads to using less cable cross-section and reducing the overall cost share of the electrical cable in the system design.

2. Validity of price-competitive system components, especially MPPT and inverters
The available components in the market that are used for DC bus based hybrid systems such as the system presented in our study, size and cost of the component is categorized according to two factors: The DC voltage range used, and the rated power required. For the 12, 24 and 48 volt range there are several available products to be used for hybrid systems in the market. However, for the 110-volt range, there were not available products oriented for OHRES available in the market at the time the study was done. Based on our market offers and price survey, the price gets more competitive with higher voltage ranges more than lower ranges.
3. Offgrid components can handle more power in the same product category
Another important criterion related to the voltage range of OHRES is that the different product categories from within a product family (MPPT or inverter/charger product family), can handle higher power requirements with higher voltage ranges. This is because the current is required to reduce for fulfilling a certain power demand. Hence, selecting a 12 V product will result in having less rated power than selecting a 48 V product in the same product category.
4. Availability of a range of commercial off-grid components in the voltage range
The availability of OHRES designed components in the market differs for the different voltage ranges and is an important criterion for our evaluation as our study has an applied research nature, and includes the development and installation of systems involving the use of state-of-the-art components available in the market. For the 12 V range, there is a huge variety of components available for the OHRES system, where on the other hand for the 110 V range there were no components available for this voltage range during the time of conducting our study.
5. DC load (particularly lighting) availability in the market
As the OHRES system design presented in the scope of this study is a DC bus coupled system, there is the possibility to use DC loads directly instead needing to involve a DC to AC inverter for supplying AC loads. Lighting is one of the major load types in the form of DC load. Lighting can be a very efficient load (especially LED DC lighting bulbs), however traditional or even LED AC lighting bulbs are less efficient, as there will be an internal AC to DC converter integrated even in the LED AC lighting bulb case, which shall reduce the overall bulb electrical efficiency.
6. Compatibility with the currently used DC loads (especially lighting) in the off-grid applications

This criteria is related to point number 6, as during our market survey we have seen that number of DC loads are not only available in the market by suppliers or manufacturers, but are also used by end-users (especially in developing countries as in our Uganda case study). DC load types such as DC TV, fridge, and radio are also available in different DC voltage ranges. However, based on our market survey it was determined that these types of DC loads mostly use the 24 V range and 12 V range, more than the 48 V range where only a few DC loads are available and used in the market. In the 110 V range, there was no DC load availability found in the market by the time of our study.

7. Compatibility with commonly used commercial available Li-ion storage systems

An important criterion for OHRES voltage level selection is the compatibility with available commercial Li-ion battery storage. As most of the newly designed and installed systems consider Li-ion storage (instead of the previous orientation of high dependability on Lead-acid battery storage), it is important in our selection to include such criteria. Based on our survey it was determined that high voltage Li-ion storage (in the range of 110 V) was available in the market. Also, there was a high focus toward 48 V Li-ion battery storage market availability and development for use applications in the residential and electro-mobility storage applications. The usage and availability of 12 V and 24 V Li-ion batteries did exist as well but not as high as in the other voltage ranges.

8. Can take advantage of the future trends of development for the storage market
This criteria point were selected taking into consideration three main aspects:

- a) The OHRES system scalability and future ability to extend the range of storage power used.
- b) The future need for battery storage replacement after the end of lifetime, which will be done according to the future storage cost in the market.
- c) In addition, taking benefit of the cost reduction due to the future market trends for developing Li-ion storage systems in certain voltage ranges which will have a positive effect on the overall future system economics.

Based on our market research it was determined that there is a clear trend toward developing 48 V Li-ion battery storage systems, especially to be used for electro-mobility applications. This will have a direct reflection on the overall storage Levelized cost for other applications as well as off-grid and residential ones. Also, the trends of using high voltage Li-ion battery storage range such as the 110 V and other range are highly predominant. For the lower voltage ranges such as 12 V and 24 V, the future trends were not that clear as for the other voltage ranges.

The evaluation outcome shows that the 48V DC system voltage level is the one matching best to the evaluation criteria compared to other voltage levels as shown in figure 2.6. It has been selected for the system technical design and products selection. The 24V DC which comes in the second place, followed by the 110V DC and the 12V DC system voltage has the least matching.

3 OHRES Techno-economic analysis and system size optimization

Chapter 3 is the second part related to the first building block of the study comprehensive methodological approach presented before in figure 1.3. This chapter covers the OHRES techno-economic assessment and system sizing related aspects in both Canada and Uganda case studies. Chapter 3 address the stages 3 and 4 of the hybrid systems development phase presented before in figure 1.2.

Chapter 3 includes four sections: The first section covers the OHRES techno-economic analysis and system sizing. Section 2 covers the Canada case study hybrid system techno-economic analysis and sizing. Section 3 covers the Uganda case study hybrid system techno-economic analysis and sizing. Section 4 highlights a techno-economic assessment for the hybrid battery storage system used in the hybrid off-grid system.

Part of the content of this chapter is based on the author's published work in Elkadragy et al. [5].

3.1 OHRES techno-economic analysis and system sizing

The techno-economic assessment and system component sizing for the hybrid system is one of the important project development phases as shown before in figure 1.2. HOMER Pro (Hybrid Optimization of Multiple Energy Resources) [50] was used as a techno-economic assessment and sizing tool. A case-study hybrid system model was constructed in HOMER Pro for each of the two locations. The HOMER Pro software by HOMER Energy is the global standard for optimizing microgrid design in all sectors, from village power and island utilities to grid-connected campuses and military bases. Originally developed at the National Renewable Energy Laboratory, and enhanced and distributed by HOMER Energy. Since its release, HOMER has been downloaded by over 250,000 people in 193 countries. This is a global community of pioneering practitioners in renewable and distributed power [50].

HOMER Pro techno-economic optimization is based on recommending the system architecture with the lowest Net Present Cost (NPC) over the system lifetime. Other economic indicators are used in selecting the most optimized system architecture such as the Levelized Cost of Electricity (LCOE) [51].

HOMER allows for many detailed inputs related to the system sizing from technical and economical perspectives. In this system analysis, we based our inputs and assumptions for the system sizing based on the following:

- Technical related inputs
 1. The Load survey done for each case study.
 2. The case study location (longitude and latitude) based on the site visits done, along with online mapping tools.
 3. Existing and planned position and orientation for the different hybrid system components such as Solar PV panels, small wind turbine, genset and load distribution.
 4. The system initial sizing HOMER renewable energy resources database [52] was used for solar, wind and temperature. In this study, there was no availability for onsite-measured reliable data for at least one year to use.
 5. Different system architectures were included in the analysis based on the system design scenarios to be investigated.
 6. Taking into consideration any existing system components that can be used in a newly designed system (as in the Canada case study).
- Economic related inputs
 1. Components costs were based on:
 - a) Offer prices for selected system components (which have been deployed in the Canada case study in later stage of the study).
 - b) In case of no price offer availability, HOMER default cost value was used.
 2. Discount and inflation rates are based on each case study's country-specific historical ranges provided by the World Bank data(Canada [53]& [54], and Uganda [55]& [56]), which have been validated through each case study end-user to replicate the remote location used rates.
 3. Project lifetime investigated 20 years

3.1.1 OHRES design layout scenarios

Different system layouts are investigated within the study, based on the selected technologies to be used and the candidate components. The diagram in figure 3.1 summarizes the eight different system design layout scenarios which are taken into consideration in the study scope. Each scenario includes different renewable or non-renewable electrical energy sources, combined with one of two battery storage options whether Li-ion battery storage only (mono storage) or hybrid lead-acid combined with Li-ion battery storage (Hybrid storage). The eight different system design layout scenarios are described in table 3.5. Only one of these scenarios is selected to be deployed in the case-studies in Uganda and Canada. The selection methodology is based on:

- i A techno-economic assessment using commercial system design and analysis tools for off-grid and decentralized systems as HOMER Energy Pro [50].
- ii The consideration of the multi-factor objectives described before and summarized in figure 2.4 into the investigated system design scenarios.

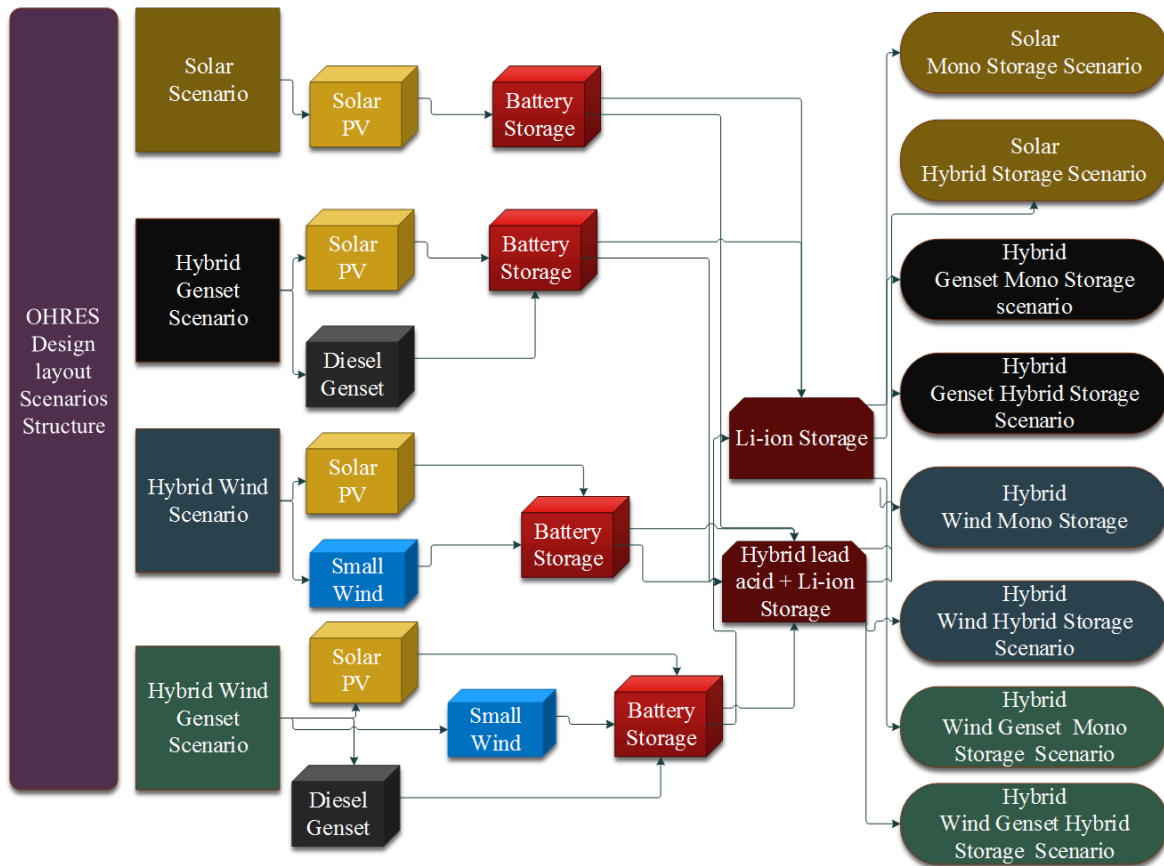


Figure 3.1: OHRES technical design layout scenarios
Figure reference: Author's illustration.

3.1.2 Hybrid battery storage modelling in HOMER

Different battery models are available in HOMER for lead-acid and Li-ion batteries. However, HOMER does not support including a direct hybrid battery storage model from its library. The modelling of our system hybrid battery storage system was challenging in HOMER, as it was needed to develop a custom-made model to integrate both battery types into one model representing a hybrid battery storage model. The development of the hybrid storage model in HOMER was done using the kinetic battery model in HOMER as a base for the hybrid battery storage modelling parameters. To provide the different needed parameters required for the HOMER kinetic battery model for the hybrid storage, an external hybrid battery storage modelling parameters calculation model was developed. The external model was used to calculate the required HOMER parameters using the manufacturer and the datasheet provided information for each of the used lead-acid (Hoppecke SUN Power VR M 6-250 [48]) and Li-ion (BOS LE300-LiFePO₄ [49]) batteries selected for our hybrid storage system. To make sure regarding our modelling approach in HOMER, an expert review was required. The external developed model was reviewed and verified by HOMER energy pro Head of Professional Services, Microgrids & Renewables through several arranged individual support and review meetings.

A hybrid battery storage model was developed in HOMER for the techno-economic

Table 3.1: OHRES different system design layout scenarios

OHRES design Layout scenario	Scenario structure description
S1: Solar-Mono Storage	Fully renewable electrical energy system based on the integration of solar PV as a renewable electrical energy source, with Li-ion battery storage to supply certain load demand based on the end-user load profile.
S2: Solar-Hybrid Storage	Similar to S1 with respect to the electrical energy sources used. However in S2 the battery storage consists of a Hybrid lead-acid combined with Li-ion storage.
S3: Hybrid Genset-Mono Storage	This system layout includes renewable and non-renewable electrical energy sources, which are the Solar PV and Genset respectively. Only Li-ion storage is used in this scenario.
S4: Hybrid Genset-Hybrid Storage	Similar to S3 with respect to the electrical energy sources used. However in S4 the battery storage consists of a Hybrid lead-acid combined with Li-ion storage.
S5: Hybrid Wind-Mono Storage	Wind energy as a renewable electrical energy source is included in this scenario in combination with solar PV. It is a fully renewable based scenario, including only Li-ion battery storage.
S6: Hybrid Wind-Hybrid Storage	Similar to S5 with respect to the electrical energy sources used. However in S6 the battery storage consists of a Hybrid lead-acid combined with Li-ion storage.
S7: Hybrid Wind Genset-Mono Storage	Wind and Solar PV are used as renewable electrical energy sources in this scenario. Combined with Genset as a non-renewable source. Storage is based on Li-ion battery storage
S8: Hybrid Wind Genset-Hybrid Storage	This scenario includes all system possible components. Wind and Solar PV represents the renewable electrical energy source. Genset is used as a non-renewable source. The system includes hybrid lead-acid and Li-ion battery storage.

assessment of our OHRES in both case study locations. The hybrid battery storage model represented two 6 Volts lead-acid batteries connected in series, and two 12 Volts li-ion batteries connected in parallel. This model configuration was selected based on the physical technical design of the hybrid battery storage in our hybrid system, to reflect a 12 Volt hybrid battery unit with a certain storage capacity, which can be used in a modular way to reach the needed system voltage level of 48 Volts and the required optimum storage usable capacity for our case studies. The parameters for

Table 3.2: Developed hybrid battery storage model parameters used in HOMER

Model Parameter	Value	Unit
Nominal voltage	12.00	Volt
Round trip efficiency	83.72	%
Minimum SoC	50.00	%
Maximum SoC	100.00	%
Initial SoC	100.00	%
Max charge current	70.00	Amp
Max discharge current	70.00	Amp
Nominal capacity	340.69	Ah
Float life	6.00	Years
Energy model	Kinetic Model	
Storage type	Battery	
Chemistry	Lead-acid and Li-ion	
String size	1	
Capital cost	766.00	Euro
Replacement Cost	766.00	Euro

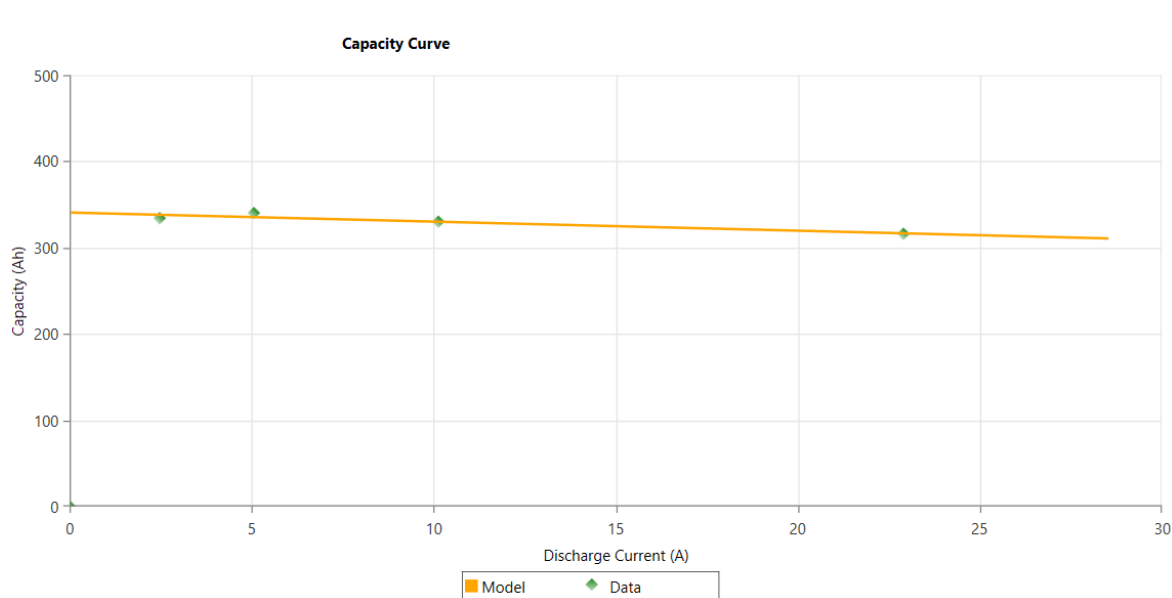


Figure 3.2: Capacity curve for the hybrid battery model in HOMER
 Figure reference: Hybrid battery storage developed model in HOMER [50].

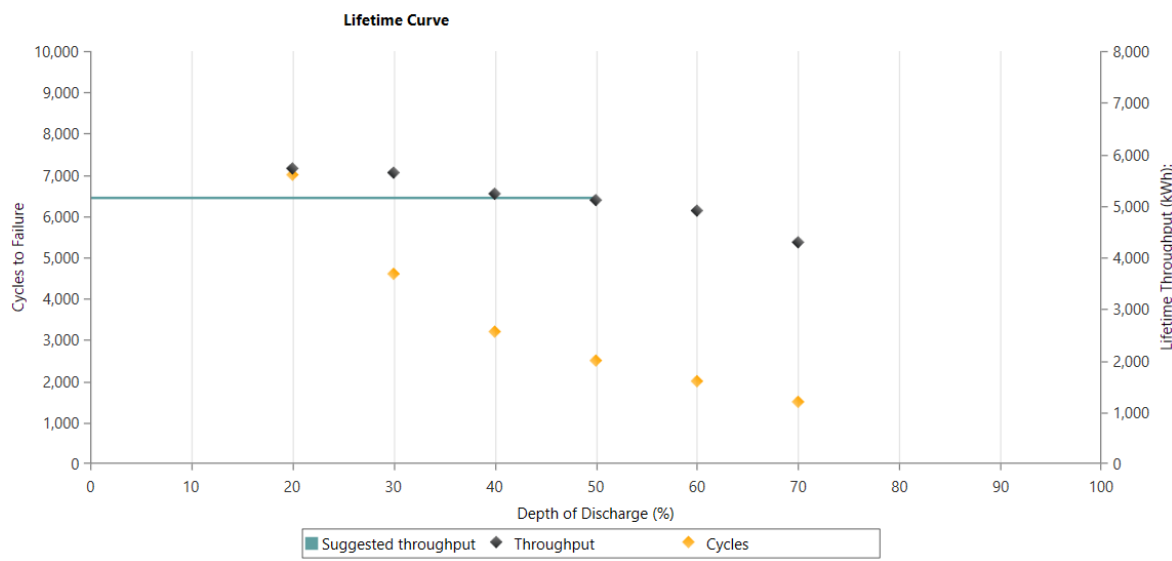


Figure 3.3: Lifetime curve for the hybrid battery model in HOMER.
 Figure reference: Hybrid battery storage developed model in HOMER. Source:
 Hybrid battery storage model details in HOMER Energy Pro [50].

the hybrid battery storage model developed which is used in HOMER are presented in table 3.2. Figure 3.2 presents the capacity curve for the hybrid battery model, which is the relation between the discharge current and the available storage capacity.

A lifetime curve for the hybrid battery model is represented in figure 3.3, which shows the depth of discharge versus the number of cycles to failure and the lifetime throughput storage energy.

The developed hybrid battery storage model in HOMER was utilized for the hybrid system modeling and techno-economic assessment for both case studies in Canada and Uganda.

3.2 Canada Case-study hybrid system techno-economic analysis and sizing

To reach the presented stage of the detailed techno-economic modelling for the Canada system, many models were investigated for each of the presented system components and the overall system architecture. Along with the presented system components here, many other components were modeled and investigated as potential to be used for the system. The presented model represents the selected shortlisted components for the system's final design. The final selected components from this analysis are already used in the system installation in the Canada case study. The techno-economic modelling in HOMER for the Canada case study took into consideration the existing system components, which can be utilized in any system upgrade.

The hybrid system modelling scheme presented in figure 3.4 represents a techno-economic assessment model used in HOMER for the different design scenarios and system architectures as illustrated before in figure 3.1. The used models in HOMER

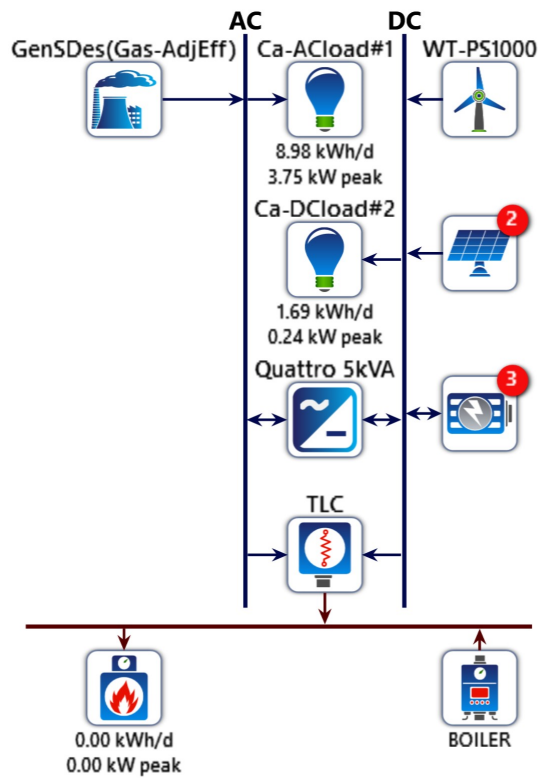


Figure 3.4: Canada case-study hybrid system modelling scheme in HOMER
 Figure reference: Canada Case study modelling in HOMER [50].

shown in figure 3.4 and its related parameter for each of the system components are described below. The assessment also includes some additional investigation aspects and sensitivity analysis factors.

Solar PV modelling: Two solar PV models are included in the HOMER system modelling.

- i PV1: Existing PV array
- ii PV2: Additional PV array

HOMER technical information summary for the used models:

- i PV1: Existing PV array
 - Rated single PV module capacity 0.220 kWp
 - Efficiency 12.5%
 - Lifetime: 25 years
 - Search space for sizing optimization: 1.32 kWp
- ii PV2: Additional PV array
 - Rated single PV module

- Rated single PV module capacity 0.320 kWp
- Efficiency 13 %
- Lifetime: 25 years
- Search space for sizing optimization: 0 or 1.92 kWp

Modelling used Abbreviation:

- i BP 3220T
- ii Sunprism 320W

Wind Turbine Modelling: One small vertical access wind turbine model is included in HOMER system modelling.

HOMER technical information summary for the used model:

- Rated capacity: 1.0 kW
- Hub height: 13 m
- Lifetime: 10 years
- Search space quantity of wind turbines: 0 and 1 (wind turbines)

Modelling used Abbreviation: WT-PS1000

Generator Modelling: One gasoline genset is included in HOMER system modelling (Gasoline fuel is more preferred than diesel fuel by case study end-user).

HOMER technical information summary for the used model:

- Minimum load ratio: 25%
- Lifetime: 15000 hours
- Search space for sizing optimization: 0, 2, 2.5, 3 or 3.5 kW

Modelling used Abbreviation: GenSDes(Gas-AdjEff)

Storage modelling: Three storage models are included in the HOMER system model.

- i Hybrid lead-acid and Li-ion
- ii Li-ion battery storage
- iii Lead-acid battery storage

HOMER technical information summary for the used models:

- i Hybrid lead-acid and Li-ion
 - Nominal capacity: 4.09 kWh

- Initial state of charge: 100%
- Minimum state of charge: 50%
- String size: 1
- Search space: 0 to 4 strings

ii Li-ion

- Nominal capacity: 1.02 kWh
- Initial state of charge: 95%
- Minimum state of charge: 10%

iii Lead-acid

- Nominal capacity: 1.03 kWh
- Initial state of charge: 100%
- Minimum state of charge: 50%
- String size: 1
- Search space: 0 to 16 strings

Modelling used Abbreviation:

i HS 2LA S - 2LI P (f-EUP)

ii LI ASM-EUP

iii LA ASM-EUP

AC load Modelling: AC load profile based on load survey for the Canada case study is used in the system modelling in HOMER.

HOMER technical information summary:

- Day to day variability: 20%
- Timestep variability: 20%
- Peak load: 3.75 kW

Modelling used Abbreviation: Ca-ACload#1

DC load Modelling: DC load profile based on load survey for the Canada case study is used in the system modelling in HOMER.

HOMER technical information summary:

- Day to day variability: 20%
- Timestep variability: 20%
- Peak load: 0.24 kW

Modelling used Abbreviation: Ca-DCload#2

Inverter/Charger Modelling: One DC/AC inverter - charger model is included in HOMER system modelling.

HOMER technical information summary for the used model:

- Lifetime: 15 years
- Efficiency: 95%
- AC generator input: active
- Search space size: 4 kW

Modelling used Abbreviation: Quattro 5kVA

Excess of energy load: Excess of energy (dump) load is modelled through the Thermal Load Controller (TCL), the Boiler, and the Thermal load.

HOMER technical information summary:

- Thermal load: blank
- Boiler efficiency: 85%

Modelling used Abbreviation: TLC , BOILER, Thermal Load#1

3.2.1 Canada case study techno-economic modelling and assessment results

The techno-economic analysis in HOMER included selected sensitivity variables as shown in table 3.3. The selected sensitivity variables are of importance to see their influence and to have a complete understating of the different hybrid system architectures. The range of the sensitivity parameters was selected based on the inputs from the case study end-user and the site surveying. Six sensitivity variables were selected which are:

- Fuel price (Gasoline)
- The AC load average energy consumption per day
- Allowed capacity shortage
- Nominal discount rate
- PV array 1 and 2 azimuth
- PV array 1 and 2 slope

The sensitivity analysis resulted has many important conclusions related to the optimal system architecture, some of which were selected to be further explained.

Table 3.3: Canada case study techno-economic modelling and assessment sensitivity analysis parameters

Fuel Gasoline price (€/L)	AC load average (kWh/day)	Capacity shortage (%)	Nominal discount rate (%)	PV array 1 (BP 3220T) existing Azimuth (°)	PV array 1 (BP 3220T) existing Slope (°)	PV array 2 (Sun-prism 320W) additional Azimuth (°)	PV array 2 (Sun-prism 320W) additional Slope (°)
1.5	8.98	1	10	0 (south orientation)	45	0 (south orientation)	45
2	4.5	10	8	90 (west orientation)	90	-90 (east orientation)	90
2.25			7				
2.5			3				
3							

PV arrays orientation

The first conclusion based on the overall results was related to the PV azimuth and orientation. It was observed that under the majority of sensitivity cases that for both PV arrays 1 and 2 Azimuth 0° and Slope 45° results in the lowest COE (€/kWh) and NPC (€).

Figure 3.5 shows a sensitivity case for the effect of the PV azimuth and orientation on the COE. The sensitivity analysis was done under the following conditions for the other sensitivity variables:

- AC load average: 8.98 kWh/d
- Capacity shortage: 1 %
- Nominal discount rate: 7%
- Gasoline price : 2 (€/L)

The graphs shows that the COE ranges between 0.784 and 0.935 (€/kWh). The lowest COE achieved when both PV arrays 1 and 2 Azimuth: 0° and Slope: 45°.

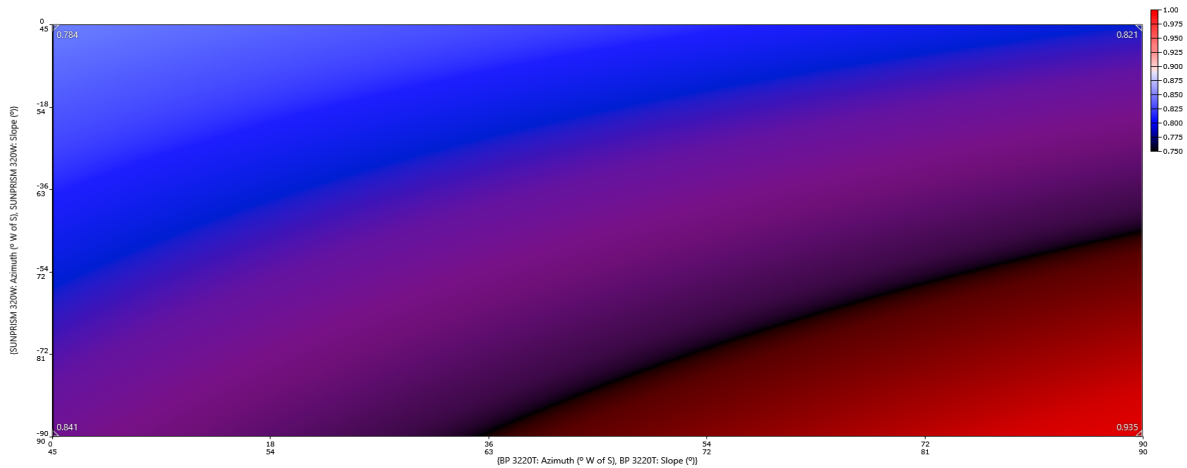


Figure 3.5: Sensitivity analysis: Effect of the PV azimuth and orientation on the COE for Canada case study hybrid system

Figure reference: Canada Case-study techno-economic modelling and analysis in HOMER [50].

Capacity shortage

The capacity shortage change does not affect the NPC, COE, and selected system architecture. The sensitivity case shown in figure 3.6 shows that there is no effect on the capacity shortage change range on the COE. The graph shows the capacity shortage on the x-axis and the nominal discount rate on the y-axis. The COE (€/kWh) is the value points shown on the graph. Due to that the minimum amount of capacity shortage 1% was fixed among evaluating the effect of other sensitivity variables with higher impact (as the nominal discount rate and fuel price).

The sensitivity analysis was done under the following conditions for the other sensitivity variables:

- AC load average: 8.98 kWh/d
- Gasoline price: 2 (€/L)
- PV 1 and 2 azimuth: 0°
- PV 1 and 2 slope: 45°

AC load average energy per day

The sensitivity of the COE to changing the AC load average energy (kWh/d) is illustrated in the sensitivity case presented in figure 3.7, where the effect of the changing range can be seen. The x-axis presents the AC load average energy (kWh/d), and the nominal discount rate (%) is on the y-axis. The sensitivity analysis was done under the following conditions for the other sensitivity variables:

- Capacity shortage: 1 %

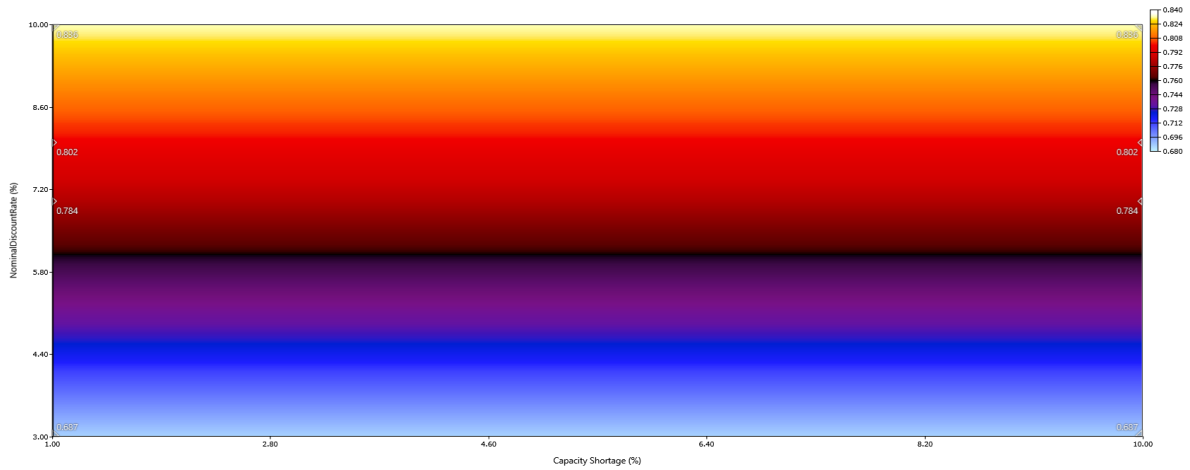


Figure 3.6: Sensitivity analysis: Effect of capacity shortage changes on the COE for Canada case study hybrid system

Figure reference: Canada Case-study techno-economic modelling and analysis in HOMER [50].

- Gasoline price: 2 (€/L)
- PV 1 and 2 azimuth: 0°
- PV 1 and 2 slope: 45°

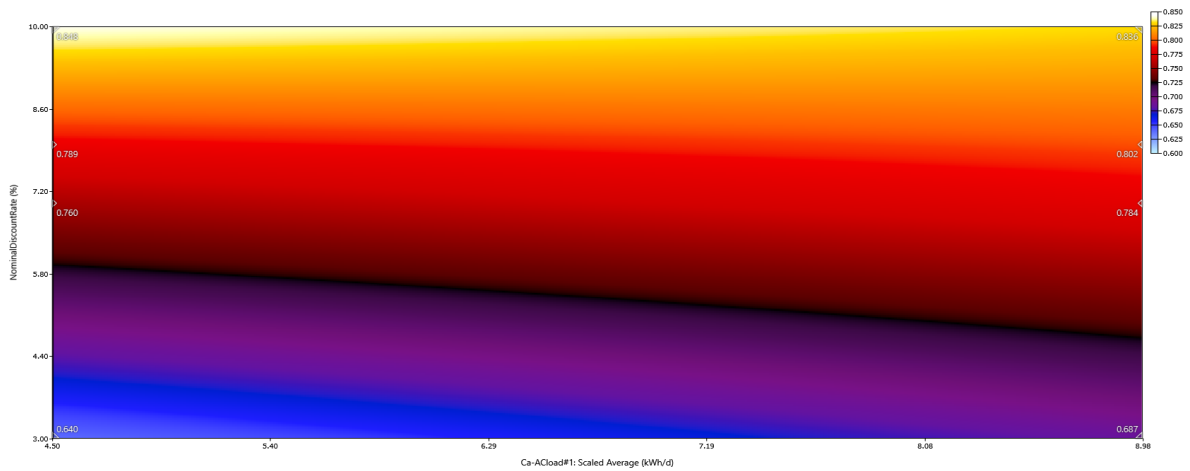


Figure 3.7: Sensitivity analysis: Effect of AC load average energy changes on the COE for Canada case study hybrid system

Figure reference: Canada Case-study techno-economic modelling and analysis in HOMER [50].

As can be seen from the graph, in certain nominal discount rates such as 7%, the change in the COE due to the effect of varying the AC load average daily energy is very minimal at 0.024 (€/kWh). The AC load daily average was considered at the worst-case consumption scenario of 8.98 kWh/d in the further sensitivity analysis cases. It is important to mention as well that the DC load average daily energy consumption was

not included as a sensitivity variable due to its very low participation in the overall load consumption compared to the AC load in the case study, which leads to having almost no effect on the system economic in case of DC loads average daily energy changes.

Canada case study system architecture sensitivity analysis

Figure 3.8 illustrates the effect of changing the nominal discount rate and the fuel price on the hybrid system architecture optimization. On the x-axis the nominal discount rate (%) varies between the defined range from 3 to 10 %. On the y-axis the fuel (gasoline) price varies between 1.5 to 3 (€/L). Other sensitivity variables are kept constant at selected values:

- AC load average: 8.98 kWh/d
- Capacity shortage: 1 %
- PV array 1 and 2 azimuth: 0°
- PV array 1 and 2 slop: 45°

The graph includes four main color areas, which represent four system architectures. The components included in the different system architectures are summarized in table 3.4.

Table 3.4: Canada case study techno-economic modelling and sensitivity analysis system architectures components

Hybrid system architecture color	Gasoline Genset	PV array 1	PV array 2	Li-ion battery storage	Lead-acid battery storage	Hybrid battery storage	Small wind turbine
Green system	Included	Included	Included	Included			Included
Red system	Included	Included	Included	Included			
Black system	Included	Included	Included			Included	
Blue system	Included	Included	Included			Included	Included

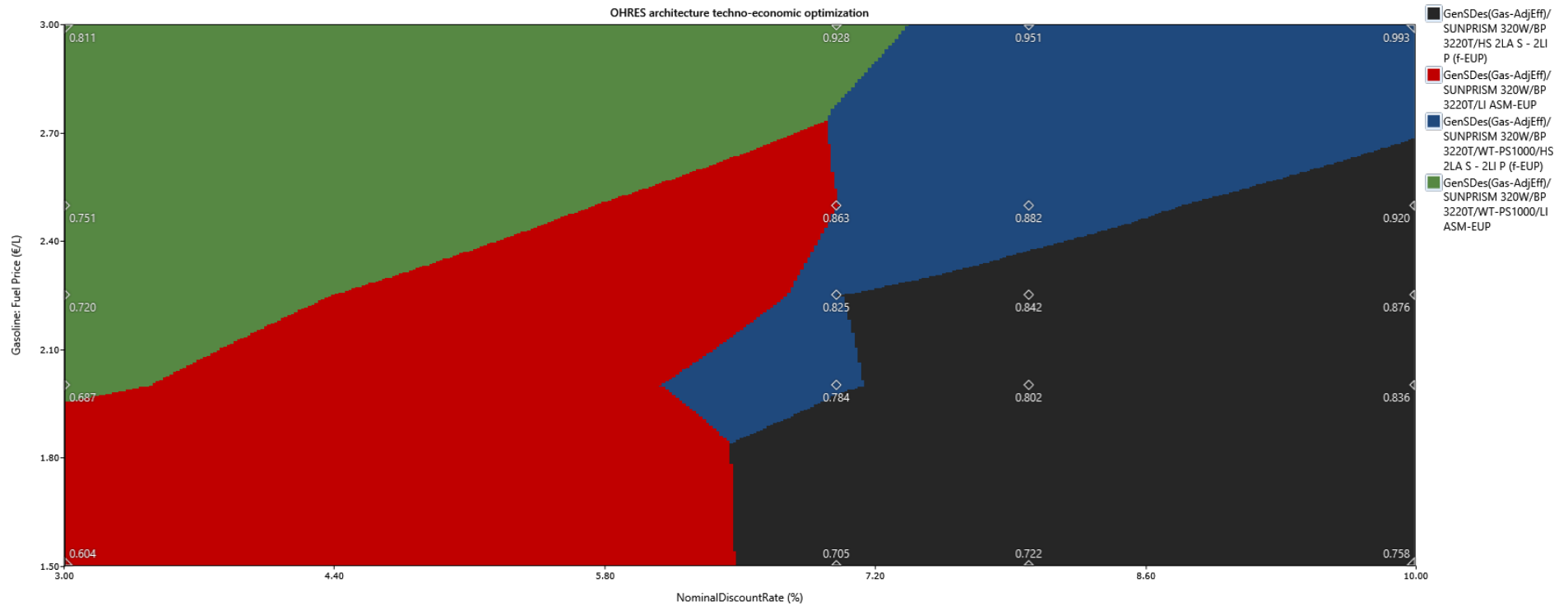


Figure 3.8: Canada case study sensitivity analysis: effect of changing the nominal discount rate and the fuel price on the hybrid system architecture optimization

Figure reference: Canada Case-study techno-economic modelling and analysis in HOMER [50].

It is clear from the OHRES optimization sensitivity analysis presented that the selected system architecture is highly dependent on the nominal discount rate and the fuel price. As seen on the graph the white dots represent the COE, which varies depending on the nominal discount rate and the fuel price from 0.604 to 0.993 €/kWh. There are wide areas of intersection between the different system architectures, which makes favoring one system architecture over another based on the lowest COE difficult, for example at a nominal discount rate of 7% and a fuel price of 2.5 €/L, both red and blue systems have almost the same COE of 0.863 €/kWh. However, the main conclusion regarding the favorable components to be used in the hybrid system can be driven by this analysis. For fuel prices higher than about 1.8 €/L including the small wind turbine becomes economically feasible in the hybrid system architecture along with a wide range of nominal discount rates as in the green and blue areas. Using a hybrid battery storage system represents the favorable economic selection for the hybrid system starting from about a 6.5% nominal discount rate and above, along with a wide range of fuel prices. Starting from about a 7.5% nominal discount rate, using a hybrid storage system is the most favorable selection along with a wide range of fuel prices. The usage of lead-acid storage systems is not presented on the graph under any sensitivity values, which means that it is more economically favorable to use whether Li-ion storage or Hybrid storage system is used.

This highlights a major conclusion that the system architecture selected should take into consideration the possibility of integrating a small wind turbine along with the usage of a hybrid battery storage system.

Canada case study selected system architecture

As clarified before in the sensitivity analysis, favoring only one system architecture over the other was not simple. Nevertheless, based on the sensitivity analysis conclusions the following criteria were selected for evaluating a winning system architecture:










- Winning System Architecture**
-  **HOMER Cycle Charging**
 -  **GenSDes(Gas-AdjEff) - 3.50 kW**
 -  **SUNPRISM 320W - 1.92 kW**
 -  **BP 3220T - 1.32 kW**
 -  **HS 2LA S - 2LI P (f-EUP) - 4.00**
 -  **Quattro 5kVA - 4.00 kW**
 -  **WT-PS1000 - 1.00**
 -  **TLC - 1,000 kW**
 -  **BOILER**

Figure 3.9: Canada case study Winning system architecture
 Figure reference: Canada Case-study techno-economic modelling and analysis in HOMER [50].

Table 3.5: Canada case study techno-economic modelling and assessment sensitivity analysis parameters

Variable	Selected value	Reason for selection
PV orientation	Azimuth: 0° (Meaning south orientation), Slope: 45°	Based on the sensitivity analysis results explained before
Nominal discount rate	7%	Based on the average nominal discount rate used in Canada, as explained before from the world bank data [53]
Capacity shortage	1%	Based on the sensitivity analysis results explained before
Gasoline fuel price	2 €/L	Average end-used price based on a total fuel ownership cost analysis done together with the Canada case-study end-user
AC load scaled average	8.98 kWh/d	Based on the sensitivity analysis results explained before

Under the selected variables, the analysis results based on the techno-economic model for the hybrid system are presented in figure 3.9. The figure shows the most techno-economic optimized system architecture (Winning system architecture).

The Winning system architecture is based on a hybrid system configuration including:

- Gasoline genset with a nominal capacity of 3.5kW.
- Two PV arrays.
- Existing PV array with an installed capacity of 1.32 kWp.
- New PV array with an installed capacity of 1.92 kWp.
- Hybrid lead-acid & Li-ion battery storage: Four strings with a total installed nominal capacity of 16.4 kWh and usable capacity of 8.18 kWh.
- Inverter charger 5 kVA.
- Small wind turbine: Rated capacity 1kW.
- Excess of energy (dump load): Represented through the thermal load controller (TLC) and the Boiler.

The net present cost (NPC) of the winning system architecture is 38381.70 €, and the COE is 0.784 €/kWh.

Base case comparison

A base case modelling the old previously existing system architecture in Canada is presented in figure 3.10. The base case model includes:

- Gasoline Genset with a nominal capacity of 2 kW
- One PV array: Existing PV array with an installed capacity of 1.32 kWp
- Lead-acid battery storage: total installed capacity 16 kWh
- Inverter charger 4 kW
- Excess of energy (dump load): Represented through the thermal load controller (TLC) and the Boiler.

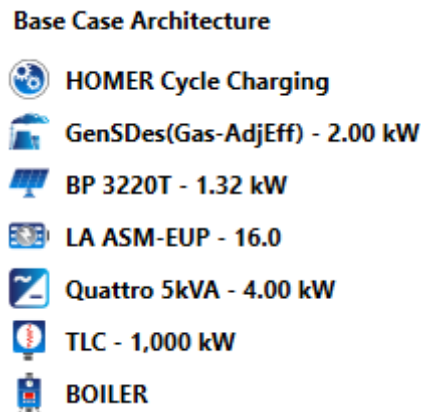


Figure 3.10: Base case modelling system architecture for Canada case study
Figure reference: Canada Case-study techno-economic modelling and analysis in HOMER [50].

The cost of electricity for the base case is 1.09 €/kWh which is 0.30 €/kWh higher than the winning architecture.

3.2.2 Canada case-study techno-economic re-assessment using measured renewable resources data

A second round of techno-economic re-assessment for the Canada case study was done at a late stage of the project. This re-assessment was not doable in earlier stages of the project as it was done using one year of measured solar and wind data, which was not available before the weather station and OHRES installation on site. For this re-assessment, one year of measured data was used, replacing the HOMER default database. Solar global horizontal irradiance (GHI) and wind measurement data from the installed weather station were used in HOMER. The data has a one-minute resolution and was measured through the weather station located at the Canada case study location through solar irradiance and wind speed sensors. The solar irradiance sensor

is measuring the GHI, and the wind sensor is located at a hub height of 13 meters above ground level.

Table 3.6 shows major differences between the two data sets in the annual averages.

Table 3.6: Major differences between the two data sets for the Canada case study in the annual averages

	Annual Average based on HOMER database	The annual average for measured data
Solar annual average (kWh/mm ² /day)	3.47	3.11
Wind annual average (m/s)	3.98	1.46

The same system architecture scenarios were investigated using the weather station solar and wind data, as in the earlier techno-economic assessment. Besides, the same sensitivity variables and ranges were included.

Canada case study re-assessment system architecture optimization

Table 3.7: Canada case study re-assessment sensitivity analysis system architecture components

Hybrid system architecture color	Gasoline Genset	PV array 1	PV array 2	Li-ion battery storage	Lead-acid battery storage	Hybrid battery storage	Small wind turbine
Red system	Included	Included	Included	Included			
Black system	Included	Included	Included			Included	

The system architecture sensitivity analysis results using the weather station measurement data is shown in figure. The following points will illustrate the main differences found between the currently presented techno-economic re-assessment, and the first techno-economic assessment using the HOMER database for the Canada case study:

- As can be seen, there are two system architectures (the red and black) included in the sensitivity results, instead of four as in the first techno-economic assessment shown in figure 3.12. Table 3.7 summarizes the components included in each system architecture.

- All scenarios including a small wind turbine were excluded as economically feasible system architecture. This is mainly due to the low wind speed measured on-site at the selected hub height.
- The currently presented COE varies from 0.672 to 1.104 €/kWh, while in the first techno-economic assessment the COE range was from 0.604 to 0.993 €/kWh.

Canada case study re-assessment selected system architecture

Under similar selected variables in the first techno-economic assessment, the result of the winning system architecture in the re-assessment included the following components as shown in figure 3.11:

- Gasoline genset with a nominal capacity of 2.5kW
- Two PV arrays
 - Existing PV array with an installed capacity of 1.32 kWp
 - New PV array with an installed capacity of 1.92 kWp
- Hybrid lead-acid & Li-ion battery storage: Four strings with a total installed nominal capacity of 16.4 kWh and usable capacity of 8.18 kWh
- Inverter charger 4 kW
- Excess of energy (dump load): Represented through the thermal load controller (TLC) and the Boiler.



Figure 3.11: Canada case study re-assessment winning system architecture
Source: Canada case-study techno-economic modelling and analysis in HOMER Energy Pro

The COE of the currently presented winning system is 0.859 (€/kWh), which is higher compared to 0.784 (€/kWh) for the first assessment winning system architecture.

Main conclusion based on the techno-economic reassessment results

- i For the hybrid system architecture, including a small wind turbine, as in the case of the first assessment winning system architecture, increases the current COE to 0.899 (€/kWh).
- ii The use of a small wind turbine at the selected hub height of 13 meters has to be re-considered as it can represent an infeasible techno-economic component in the hybrid system.
- iii Consideration of further wind speed measurement campaigns on higher hub heights could enhance the economics of the whole hybrid system and lower the COE if a small wind turbine represents an economically attractive part of the hybrid system.
- iv Including a hybrid battery storage system in the system architecture still represents the most economically feasible solution.

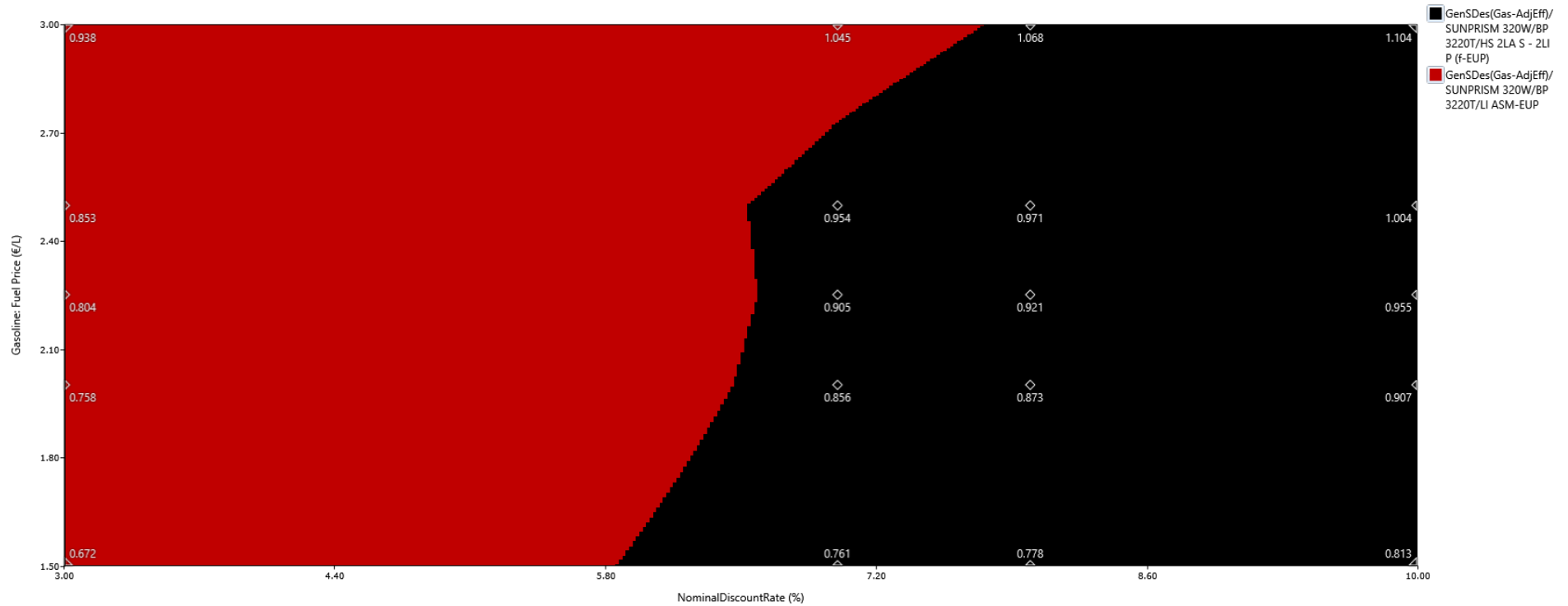


Figure 3.12: Canada case study re-assessment sensitivity analysis: effect of changing the nominal discount rate and the fuel price on the hybrid system architecture optimization

Figure reference: Canada Case-study techno-economic modelling and analysis in HOMER [50].

3.3 Uganda case-study hybrid system techno-economic assessment and system size optimization

This section will highlight some major points related to the techno-economic analysis and hybrid system sizing using HOMER for the Uganda case study. A similar analysis process as described before in the Canada case study was applied to the Uganda case study in order to reach a techno-economic optimized system architecture. The techno-economic modelling in HOMER for the Uganda case study took into consideration the inputs gathered during the site surveys to the system installation location (School). This includes:

- Limitations on the space available for the solar PV panel installation on the main building rooftop.
- PV panels orientation: south – east (-30°), due to rooftop orientation.
- The possible slope for local PV stands, minimum of 10° .
- Installation hub height for a small wind turbine of 13 m.

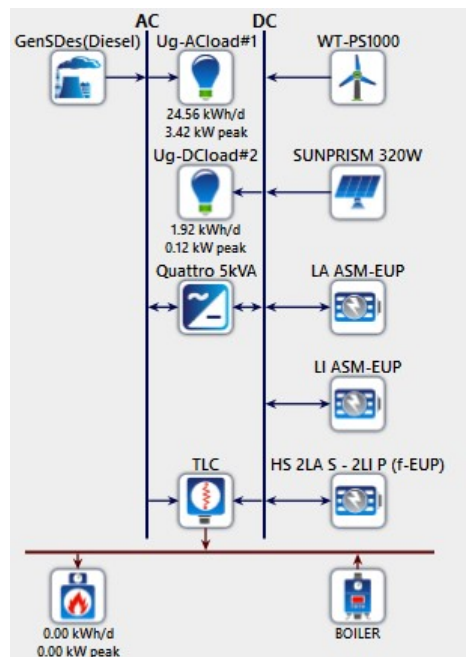


Figure 3.13: Uganda case-study hybrid system modelling scheme in HOMER
Figure reference: Uganda Case-study modelling in HOMER [50].

The hybrid system modelling scheme presented in figure 3.13 represents a techno-economic assessment for the different design scenarios and system architectures. The assessment also included some additional investigation aspects and sensitivity analysis factors as in the Canada case study.

Solar PV modelling: One solar PV model is included in the HOMER system modelling.

HOMER technical information summary for the used model - PV1: Solar PV array

- Rated single PV module capacity 0.320 kWp
- Efficiency 13 %
- Lifetime: 25 years
- Search space for sizing optimization: 0 or 3.84 kWp

Modelling used Abbreviation: Sunprism 320W

Wind Turbine Modelling: One small vertical access wind turbine model is included in HOMER system modelling.

HOMER technical information summary for the used model:

- Rated capacity: 1.0 kW
- Hub height: 13 m
- Lifetime: 10 years
- Search space quantity of wind turbines: 0 and 1 (wind turbines)

Modelling used Abbreviation: WT-PS1000

Generator Modelling: One Diesel genset is included in HOMER system modelling.

HOMER technical information summary for the used model:

- Minimum load ratio: 25%
- Lifetime: 15000 hours
- Search space for sizing optimization: 0, 2, 2.5, 3 or 3.5 kW

Modelling used Abbreviation: GenSDes(Diesel)

Storage modelling: Three storage models are included in the HOMER system model.

- i Hybrid lead-acid and Li-ion
- ii Li-ion battery storage
- iii Lead-acid battery storage

HOMER technical information summary for the used models:

- i Hybrid lead-acid and Li-ion
 - Nominal capacity: 4.09 kWh

- Initial state of charge: 100%
- Minimum state of charge: 50%
- String size: 1
- Search space: 0 to 4 strings

ii Li-ion

- Nominal capacity: 1.02 kWh
- Initial state of charge: 95%
- Minimum state of charge: 10%

iii Lead-acid

- Nominal capacity: 1.03 kWh
- Initial state of charge: 100%
- Minimum state of charge: 50%
- String size: 1
- Search space: 0 to 16 strings

Modelling used Abbreviation:

i HS 2LA S - 2LI P (f-EUP)

ii LI ASM-EUP

iii LA ASM-EUP

AC load Modelling: AC load profile based on load survey for the Uganda case study is used in the system modelling in HOMER.

HOMER technical information summary:

- Day to day variability: 10%
- Timestep variability: 10%
- Peak load: 3.42 kW

Modelling used Abbreviation: Ug-ACload#1

DC load Modelling: DC load profile based on load survey for the Uganda case study is used in the system modelling in HOMER.

HOMER technical information summary:

- Day to day variability: 10%
- Timestep variability: 10%
- Peak load: 0.12 kW

Modelling used Abbreviation: Ug-DCload#2

Inverter/Charger Modelling: One DC/AC inverter - charger model is included in HOMER system modelling.

HOMER technical information summary for the used model:

- Lifetime: 15 years
- Efficiency: 95%
- AC generator input: active
- Search space size: 4 kW

Modelling used Abbreviation: Quattro 5kVA

Excess of energy load: Excess of energy (dump) load is modelled through the Thermal Load Controller (TCL), the Boiler, and the Thermal load.

HOMER technical information summary:

- Thermal load: blank
- Boiler efficiency: 85%

Modelling used Abbreviation: TLC , BOILER, Thermal Load#1

Uganda case study system architecture sensitivity analysis

As in the Canada case study, selected sensitivity variables were investigated in the Uganda case study techno-economic assessment to reach the economically optimized system size and architecture. Table 3.8 summarizes the sensitivity variable ranges for the four sensitivity variables:

- Fuel price (Diesel)
- Allowed capacity shortage
- Nominal discount rate
- PV array slope

Figure 3.14 illustrates the effect of changing the nominal discount rate and the diesel fuel price on the hybrid system architecture optimization. On the x-axis, the nominal discount rate (%) varies between the defined range from 5 to 20 %. On the y-axis, the fuel (gasoline) price varies between 1.25 to 3 (€/L). Other sensitivity variables are kept constant at selected values:

- Capacity shortage: 1 %
- PV array Slop: 10°

Table 3.8: Uganda case study techno-economic modelling and assessment sensitivity analysis parameters

Fuel Diesel price (€/L)	Capacity shortage (%)	Nominal discount rate (%)	PV array (Sun-prism 320W) existing Slope (°)
1.5	1	20	10
2	10	15	20
2.25		10	
2.5		5	
3			

Table 3.9: Uganda case study techno-economic assessment results - system architecture components

Hybrid system architecture color	Diesel Genset	PV array	Li-ion battery storage	Lead-acid battery storage	Hybrid battery storage	Small wind turbine
Green system	Included	Included	Included			Included
Orange system	Included	Included		Included		
Black system	Included	Included			Included	
Blue system	Included	Included			Included	Included

The graph includes four main color areas, which represent four system architectures. The components included in the different system architectures are summarized in table 3.9

It is clear from the OHRES optimization sensitivity analysis presented that the selected system architecture is highly dependent on the nominal discount rate and the fuel price. As seen on the graph the white dots represent the COE, which varies depending on the nominal discount rate and the fuel price from 0.495 to 0.934 €/kWh. As can be seen, there are wide areas of intersection between the different system architectures, which makes favoring one system architecture over another based on the lowest COE difficult. However, the main conclusion regarding the favorable components to be used in the hybrid system can be driven by this analysis. For fuel prices higher than about 2 €/L and a discount rate of 15 % or higher, including the small wind turbine becomes economically feasible in the hybrid system architecture as represented by the blue system area in the graph. Using a hybrid battery storage system represents the favorable economic selection for the hybrid system starting from about

14 % nominal discount rate and above, along with a wide range of fuel prices. This drives to a major conclusion that the system architecture selected should take into consideration the possibility of integrating a small wind turbine along with the usage of a hybrid battery storage system, as in the case for the Canada case study system techno-economic optimization results as well.

Uganda case study selected system architecture

Based on the sensitivity analysis conclusions, the following criteria presented in table 3.10 were selected for evaluating a winning system architecture.

Table 3.10: Uganda case study selected variables for the winning system architecture techno-economic evaluation

Variable	Selected value	Reason for selection
PV slope	Slope: 10°	Based on the sensitivity analysis results explained before
Nominal discount rate	15%	Based on the average nominal discount rate used in Uganda, as explained before from the world bank data [55]
Capacity shortage	1%	Based on the sensitivity analysis results explained before
Diesel fuel price	2 €/L	Average end-user price based on a total fuel ownership cost estimation

The components of the winning system architecture under these parameters is represented in figure 3.15, and includes:

- Diesel genset with a nominal capacity of 2 kW
- PV array with an installed capacity of 3.84 kWp
- Hybrid lead-acid & Li-ion battery storage: Four strings with a total installed nominal capacity of 16.4 kWh and usable capacity of 8.18 kWh
- Inverter charger 4kW
- Small wind turbine: Rated capacity 1kW
- Excess of energy (dump load): Represented through the thermal load controller (TLC) and the Boiler.

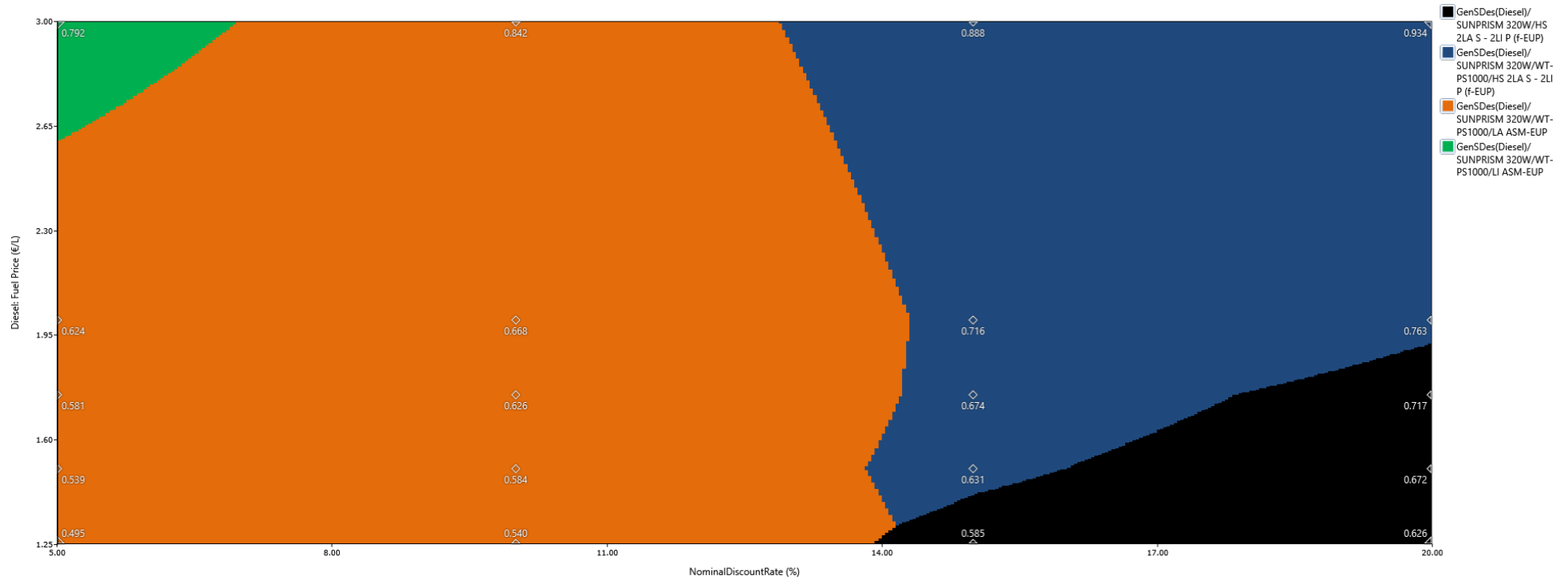


Figure 3.14: Uganda case study sensitivity analysis: effect of changing the nominal discount rate and the fuel price on the hybrid system architecture optimization

Figure reference: Uganda Case-study techno-economic modelling and analysis in HOMER [50].

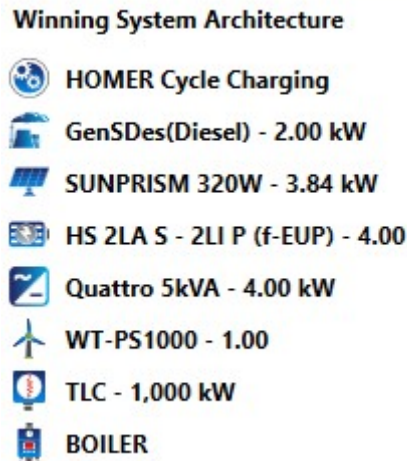


Figure 3.15: Uganda case study Winning system architecture
 Figure reference: Uganda Case-study techno-economic modelling and analysis in HOMER [50].

The total NPC of the winning system is 53590.54 €/L and the COE is 0.723 €/kWh.

3.4 OHRES Hybrid Battery Storage (HBS) techno-economic assessment

The techno-economic analysis for the hybrid battery system used in our OHRES system design is shown in figure 3.16. In this analysis, we have compared three different scenarios for the battery storage system design:

- i Reference Case: hybrid lead-acid and Lithium ion (li-ion) bases battery storage
- ii Alternative Case 1: li-ion based battery storage
- iii Alternative Case 2: Lead-acid based battery storage

Such economic analysis can be based on two financial analysis options:

- i A static financial analysis: Where the value of money is fixed along the system lifetime or analysis period.
- ii A dynamic financial analysis: Where the value of money changes based on when it is expected to take place (in which year) as in or out cash flow. In this case, an interest or discount rate is used for the dynamic calculation of the cash flow value.

In the presented, economic analysis is based on a dynamic financial analysis, based on the cost future value (CFV). The CFV takes into consideration that money (cost) value will vary from its initial value, based on a certain assumed interest rate for all future costs. In this analysis, the assumed interest rate was based on the average inflation rate

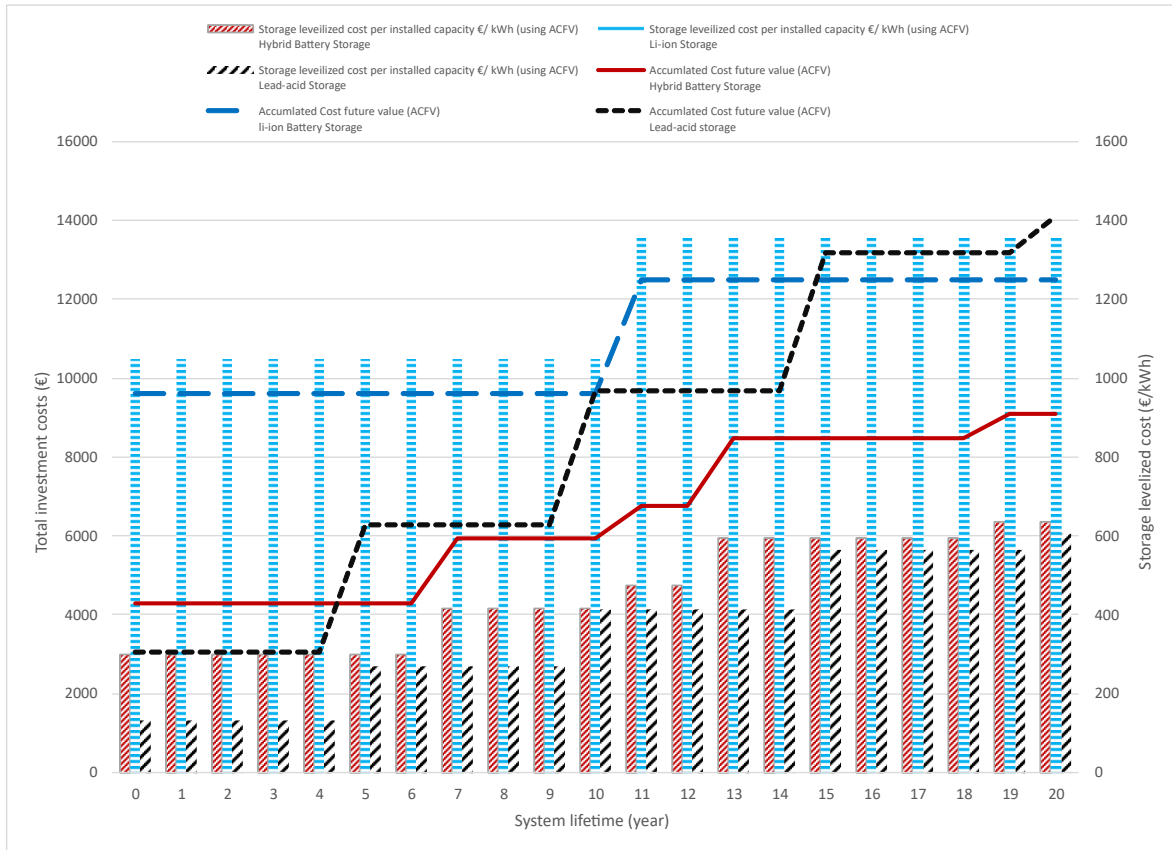


Figure 3.16: Dynamic financial assessment for OHRES storage systems
Figure reference: Author's illustration, published in [5].

in developed economies, where most of the products used in the analysis (batteries) are developed and manufactured. The dynamic economic assessment shown completed based on certain assumptions. The graph shows three different battery storage systems cases. The costs shown are based on the accumulated cost future value (ACFV) using the assumed discount rate, to add a dynamic financial analysis dimension to the value of money changes over the project's 20 year lifetime. The economic analysis was done based on the actual prices offered at the time of building our OHRES system, which has been installed in the Canada case study.

The cost future value is calculated as the following:

$$FV_n = PV \cdot (1 + i)^n \quad (3.1)$$

where;

- FV_n = The future value in year (n) of a cash flow
- PV = The present value of the cash flow
- i = The interest rate for the future value calculation
- n = number of years

The lines represent the total investment cost (€), and the bars represent the levelized cost per usable storage capacity (€/kWh) for each of the three storage cases. Important assumptions made for the analysis are shown in table 3.11, table 3.12 and table 3.13

. General assumptions listed in table 3.11 are applicable for all three scenarios. Case-specific assumptions are listed in tables 3.12 and 3.13 .

Remarks on assumptions:

- It is very important to consider the difference in the effectively usable capacities between the three cases, as they are all not the same. This is because the electrical design restrictions and necessary voltage level cannot be avoided in our analysis in order to be able to compare realistic design scenarios. Later, these scenarios can be translated into physical system components to be used on-site for our OHRES system. Also, different battery types couldn't be selected due to the need of comparing the same battery types used in the hybrid storage system.
- Lead-acid battery lifetime assumption: Due to the technical behavior of the hybrid system, it is expected that the lifetime of the lead-acid batteries shall be higher than the case of using a pure lead-acid storage system, as the batteries are not facing the load demands alone. Also, the hybrid system behavior operation strategy makes sure that the lead-acid batteries have the priority in staying fully charged most of the time until the lithium-ion batteries cannot fulfill the load needs or high load demands are required. It is therefore expected that in the reference case the lead-acid batteries would have more years in operation than the alternative case 2 where lead-acid batteries are only used for storage.

Techno-economic analysis discussion:

Under the given assumptions, the ACFV shows that hybrid battery storage represents the most economical solution for our OHRES residential application over its lifetime. The installation cost of the hybrid battery storage (reference case) is higher than the lead-acid (alternative case 2), as is the levelized initial cost. While the lead-acid system is cheapest in the short-term, after 4 years of operation the accumulated total investment cost of the lead-acid battery system exceeds that of the hybrid system. Over the long term, due to the need of exchanging the lead-acid batteries over the years, the lead-acid system becomes expensive in terms of an accumulated total investment cost than both other storage systems.

The hybrid storage system was selected and implemented in the hybrid system as it was deemed to be the most cost-effective storage solution under the given assumptions. As there is limited existing research on how hybrid storage performs under remote and harsh environments such as the Canada case study, selecting a hybrid storage system represents a novel and innovative approach.

It is important to mention that such an analysis cannot be generalized, as it is for a specific application category as mentioned previously. In addition, the assumptions made can vary based on the application, the region of components implementation or purchasing, or the user behavior. This can have an influence on the outcome results, which must be carefully analyzed on a case-by-case basis for each OHRES design and analysis.

Table 3.11: Hybrid battery storage techno-economic assessment general assumptions

General Assumption Category	Assumption
System lifetime	20 years
Interest rate	2%
Lead-acid battery DOD	50%
Li-ion battery DOD	85%
Voltage level target for the storage system	48V
Lead-acid battery one unit voltage	6V
Li-ion battery one unit voltage	12V
Targeted usable storage capacity for the system	About 8kWh
Maintenance and replacement costs	Replacement cost only. No maintenance cost is assumed for batteries.
Lead-acid batteries	Hoppecke SUN Power VR M 6-250 [48] AGM (absorbent glass mat) batteries
Li-ion batteries	BOS LE300 [49] LiFePO ₄ (Lithium iron phosphate)
Application	Off-grid and decentralized hybrid systems for residential applications

Storage price reduction assumptions

Li-ion storage price reduction assumption	<ul style="list-style-type: none"> • 10% for year 1 to 5 • 5% for year 5 to 10 • 1% for year 10 to 20
LA price reduction assumption	<ul style="list-style-type: none"> • 1% along the system lifetime

Table 3.12: Case-specific assumptions related to storage technical aspects

	Reference case: hybrid lead-acid and Li-ion bases battery storage	Alternative case 1: Li-ion based battery storage	Alternative case 2: Lead-acid based battery storage
Number of Li-ion batteries	8	28	0
Number of Lead-acid batteries	8	0	16
Li-ion total Capacity kWh	2.6	9.2	0.0
Lead-acid total capacity kWh	11.7	0.0	23.3
Battery storage installed capacity (kWh)	14.3	9.2	23.3
Li-ion usable capacity (%)	85.0%	85.0%	
Li-ion operation state of charge (SoC) window (%)	Minimum SoC: 10% Maximum SoC: 95%	Minimum SoC: 10% Maximum SoC: 95%	
Lead-acid Usable capacity (%)	50.0%		50.0%
Lead-acid operation state of charge (SoC) window (%)	Minimum SoC: 50% Maximum SoC: 100%		Minimum SoC: 50% Maximum SoC: 100%
charge (SoC) window (%)	Maximum SoC: 100%		Maximum SoC: 100%
Battery storage usable capacity (kWh)	8.1	7.8	11.7
Voltage (V)	48.0	48.0	48.0

Table 3.13: Case-specific assumptions for battery configuration, initial cost and lifetime

	Reference case: hybrid lead-acid and Li-ion bases battery storage	Alternative case 1: Li-ion based battery storage	Alternative case 2: Lead-acid based battery storage
Battery system configuration			
Battery storage system configuration	<ul style="list-style-type: none"> • Lead-acid one string: all 8 batteries connected in series. • Li-ion batteries two strings: the 8 li-ion batteries are split into two parallel strings (with 4 batteries in series in each string). • The lead-acid battery string connected in parallel with the two Li-ion battery strings, forming a 48V hybrid battery storage system. 	<ul style="list-style-type: none"> • Seven strings of four Li-ion batteries are connected in series to reach the storage voltage of 48V. • These seven strings are connected in parallel to reach the needed usable storage capacity 	<ul style="list-style-type: none"> • Two strings of eight lead-acid batteries are connected in series to reach the storage voltage of 48V. • These two strings are connected in parallel to reach the level of the required usable storage capacity.
Total storage system Weight (kg)	360.0	112.0	656.0
Initial storage system cost (€)			
Li-ion batteries cost (€)	2748.0	9618.0	
Lead-acid batteries cost (€)	1536.0		3072.0
Total Cost (€)	4284.0	9618.0	3072.0
Lifetime assumptions			
Li-ion battery lifetime	10 years	10 years	
LA battery lifetime	6 years		4 years

4 OHRES hardware functionality and optimization, dynamic testing, and on site commissioning

Chapter 4 is the third and last part related to the first building block of the study comprehensive methodological approach presented before in figure 1.3. This chapter covers the OHRES hardware aspects and functionality optimization, as well as the system dynamic testing and on site commissioning activities in both case studies in Canada and Uganda.

Chapter 4 address many phases along the hybrid system deployment phases presented before in figure 1.2: From the development phase stage 5 (System components selection, purchasing and integration), through the deployment phase stages, to the operation and monitoring phase stage 12 (End user on-site training for system operation and troubleshooting).

The chapter includes seven sections: The first section covers the OHRES System remote Monitoring and Weather Station (SMWS) and hardware aspects. Section 2 addresses the hybrid system operation and safety developed functionalities. Section 3 covers the hybrid system dynamic testing and functionality optimization. Section 4 describes the OHRES on-site installation and commissioning. Section 5 describes the Canada case study OHRES installation and commissioning. Section 6 covers the Uganda case study on-site installation and commissioning. Section 7 focuses on highlighting the major differences experienced between the case studies in Canada and Uganda.

Part of the content of this chapter is based on, and from the author's published work in Elkadragy et. al [1] [5] [8].

4.1 OHRES System remote Monitoring and Weather Station (SMWS), and hardware aspects

One of the most neglected aspects in most of the installed off-grid renewable electrical energy system is the ability to fully monitor, take control actions remotely and evaluate the system operational performance against the available renewable resources in the system installation area. In our technical system design we have taken into high consideration how to cover this gap, using a remote system monitoring and weather station (SMWS). The main components of the SMWS are:

- Self-powered weather station

- Hall effect sensors (voltage / current measurement)
- Controller and data acquisition unit
- Internet connection provided through GSM modem as the case of Uganda case study, or Satellite internet connection as the case of Canada case study.

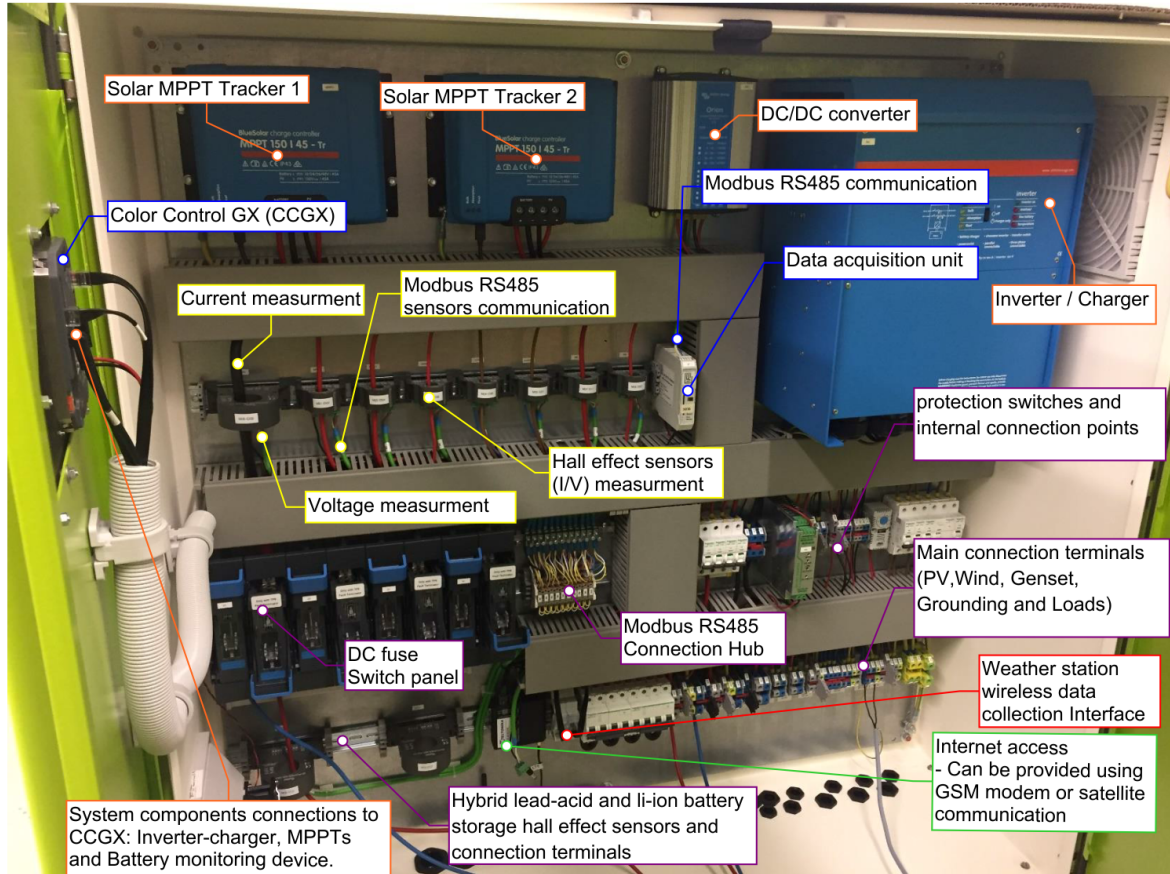


Figure 4.1: OHRES system cabinet hardware and SMWS in-door components
Figure reference: Author's figure, published in [5] [8].

Figures 4.1 and 4.2 shows the detailed hardware structure of the SMWS including the measurement sensors, data acquisition unit, and the weather station responsible for the renewable energy resources and weather-related measurements. Each of these components provide a unique functionality and the different components are integrated together within the OHRES to provide a full remote monitoring and performance assessment functionality. The weather station provide the needed weather and available renewable resources measurements as: solar irradiation, wind speed, wind direction, ambient temperature, humidity, atmospheric pressure and PV module temperature. The station is self-powered using a small PV panel and integrated battery. Measured data is transmitted wireless to a wireless interface, which is connected to the controller and data acquisition unit. For the monitoring of the system functionality and flow of energy, Hall effect current and voltage sensors are used in selected system positions. The data from the weather station and the monitoring sensors are transmitted to the

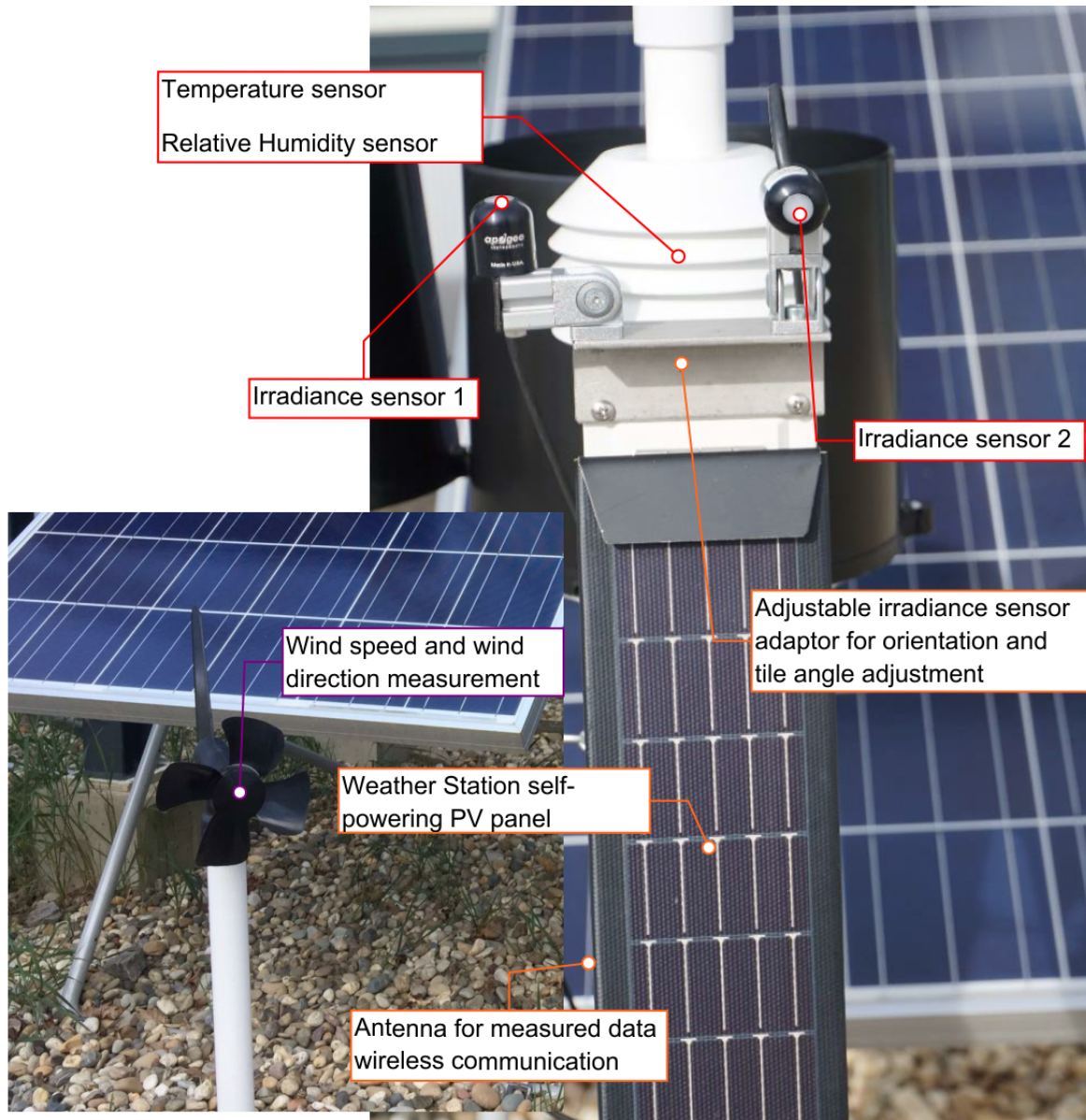


Figure 4.2: Weather station sensors and out-door components as provided
 Figure reference: Author's figure, published in [5] [8].

controller and data acquisition unit using Modbus RS485 as communication protocol. The controller and data acquisition unit was developed in cooperation with an industrial partner, and is capable of handling multiple functions within the system. In our system setup its main functionality is the data collection, cleansing, pre-processing and communication using Internet connection. The Internet connection can be provided using common LAN connection, GSM modem or satellite connection. One of the important functionalities of this unit is optimizing the size of data files sent remotely, in order to minimize the communication capacity needed which is a typical condition in most of the off-grid locations. The data transmitted is represented on a web based user interface which allows data monitoring and download, an example of the user interface is shown later in figure 4.7.

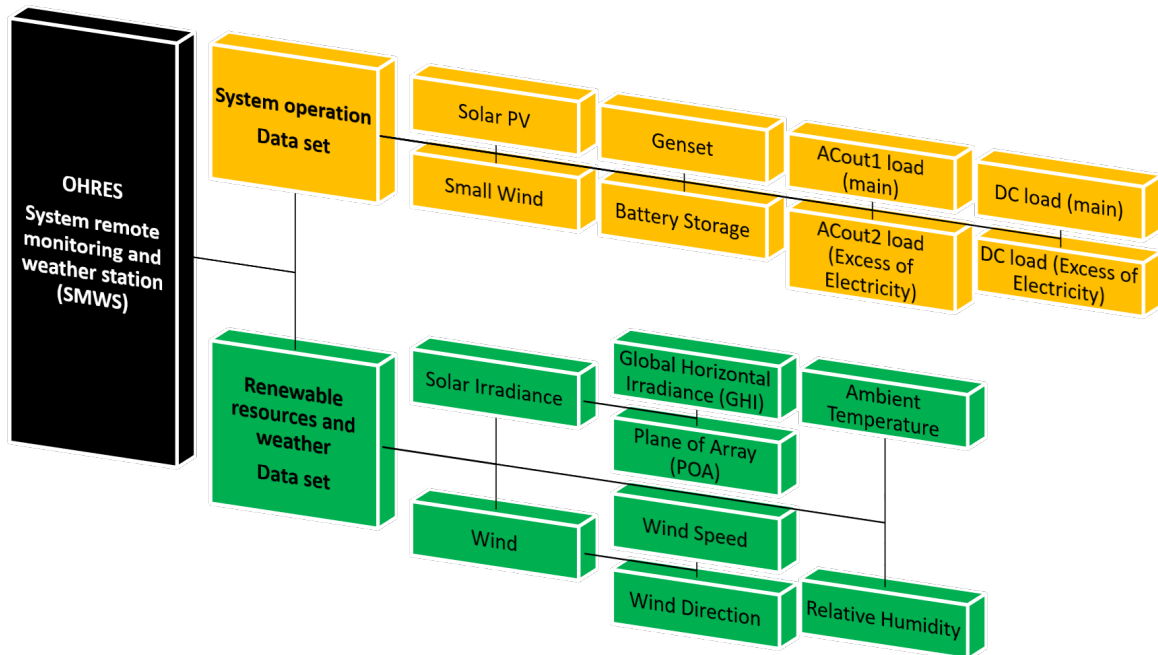


Figure 4.3: OHRES System remote Monitoring and Weather Station(SMWS) data sets.
Figure reference: Author’s figure, published in [8].

This section focuses on the data types collected from the hybrid systems, and where the measurement data points are allocated. The OHRES System remote Monitoring and Weather Station (SMWS) consists of two major parts:

- i System operation and performance measurement devices, and
- ii Renewable resources and weather measurement devices.

There are two major data sets as illustrated in figure 4.3:

- i System operation data set.
- ii Renewable resources and weather data set.

Each of these major datasets includes a variety of measured parameters, which will be highlighted in more detail in the following sections.

4.1.1 System operation data set

Selected Data and collection points in the hybrid system

The system operation data set includes eight different measured parameters as shown in figure 4.3. For each of these parameters, voltage and/or current measurements are taken using Hall Effect sensors. The selected sensor positions for each of the measured parameters are illustrated in the single line electrical diagram in figure 4.4.

Together with table 4.1 a complete understanding of the system measurement points can be formulated. The table includes a detailed description of technical criteria for each measurement point including the type of sensor used, measured voltage and current range and physical sensor position.

Table 4.1: OHRES sensor details for the voltage and current at selected measurement points

Measuring Point	Sensor Type	Measuring Voltage range	Measuring Current range	Physical sensor Position
M1	Qi-Power-485	150VDC	45A	Between PV Array and Solar Maximum Power Point Tracker (MPPT1).
M2	Qi-Power-485	150VDC	45A	Between and PV Array and Solar Maximum Power Point Tracker (MPPT2).
M3	Qi-Power-485-LV	Not applicable (same as M6)	32A	Between battery and wind turbine.
M4	Qi-Power-485	120/240VAC	24/13A	Between inverter and generator.
M5	Qi-Power-485	120/240VAC	18/33A	Between inverter and AC load (main).
M6	Qi-Power-485-300-LV	48VDC	100A	Between battery/charge controller and inverter.
M7	Qi-Power-485-LV	Not applicable (same as M6)	50A	Between battery and DC load (excess of electricity).
M8	Qi-Power-485-LV	Not applicable (voltage fixed to 12VDC)	5A	Between battery and 12VDC distribution.
M9	Qi-Power-485-300-LV	48VDC	100A	Between lead/acid battery and charge controller/inverter.
M10	Qi-Power-485-300-LV	48VDC	100A	Between lithium battery and charge controller/inverter.

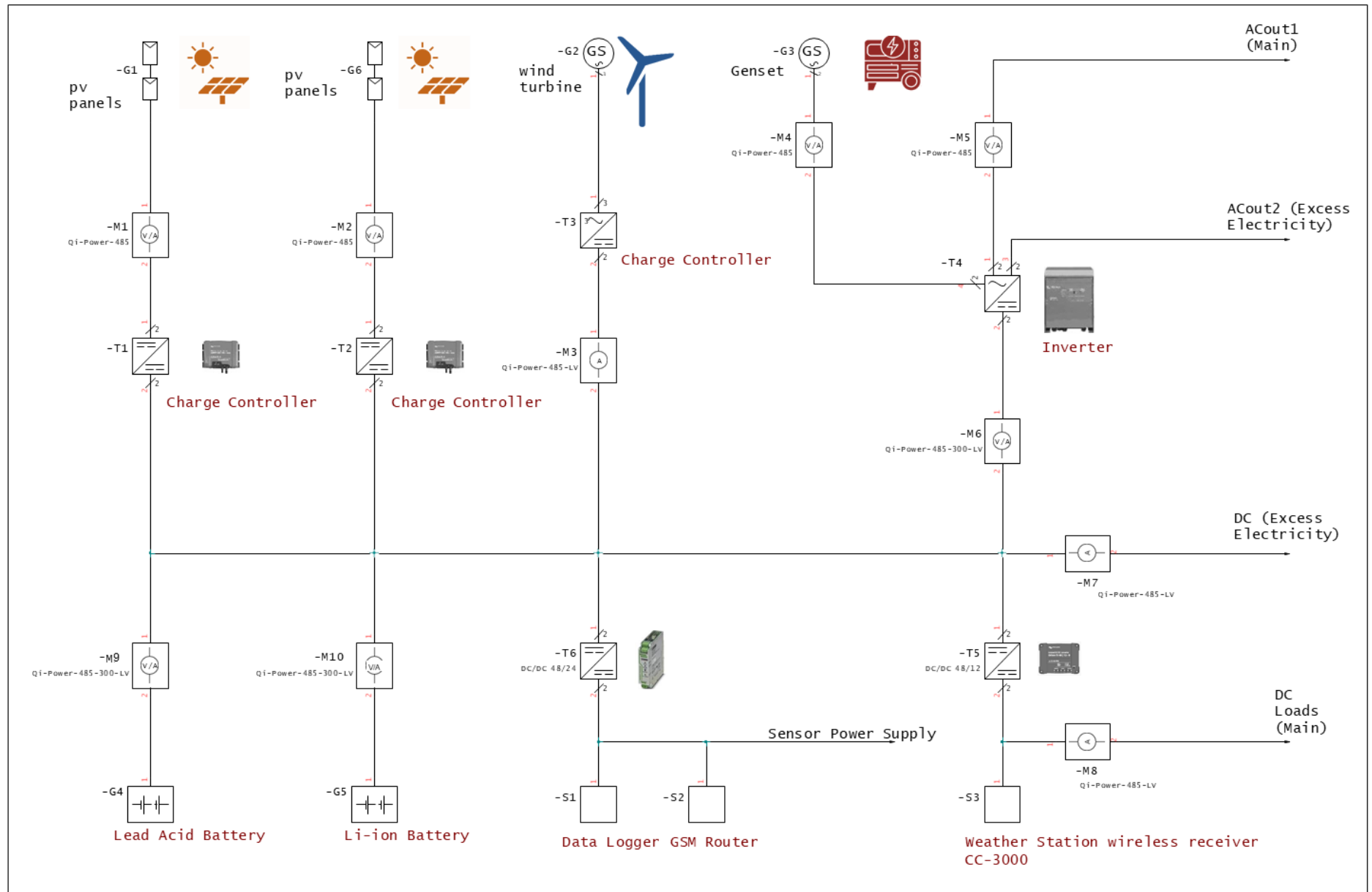


Figure 4.4: OHRES electrical and sensors measurement positions single line diagram layout.

Figure reference: Author's illustration, published in [8].

4.1.2 OHRES integrated components measurements and controller

Along with the previously mentioned sensors, another source for our system-related data collection is the integrated controller Color Control GX (CCGX)[57].

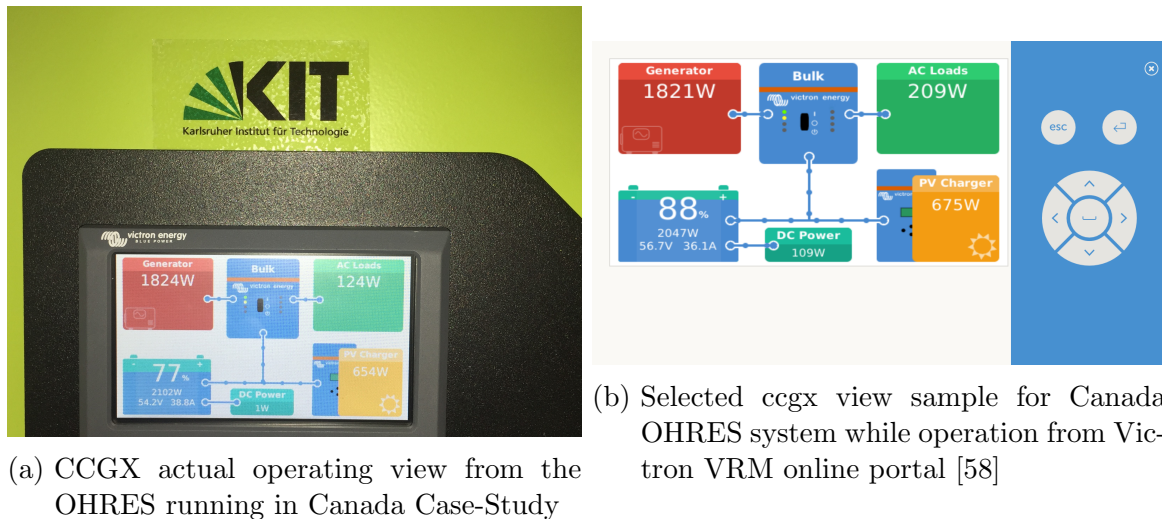


Figure 4.5: CCGX selected views from the OHRES operation in Canada case-study household

Figure reference: Author's figure, published in [8].

As shown in figure 4.5, the CCGX collects also important measured parameters from the different system components including the Solar PV Maximum Power Point Trackers (MPPTs), inverter and the battery-monitoring device (BMV). The CCGX measurements play a role in our measurement strategy, as they can be used in case of sensor measurement failure or validation requirements. As well as the calculation of not frequently used load outputs. As in our case the AC output 2 (excess of electricity), Which is only activated in case of excess of electricity production. AC output 2 utilizes this excess energy for a productive energy use application, as in the case for the OHRES installed in Canada where excess energy is used for water heating.

Important remarks regarding the measurement parameters

- i The measured AC voltages are both 120VAC and 240VAC, depending on the standard used AC voltage with respect to our case-study location in Canada and Sub-Saharan Africa (Uganda).
- ii Not all sensor measurements include current and voltage, as some measurement points share a common voltage due to the hardware connection. This is the case of M3 and M7, which have the same voltage level of the DC bus measured with M8. In that case, only one voltage measurement is enough for the other measurement points as well. Also in the case of M8, no voltage measurement is required as the DC/DC converter ensures that the output voltage is always 12VDC.

- iii There is no need for a dedicated sensor for measuring the voltage and current of ACout2 (excess of electricity), as these values are calculated based on the measured data from the CCGX and the ACout1 sensor.
- iv All Hall Effect sensors measurements (voltage and current) were validated against a calibrated electrical multi-meter measurement device, as part of the system testing and cold-running procedure. Such a measurement check and validation protocol proved that it is very important to be done in the testing phase, as one sensor had to be replaced due to inconsistency in its current measurement values.

4.1.3 Renewable resources and weather Data set

Six selected renewable energy resources and weather parameters measured within this data set scope:

- i Solar related parameter irradiance
 - a) Global Horizontal Irradiance (GHI)
 - b) Plane of Array (POA) irradiance
- ii Wind-related parameters
 - a) Wind speed
 - b) Wind direction
- iii Weather-related parameters
 - a) Ambient temperature
 - b) Relative humidity

Data collection

These measured parameters are collected using a self-powered weather station as part of the SMWS shown in figure 4.2. The weather station type used in all of our current systems is the Rainwise PVmet300 [59], more details about the weather station provided in [1]. Table 4.2 includes the main criteria related to the measurement sensors used for each parameter in the renewable resources and weather dataset.

As described later in section 4.5, figure 4.21 shows the current allocation of the weather station for our system installed in Canada.

4.1.4 Remote monitoring and primary data transmission

The primary data collected based on both the system operational data and the renewable resource and weather data has to be monitored and transmitted from the hybrid system locations in our case-studies from Canada and Uganda to our database and remote monitoring platform in Germany.

This is done using the Data Accumulation Unit (DAU) (or data logger) of the SMWS as shown in figure 4.1. The DAU is responsible for the collection of the primary data and

Table 4.2: Renewable resources and weather data-set measurement sensors technical criteria

Renewable resource and weather parameter	Sensor used	Sensor allocation and positioning
GHI	Solar irradiance sensor 1(Pyrometer)	South orientation with zero degree tilt angle for GHI measurement. Allocated on the ground level as near as possible to the PV panels installation.
POA	Solar irradiance sensor 2(Pyrometer)	The same orientation and tilt angle of the system installed PV panels. Allocated on the ground level as near as possible to the PV panels installation.
Wind speed	Weather station integrated wind measurement kit	Measurement Hub height 12 meters Wind direction Weather station integrated wind measurement kit Measurement Hub height 12 meters.
Ambient temperature	Integrated weather station temperature sensor	Allocated on the ground level as near as possible to the PV panels installation.
Relative Humidity	Integrated weather station temperature sensor	Allocated on the ground level as near as possible to the PV panels installation.

sending it remotely using an internet connection. The internet service provided in the Canadian case study using a satellite communication network due to the location's very remote nature, and in Uganda using a GSM modem. The general data flow sequence is illustrated in the layout of the Off-grid and decentralized Systems Data Analysis Platform (OSDAP) data shown in figure 4.6. More details about OSDAP is provided later in chapter 6.

The primary measured data is collected in three seconds resolution, which makes it suitable for our further process and analysis purposes which require minutely and hourly averaged primary data (as the next sections of this chapter will describe in detail).

OHRES real-time monitoring and remote access

All measured parameters can be real-time monitored for our OHRES. There are two main platforms used for the live monitoring of the parameters:

- i SMWS real-time monitoring Platform

This platform developed together with one of our industrial partners (Ferntech[60] previously known as infinite Fingers) includes all necessary parameters related to system operation and weather station in one location. It allows for five-second

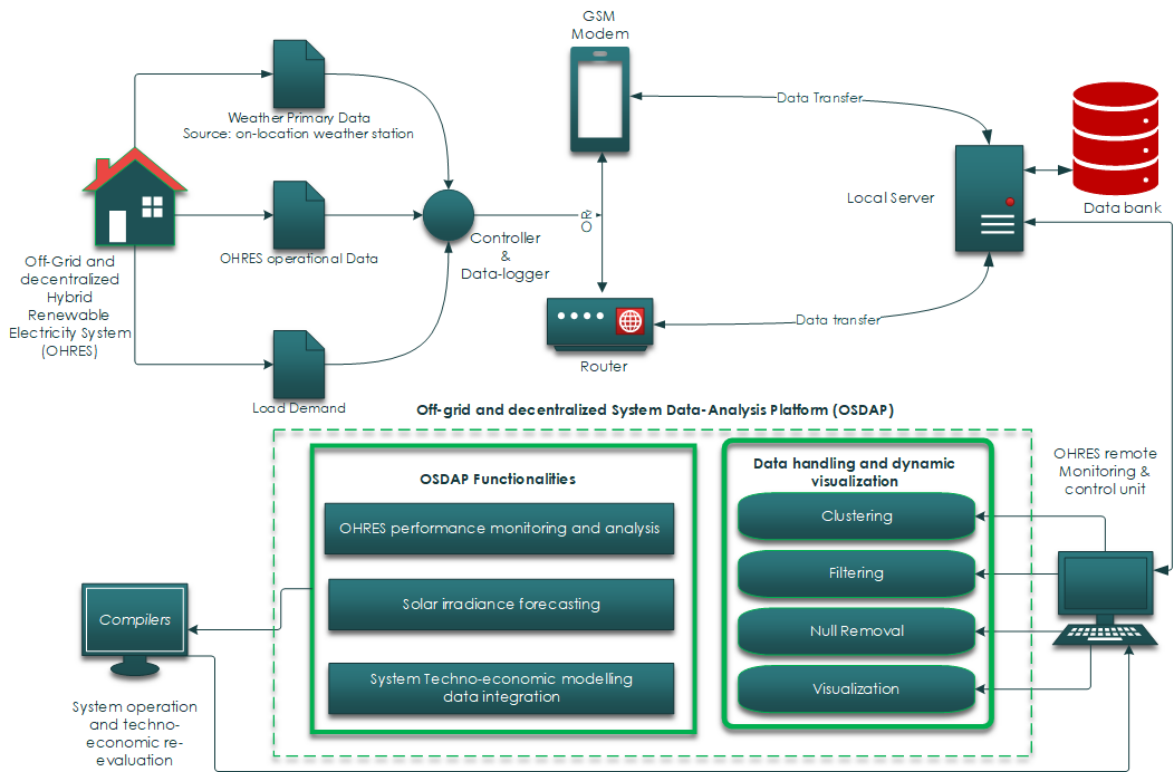


Figure 4.6: Off-grid and decentralized Systems Data Analysis Platform (OSDAP) general layout

Figure reference: Author's illustration, published in [1] [47] [8].

updated real-time monitoring for all parameters illustrated in figure 4.3 In addition, it includes selected system operation parameters from the CCGX. Figure 4.7 shows a selected example of the portal view for the Canada hybrid system.

The platform allows real-time monitoring and primary data download for desired times, which can be used for our system performance analysis as will be described further in the upcoming sections of this chapter.

ii Components integrated remote management

The second remote platform is the Victron Remote Management (VRM) [58], Which is a monitoring and management integrated functionality in some of the OHRES components used and connected to the CCGX as the solar charge controllers, inverter and the battery monitoring device. The VRM allows access and monitoring functionally related only to the CCGX. VRM portal example is shown in figure 4.8. The VRM allows for the monitoring of the CCGX connected victor devices as in our case the solar chargers, inverter, and battery monitoring device. As well as, a level of remote control and management for these devices as firmware update, settings remote changing and device ON/OFF control. These control functionalities are very useful for the system remote operation and troubleshooting. This makes the VRM a complimentary control platform to the SMWS platform.

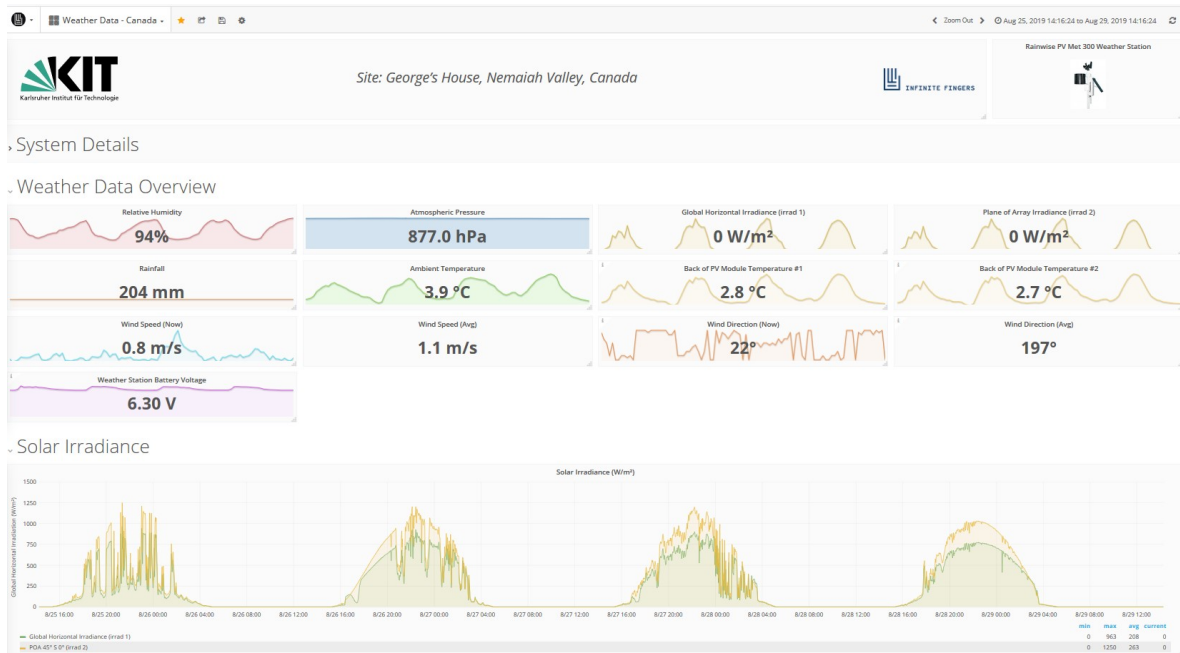


Figure 4.7: SMWS monitoring and data-logging online platform
 Figure reference: OHRES online portal, developed together with our industrial partner Ferntech [60].

Using both the SMWS platform and the VRM platform creates a very high level of OHRES remote monitoring and operation, which is a milestone for the sustainable and successful utilization of remote hybrid systems.



Figure 4.8: SMWS monitoring and data-logging Victron Energy online platform.
 Figure reference: Victron Energy VRM portal for Canada Case study [58].

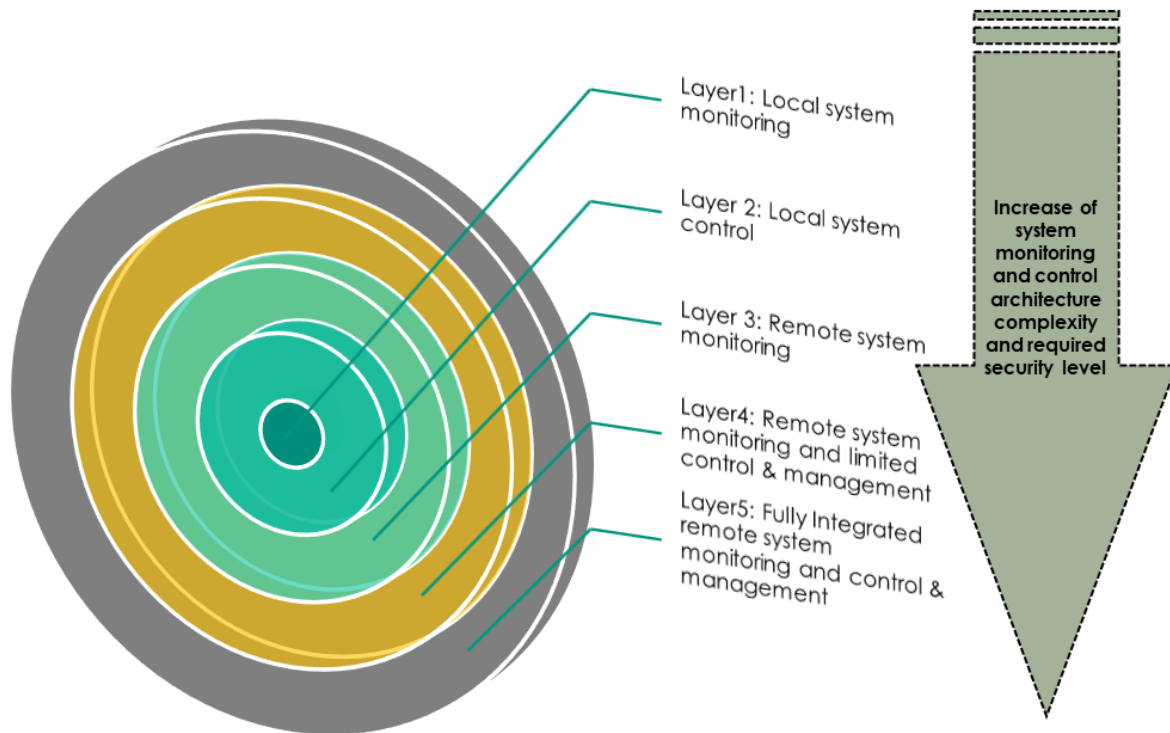


Figure 4.9: Multi-Layer Remote Access (MLRA) Model for OHRES.
 Figure reference: Author’s figure, published in [8].

Remote monitoring and management security aspects

On one hand remote monitoring and management functionality is needed, but on the other hand, there is also another important side related to cybersecurity.

The Multi-Layer Remote Access (MLRA) Model proposed in figure 4.9 remote security for off-grid and decentralized systems helps to understand the different access layers, which are associated with the monitoring, control, and management of such systems.

There are mainly five layers in the MLRA mode, each layer includes the access level right of the previous one, plus the specified layer functionalities.

- Layer 1: Local system monitoring.
 This is the core and minimum level access layer. It allows the user to monitor only the system operation and performance. It does not give any access rights for any major system control and management actions as in the case of OHRES systems for settings changing for components as solar chargers, wind controllers, inverter chargers, battery monitors and controllers and genset.
- Layer 2: Local system control.
 In addition to the functionalities allowed in layer 1, this layer allows the local control and management actions for the OHRES components and settings. In this layer, it is necessary that the communication and control actions are communicated using physical hardware connection (cable connection), with a certain specified communication protocol and software tools. There is no possibility for

any monitoring or control functionalities using the internet connection up to this layer.

- **Layer 3: Remote system monitoring (RSM).**
In this layer, the remote interaction with the hybrid system components and data starts, but in a monitoring only mode. Through centralized controllers with data logging and network (internet) communication abilities, selected components and parameters of the hybrid system can be monitored as in our case the weather and system operational data. Remote access level to any changes in the system settings, components firmware or control abilities does not exist as only monitoring related functionalities are possible.
Although the level of remote control does not exist in that layer, a certain level of cybersecurity and remote access protection is needed for data access protection since the system has a remote access capability for monitoring. This security level can be realized through secured access restricted online monitoring portals as done in the case of our system.
- **Layer 4: RSM and limited control & management.**
Along with the remote monitoring functionalities for hybrid system components and related operation data. Selected control actions and management functionalities can be carried out remotely as well. The cybersecurity criticality gets higher here than the previous layers, due to the direct effect, which can be caused due to some of the selected system control actions on the system performance and safety. It is highly recommended if the OHRES operates under this remote access layer to pay high attention to:
 - i The selected control and management actions, which are allowed to be taken remotely.
 - ii The cybersecurity level for the remote monitoring and control portals, in order to avoid hacking action or data monitoring miss-use. This is provided in our hybrid system architecture together through our industrial partners.
- **Layer 5: Fully integrated remote monitoring and control.**
This is the top layer, which includes all the access levels and control rights for all previous layers. In addition to the ability of carrying-on all control and management actions remotely without any physical hardware restrictions, it involves the integration of centralized or de-centralized controllers with network (internet) access functionality.

Optimal remote access layer recommendations for OHRES: Based on the MLRA Model described in previous layers, it is recommended to operate OHRES under layer four and take into consideration in the system design phase the integration of the required hardware components and software packages needed to reach this level of remote access. This recommendation is based on lessons learned and practical experiences gathered from the OHRES deployment and operation in our case study in Canada, which can be summarized in the following points:

- i Having a defined access level for hybrid systems located in remote areas through reliable remote connection is required for both the system end-user (for example in our case household or school residents) for basic system easy monitoring, and for system developers for adapting any changes in the operation condition into selected system parts settings.
- ii Integrating remote monitoring capabilities in addition to data logging supports gathering primary data related to the system operation and the renewable resources as in our OHRES case. This allows for remote data analysis important functionalities, such as system or components performance analysis as described in an upcoming chapters of this study.
- iii Handling the trouble-shooting process in a more effective way, through having the ability to do a “first troubleshooting actions round” remotely and see its effect on overcoming some basic system operational problems, before going into deeper troubleshooting local process if required.
- iv Positive effect on the system techno-economic aspects, due to the continuous remote monitoring, system primary data gathering and analysis and easier system operation and troubleshooting process. These factors should play a major role in increasing system utilization and reliability.

On the other hand, for OHRES it is not recommended in most application cases (as in our case residential applications) to operate under layer 5 conditions for the following reasons:

- i Hybrid system users in most of the cases have frequent interaction with the system. In the case-studies the users have a daily interaction with the hybrid system as they depend on the electrical energy produced from the hybrid system as the main energy resource.
- ii A detailed risk assessment is required due to exposing safety-critical functionalities to remote access and a highly reliable cybersecurity level needs to be guaranteed.
- iii The need for having a full remote control functionality must be carefully assisted. This functionality involves including major technical aspects and dedicated components, which if not utilized can result in a negative effect on the techno-economic feasibility of the hybrid system instead of supporting it through increasing the system’s reliability.

Our OHRES is designed to operate under access layer four, which leads to isolate any safety-critical control action from being exposed to any online or remote access possibilities. The only possibility to take these critical actions is through physical hardware interface, and allow some control and functionality actions to be taken remotely for remote operation and troubleshooting purposes. Solid examples of these actions in our OHRES system architecture are described in table 4.3.

Table 4.3: OHRES remote monitoring and control architecture

OHRES system part	OHRES component	Control or management action	Remote access for control or management action	Functionality description
Control cabinet	Inverter charger	<ul style="list-style-type: none"> • Reset (ON/OFF) • Settings modifications and firmware updates 	Allowed	As the main coupling component between the DC and AC side of the system, it is allowed to make remote settings modifications, firmware updates and remote reset (ON/OFF).
Battery Storage	Deep-discharge	protection controller switch ON/OFF switching	Not allowed	The deep-discharge protection switch for the hybrid battery system is responsible for disconnect the hybrid battery system from the load, in case of a low State of Charge (SOC) set point.
Battery Storage	Battery monitoring device	Settings modifications and firmware updates	Not allowed	The changes in the battery monitoring device are done only locally, as it includes set points for the hybrid battery storage SOC alarms, beside the control signal (relay) for the Deep-discharge protection controller switch.
Battery Storage	Battery Management System (BMS) of the Lithium-Ion (Li-ion) batteries	Settings modifications and firmware updates	Not allowed	The firmware management of the Li-ion batteries can only be managed or updated through local communication due to the safety implication it can have on the Li-ion batteries in particular, and the whole system.

4.2 System operation and safety developed functionalities

4.2.1 System operational developed functionalities

Functionalities responsible to avoid user misuse that can cause damage important parts of the hybrid system has been integrated through developed hardware parts. The misuse proof concept is centered around protecting the battery storage system as it is the most user dependent part of the system and can be damaged due to misuses such as deep discharging. Many layers of protection were built around this centralized part as shown in figure 4.10. The misuse proof concept includes different action layers. Each action is activated based on triggering set points for selected parameters, which are integrated in the hybrid system's control algorithm. The parameters selected for triggering the misuse, proof actions are:

- i The hybrid battery storage system SOC
- ii The hybrid battery storage system Voltage

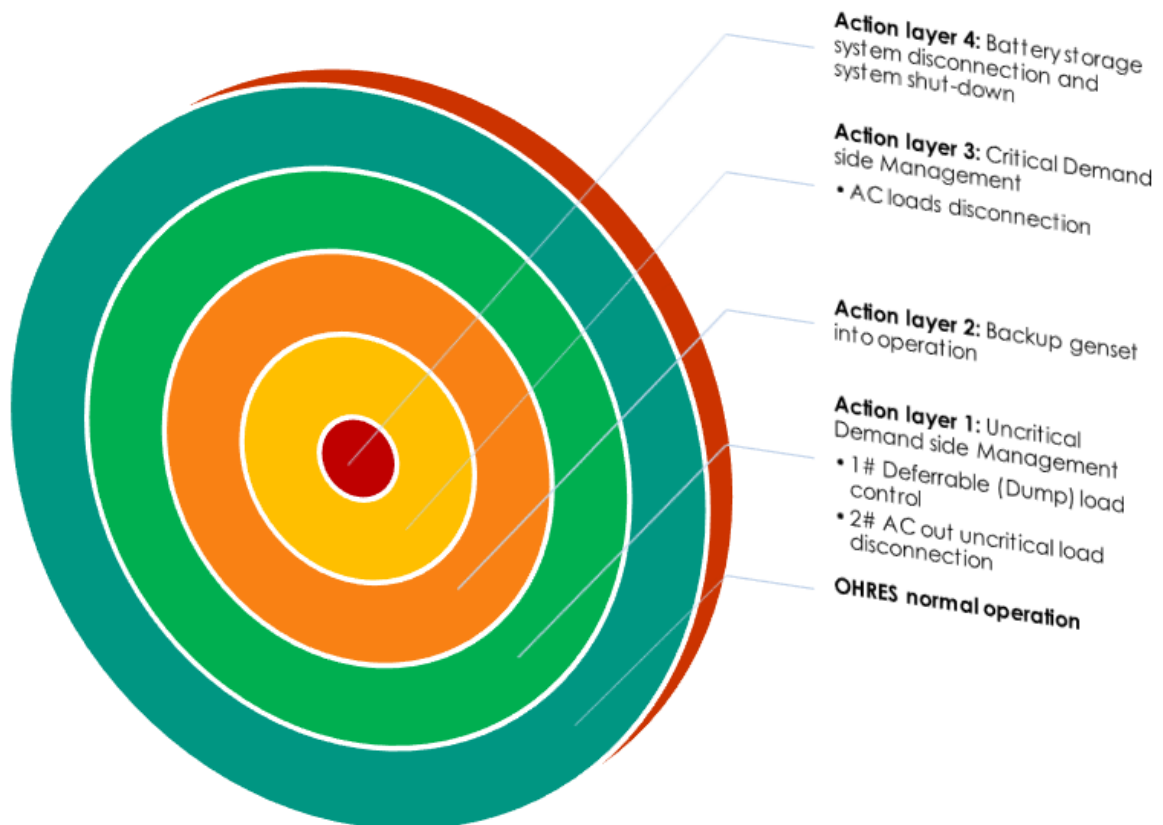


Figure 4.10: OHRES operation and protection layers
Figure reference: Author's illustration.

Certain set points are selected for these two parameters (including minimum time in the case of the voltage, where the set point has to be active), as triggering conditions

for the control algorithm in order to activate control actions. There are four action layers in the control concept for the off-grid hybrid system:

Action layer 1: Uncritical demand side management

In this action layer, uncritical loads are disconnected using several automated hardware parts of the system based on certain storage SOC or voltage set points. The controller waits for the set point to be activated for a defined time period, and then sends control signals to different system hardware parts to take the necessary actions. The loads disconnected in this action layer are:

i The dump loads

This action is taken through the DC dump load controller integrated in the system hardware, as shown in figure 4.11.

ii AC uncritical loads

This action is taken by the AC inverter, which includes two AC outputs: AC Output 1 (ACO1) and AC Output 2 (ACO2). The ACO1 is assigned for the AC main and critical loads, which for example includes (but is not limited to) in the Canada study case: fridge, satellite internet connection, telephone power supply. The ACO2 is assigned for the AC uncritical and dump loads, which for example includes: AC water heating elements, washing machine, TV. Based on certain set points, the ACO2 connected loads are disconnected first but the power supply to ACO1 loads still operates normally.

Action layer 2: Backup genset into operation

Action layer 2 is activated in case the system is still supplying its necessary power from the battery storage system even after the activation of action layer 1. The action layer 2 is activated (beside action layer 1) if programmed storage SOC or voltage set points are reached for a certain defined time period. In action layer 2 the backup genset is activated using an auto starting control signal generated from the hybrid system main controller (CCGX). The genset runs at full capacity to supply the load demands and charge the batteries. If the genset-generated power is enough, the storage system SOC and voltage conditions will get higher. After the batteries are fully charged the system would return to normal operation and the backup genset would be turned off.

Action layer 3: Critical demand side management

Action layer 3 is activated in case the genset could not supply the energy needed due to low or no fuel availability level, or there is not enough energy provided from renewable energy sources. Then Layer 1 and 2 are active and the system control algorithm proceed to action layer 3.

By reaching the activation of this action layer the AC output main loads connected to ACO1 for the inverter are disconnected. DC loads are also disconnected, which means that all AC, DC and dump loads are disconnected. The only source of energy

consumption is the internal consumption of the system components, which is very low compared to the external connected loads.

This layer activation is a major warning for the system user, which requires fast interaction in order to avoid deep battery discharging and getting the battery to critical SOC condition.

Action layer 4: Battery storage system disconnection and system shut-down

This layer represents the last defense action layer for the hybrid system towards protecting the battery storage system from reaching critically low SOC conditions due to end user misuse, or ignorance to take proper corrective actions to support getting the system back to normal operation .

Critical SOC conditions are harmful for the lead-acid batteries due to their sensitivity to deep discharging which would have an effect on its lifetime. Critical SOC conditions are also harmful to the li-ion batteries because in that layer it is already at its lowest allowed SOC and disconnected through its internal integrated BMS.

In this layer, the battery storage system is disconnected and separated from the main DC bus and other hybrid system components, which causes a total system shut-down. The shutdown is done through sending a control signal to an automated disconnected power switch connecting the battery storage system to the main DC bus. The switch also disconnects the interconnection between the lead-acid and the li-ion batteries within the hybrid storage system to avoid energy exchange between the two batteries. Figure 4.11 shows the battery storage disconnect switch. Once the battery disconnect switch is off, the solar PV inputs are also disconnected through two automated disconnect switches shown in figure 4.12. The PV switches includes a sensing functionality for the DC bus voltage, and once the voltage drops to zero the switches are immediately disconnected. This function is very important in order to protect the MPPTs from getting defected, as the MPPTs used in our hybrid system should not be exposed to PV connected input without existing batteries connection first. The electric diagram of the PV disconnect breakers connection to the MPPTs is shown in figure 4.13.

Manual hybrid system reset

After action layer 4 is activated, a manual system reset is required. This allows for troubleshooting the cause of reaching this layer. The manual reset is done through a hardware interlock switch. By using the interlock switch, the battery switch can be set back to ON and the batteries are connected back to the system. This allows for manually charging the batteries using the genset and using the available renewable energy resources. If the batteries' SOC or Voltage level did not reach a certain defined level within the allowed time period, the battery switch will again set to off and the system will shut down giving the end user a warning signal that the manual resetting process is not done correctly. Once the batteries are charged to the defined minimum level, the system can be restored back to normal operation. It is also recommended for the end user to get the hybrid battery system fully charged once a manual reset process is needed, before interconnecting heavy loads.

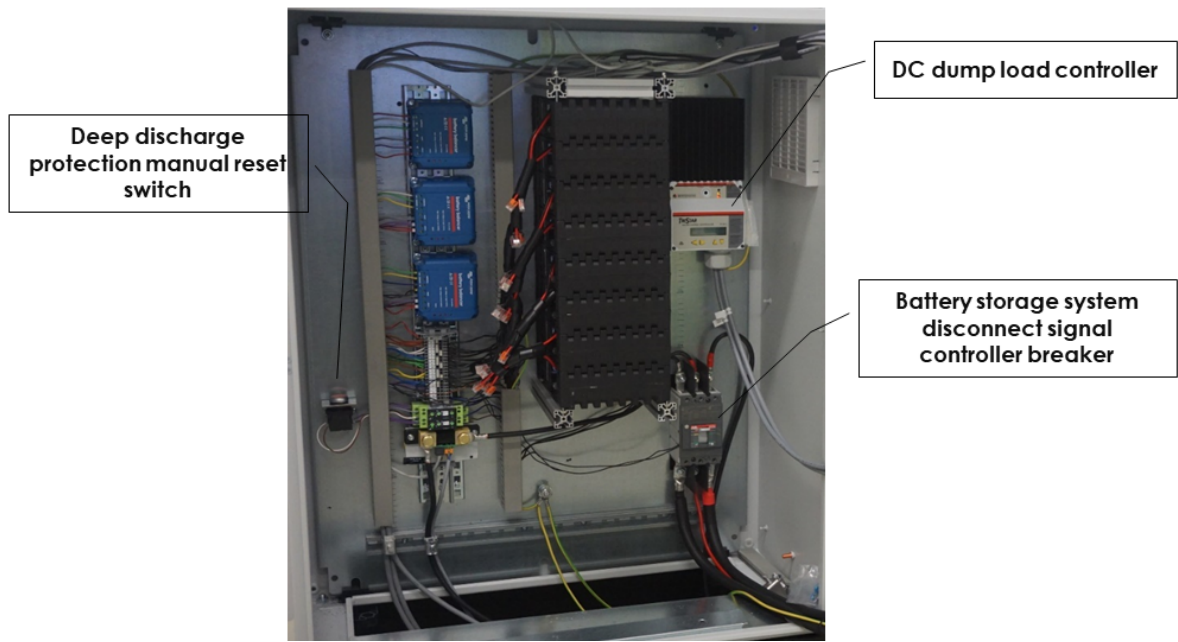


Figure 4.11: Battery storage system disconnect breaker and DC dump load controller.
Figure reference: Author's figure.

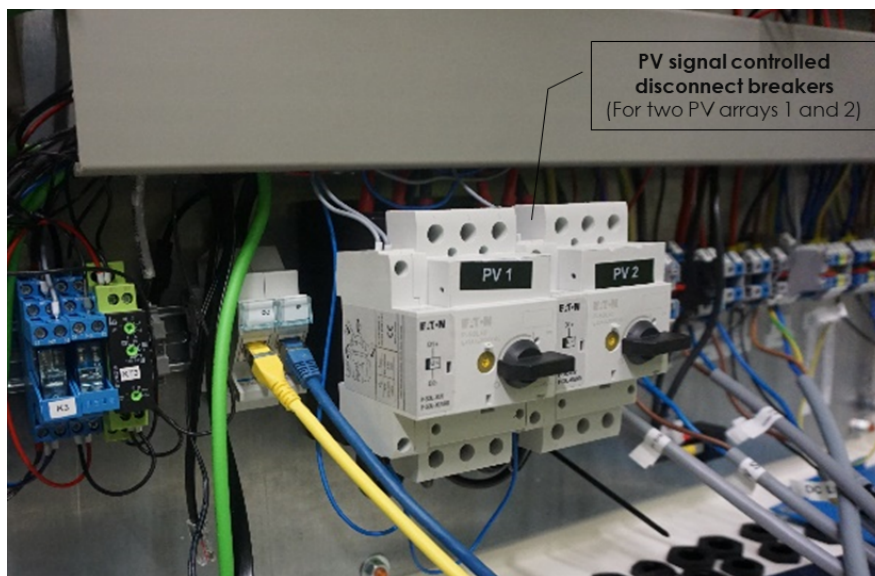


Figure 4.12: PV disconnect controller breakers.
Figure reference: Author's figure.

4.2.2 Other important integrated functionalities

Through our industrial partner specialized in off-grid systems components integration, OHRES also included standard required electrical protection functionalities such as: short circuit protection for the DC side components and connection points using DC fuse switches, AC side components and connection points using AC circuit breakers, low voltage signals and internal communication parts, small fuses were integrated into the circuit design, and earth leakage protection.

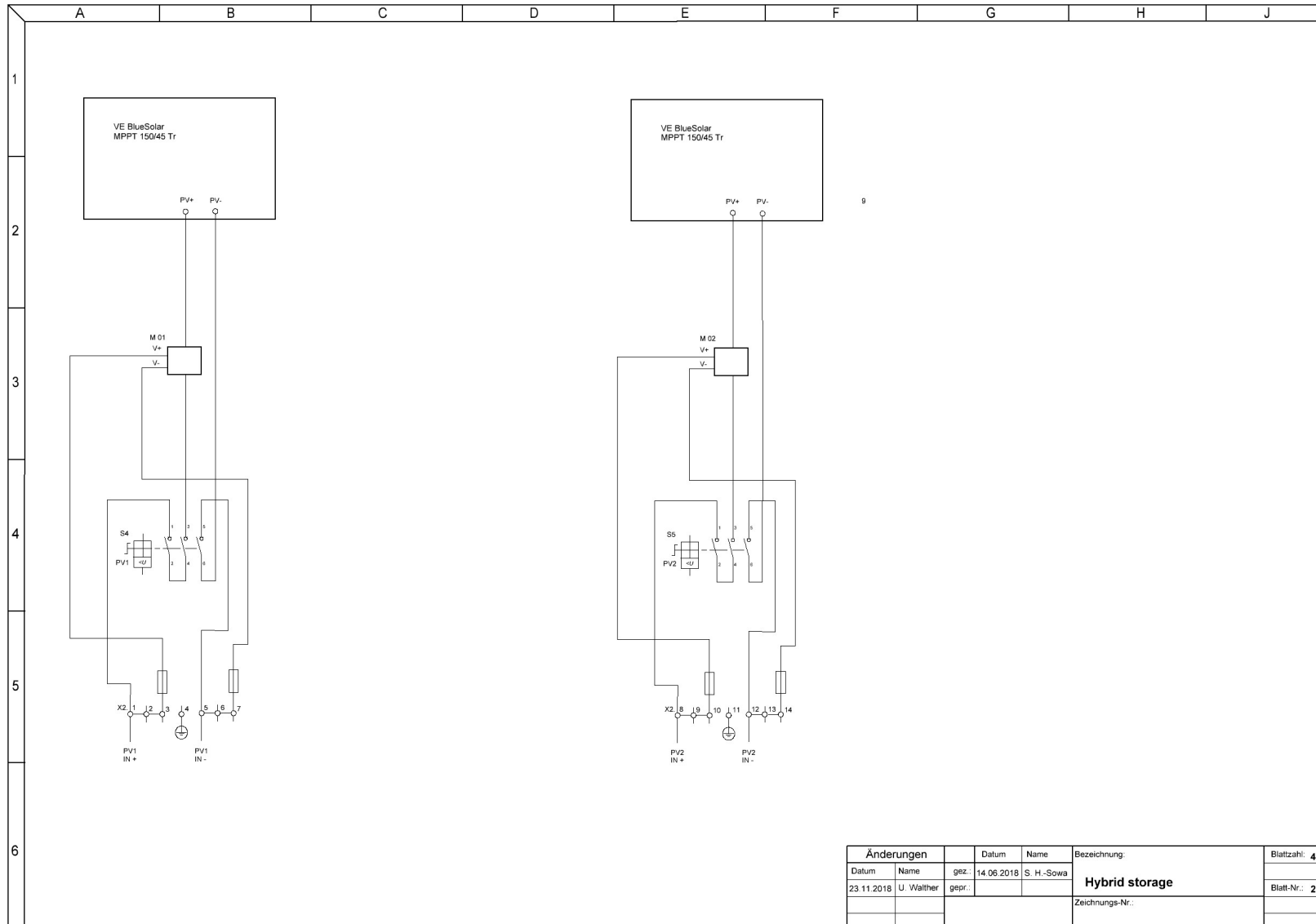


Figure 4.13: Electrical circuit diagram - Connection of the MPPT and PV disconnect controller breakers
Figure reference: Author.

This is beside the internal protection functionalities integrated in the industrial system main components.

All hardware components used in the OHRES are also industrial certified components, from major components as main inverters, MPPTs, converters and sensors, to minor components as internal cables and circuit breakers. The safety aspect was taken into consideration in the battery system installation and housing selection. Industrial explosion-proof cabinets were used for the lead-acid batteries to reach a high safety level in case of any gas leakage during operation.

All these functionalities are essential in order to reach an industrial level system design, ready for international shipment and safe operation.

4.3 System dynamic testing and functionality optimization

A major aspect of having a sustainable and successfully running OHRES for remote areas is having a comprehensive pre-commissioning testing and cold-running process strategy. The main objectives of the testing methodology is to understand the system's dynamic operation as if in reality when the system installed and used in the case study location. As well, making sure that under different operating scenarios all components are operating healthily. This is an extremely important task to do in a controlled testing environment, as once the system is shipped to the remote location there will not be the possibility to carry on most of the testing procedure. Also, component or system early failure due the lack of pre-testing can result in a highly time consuming and costly process for getting the system back up and running.

It is crucial to get a clear understanding of the hybrid system operation under different testing scenarios based on what is expected in real operating conditions, and to test as much as can be tested before system shipment on both components and system overall levels. The availability of testing methodologies including innovative off-grid hybrid system parts, as in our case the hybrid battery storage, is very limited. For example the IEC TS 62257: Recommendations for renewable energy and hybrid systems for rural electrification [61], many parts which includes very useful recommendations related to safety and system sizing for renewable energy and hybrid systems for rural electrification, as well as many other project management aspects. However, it does not include specific testing procedure which can be directly used to fulfil our testing objectives. There is a need for developing such standards including testing methodologies for state-of-the-art off-grid and decentralized hybrid systems with different capacities, as well as recommendations and standards for other system deployment stages along the value chain. A testing methodology for our OHRES has been developed with certain objectives, which could represent a step towards such a goal.

The testing methodology developed for the OHRES targeted certain test objectives on both levels:

- i Individual system components level
- ii System overall level (which include all system components interaction during operation).

Three major testing objectives are focused on for each testing level

Two of them are on each of the individual components level, which are:

- i Functionality and Performance for individual system components and overall system.
- ii Dynamic operational characteristics for each component individually or in interaction with other systems components. In addition, operational characteristics related to the hybrid system overall.

The third one is on the overall hybrid system level:

- iii System overall dynamic operation and safety functionalities

More details about the testing objective are the provided in the upcoming sections.

4.3.1 System dynamic operation testing and functionality optimization

Hybrid system test bench

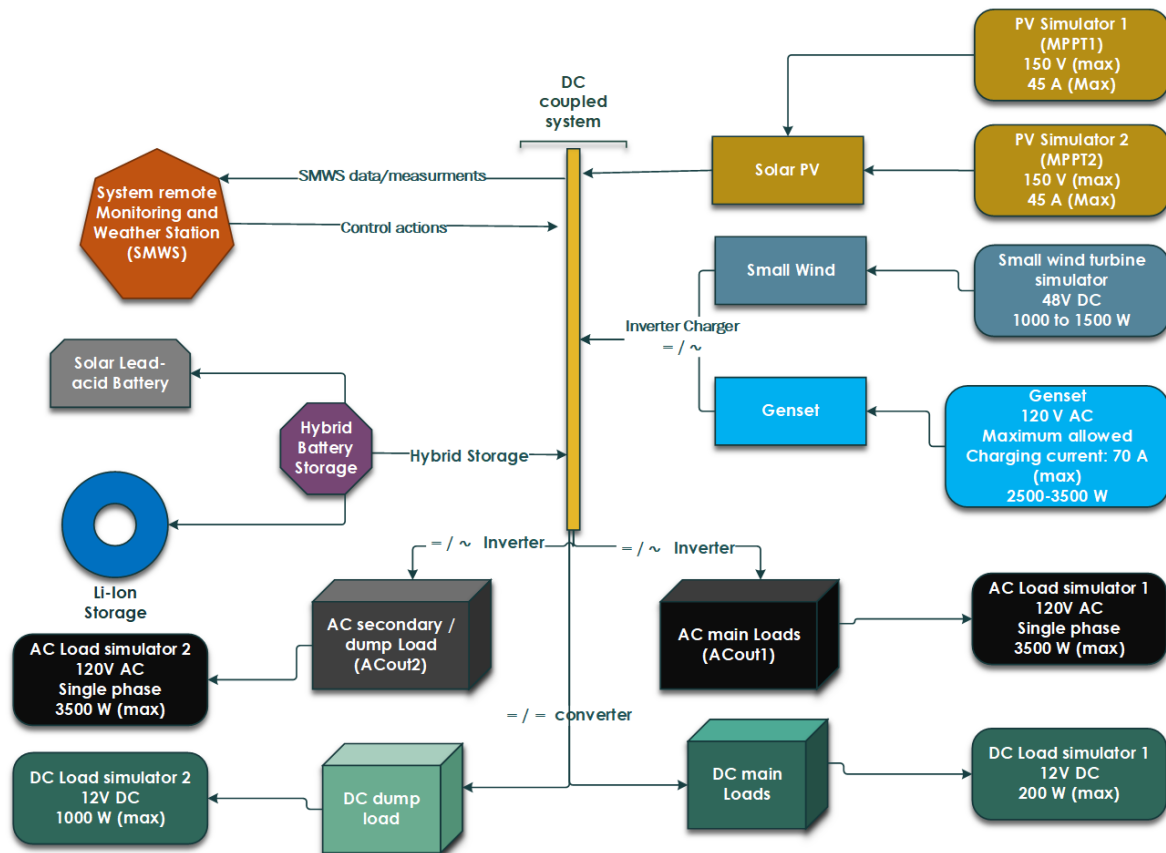


Figure 4.14: OHRES test bench diagram.

In order to fulfill our testing objectives the hybrid system pre-commissioning and cold-running testing must be carried out according to the following criteria:

- i Creating a controlled test environment where each individual component test objective can be achieved, in addition to the system overall testing objectives.
- ii Applying as many testing scenarios as possible. Taking into consideration the design of the testing scenarios based on the reference case study conditions as load profile, renewable and non-renewable resources availability, and environmental conditions

The selected case study for the first system installation was the Canada case study household. For the testing criteria given, all the hybrid system different components were gathered from different suppliers around the world in the pre-commissioning and testing lab location at the Battery Technical Center (BATEC) at Karlsruhe Institute of Technology (KIT). The different OHRES components were installed and integrated as in the final installation planned in the case study location. The system monitoring and weather station was installed and integrated for the testing process.

In order to apply the different testing scenarios, programmable simulators were used in the test bench for both renewable energy resources and loads. The load simulators are programmable and can carry multiple back to back days or even week long testing scenario. Figure 4.14 shows the overall test bench diagram, and table 4.4 summarizes the used hardware components and their technical related data ranges (Voltage, Current and Power).

Solar PV: For the Solar PV inputs on the two Maximum Power Point Trackers (MPPT) used in the OHRES design (MPPT 1 and 2), two separate PV programmable simulators were used (each for one of the MPPT used). Based on the PV array design the maximum open circuit voltage (Voc) range required to be simulated was 150 V DC, and the maximum short circuit current (Isc) range required was 45 A DC.

Small wind: A programmable DC power source was used to simulate the power input of a small wind turbine operating with 48 V DC, and in the power range of 1000 W.

Genset: A dual fuel genset was used which is part of the system components to be installed and used later in the case study final location. The Genset operates with gasoline or propane as a fuel. The operating voltage of the Genset is 120 V AC, as this is the standard used voltage in the system installation location in Canada. The AC rated power is 3500 W.

Table 4.4: OHRES test bench used hardware components technical summary

System component	Test device	Quantity	connected to	Voltage range (V)	Current range (A)	Power range (W)
Solar PV	PV simulator 1	1	MPPT1	150 V DC (maximum)	45 A (maximum)	6750 W (maximum)
	PV simulator 2	1	MPPT2	150 V DC (maximum)	45 A (maximum)	6750 W (maximum)
Small wind	Small wind turbine simulator: Controlled power source	1	Small wind turbine input terminals in the OHRES main cabinet	48 V DC	Between 20 to 32 A	Rated power range 1000 to 1500 W
Genset	Dual fuel genset: gasoline/propane	1	Genset input terminals in the OHRES main cabinet	120 V AC	Maximum allowed charging current: 70 A	rated power range 2500-3500 W
AC loads	Load simulator 1	1	Inverter ACout 1 - Main AC loads output terminals in the OHRES main cabinet.	120 V AC		2500-3500 W
	Load simulator 3	1	Inverter ACout 2 - Secondary/Dump AC loads output terminals in the OHRES main cabinet.	120 V AC		2500-3500 W
DC loads	Load simulator 2	1	DC main loads output terminals in the OHRES main cabinet.	12 V DC		200 W
	Load simulator 4	1	DC dump loads output terminals in the OHRES main cabinet.	12 V DC		500 W

AC Load

Main AC loads: AC load simulator 1 was used to simulate the load curve of the different load scenarios expected to take place during system operation. The AC load voltage is 120 V AC and range of power is up to 3500 W. The simulator was connected to the main AC output (ACout1) of the system inverter. Different load curves were used to program the load simulator based on the load profile of the Canada case study.

Secondary / dump AC loads: AC load simulator 2 was used for testing the functionality of the secondary AC out (ACout2) of the inverter. This secondary output can be used for uncritical AC loads which can be turned off first in case of low power availability in the hybrid system. It can also be used for excess of energy (dump) AC loads. In the Canada case study the ACout2 is utilized and programmed with certain conditions to utilize any extra energy produced in the system (from solar PV for example during summer period and full battery SoC), into an AC water heating elements connected to a water tank for producing hot water as a way of utilizing and storing such excess energy.

DC Load

Main DC loads: DC load simulator 1 was used to simulate the main DC loads. The DC loads used in the Canada case study are all lighting loads with a DC load voltage of 12 V DC and range of power is up to 200 W. The load simulator connected to the main DC load connection terminal located on the output terminals of a 48 V / 12 V DC-DC converter.

Excess of energy (dump) DC loads: DC load simulator 2 was used to simulate the dump or excess of energy DC loads. A DC dump load controller was programmed with certain operational conditions these non-critical loads only in case of the presence of excess of produced energy (from solar PV for example during summer period, and full battery SoC). This gives the end user the possibility to connect not only AC but also DC dump loads, and maximize the utilization of any excess produced energy into productive use. For example in the Canada case study DC water heating elements can be used in a water tank as a mean of excess energy utilization and storage.

These different simulators and components were integrated in an off-grid and hybrid system test bench together with the OHRES components and the system monitoring and weather station (SMWS) components. Using our online data logging functionality the different testing scenarios results are requested for proper analysis against the defined testing objectives

System testing methodology and objectives

A detailed pre-commissioning testing objectives map was developed for hybrid system. For each system component the three major testing objectives related to performance and operation as clarified before, are illustrated into more detailed sub-objectives and

testing actions related to the hardware individual components used in the hybrid system, and the overall system as well.

The testing map included the following testing branches:

- Solar PV
- Small Wind
- Genset
- Inverter – Charger
- Loads: AC loads, DC loads and excess of energy (Dump) load
- System monitoring and weather station (SMWS)
- System level

Under each of these seven testing branches there is a sub-level that includes major, sub objectives related to the performance, dynamic operational behavior, and in the case of the system level the overall system safety.

Covering all these test objective resulted in performing 221 different test cases, all performed on the hybrid system on the developed test bench before system shipment to the final location. Different testing condition scenarios were used in these test cases: using different solar PV array orientations and tilt angles, various load profiles based on the TCL and ACL load curves from the Canada case study load survey, and different testing period varying from several hours to several days long testing periods. In these test cases, satellite based data for solar PV irradiance and wind speed from the SODA HelioClim Sat database [62] were used for the nearest location possible to the case study area with available satellite data.

Selected critical test objectives were organized based on priorities of: A) Must be tested before system shipment, and B) Can be tested directly in final location after installation.

Detailed example of OHRES testing case and its results is presented later in chapter 6.

Besides the three major testing objectives mentioned before on the components and overall system levels, there are two important side objectives in the pre-commissioning testing and cold-running process :

Side objective 1: Validation of the system monitoring Hall Effect sensors used in different selected measurement points (in total 10 sensors as clarified in details before in figure 4.4). As described before in section 4.1, ten hall effect sensors are used in selected measuring positions as shown in figure 4.4. As a necessary testing and validation action for the OHRES, the sensors measured values, which are mainly current and voltage measurements, needed to be validated before system shipment to the final location in the Canada case study household. The validation methodology used for the sensors validation was based on comparing the voltage and current measurements from the installed sensors, against calibrated multi-meter manual measured values.

The installed sensors measurement values were monitored and registered through the live system monitoring online platform, which is a part of the SMWS as shown before in section 4.1. The online platform had a three seconds measurement resolution and measurement values are updated each five to ten seconds.

The sensors validation measurements were taken during four different system operation modes:

- i Charging only mode In this mode, the system was running using the simulators in the test bench in order to charge the hybrid batteries. No loads are activated so the input energy flow is only toward the battery system.
- ii Discharging only mode The AC and/or DC load simulators are activated and the power required is provided only by the battery system. Solar, wind and genset input energy sources are not activated.
- iii Standby mode The system components are interconnected, but there is no energy input (sources) or output (loads) activated. There is a minimum power flow due to the internal self-consumption.
- iv Reference operation mode This is the nominal operation mode, where energy input from different sources as Solar PV, Wind and Genset are active, and there is simultaneous consumption from the AC and DC loads. Depending on how much input energy is available and required energy from loads required, the power flow varies from or to the battery storage system.

During the validation process, certain measurement and validation criteria had to be followed including the following points:

- i The manual current and voltage measurements are done as near as possible to the sensor installation position, in order to avoid any measurement losses or interference. Due to the sensors installation free positions within the main cabinet this was doable for all ten sensors.
- ii There is a measurement value time delay between the manual measured value, and the registered value on the live online system-monitoring platform. This delay is due to the time required for the online platform to update its values, which were in the range of 5 to 10 seconds. This has been taken into consideration during the validation process. To overcome this delay the measurements were taken after the voltage and current value stabilized for at least one minute, in addition to having a time stamp comparison between the manual and the online registered values.
- iii A +/- 5% tolerance was allowed as measurement difference between the manual and online sensor measured values. It is important to mention that during the validation process, one of the sensors was detected as defected and was replaced. All other sensors passed the validation procedure successfully.

Side objective 2: Measuring the system control components internal power consumption in system standby mode. While the system different components are interconnected without any input or output power flow, the power consumption was indicated on the main system controller and on the battery-monitoring device as well. This indicates the internal consumption of the OHRES components, which included power electronic component, sensors, communication routers, controllers and other system internal losses. The range of the internal power consumption was between 56 and 58 Watts.

4.4 OHRES on-site installation and commissioning

Previously we did cover the development phase different stages as illustrated in figure 1.2. This section and the following sections, will focus on the OHRES deployment phase different stages and the early stages of the operation and monitoring phase. There have been many challenges and efforts related to the deployment phase, which did provide very good practical experience and lessons learned, and on the other side consumed a lot of effort and time to overcome them successfully. In the current context, not all of them can be addressed in a detailed manner. Below is a summary of the major challenges related to some of the stages in the deployment phase.

Major challenges related to hybrid system decommissioning after testing

Major challenges related to the decommissioning of the system after ending the testing process and preparing all components for shipment can be summarized as:

- The Decommissioning process has to be developed and implemented with a clear objective of making the installation and re-assembly of all the different system components as smooth and clear as possible in the final location.
- Compensating any missing or defective parts from the local market would not be possible in most cases, even for small system parts as a fuse, switches, connection points, . . . etc.
- Components packing for shipment have to take into consideration the challenging nature of having no direct and single shipment method to the system's final destination. Also the risk of local transportation of the components from the port location using very rough roads to reach the remote final destination in both case studies.
- Specific special packing restrictions and requirements have to be followed as the case for Li-ion batteries.

Major logistics related challenges

The logistics process seems to be one of the easiest stages in the system deployment phase, however, it is not as it includes its own challenges, and effects on the whole planned timeline. Some of these challenges are:

- The demanding timeline for our study left us with the only choice of using air shipment as an option for the long-distance shipment, besides using local road transportation for the rest of the system logistics journey to its final installation location. Other means of long-distance shipment as sea freight for example was not an option due to the very long period of several months it would take for the hybrid system to reach the nearest available port, then be transferred by road.
- High restrictions of Li-ion batteries shipment by air, which is a key part of our hybrid battery storage system that the whole hybrid system cannot function without.
- Coordination and management of the local system transportation phase, after delivery to the nearest airport.
- Arrangement of international and local logistics requirements and certifications for all parts of the system. Especially in the Canada case study where different standards have to be fulfilled, rather than the European standards.
- Customs clearance was very challenging, especially in the Uganda case. Even that not all system components were sent to the Uganda case study location, but handling the customs clearance for the sent components as the weather station and PV solar panels was not done in the expected and planned manner. This is mainly due to the lack of getting in force the local announced regulations related to tax exemption for renewable energy components as PV solar panels for example. These announced regulations were not applied to our system components, besides that there was lacking information on why it could not be applied. This made the customs clearance process very time and extra cost demanding.

Installation and commissioning in the case study or end-user location

The on-site installation and commissioning stage is a very critical one, including many details to take care of and challenges to overcome directly in the final system installation location. This makes the type of challenges faced in this stage unique and can differ a lot from one location to another. Major challenges faced during this stage can be summarized as:

- In such remote locations where our case studies are located, getting specialized technical support if required is extremely hard besides being very costly from both financial and time perspectives.
- Local required tools availability (as mechanical, electrical tools) is rather limited or even does not exist in case of requirement of any special tools.
- A Harsh working environment with extreme outdoor weather conditions related to temperature, amount of dust, sun exposure effects, wildlife surrounding risk, and unprojected weather sudden changes.
- Sourcing of the minimum amount of local human resources needed for the installation and commissioning.

- Implementation of safety measures aspects for all the system's different components, and the working local team along the period required for the system commissioning.

System hot running testing on-site using end-user loads

Overcoming all previous challenges and completing previous phases shall lead to having the system ready for the hot running test under real-life conditions. In case all previous stages are completed successfully, the challenges that appear in this stage are few but on the other hand, can be very time-consuming due to the fine-tuning and many test scenarios needed to be covered. Major challenges related to the deployment phase are:

- Covering all possible operational scenarios under real load conditions during the hot running testing.
- A time-consuming process, due to the settings and setup fine tuning required which can take place only on-site under real-life conditions.

A major part of these challenges could not be planned for beforehand, due to the complexity of the international project nature and the lack of previous related practical experience. Besides that, there is a major difference between not only case studies and projects in different countries but rather between different use cases within the same area. This makes the challenges that can be faced in each system deployment differ from another.

Methodological aspects used to address deployment phase challenges

To address and overcome the previously mentioned challenges, the following methodological aspects were followed:

- Plug and play commissioning philosophy Having a plug and play commissioning process was the core philosophy used in the hybrid system preparation for shipment and on-site installation. Most of the complex connections and components integration were pre-prepared before the system shipment to its final destination. Only interconnections between different cabinets as between the main control cabinet and the batteries cabinets were left to be done on-site. Also, the different system inputs and outputs for energy sources, batteries, and load connections were all gathered on one cabinet so the user interface and connection work is done in one location, and in a clear plug and play manner.
- Well documented system parts Labeling and documenting all system parts was essential for having a failure-free commissioning process on site. Not only on the high level of system major components but also labeling and documenting detailed items and components (even that they could be challenging to follow and cover them all).
- A detailed user installation, commissioning and operation manual was developed for the OHRES installation different stages in detail and operation requirements.

This is crucial for supporting both the on-site installation and commissioning and providing the end-user with the required information needed for the system operation.

- Early site visits for the case studies locations Having an early site visit to the case studies remote location is a very important factor, which affects dramatically identifying many challenges along the value chain of the hybrid system's deployment. Many local challenges were never to be identified and taken into consideration in our system design and planning unless this step was taken (especially in the Uganda case study) and local experience and surveys were gathered and carried out.
- Close involvement of the case study end-users along with the different phases One of the key factors we based our methodology on is the involvement of the end-user along with the different system planning and implementation phases. Specially to overcome the international logistics and transportation challenges, close involvement of the end-user was highly required to be able to realize realistic planning and overcome many local obstacles.
- Early identification of local resources and local capacity building One of the major advantages of having an early site visit as well as the identification of locally available resources from both human and required materials sides. Local technical partners and selected human resources were identified for providing the local technical support needed for the system deployment and operation. Local capacity building as well as a key factor, which helped to create technically qualified local human resources needed for overcoming the lack of specialized technical support during the system implementation stages.

4.5 Canada case study OHRES installation and commissioning

The following section focuses on selected highlights related to the OHRES deployment phase in the Canada Case Study.

4.5.1 Canada hybrid system logistics handling

After completing the testing phase each of the system's main components was de-commissioned and packed to be ready for shipment. Some of the previously mentioned challenges related to the logistics and system transferred did appear during the logistics handling process, however, overcoming these challenges was successful through utilizing our methodology described earlier. It was mandatory to provide the required certificates for each system component, which complies with the required logistics needs. Besides, some components had to comply with the European besides North American and Canadian standards. Air shipment was selected, due to the project timeline requirement and the very long shipment periods (several months) which other shipment methodizes as sea freight for example can take to reach our case study remote location.

All hybrid system components did arrive at the final case study destination at British Columbia (BC), Canada in July 2019. Figure 4.15 shows the last transportation phase of the system using road transportation in BC, Canada.



Figure 4.15: Canada case study system last transportation phase
Figure reference: Taken by Canada Case study end user.

Hybrid batteries logistics handling

It is important to highlight that the shipment of li-ion batteries by air is a very critical and demanding process. As it is considered a dangerous good for air freight, there are specific regulations that our batteries had to comply with before being allowed to be shipped by air. These regulations are defined by the International Air Transport Association IATA [63], and includes:

- i The compliance of the li-ion batteries to the UN3480 standard,
- ii A certain li-ion battery packing procedure to follow.
- iii The batteries have to be discharged below 20% SOC for air shipment.
- iv The batteries shipment box total weight has to stay below a certain defined weight.

Besides many other forms and regulations to take into consideration.

It was not allowed to ship all of our eight batteries in the battery cabinet as one stack, even if they were not interconnected. Figure 4.16 summarize the different packing steps for the li-ion batteries to make it ready for air shipment.



Figure 4.16: Different packing steps for the li-ion batteries for air shipment.
Figure reference: Author's figures.

Packing Step 1: included separating the battery units and isolating them electrically. Also checking that any protection devices are in place as fuses for example.

Packing Step 2: using a carton box for each battery unit. Plus surrounding the battery unit with special flame absorption foam material (developed especially for li-ion batteries flame treatment).

Packing Step 3: sealing each battery box with a special non-flammable tap defined for li-ion batteries shipments.

Packing final step: placing all battery carton boxes in a special material carton box, and sealing it using the special tap. Plus adding the required safety signs and information needed for air freight. Then the batteries are ready for air shipment.

On the other hand, the shipment of sealed lead-acid batteries is very simple, as they are not classified as dangerous goods as in the case of Li-ion batteries.

4.5.2 OHRES hot-running test and full commission for the Canada Case study

The OHRES installation and commission for the Canada case study was planned to take place during summer, as due to the harsh weather conditions in the case study location almost along the year (except during summer) it would be not possible to complete the installation of the system. The commissioning was carried out during August 2019. The commission included indoor and outdoor installation activities for the hybrid system components and the weather station. Figure 4.17 shows part of the outdoor installation during the commissioning actives in the final system location in Canada.



Figure 4.17: Canada case study hybrid system outdoor installations.
Figure reference: Author's figure.

The indoor installation included the main control cabinet and the hybrid battery storage parts. The installation was done in the house basement, replacing the old installed electricity system. Figure 4.18 shows part of the system indoor installation preparations. Due to the plug-and-play philosophy for the system commissioning, it took only about 6 hours to build the system interconnections and make it ready for on-site testing and operation.

Besides the hardware installation and commissioning, different load scenarios were



Figure 4.18: Canada case study hybrid system indoor installations and commissioning.
Figure reference: Author's figure.

tested in the household in order to achieve three main objectives:

- i Assure the system operation reliability under all possible load and operation conditions, including total connected load peaks and transient loads.
- ii Final Fine-tuning of the control algorithm set points (explained previously), which was expected to be a simple process due to the comprehensive testing process for the system under lab conditions. However, it turns out to be a time-consuming process under real operation conditions, including all uncontrolled variables from renewable energy resources availability sudden change, to load behavior changes and requirements for Genset fast response time to avoid loss of power supply.
- iii On-site capacity building and training for the case study end-user, who was involved in all the hot running testing scenarios and commissioning process as well.

The system is put into operation on 23 August 2019, and the household is dependent on it as the main source of electrical energy since then. The old existing hybrid system which has been used before the new current system installation is still in place, but

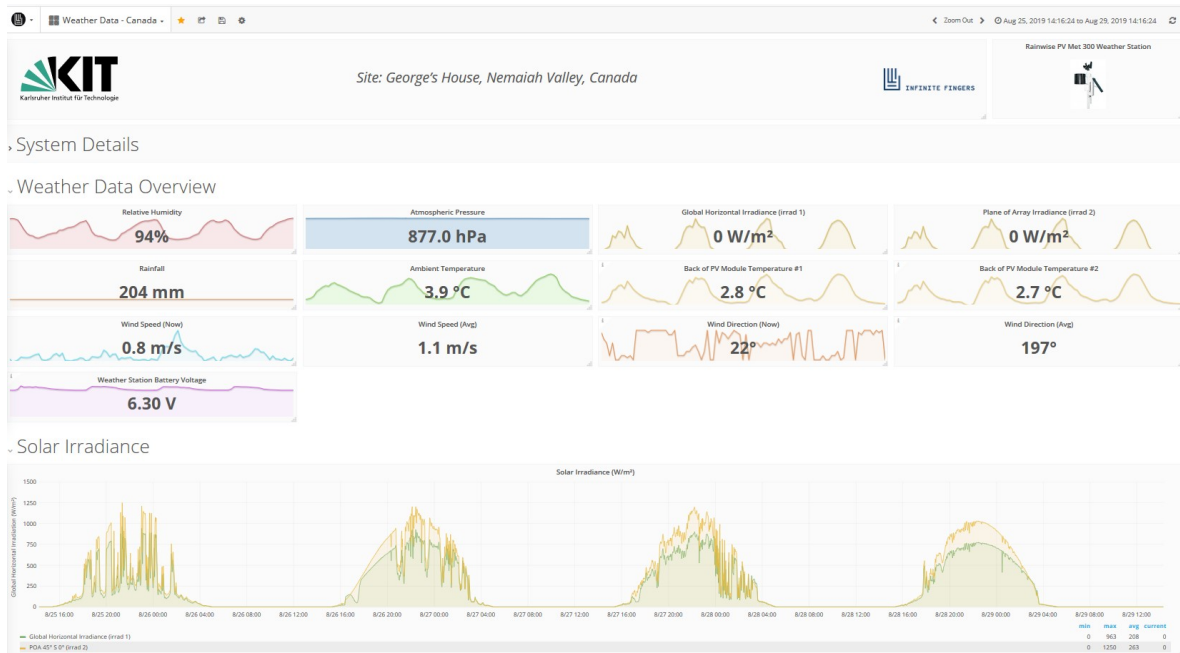


Figure 4.19: Canada case online monitoring portal - Weather station data monitoring.
Figure reference: Canada case-study online monitoring portal.

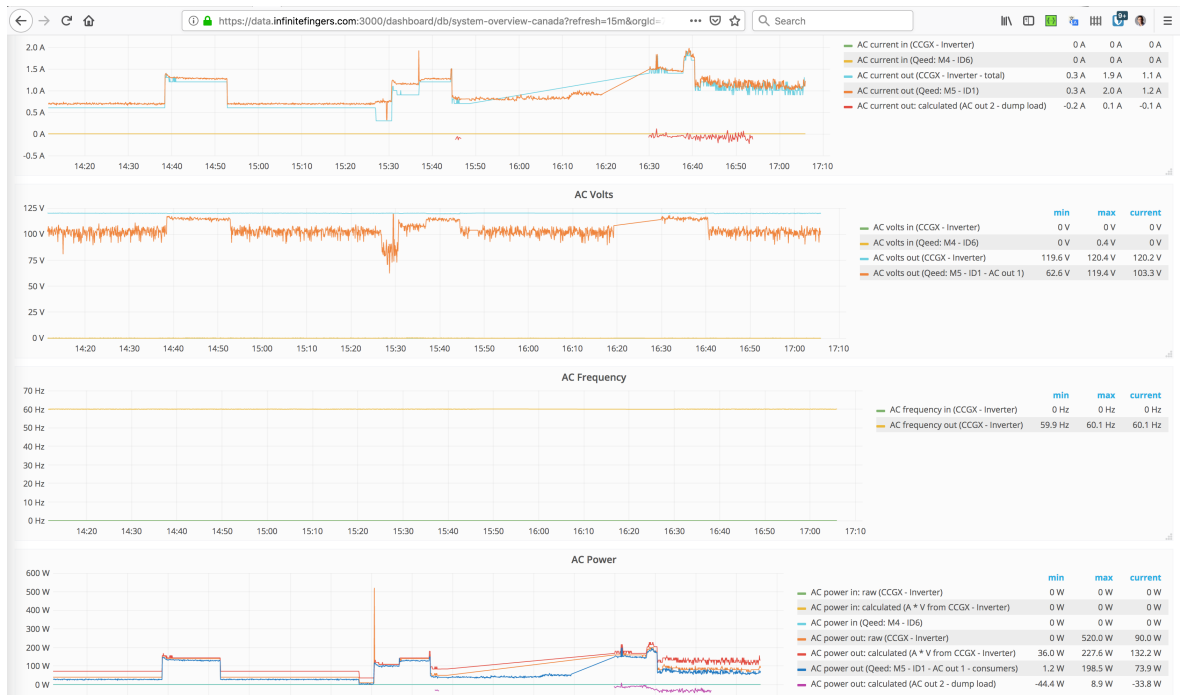


Figure 4.20: Canada case online monitoring portal - AC related measurements example.
Figure reference: Canada case-study online monitoring portal [60].

not operating anymore. The first year of operation went without any system failures reported, even during the harsh winter period in the case study location, which is a major success milestone for our study. To our knowledge, such hybrid system architecture including hybrid li-ion and lead-acid battery storage is the first of its kind for

the remote community where our case study is located, if not in the whole of Canada (to our knowledge by the time of the system installation).

Figure 4.19 show a screenshot of the system remote monitoring online portal for the Canada case study during and after the hybrid system commissioning. Figure 4.20 shows an example of the AC related different measurements remote monitoring as currents, voltages, frequency, and powers.

The indoor and outdoor OHRES installation and commissioning is summarized in figure 4.21. The only part of the hybrid system which was postponed to be installed is the small wind turbine. This is due to the requirement of having at least one year (optimal two years) of wind speed measurement at the selected hub height of 14 meters above ground level, which was not completed by the time of the system installation. Based on the wind measurement campaign results it can be decided if it is economically feasible to install the wind turbine at this hub height to produce enough energy yield for the system, or it could be required to get to higher hub heights for better wind regime. Figure 4.22 shows the electric circuit diagram of the OHRES main electrical cabinets and components interconnection.

4.5.3 On-site installation and commissioning failures and experience highlights

It is important to highlight some of the deployment phase process related failures and experience points, which affected our plans and had implications on both time and cost of the system deployment.

Defected batteries during logistics: It was remarkable that all hybrid system components sent from the pre-commissioning and testing location at KIT, Germany to the final case study destination at BC, Canada arrived in healthy condition. Only one of the eight lead-acid battery units had some severe damage and was not safe to be installed. Figure 4.23 shows the defected battery with damage on the positive electrode and casing cracks. Unfortunately it was not clear in which stage of the system logistics this damage happened, as it was discovered after the unpacking of the different components in the case study final destination.

It was very time critical to find a replacement for the defected battery, to avoid delaying the commissioning of the system for up to one year in case it is not completed during the planned summer period. A replacement for the battery unit could not be resourced locally in Canada within the required time frame. It was planned to have two lead-acid battery units as back-up reserve for any defects during the testing, transportation or commissioning, which was our fast and suitable solution for replacing the defected battery. The battery units were both shipped from Germany to Canada for a quick replacement and providing local back-up for at least one battery unit in the case study location. Having these back-up batteries available for immediate shipment turned out to be a reason for avoiding severe implications on the system commissioning timeline.

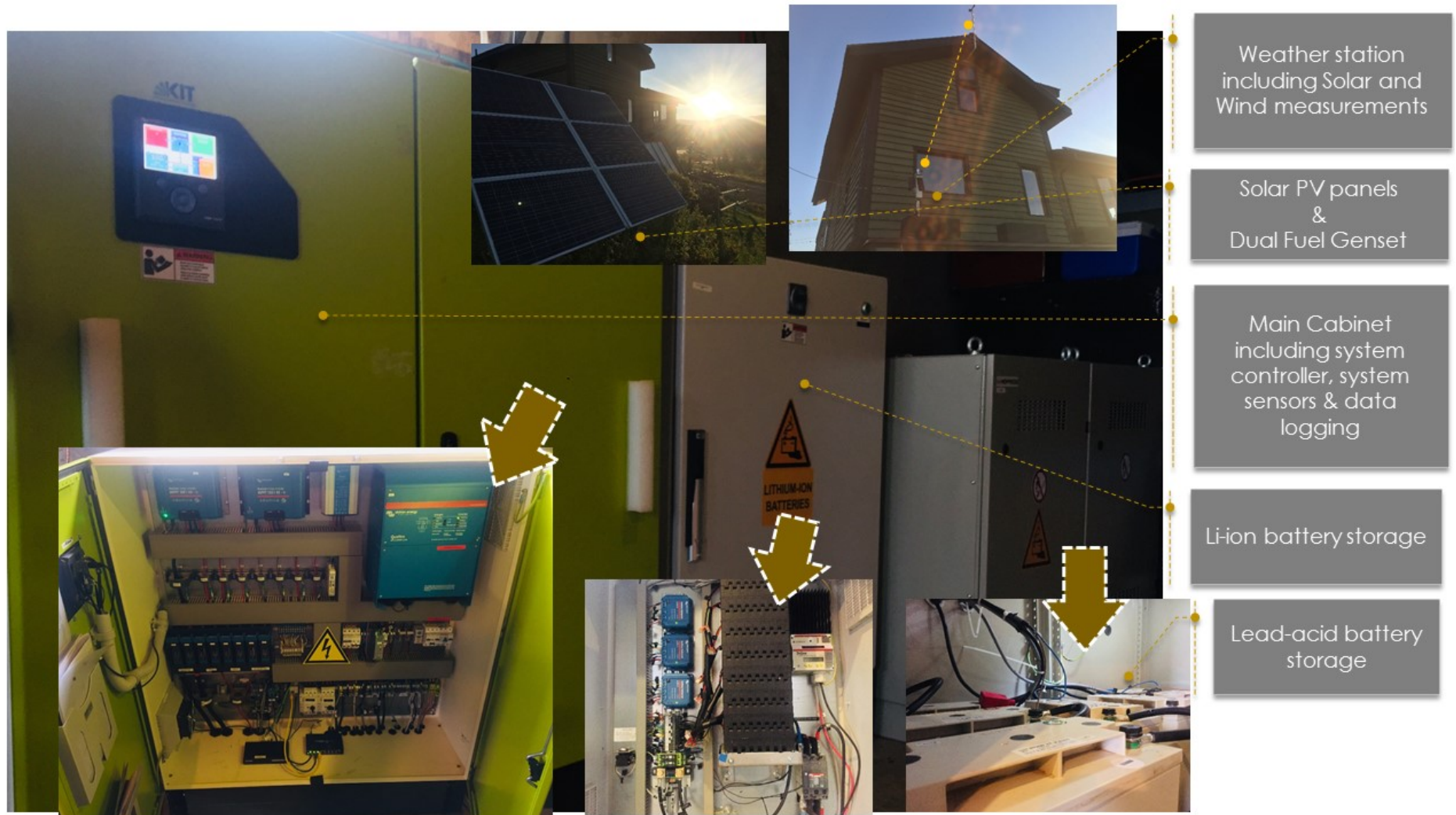


Figure 4.21: Canada case indoor and outdoor OHRES installations summary.
 Figure reference: Author's figure, published in [5] [8].

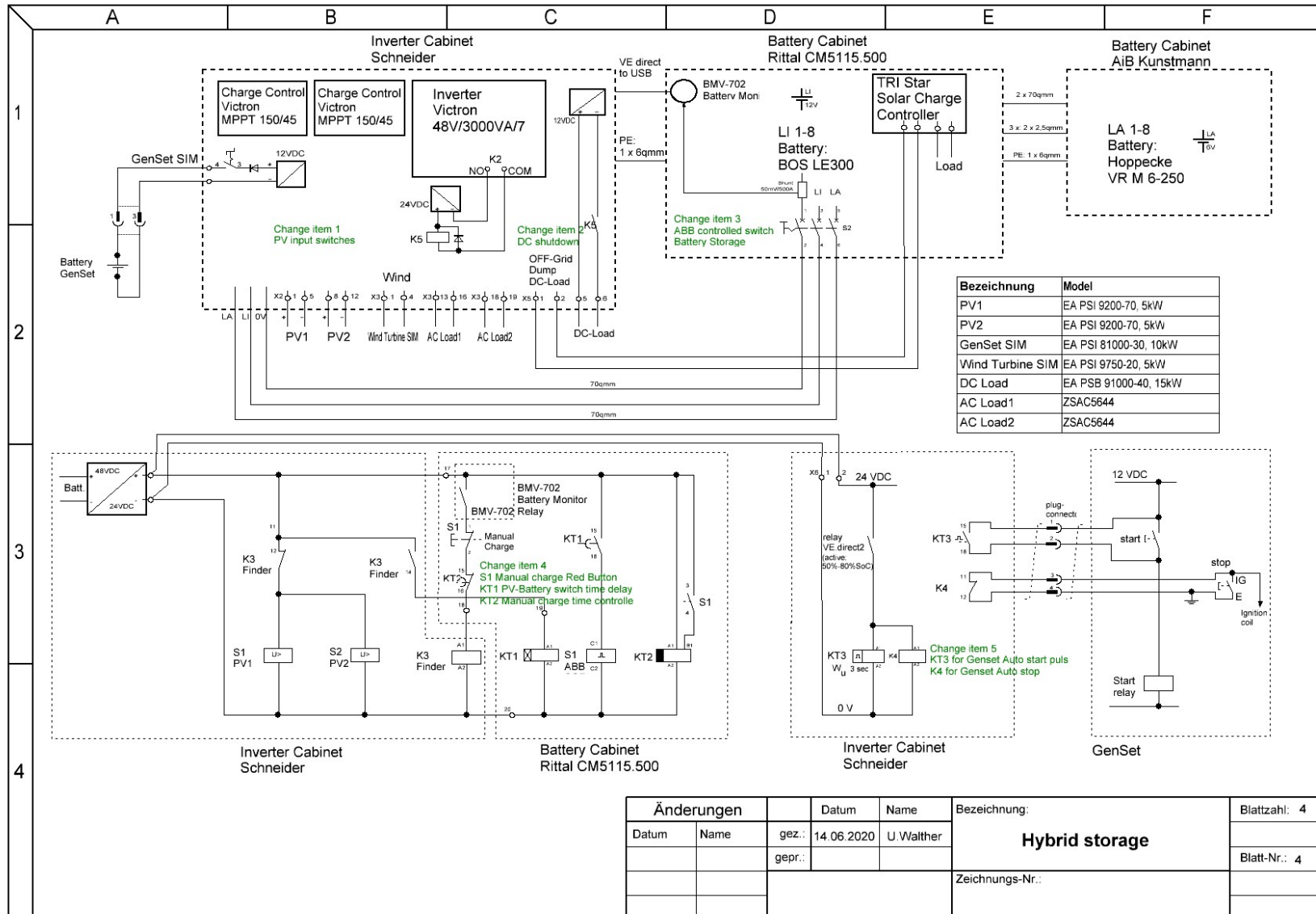


Figure 4.22: Electrical circuit diagram - Off-grid Hybrid Renewable Electricity System (OHRES) electrical main components
 Figure reference: Author.



Figure 4.23: Defected lead-acid battery during Canada hybrid system logistics process.
Figure reference: Author's figure.

Weather conditions very dependent timeline: In the case of the Canada case study (and other similar locations not only in Canada but globally sharing the same weather conditions), the installation and commissioning time window is very narrow along the year (mostly during the summer period). This forces the project timeline to be extremely dependent on the summer window and weather conditions, which can result in not only few weeks of plan delays but up to one year as well. This fact represented a major challenge and source of high risk for our planning process, which cannot be neglected or underestimated.

Unplanned delays in the system logistics: One of the underestimated processes that had an effect on the project timeline was the local logistics delays. It was expected that once the air shipment phase of the system was completed, the road transportation phase of the system within Canada would be done according to the planned timeline and process defined by the local transportation partner. However, the local logistics ended up taking several weeks longer than planned. This was due to the availability of only one freight handling partner recommended from our end-user for handling the local logistics, with limited working capacity and sub-optimal query handling capabilities. There was also the need to coordinate among many parties, as the last stage of the

system transportation had to be made by the end-user himself, as the freight partner service was limited only to the nearest town.

Outsourcing on spot required parts: Although all required cables for the system interconnections were planned and shipped, external cable extensions were required for connecting the AC and DC loads. Sourcing such cables (even slandered cable types) on quick timelines was not possible through the local remote community shops. There were two main ways to overcome such a challenge.

- i Finding more resources in the nearest town (as is the case for many remote communities), which can involve at least 6 to 8 travelling hours.
- ii Search within the local community for suitable cables to be used (leftovers from previous projects or local private stocks).

Using both of these solutions helped this challenge to be solved, giving a clear example for a lesson learned: that providing everything required for remote installations involves deep planning and is a very challenging and under-estimated part of such systems deployment process.

4.6 Uganda case study on-site installation and commissioning

The following section focuses on selected highlights related to the OHRES deployment phase in the Uganda Case Study.

Early deployment of hybrid system first phase (weather station) in Uganda

One of the most critical pre-requisites for a successful off-grid systems design is a very early site survey, due to the fact that each off-grid location is unique (as described before). This aspect is taken into high consideration in our study, especially for the developing country case-study in Uganda where is not enough information and data available which reflects the practical facts and challenges on the ground. In beginning 2018 a site visit was done to the case-study location in Uganda. The visit included several activities and objectives, each of these objectives has a list of needed actions in order to achieve the needed objective result (the detailed action plan is not shared here). The main objectives of the site visit can be summarized into four main categories as follows:

- Technical visit related objectives
 - i School location detailed site assessment and survey.
 - ii Installation and commissioning of the system first phase, the weather station in a selected testing location.
 - iii Having a preliminary assessment of the available renewable and non-renewable energy resources in the case-study area.

- iv Selection of the OHRES different components (PV panels, battery storage system, small wind turbine, Control unit cabinet, SMWS) installation spots in the school location.
 - v Collecting a realistic impression and having a close practical view for the case-study technical needs (e.g. load distribution).
 - vi Commissioning of the remote data acquisition unit including the GSM modem and having a hot-running test of the data streams from Uganda to our database in Germany.
- Economical visit related objectives
 - i Survey the locally available renewable electrical energy financing mechanisms, with focus on small-scale systems for private owners.
 - ii Collecting preliminary general overview about the level of maturity for using off-grid systems especially within rural remote areas.
 - iii Having a realistic understanding for the financial capabilities of the targeted private owners for off-grid electrical systems in rural areas.
 - iv Getting in contact with governmental entities and representatives (if possible) to measure the real level of utilization for the off-grid applied support mechanisms, and it's implication on the system economic feasibility.
 - v Check the level of market maturity and understanding for the economic aspects and investment nature of renewable energy projects in general, and in particular off-grid electrical energy systems.
 - Social visit related objectives
 - i Measure the awareness regarding renewable energy.
 - ii Getting a close understanding of the social interaction in the case study location.
 - iii Experience the life-style of end-consumers through living in the same life conditions if possible.
 - Project management related objectives
 - i Getting introduced and establish communication channels with the members of the local project partner Sofraa Worldwide Organization [64].
 - ii Building local support capacity (especially for technical troubleshooting) from selected local project partner members, who have basic technical capabilities and potential to receive a technical training.
 - iii Identification of reliable local partner companies in the field of renewable energy off-grid systems, and create mutual-interest for partnership within the case-study project scope.
 - iv Revise the project stakeholder analysis, especially the importance and influence of each of the stakeholder on real-life practical basis.

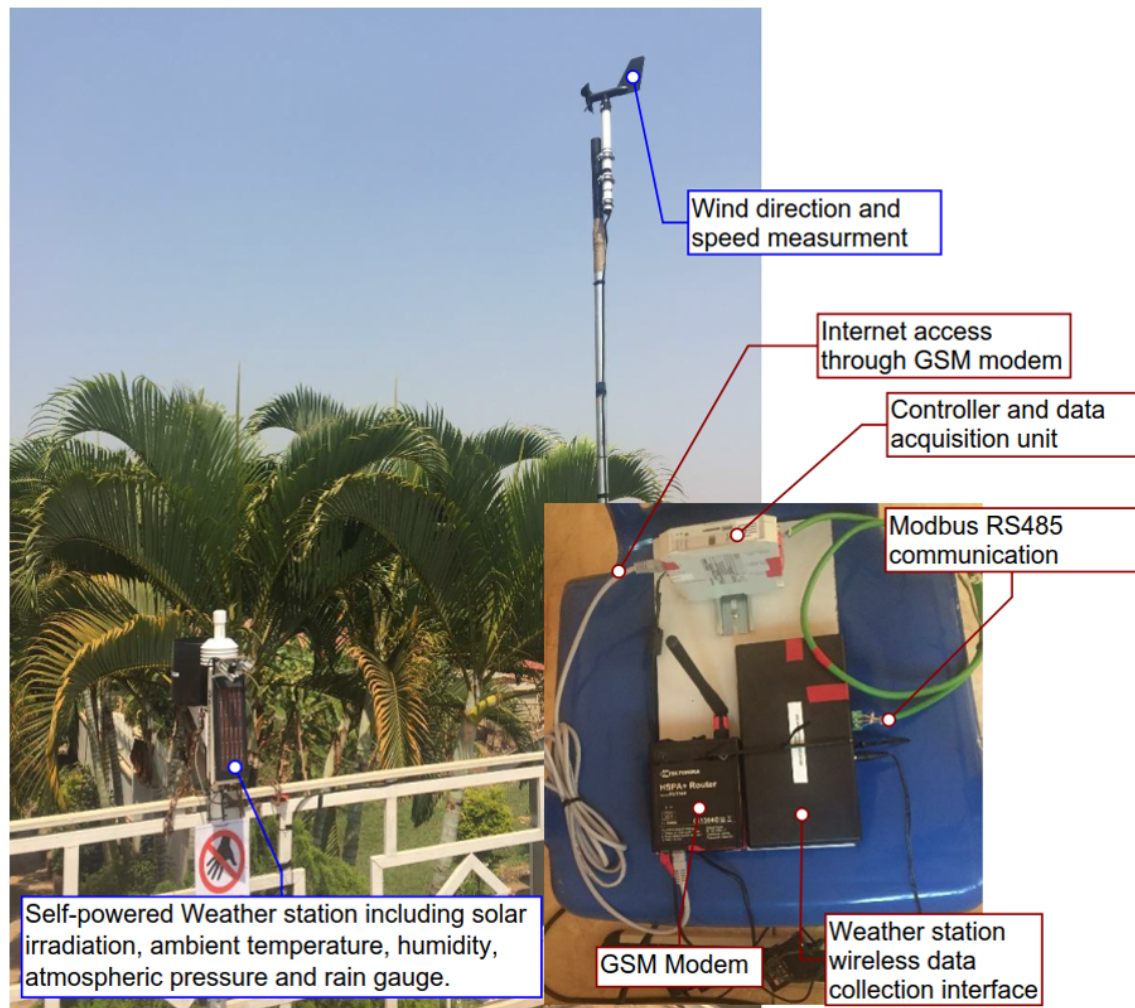


Figure 4.24: Weather station and remote data acquisition commissioning and hot-running test in Uganda, Jinja.

Figure reference: Author's figure, published in [1].

- v Identify real risk potentials and possible practical mitigation methodologies for them.
- vi Have an early estimation of the bottle-necks in the project life-cycle which can have major influence on the estimated project work break-down-structure and time-line.

Figure 4.24 shows the deployment of the weather station and the remote data acquisition system, including a GSM modem for providing internet connection in Uganda. The weather station is installed for the hot-running test in a near secured testing location to its planned final installed location in the Sofraa organization school. It is planned that the weather station will be transferred to the final installation location once the school starts its full operation, which is planned for this year (2019). The weather station is self-powered using a PV panel and integrated battery for powering the sensors and externally installed components. The measured data from the sensors

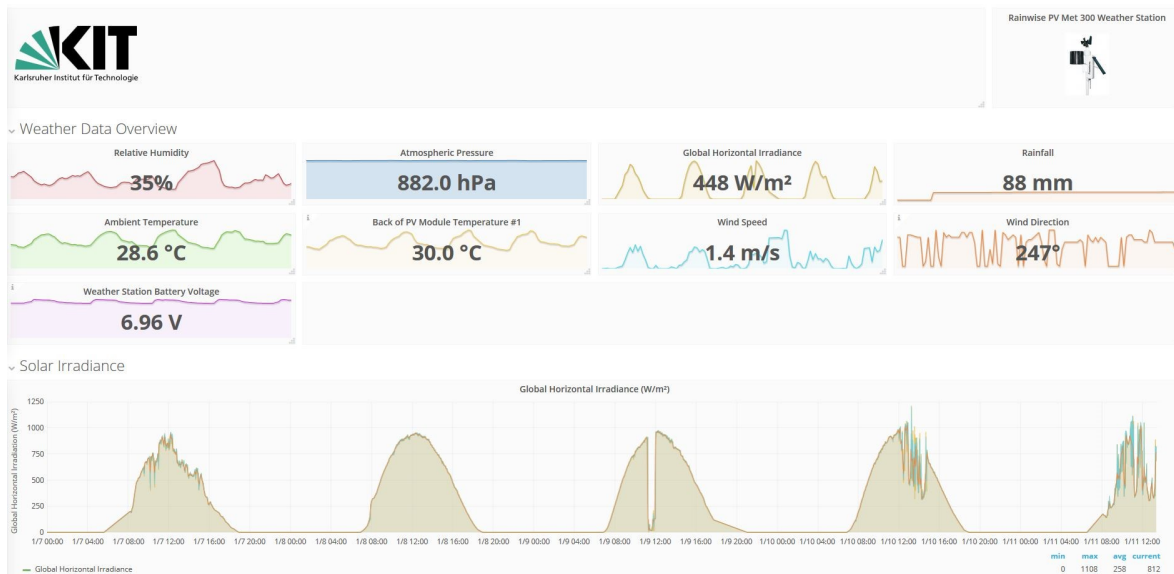


Figure 4.25: Data monitoring and analysis portal for remote SMWS

Figure reference: Uganda online monitoring portal, developed in cooperation with our industrial partner Ferntech [60].

in the weather station is transferred using wireless communication to the weather station wireless receiving unit installed indoor. The data is transferred to the data acquisition and control unit using Modbus RS485 protocol. A GSM modem using the local GSM network provide Internet communication for the data transfer from the data acquisition and control unit to the data-bank. The data can be accessed and downloaded using an online web portal. Figure 4.25 shows a real example of how the data is illustrated on the web portal based on the data transferred from the weather station in Uganda. The SMWS and the data portal is developed in cooperation with our industrial partner Infinite Fingers [60].

4.6.1 Installation and commissioning of weather station in its final location

Since 2019 the Uganda weather station has been transferred and is operating at its final installation location at the Sofraa School in Wakisi – Jinja.

As shown in figure 4.26, the weather station was installed on the rooftop of the school’s main administrative building as it is the safest location away from the direct contact or reach of students. The wind measurement sensor was installed few meters away from the main weather station, about four meters above the height of the rooftop where a potential installation location for a small wind turbine is. The wind measurement total hub height is 13 meters above ground level.

The installation was completed with the support of our local case study partner Sofraa Organization, who provided us with the necessary on-ground logistical support and materials needed. Tthe organization also provided us with local team members who have been trained for supporting the capacity needed for the installation as part of our local capacity building plan. The local team was also trained for the troubleshooting of



(a) weather station installation in its final location
 (b) Final rooftop installation of the weather station in the Uganda case study

Figure 4.26: Uganda case study - weather station installation and commissioning in its final location at Sofraa school.

Figure reference: Author's figure.

the weather station's different components. Figure 4.27 show part of the local activities for the installation and capacity building in Uganda case study.

Side activities and objectives during site visits

Weather station irradiance sensors functionality testing: Due to the harsh conditions, especially regarding dust accumulation, it was necessary to check the effects of this environment on sensitive sensors as the irradiance sensors. Before the re-allocation of the weather station in its final location, a validation process for both installed irradiance sensors was done. The validation was carried out by comparing the measurements of each sensor against the measurements of a brand new irradiance sensor used at the same orientation and tilt angle of the installed ones. The validation process results was positive and no measurement differences were found between the installed and the new irradiance sensor used for validation.

Raising local awareness about the project activities: One of the key factors for success in rural areas in a developing economy country such as the Uganda case study is the local social acceptance and support for the ongoing activities, especially if it is carried out through a third party. This was taken into consideration and planned to be part of the side activities carried out during the site visits. Raising awareness about the benefits of electrical energy access and the hybrid systems components was very necessary especially for the students of the school who will get to benefit from the electrical energy access, and get to know the hybrid system.

System deployment current status

The installation of the weather station in its final location was planned as the first phase of the hybrid system as in the case for the Canada case study. The system installation was planned at the end of the second quarter of 2020, however the system deployment



(a) Local technicians training for the installation of the wind met mast and weather station parts



(b) Local technicians training for weather station trouble-shooting



(c) Introducing installed parts functionalities for school students and teachers



(d) Raising awareness regarding renewable energy for school students

Figure 4.27: Uganda case study - weather station part of the local capacity building activities.

Figure reference: Author's figure.

had to be put on hold due to the global pandemic. The effect of the global pandemic was dramatic on the project plans as there was local country shut down in Uganda and very high travel restrictions, besides the other high health risks. In addition, material and supplier availability were also affected negatively. Under these conditions the last stage of the Uganda hybrid system integration, testing and commissioning was not possible to be carried out as planned.

4.7 Highlight on the major differences experienced between the case studies in Canada and Uganda

Through the on-ground activities carried out during the study period, it was clear that there are major differences between the two case studies. Each case study had its own challenges, some of which common between both of them, but others were unique. In the following section, we highlight some of the differences between the experience and

challenges faced between the case studies.

More reported technical problems from Uganda case study compared to Canada case study

In the Canada case study a complete hybrid system was installed, whereas only the first part of the system was installed in Uganda, which is the weather station. The amount of reported technical problems from the Uganda case study was more during the first year of operation than from the Canada case study. In fact, there were no reported major technical problems reported related to the Canada case study system. However, many failure cases were reported from the Uganda case study due to many reasons, which can be summarized as:

- Data flow loss due to loss of internet connection (through GSM modem).
- Hardware failure in the weather station: For example defects in the weather station integrated small powering battery, which leads to communication and measurements loss over night periods where there is no solar power available for powering the weather station through its integrated solar panel.
- Other hardware failures which lead to missing data collection.

It is important to mention that the support of our local partner in Uganda was remarkable for overcoming the technical problems in a very good response time. One of the reasons which can explain such a difference is the level of awareness of the end-users regarding off-grid and decentralized systems operation and troubleshooting. In the Canada case study, the end-user had a very high level of technical experience and awareness of the system operation requirements. However in Uganda this knowledge is very limited, and it was exclusively built up through the technical training conducted on site during our site visits.

Logistics handling

Even though logistics had many common challenges for both case studies. However, the logistics handling for the Uganda case study was much more challenging than the case of Canada. This was mainly due to two main factors:

- i The customs clearance handling, even for the tax exempted goods such as the renewable energy system parts. For example, when the weather station was shipped to Uganda, all documents required were provided with the shipment and it was expected to arrive a few months before our first site visit to the final case study remote location. However, we had to pick up the weather station ourselves from the customs location in Kampala airport and finalize the local customs requirements that could not be clarified from our global logistics partner. This involved very long local travelling hours from the remote case study area to the main airport in Kampala, extra unplanned costs and losing few days from our site visit in clarifying the shipment status and location.

- ii Defected parts during the transport process of the PV panels. Many PV panels were defected in the two shipments made to Uganda. Even though air shipment was used for both shipments, defected panels were always reported after the shipment opening in the final case study location.

These issues were more prevalent for shipment to to Uganda case study even though the total shipping distance for the Canada case study was longer. The parts that were defected during the shipping and logistics to Canada were very few compared to what was reported from Uganda.

Lack of information in the early planning stage

Gathering required information related to each case study in the early study stages was much easier and more reliable for Canada than for the Uganda case study. A clear example was gathering reliable information related to load curves and local conditions could be done through remote communication in the case of Canada. On the other hand, to reach the same level of information in Uganda required an early site visit. This made handling both case studies very different in terms of the investment of effort, and the communication methods.

5 HOTE M: Hybrid off-grid and decentralized system Techno-Economic model

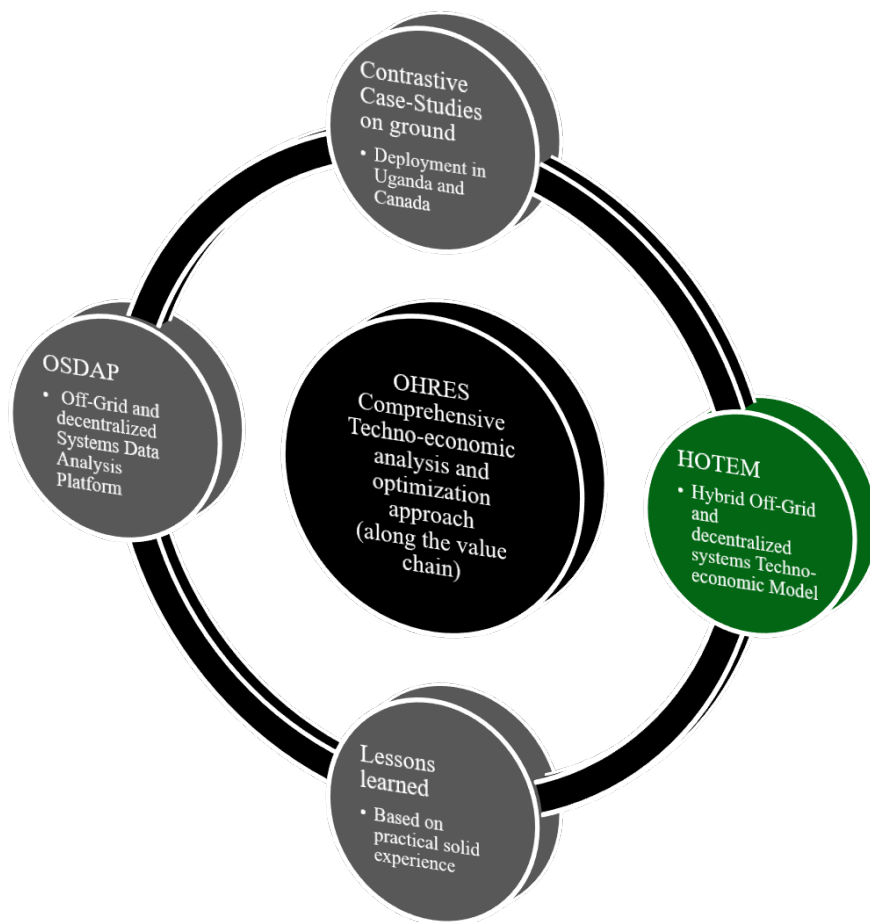


Figure 5.1: Second building block of OHRES Comprehensive Techno-economic analysis and optimization approach - HOTE M.

Chapters 2, 3, and 4 covered in details the first building block of the comprehensive approach related to the contrastive case studies and the off-grid hybrid systems deployment. Chapter 5 covers all details related to the second building block shown in figure 5.1, which is related to off-grid and decentralized systems techno-economic modeling and sizing tool development. This chapter will cover in detail the Hybrid off-grid and decentralized system Techno-Economic model (HOTE M) structure and development aspects.

Chapter 5 includes four sections: Section 1 covers HOTEM structure and development methodology. Section 2 address HOTEM optimization targets and power dispatch strategy. Section 3 covers a case study description where HOTEM is used for system sizing, and the modelling results. Section 4 presents a benchmarking for HOTEM against a commercially used tool (HOMER) for off-grid and decentralized hybrid systems techno-economic analysis and system sizing.

The work presented in chapter 5 is related to stages 3 and 4 of the hybrid systems development phase presented before in figure 1.2.

HOTEM is a techno-economic assessment model for off-grid and decentralized hybrid systems. It is a system sizing and economic evaluation software tool, which is used for the sizing and assessment of electrical energy systems which are not grid connected. This chapter illustrate the technical details related to HOTEM and its sub-models used for the different hybrid system components.

The content of this chapter is based on the supervised scientific work of Iqbal et al. [7], and Awad et al. [6], and part of its content is from the author's published work in Elkadragy et. al [5].

5.1 HOTEM structure and development methodology

The Hybrid Off-grid and decentralized systems Techno-Economic Model (HOTEM) presented here is based on a reference model originally developed by Bonhanazard [65] and adopted by Marcelino et. al [30]. The internally developed model is called Hybrid Micro Grid Systems (HMGS). The HMGS model optimization aims to minimize the loss of power supply probability (LPSP), the levelized cost of electricity (LCOE) and to increase the share of renewables within grid-connected systems. This is achieved by finding the best composition of generation units and optimum energy storage operation mode under the given optimization goals. An alternative algorithm called "Canonical particle swarm optimization Algorithm" is used to solve this optimization problem. C-DEEPSO is a new population-based method built upon swarm intelligence and differential evolutionary technique. It is used as a solving algorithm instead of an original particle swarm optimization due to a higher robustness of results [66]. More details about the C-DEEPSO algorithm and its properties as wells as the HMGS model can be found in [30], [67], [66], [68] and [69].

The main objective of HOTEM is to perform an hourly based optimization to minimize the Cost of Electricity (COE) and Loss of Power Supply Probability (LOLP) as well as maximize the share of locally available renewable generated electricity (RE_{factor}). This can be achieved by optimally adjusting the install capacity of the PV panels, wind turbines, diesel generator and battery capacity based on hourly demand and available primary energy resources. The original model described by Marcelino et al. [30] is a grid-connected hybrid system that uses the C-DEEPSO algorithm [66] in combination with multi-criteria decision making tools.

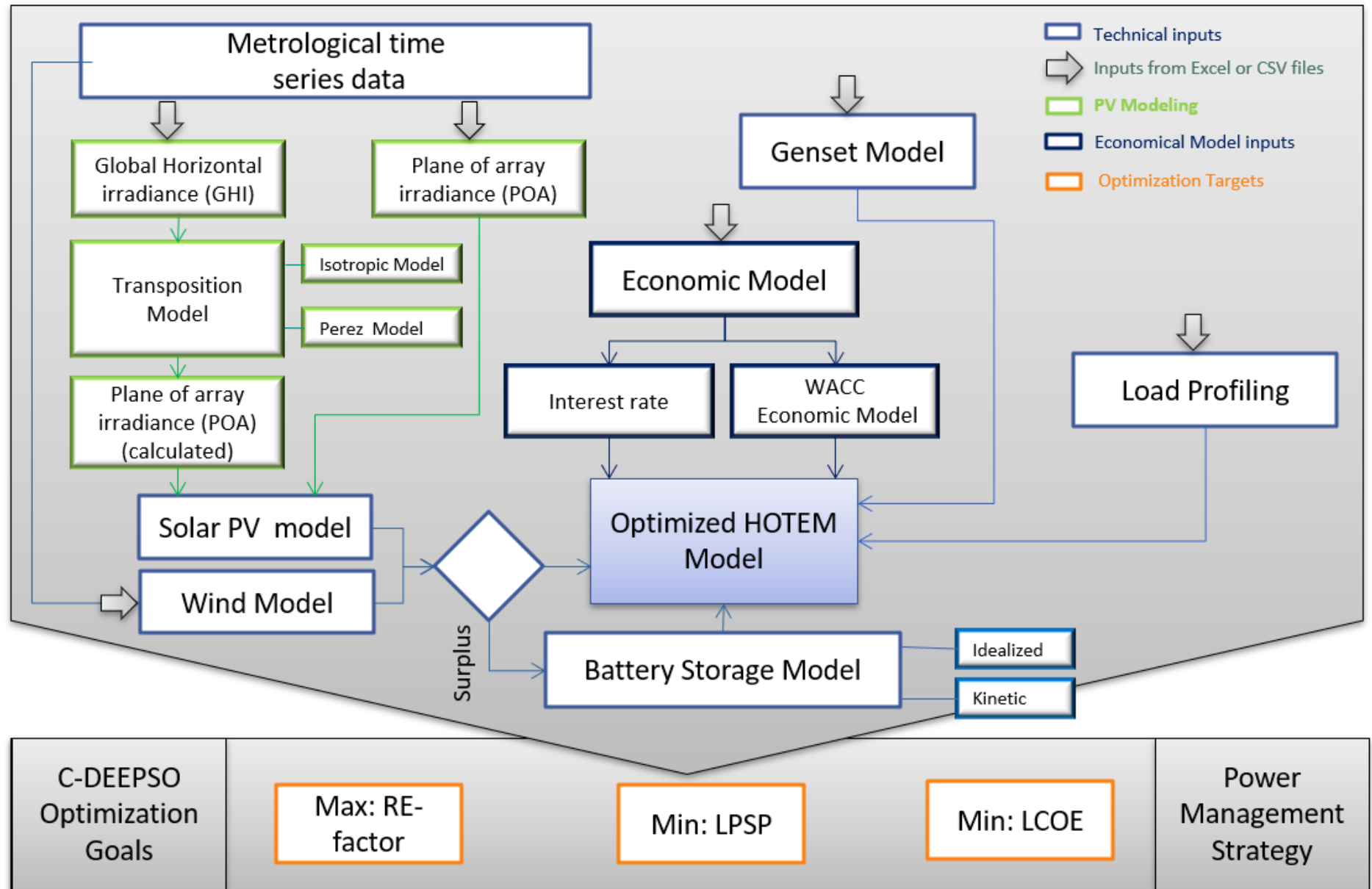


Figure 5.2: HOTEM layout and sub-models structure.

Figure reference: Author's illustration, published in [5] and supervised work [7].

Marcelino et al's model is totally reformulated to achieve the current reliable HOTEEM status for an off-grid and decentralized hybrid system. Gen-set is modeled as a back power source. The modeling makes sure that whenever a Generator is required, it operates at full capacity, and surplus power charges the battery bank. Furthermore, the transposition model is developed to convert Global Horizontal Irradiance (GHI) to Plane of Array Irradiance (POA) by any define slope and azimuth angle. For a better performance of the storage system, an idealized battery model is designed for lithium-ion batteries to protect them for overcharging and discharging.

A load management system is introduced to add randomness to the load to generate a more realistic load profile.

A new Weighted Average Cost of Capital (WACC) model is developed for a better economic analysis and a mechanism to determine the replacement cost of each component of the hybrid system is also introduced.

A complete scheme of HOTEEM is presented in Figure 5.2. In the following sections, detailed description of HOTEEM used models and operation description is presented.

5.1.1 PV modeling

The output of a solar array depends on solar irradiance which that is mostly measured in a horizontal plane. A solar array can be placed on a tilted surface to receive maximum sun irradiance that eventually maximizes the PV output power. To calculate solar irradiance from GHI depending on the title angle. The mathematical formulation to calculate the PV output is given in Eq. (5.1) [70]. This calculation method is commonly used also by commercial modelling tools such as HOMER Energy for example. The difference between HOTEEM difference fromand HOMER is the calculation of cell temperature. HOMER has its own mathematical relations to calculate the cell temperature wWhile in HOTEEM tThe cell temperature T_c is calculated through Eq. (5.2) [70].

$$P_{power} = P_r \times D_r \times \left(\frac{G_T}{G_{ref}}\right) \times [1 + K_T(T_c - T_{ref})] \quad (5.1)$$

where;

P_{power} = Solar PV power output [kW]

D_r = PV derating factor [%]

P_r = Rated power at reference condition [kW/m²]

G_T = Solar radiation received on plane in current time step [kW/m²]

G_{ref} = Solar radiation at reference condition [$G_{ref}= 1kW/m^2$]

K_T = Temperature coefficient of the maximum power

T_c = Cell temperature [°C]

T_{ref} = Cell temperature at reference condition [$T_{ref} = 25^\circ\text{C}$]

$$T_c = T_{amb} + (0.0256 \times G_T) \quad (5.2)$$

where;

T_c = Cell temperature [°C]

T_{amb} = Ambient temperature [°C]

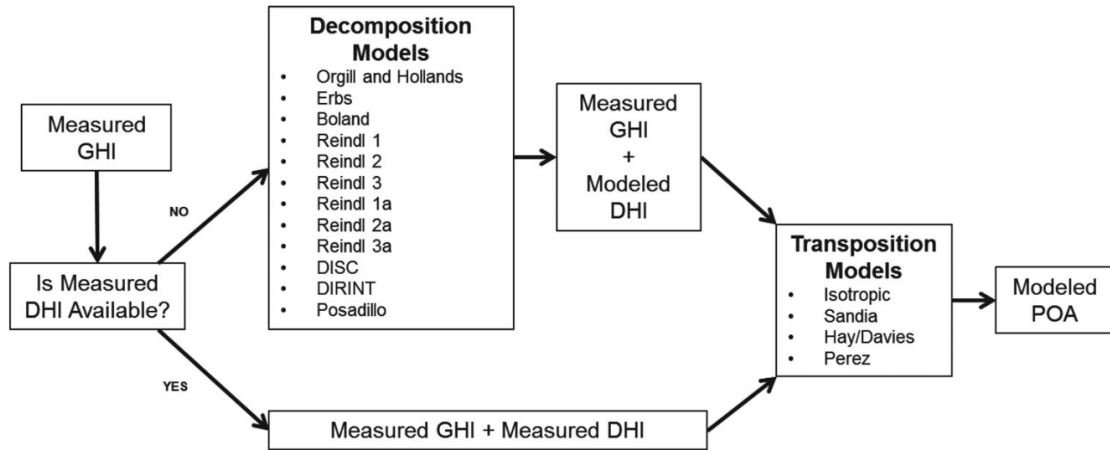


Figure 5.3: Flowchart of modeling POA irradiance from measured GHI [2].

G_T = Solar radiation received on plane in current time step [kW/m^2]

In the best case scenario, measured high-resolution irradiance data would be available for the p Plane-of-array (POA) in the location of the hybrid system installation. The POA measurement also has to must have the same tilting angle and azimuth angle of the planned installed PV array, in order to have a realistic PV power production calculation from the modelling tool. However, as most irradiance measurements from satellite or installed on ground radiance measurements and data are available for global horizontal irradiance (GHI), this represented a necessity in case of including necessitated the inclusion of transposition models in HOTEM in order to estimate the Plane-of-array (POA) irradiance from the GHI. Many transpositions models are available such as REINDL, ISOTROPIC, PRERZ, HAY/DEVIES, and SANDIA, as shown in figure 5.3 [2].

HOTEM transposition modelling is based on two transposition models, isotropic and Perez. According to [71], the isotropic model performs better at smaller tilt angel while for larger tilt angle Perez model has a better performance. So an angle of 40 degree is selected as the threshold point below which HOTEM follows the isotropic model and for tilt angle above or equal to 40 degree HOTEM follows the Perez model. Other commercial PV modelling specialized tools as *PVsyst*[72] software also uses Perez transposition model to calculate the Plane of array irradiance (irradiance at any tilt and azimuth angle), other modelling tools as *HOMER Energy*[51] uses REINDL model.

Transposition model:

To calculate the irradiance at tilt angle from GHI, the following steps are involved [73]:

1. Decomposition of GHI into direct and diffuse components expressed as diffuse horizontal irradiance (DHI) and direct normal irradiance (DNI).
2. Transposition of these components to POA of the modules.

The mathematical modeling implemented in HOTEM to determine POA is formu-

lated as follows [74] [73]:

$$G_{POA} = G_{d,t} + G_{b,t} + G_{r,t} \quad (5.3)$$

where;

G_{POA} = Plane of array irradiance [W/m^2]

$G_{b,t}$ = Beam component of solar irradiance [W/m^2]

$G_{r,t}$ = Ground reflected component of solar irradiance [W/m^2]

$G_{d,t}$ = Sky diffuse component of solar irradiance [W/m^2]

The following section describes the determination of each component of the POA irradiance adopted. The complete PV modeling including the transposition model is summarized in Figure 5.4.

Beam irradiance component

The beam irradiance is the component of sunlight which directly falls on the solar module making an incident angle to the normal of the plane.

It can be calculated using the direct normal irradiance and angle of incident [75].

$$G_{b,t} = DNI \times \cos(AOI) \quad (5.4)$$

where;

DNI = Direct normal irradiance [W/m^2]

AOI = Solar angle of incidence on module plane [$^\circ$]

Direct normal irradiance (DNI) can be estimated with the help of global horizontal irradiance [75].

$$DNI = \frac{GHI - DHI}{\sin\theta_z} \quad (5.5)$$

where;

GHI = Global horizontal irradiance [W/m^2]

DHI = Diffuse horizontal irradiance [W/m^2]

θ_z = Sun zenith angle [$^\circ$]

Angle of incidence (AOI) is the angle between the sun beam and the PV plane, which can be estimated as [2]:

$$AOI = \cos^{-1} [\cos(\theta_Z)\cos(\theta_T) + \sin(\theta_Z)\sin(\theta_T)\cos(\theta_A - \theta_{ar})] \quad (5.6)$$

where;

θ_z = Sun zenith angle [$^\circ$]

θ_A = Sun azimuth angle [$^\circ$]

θ_T = Surface tilt angle of array [$^\circ$]

θ_{ar} = Azimuth angle of the array [$^\circ$]

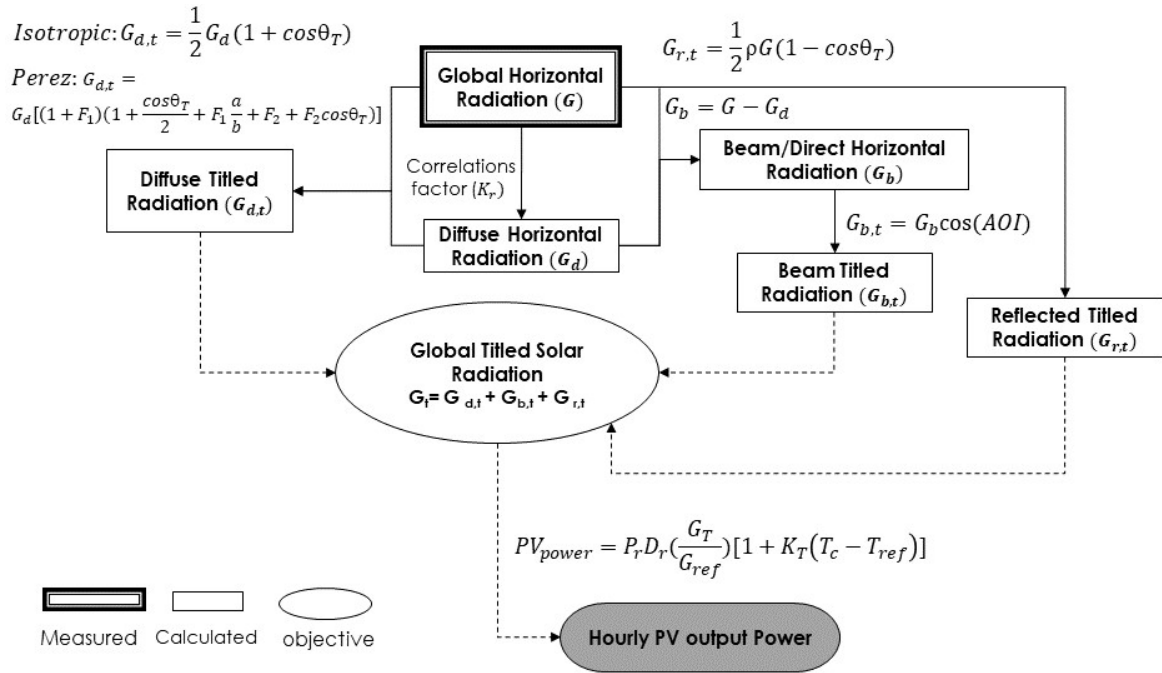


Figure 5.4: Solar irradiance Transposition model for the calculation of POA from GHI. Figure reference: Author's publication [5], and supervised work [7].

Ground reflected component

The ground reflected component is the irradiance that the solar plane received after reflecting off the ground. It can be calculated as follow [76]:

$$G_{r,t} = GHI \times \rho * \frac{1 - \cos\theta_T}{2} \quad (5.7)$$

where;

ρ = Ground albedo

θ_T = Surface tilt angle of array [°]

Ground albedo is the ratio of GHI incidence on the ground to that reflected. Its value varies from 0 to 1 depending on the properties of the ground. In HOTEM the value of albedo is by default fixed to 0.2.

Sky diffuse component

Two different transposition models are designed in HOTEM to calculate the sky diffuse component.

Isotropic sky diffuse model

The isotropic model is based on the assumption that the diffuse irradiance from the sky dome is uniformly distributed across the sky dome [77], it is calculated as follows:

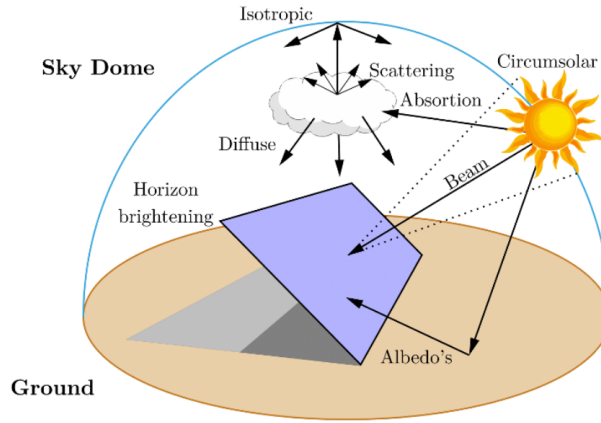


Figure 5.5: Solar beam (direct), sky-diffuse, and ground-reflected radiation on an inclined planar surface [3].

$$G_{d,t} = DHI \times \frac{1 + \cos\theta_T}{2} \quad (5.8)$$

where;

$G_{d,t}$ = Isotropic sky diffuse irradiance [W/m^2]

θ_T = Surface tilt angle of array [$^\circ$]

Perez sky diffuse model

The Perez sky diffuse model allows a more detailed analysis in relation to the isotropic model by considering the effect of horizon and circumsolar horizon brightening components that were neglected in the isotropic model (Figure 5.5). This leads to two empirical functions F1 and F2, then finally summed up to calculate the total sky diffuse irradiance [77]. The mathematical formulation is described in Eq. (5.9)

$$G_{d,t} = DHI \times \left[(1 - F1) \left(1 + \frac{\cos\theta_T}{2} + F1 \frac{a}{b} + F2 \sin\theta_T \right) \right] \quad (5.9)$$

where;

$G_{d,t}$ = Perez sky diffuse irradiance [W/m^2]

F1 = Circumsolar coefficients

F2 = Horizon brightness coefficient

Coefficients a and b take into account the incidence angle of the sun on the considered slope. These terms are computed in Eq. (5.10) and Eq. (6.10).

$$a = \max(0, \cos\theta) \quad (5.10)$$

$$b = \max(\cos 85, \cos\theta_z) \quad (5.11)$$

The brightness coefficients F1 and F2 depends on two conditions of sky which are Clearness ϵ and brightness δ , as defined in Eq. (5.12) and Eq. (5.13) [77].

$$\epsilon = \frac{\frac{DHI+GHI}{DHI} + 5.53 \times 10^{-6}\theta_Z^3}{1 + 5.53 \times 10^{-6}\theta_Z^3} \quad (5.12)$$

$$\delta = AM \times \frac{DHI}{E_a} \quad (5.13)$$

where;

AM = Air mass

E_a = Extraterrestrial Irradiance [W/m²]

The coefficients F1 and F2 are then computed in Eq. (5.14) and Eq (5.15).

$$F1 = \max \left[0, \left(\rho_{11}, \rho_{12} + \frac{\pi\theta_z}{180}\rho_{13} \right) \right] \quad (5.14)$$

$$F2 = \rho_{21} + \rho_{22} + \frac{\pi\theta_z}{180}\rho_{23} \quad (5.15)$$

The coefficient $\rho_{11}, \rho_{12}, \rho_{13}, \rho_{21}, \rho_{22}$ and ρ_{23} are based on statistical analysis.

Perez has published a number of different versions of the coefficients ρ fitted to various data sets [78, 79]. One set of the coefficients was used for HOTEM as given in table 5.1.

Table 5.1: Perez model coefficients for irradiance (Author's publication [5]).

ϵ bin	ρ_{11}	ρ_{12}	ρ_{13}	ρ_{21}	ρ_{22}	ρ_{23}
1	-0.008	0.588	-0.062	-0.06	0.072	-0.022
2	0.13	0.683	-0.151	-0.019	0.066	-0.029
3	0.33	0.487	-0.221	0.055	-0.064	-0.026
4	0.568	0.187	-0.295	0.109	-0.152	-0.014
5	0.873	-0.392	-0.362	0.226	-0.462	0.001
6	1.132	-1.237	-0.412	0.288	-0.823	0.056
7	1.132	-1.237	-0.412	0.288	-0.823	0.056
8	0.678	-0.327	-0.25	0.156	-1.377	0.251

5.1.2 Wind turbine

The output of wind turbines is highly affected by the hub height (h_2). and the surface conditions (α). Therefore, the measured wind speed at anemometer height (h_1) must be converted corresponding to the desired hub heights. HOTEM uses the power-law equation given in Eq. (5.16) [80] [30] to calculate the wind speed at a given hub height.

$$\frac{V_2}{V_1} = \left(\frac{h_2}{h_1} \right)^\alpha \quad (5.16)$$

The power output of the wind turbine in HOTEEM is approximated according to the following relation described in Eq. (5.17) [80] [30].

$$\begin{cases} 0, & V_{c-out} < V < V_{c-in} \\ V^3 \left(\frac{P_r}{V_r^3 - V_{c-in}^3} \right) - P_r \left(\frac{V_{c-in}^3}{V_r^3 - V_{c-in}^3} \right), & V_{c-in} < V \leq V_r \\ P_r, & V_r \leq V \leq V_{c-out} \end{cases} \quad (5.17)$$

where;

V_{c-in} = Cut in velocity

V_{c-out} = Cut out velocity

V_r = Nominal wind velocity

V = Wind velocity in current time step

P_r = Rated power

5.1.3 Battery storage system

Two generic battery models are used in HOTEEM: the Idealized Battery Model and the Kinetic Battery Model (KBM). Both battery models can be used within HOTEEM to model Lead-acid and Li-ion batteries. Both models are also used in the Hybrid battery storage system modeling in HOTEEM as illustrated later in the current section.

The idealized model treats the battery bank like a tank of charge. It removes and adds the charges as shown in figure 5.6 according to the equations given below [4]:

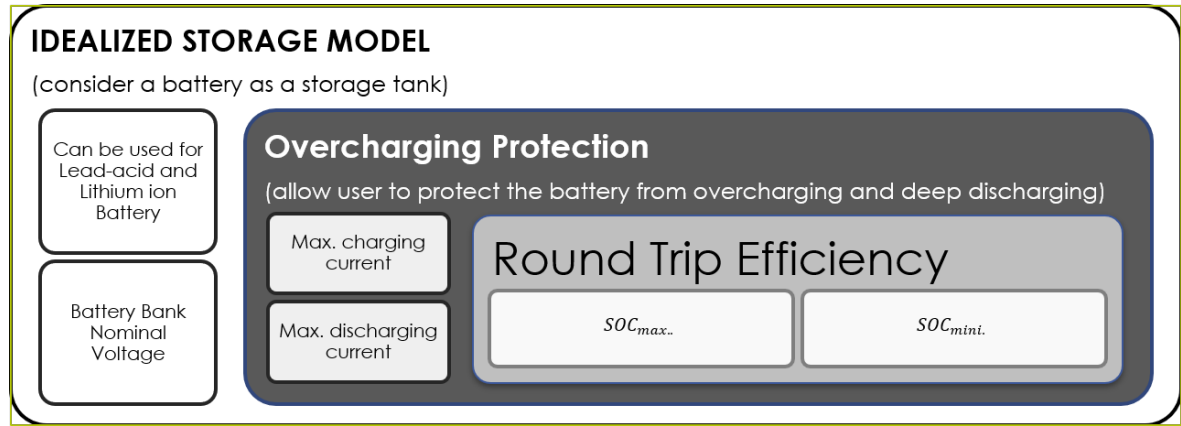


Figure 5.6: Idealized battery model overview.

Figure reference: Author's illustration, based on the description in [4].

Charging:

$$q_t = q_{t-1} + I\Delta t \quad (5.18)$$

Discharging:

$$q_t = q_{t-1} - I\Delta t \quad (5.19)$$

where;

- t = time in hours [h]
 q_t = battery capacity at time t [Ah]
 I = charging / discharging current [A]
 Δt = time step in hours [h]

The Kinetic Battery Model (KBM) treats the battery bank as two tanks with a conductance in between, and it is used to account for modeling Peukert's law which expresses the changes in the battery's available capacity concerning the different discharge current rates (as shown in the results example in figure 5.8). As shown in the KBM representation in figure 5.7 one tank holds the immediate available capacity q_1 and the other tank contains the chemically bound capacity q_2 , where k' represent the conductance between the two charge tanks defining the relation between the bounded capacity and the available capacity (where it can represent also the charge and discharge different C-rate used in Li-ion batteries). Both tanks have different widths, the c represents the width of the available tank, and $1 - c$ that of the bound one. R_0 represents the constant internal resistance, and I is the battery current [81].

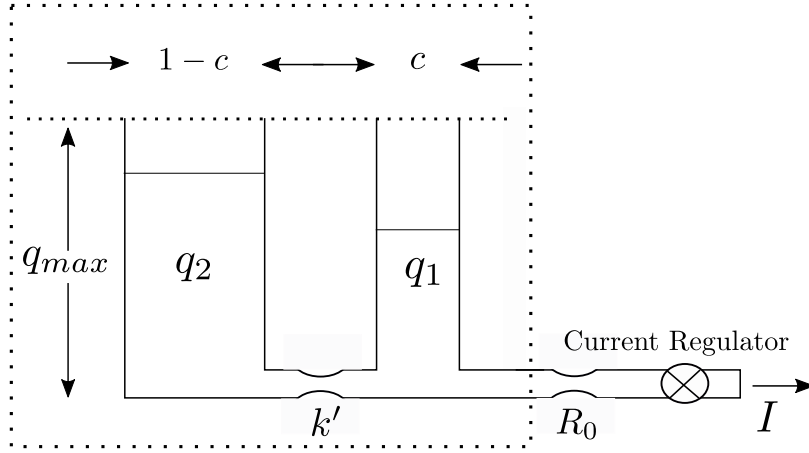


Figure 5.7: Kinetic battery model representation.
Figure reference: Source [81]

Each time step, the model calculates both quantities and the total charge q as follows [81]:

$$q_1 = q_{1,0}e^{-k\Delta t} + \frac{(q_0kc - I)(1 - e^{-k\Delta t})}{k} - \frac{Ic(k\Delta t - 1 + e^{-k\Delta t})}{k} \quad (5.20)$$

$$q_2 = q_{2,0}e^{-k\Delta t} + q_0(1 - c)(1 - e^{-k\Delta t}) - \frac{I(1 - c)(k\Delta t - 1 + e^{-k\Delta t})}{k} \quad (5.21)$$

$$q = q_1 + q_2 \quad (5.22)$$

where;

q_1	= available charge [Ah]
q_2	= bound charge [Ah]
q	= total charge [Ah]
$q_{1,0}$	= available charge at beginning of time step [Ah]
$q_{2,0}$	= available charge at beginning of time step [Ah]
q_0	= total charge at beginning of time step [Ah]
k	= rate constant [h^{-1}]
c	= capacity ratio [-]

Capacities for at least three different discharge rates are required from the battery manufacturer's data sheet, to calculate the values for k and c . The user is requested to enter the value for the capacities and their correspondent discharge rates in an excel sheet. From these values the following ratio for different capacities can be calculated [81]:

$$F_t = F_{t_1, t_2} = \frac{q_{T=t_1}}{q_{T=t_2}} \quad (5.23)$$

where;

$q_{T=t}$ = discharge capacity at discharge time $T = t$ [Ah]

Using equation (5.24) [81] the values for c and k can be determined as follows:

$$c = \frac{F_t(1 - e^{-kt_1})t_2 - (1 - e^{-kt_2})t_1}{F_t(1 - e^{-kt_1})t_2 - (1 - e^{-kt_2})t_1 - kF_t t_1 t_2 + kt_1 t_2} \quad (5.24)$$

Equation (5.24) is calculated for the same value of k (range from 0 to 1) twice, each time for a different value for F_t (for example, $F_{1,10}$ and $F_{1,20}$). When the same result (c) for the two calculations is obtained, these values are the k and c to be used for the model. If more values for F_t are available, a least square fit is applied to obtain best values for c and k by using equation (5.25) [81]:

$$F_{t_1, t_2} = \frac{t_1((1 - e^{-kt_2})(1 - c) + kct_2)}{t_2((1 - e^{-kt_1})(1 - c) + kct_1)} \quad (5.25)$$

Using the c and k values, the maximum theoretical capacity of the battery can be estimated using a slow discharge rate value (e.g. 20-hour discharge rate):

$$q_{max} = \frac{q_{T=20}((1 - e^{-20k})(1 - c) + 20ck)}{20ck} \quad (5.26)$$

Moreover, the maximum charge and discharge current for a time step can be calculated:

$$I_{d,max} = \frac{kq_{1,0}e^{-k\Delta t} + q_0kc(1 - e^{-k\Delta t})}{1 - e^{-k\Delta t} + c(k\Delta t - 1 + e^{-k\Delta t})} \quad (5.27)$$

$$I_{c,max} = \frac{-kcq_{max} + kq_{1,0}e^{-k\Delta t} + q_0kc(1 - e^{-k\Delta t})}{1 - e^{-k\Delta t} + c(k\Delta t - 1 + e^{-k\Delta t})} \quad (5.28)$$

The required battery capacity measured in kWh of the system is designed depending on the load demand and autonomy days given in equation (5.29).

$$E_b = \frac{E_L \times AD}{\eta_{inv} \times \eta_b \times DOD} \quad (5.29)$$

where;

- E_b = Required battery capacity [kWh]
- E_L = Load demand [kWh]
- AD = Days of Autonomy
- η_{inv} = inverter efficiency
- η_b = Battery efficiency
- DOD = Depth of discharge [%]

DOD depends on the SOC_{min} and SOC_{max} and is measured as:

$$DOD = \frac{(100 - (SOC_{min} + (100 - SOC_{max})))}{100} \quad (5.30)$$

where;

- SOC_{min} = minimum state of charge of battery
- SOC_{max} = maximum state of charge of battery

DoD is calculated for each time step t , considering the given boundaries of the SOC_{min} and SOC_{max} .

HOTEM uses both idealized and Kinetic battery models for modeling different battery technologies (mainly lead-acid and Li-ion) where the user can choose which model to be used for which battery technology. In our case studies modeling represented Idealized model is used for Li-ion battery modeling, as it is in most cases challenging to get the required level of detailed parameters from Li-ion battery manufacturing data sheets to fulfill the kinetic model modeling required parameters. Also, HOMER Energy uses in its standard Li-ion battery library idealized battery model for different battery manufactures. On the other hand, for lead-acid batteries the kinetic battery model is used as the provided details regarding the battery behavior parameters are fulfilling what is required for the KBM. Figure 5.8 shows an example of the KBM modeling and the peukert's effect for a lead-acid battery model, compared to the manufacturer datasheet (Hoppecke SUN Power VR M 6-250 [48]) provided for the lead-acid battery selected to be used for our OHRES in Uganda and Canada Case studies. In the hybrid lead-acid and Li-ion battery modelling, both battery models can be used based on user preference. Where in our case study presented as mentioned idealized model and KBM, are used for Li-ion and Lead-acid respectively in the HBESS.

The following modelling features as degradation, battery voltage modelling and temperature effect modelling can be used in HOTEM for the different battery technologies as well (lead-acid or Li-ion), also can be included in the hybrid battery storage modelling.

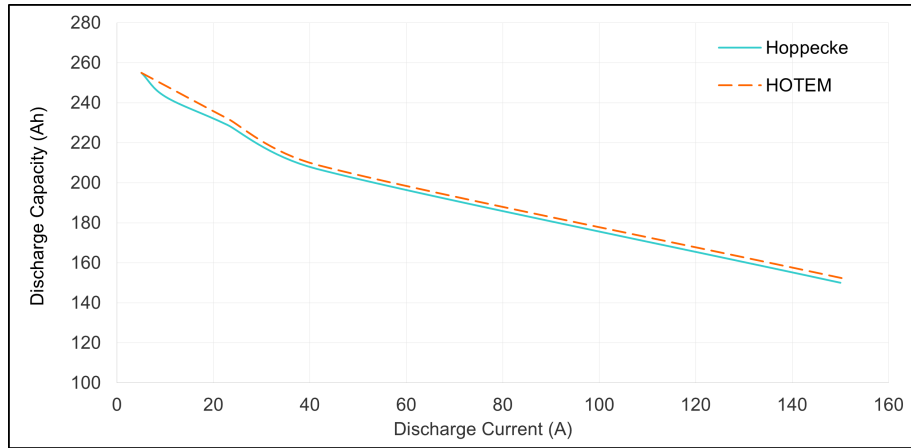


Figure 5.8: KBM modelling and the peukert's effect for a lead-acid battery results compared to the manufacturer datasheet for our OHRES selected case-studies lead-acid battery (Hoppecke SUN Power VR M 6-250).

Figure reference: Supervised work [6].

Degradation modelling

A rainflow counting algorithm [82] is used for the calculation of battery degradation due to battery cycling charging and discharging. The algorithm calculates both the number and range of cycles done by the battery during the simulation process. The user is required to enter data (available in used battery data sheet) for the number of battery cycles to failure versus depth of discharge DOD . HOTEM builds the relation between the two quantities by Marquardt non-linear least square procedure using equation (5.31). [83]

$$C_F = a_1 + a_2 e^{a_3 R} + a_4 e^{a_5 R} \quad (5.31)$$

where;

C_F = cycles to failure

a_i 's = fitting constants

R = range of cycle (depth of discharge of each cycle)

For each cycle, C_F is calculated. At the end of a simulation the total damage to battery D is calculated:

$$D = \sum_{i=1}^n \frac{1}{C_{F,i}} \quad (5.32)$$

where;

n = total number of cycles during simulation

$\frac{1}{C_{F,i}}$ = fraction of battery life used up during cycle i

When D reaches the value of 1.0, it means the battery is used up completely and needs to be replaced.

Battery voltage Modelling

The voltage model is based on the work in [84]. It is a generic model that requires parameters from the user. The parameters can be extracted from the battery's manufacturer data sheet. The model calculates the battery's terminal voltage in relation to the charge in the battery at each time step t .

Figure 5.9 shows the different parameters required for the model performance.

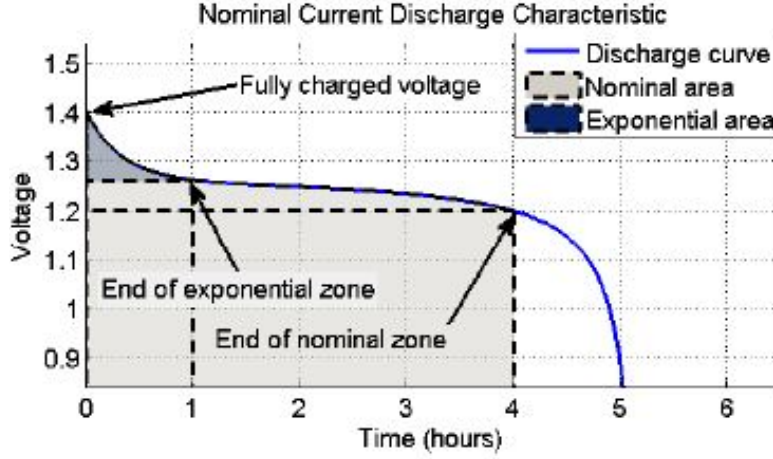


Figure 5.9: Different required parameters for the voltage model
Figure reference: Source [85].

The following equations are used for the calculation of the batteries terminal voltage.

$$V(t) = V_0 - IR - K \left(\frac{q_{full}}{q_{full} - (q_{full} - q(t))} \right) + ae^{-B(q_{full} - q(t))} \quad (5.33)$$

where $V(t)$: terminal voltage at time step t [V]
 V_0 : battery constant voltage [V]
 I : battery current [A]
 R : battery internal resistance [Ω]
 K : polarisation voltage [V]
 q_{full} : capacity at full charge [Ah]
 $q(t)$: capacity at time step t [Ah]
 a : exponential zone amplitude [V]
 B : exponential zone time constant inverse [Ah^{-1}]

$$a = V_{full} - V_{exp} \quad (5.34)$$

$$B = \frac{3}{q_{exp}} \quad (5.35)$$

$$K = \frac{(V_{full} - V_{nom} + a(e^{-Bq_{nom}} - 1))(q_{max} - q_{nom})}{q_{nom}} \quad (5.36)$$

$$V_0 = V_{full} + K + RI - a \quad (5.37)$$

where V_{full} : voltage at full capacity [V]
 V_{exp} : voltage at end of exponential zone [V]
 q_{exp} : percentage of q_{full} that is depleted by the end of the exponential zone [%]

HOTEM use the values in table 5.2 as default values [86] for both technologies lead acid and lithium ion. These values are used in case the required parameters are not given in the battery's data sheet.

Table 5.2: Default values for voltage model parameters used in HOTEM (Supervised work [6]).

	Lead-acid	Li-ion
q_{exp} (%)	0.25	2.17
q_{nom} (%)	90	88.9
V_{full} (V)	2.2	3.6
V_{exp} (V)	2.06	3.4
V_{nom} (V)	2.04	3.2

Temperature effect modelling

Capacity fade due to increase in battery's temperature is calculated in HOTEM. The model uses equation 5.38 to model the relation of the battery life to the battery's temperature.

$$BL = a_1T^2 - a_2T + a_3 \quad (5.38)$$

where BL : battery life percentage [%]
 a_i 's : fitting constants
 T : battery temperature [celsius]

The user enters a minimum of three values for battery life percentage versus battery temperature. HOTEM calculates the fitting constants based on these values and models the relation as shown in figure 5.10

Hybrid battery storage modelling

A hybrid battery storage model is developed. The models for lead acid and lithium ion batteries work next to each other in the same system. Each model works with its separate parameters under the control of a power management strategy. The user enters the data required for the modeling of each battery technology, and additionally, a ratio for the nominal capacity of the lithium ion battery bank to that of the lead acid battery bank. The power management strategy is that the lead acid battery bank serves as the back up in case of discharging and has the priority in case of charging.

In a hybrid battery storage system configuration including Lead-acid and Li-ion batteries, different battery strings technologies shall not be connected directly without the existence of important components which regulate the interaction between both battery technologies. Figure 5.11 shows a simplified configuration of the hybrid system

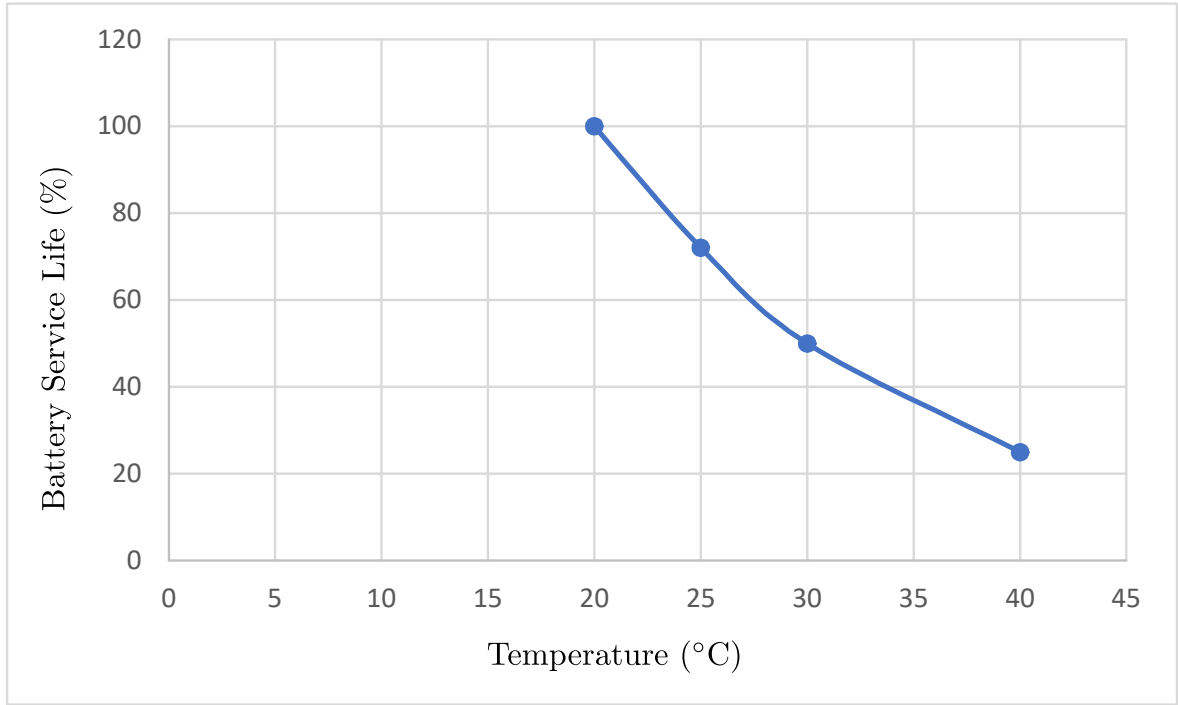


Figure 5.10: Effect of temperature on a Lead-acid OPzV battery lifetime.
Figure reference: Supervised work [6].

used our OHRES system design (which is already implemented in our Canada case-study) that HOTEM is based its hybrid energy storage system modelling on. The hybrid battery storage system was design for 48V DC so the lead-acid and Li-ion batteries both has to be selected to fulfill this voltage level. The lead-acid battery is connected to the main DC bus terminal through a charge controller, which is in practical aspect a part of the Inverter / Charger as descried before in Chapter 4 and shown in figure 4.1. The Li-ion battery is connected in parallel to the lead-acid battery (using internal integrated circuit breaker and protection relays in the li-ion battery), and the flow of energy beside other functionalities as charge, discharge rates of Li-ion, safety related functionaries and operation control aspects is controlled using the internal integrated Battery Management System (BMS), which exists in practical design in each Li-ion battery unit used for our OHRES system.

Equations 5.39 to 5.42 show the necessary calculations for determining the charging and discharging currents of the batteries.

$$I_{c,PbA}(t) = \frac{P_{ch,bus}(t)\eta_{cc}}{V_{PbA}(t-1)} \quad (5.39)$$

$$I_{d,PbA}(t) = \frac{P_{dch,bus}(t)}{V_{PbA}(t-1)\eta_{cc}} \quad (5.40)$$

$$I_{c,LI}(t) = \frac{P_{ch,bus}(t)\eta_{conv}\eta_{cc}}{V_{LI}(t-1)} \quad (5.41)$$

$$I_{d,LI}(t) = \frac{P_{dch,bus}(t)}{V_{LI}(t-1)\eta_{conv}\eta_{cc}} \quad (5.42)$$

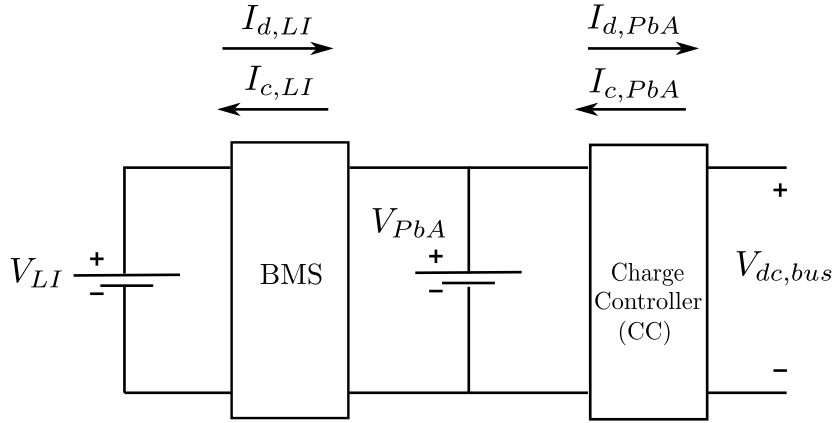


Figure 5.11: Hybrid Battery Energy Storage System (HBESS) simplified architecture and adapted configuration in HOTEM.

where	$I_{c,PbA}(t)$: current charging Lead-acid battery at t [A]
	$I_{d,PbA}(t)$: discharge current from Lead-acid battery at t [A]
	$V_{PbA}(t - 1)$: terminal voltage of Lead-acid battery at $t - 1$ [A]
	$I_{c,LI}(t)$: current charging Li-ion battery at t [A]
	$I_{d,LI}(t)$: discharge current from Lead-acid battery at t [A]
	$V_{LI}(t - 1)$: terminal voltage of Li-ion battery at $t - 1$ [A]
	η_{cc}	: efficiency of charge controller [-]
	η_{conv}	: efficiency of DC-DC converter [-]

The lead-acid and Li-ion battery models are connected in an algorithm shown in Figure 5.12. The model is designed so that the Li-ion do most of the cycling and the Lead-acid is the back up. During charging the Lead-acid battery has the priority and if it is fully charged the Li-ion battery is charged, this is resembled as the Lead-acid battery Charge box. During discharging the Li-ion battery get discharged first, if the Li-ion battery is fully discharged or the load required power is higher than the power which the Li-ion battery string can provide, the Lead-acid battery starts discharging, this is resembled by the Li-ion battery Discharge box.

Table 5.3 present symbols used in the model algorithm along with their corresponding definitions and units. Equations (5.43) to (5.48) shows the definition of these terms in HOTEM.

Table 5.3: Symbols used in the model algorithm (Supervised work [6]).

Symbol	Definition	Unit
$P_w(t)$	Output power from wind turbine in time step t	[kW]
$P_{pv}(t)$	output power from PV in time step t	[kW]
$P_l(t)$	power required by load in time step t	[kW]
E_b	energy stored in battery	kWh
$q(1)$	charge in battery at full charge	kAh
E_{ch}	energy charged into battery	kWh
E_{dch}	energy discharged from battery	kWh
E_{dump}	surplus energy	kWh
q_{dump}	surplus charge	kAh
B_{rep}	number of battery replaced	-

$$E_{ch}(t) = \frac{1}{2} I_{ch}(t)(V(t) + V(t-1))\Delta t \frac{1}{\eta_{batt}} \quad (5.43)$$

$$E_{dch}(t) = \frac{1}{2} I_{dch}(t)(V(t) + V(t-1))\Delta t \quad (5.44)$$

$$E_{dump}(t) = \frac{1}{2} q_{dump}(t)(V(t) + V(t-1)) \quad (5.45)$$

$$E_b(t) = \frac{1}{2} q(t)(V(t) + V(t-1)) \quad (5.46)$$

$$E_b(1) = q(1)V(1) \quad (5.47)$$

$$SOC(t) = \frac{q(t)}{q(1)} \cdot 100 \quad (5.48)$$

where $I_{ch}(t)$: charging current at t [A]
 $I_{dch}(t)$: discharge current at t [A]
 $q_{dump}(t)$: dumped charge at t [Ah]
 $q(t)$: charge in battery at t [Ah]
 $q(1)$: charge in battery at full charge, at $t = 1$ [Ah]

Results examples of the Hybrid Battery Energy Storage System (HBESS) modelling results in HOTEM are shown represented in Figures 5.13, 5.14, and 5.15. It can be seen that the Li-ion battery is doing most of the cycling and the lead-acid is serving as back up or for covers the load requirement in case the Li-ion battery can't fulfill the power demand. The lead-acid SOC can be seen to being kept at its maximum in most of the time periods, as long as the Li-ion battery hasn't reached its minimum state of charge. Once the Li-ion reaches its minimum state of charge the lead-acid battery starts discharging.

5.1.4 Generator

The required amount of energy storage can be reduced by utilizing diesel generators in remote communities. This results in a more cost-effective and reliable system, when

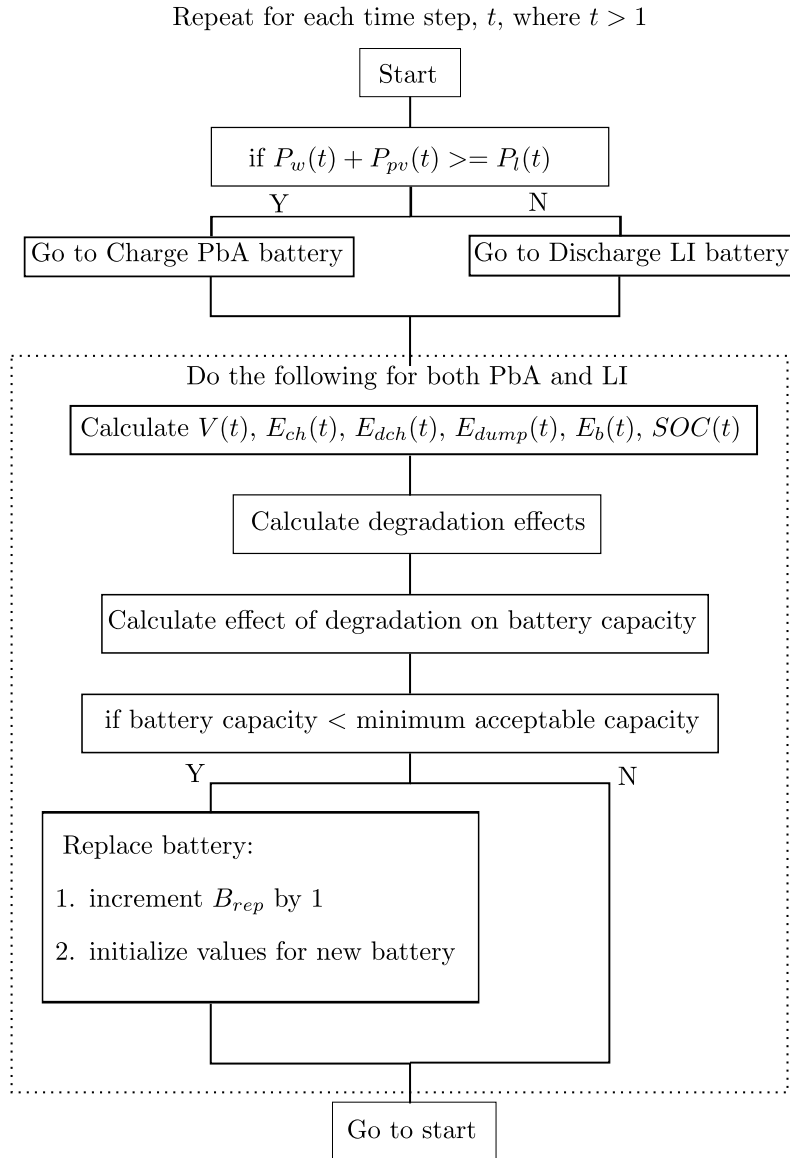


Figure 5.12: Hybrid battery storage dispatch algorithm.
Figure reference: Supervised work [6].

the both components are sized in a way that they complement each other in a optimal way.

When the battery has not enough energy to cover the load, which mostly happens during peak load demand, the diesel generator will work as a secondary energy source.

The efficiency and hourly fuel consumption are two important parameters in sizing the diesel generator in a hybrid system. HOTEM uses the modeling in Eq. (5.49) to calculate the hourly fuel consumption [87].

$$F(t) = a \times P(t) + b \times Pr \tag{5.49}$$

where;

$F(t)$ = Fuel consumption [L/h]

$P(t)$ = Generated Power [kW]

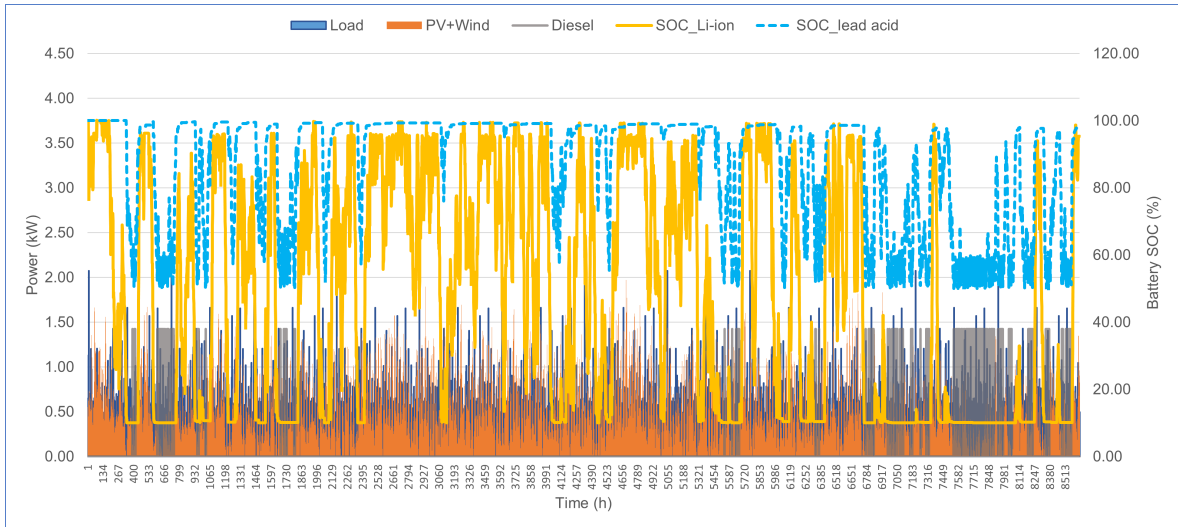


Figure 5.13: HBESS Modelling results - OHRES simulation Complete year time period
 Figure reference: Author's publication [5], and supervised work [6].

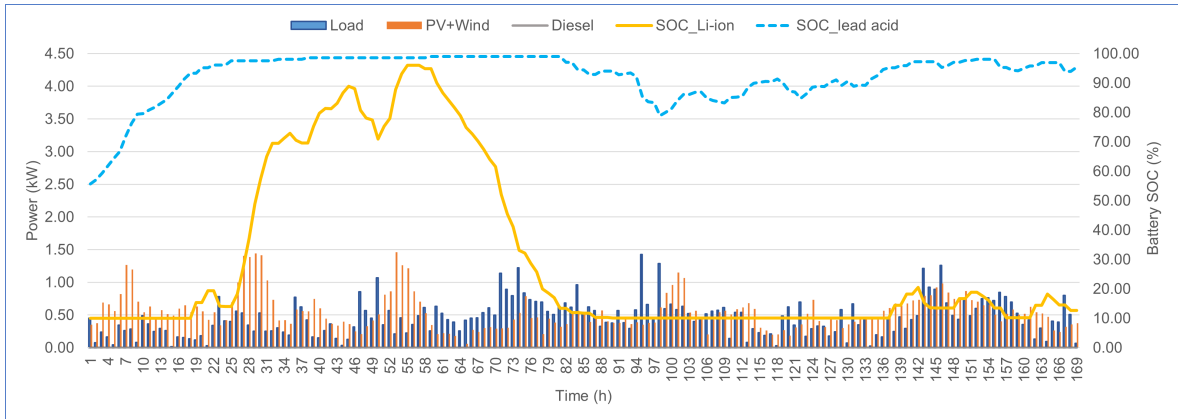


Figure 5.14: HBESS Modelling results - OHRES simulation Week time period

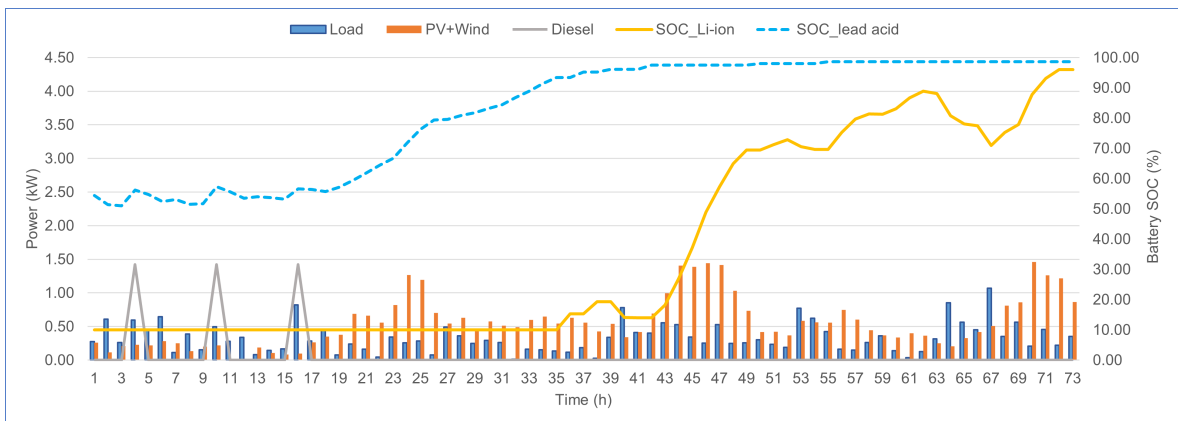


Figure 5.15: HBESS Modelling results - OHRES simulation Multi days time period

$$Pr = \text{Rated Power [kW]}$$

a and b represent the coefficients of fuel consumption in L/kW. They are constant parameters and their default value in HOTE M are 0.246 L/kW and 0.028415 L/kW respectively[87].

5.1.5 Inverter

Conversion between DC powers (renewable energy resources power, battery storage) and AC powers (AC loads, Genset) in OHRES is done through the inverter which is included as part of the HOTE M hybrid system modelling. HOTE M uses four main parameters for the inverter modelling, which is inputted through the HOTE M model input sheet:

- i Inverter efficiency for DC/AC conversion ($u_{inv}[\%]$).
- ii Inverter charger efficiency for genset power conversion ($U_{invchr}[\%]$)
- iii Inverter rated power (INV MAX [kW])
- iv Inverter cost (INV CKW [\$/kW])

These four parameters are used in different modelling positions within the structure of HOTE M to include the inverter technical effects on power conversion from different DC and AC components and power flows in the hybrid system, and economical aspects within the OHRES techno-economic modelling.

5.1.6 Load profiling and random variability

The most critical area in designing a hybrid study is to analyze the load profile of an area or a house. The sizing and modeling of battery are highly dependent on load profiles. Furthermore, the reliability of system is also affected by peak load times and behavior of consumers and eventually, it affects the sizing of hybrid system components and price of electricity.

The HOTE M allows a user to add randomness to the load so that the load profile looks more realistic. Two types of randomness are modeled in the analysis on hand, namely *Day-to-day variability (D-t-D)* and *Time-Step-to-Time-Step variability (Ts-t-Ts)*. The following section will explain in detail the load randomness by considering a load profile of a typical rural household shown in Figure 5.16.

Day-to-day variability (D-t-D)

In the first step, the user can input the hourly profile of the first day of the year. The HOTE M assumes the same profile and repeats it for each day of the whole month. A plot of the first week of the year is shown in Figure 5.16. It can be seen that the load profile repeats itself day after the day without any added variability.

However, realistically the size and shape of the load profile varies from day by day. Therefore adding variability makes the data more realistic. HOTE M allow user to enter D-t-D (%). It then changes the load profile of each day defined by user at a random amount, so the load retains the same shape of each day but it scaled upward

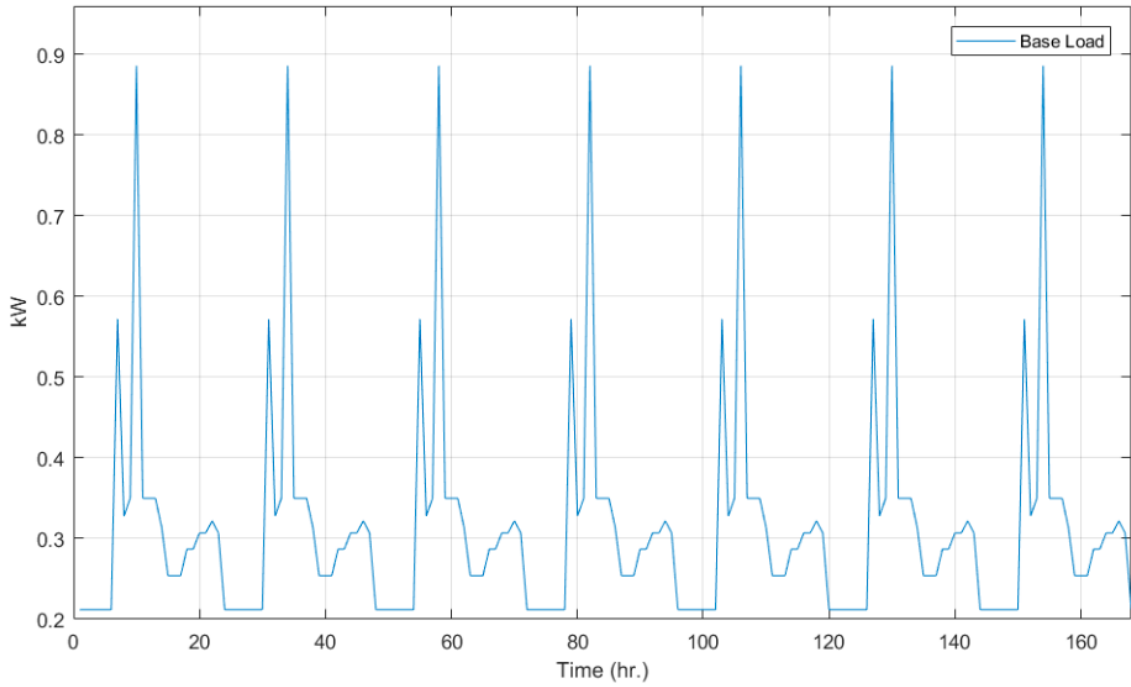


Figure 5.16: Load profile of the first week of the year without variability.
Figure reference: Author's publication [5], and supervised work [7].

or downward. Figure 5.17 shows the load profile of the first week of the year with and without D-t-D variability. It can be also seen in Figure 5.17 , the peak load is scaled up from 0.88kW to 1.22kW respectively but the shape of each day load profile is the same.

Time-Step-to-Time-Step variability (Ts-t-Ts)

Unlike D-t-D variability, the Ts-t-Ts variability changes the shape of the load profile without affecting its size. The user can also enter any Ts-t-Ts variability. Figure 5.18 shows the load profile of first week of the year with 15% Ts-t-Ts. It can be also be seen from Figure 5.18 , the peak load is scaled up from 0.88kW to 1.25kW respectively.

By entering both D-t-D and Ts-t-Ts variability, a user can combine their effect to create realistic-looking load profile data. Figure 5.19 represents the first week of the year with 20% D-t-D and 15% Ts-t-Ts variability.

The mechanism of adding D-t-D and Ts-t-Ts variability is given in Eq. (5.50). First, HOTEM assembles the hourly data of the month from daily profile specified by the user. Then, it steps through that time series, and, in each hour, it multiplies the value in that hour by a perturbation factor (α), then assumes the same profile for each month of the year.

$$\alpha = 1 + \delta_d + \delta_{ts} \quad (5.50)$$

where;

δ_d = daily perturbation

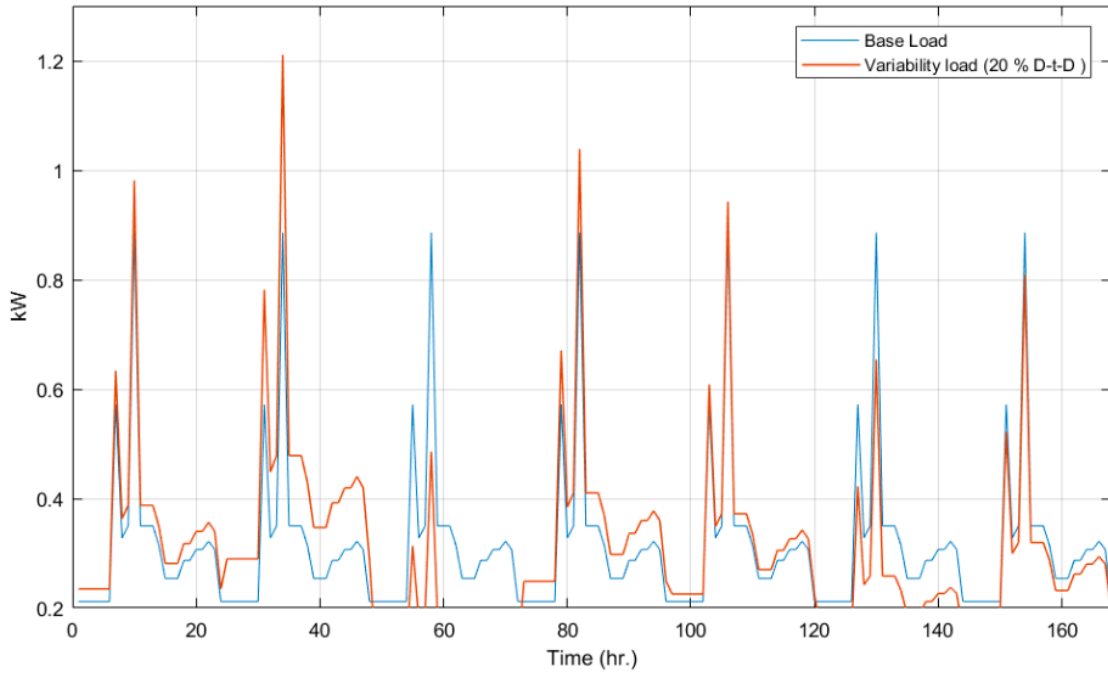


Figure 5.17: Load profile of the first week of the year with 20% Day-to-Day variability. Figure reference: Author’s publication [5], and supervised work [7].

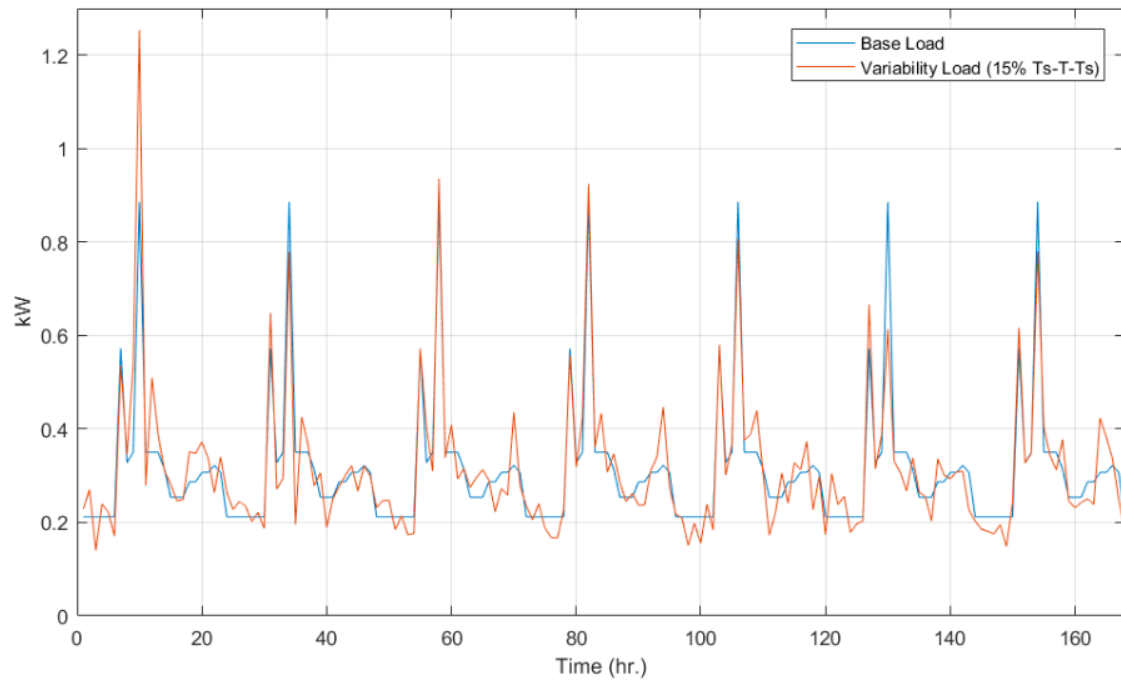


Figure 5.18: Load profile of the first week of the year with 15% Ts-t-Ts variability. Figure reference: Author’s publication [5], and supervised work [7].

δ_{ts} = time step perturbation value

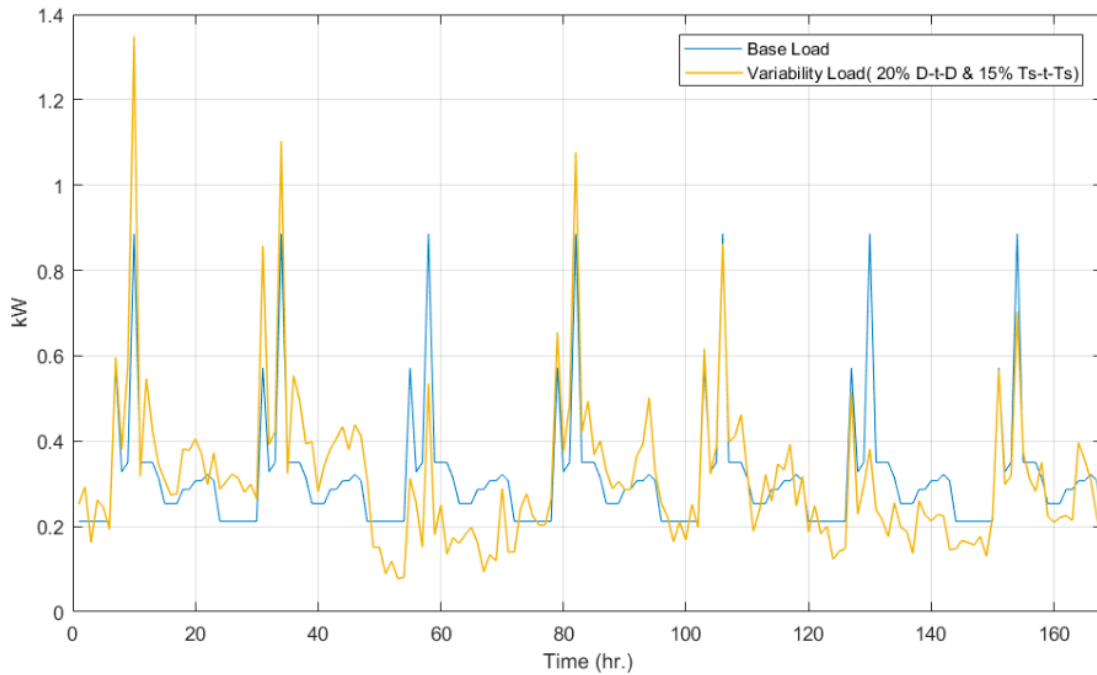


Figure 5.19: Load profile of the first week of the year with 20% Day-to-Day and 15% Ts-t-ts variability.

Figure reference: Author's publication [5], and supervised work [7].

HOTEM randomly draws the daily perturbation once per day from a normal distribution with a mean of zero and standard deviation equal to D-t-D variability entered by a user. Similarly, HOTEM randomly draws the time step perturbation for each hour from a normal distribution with a mean of zero and standard deviation equal to Ts-t-Ts specified by the user.

5.1.7 Economic modelling

This section shows the economic models used in HOTEM for defining the discount rate used in the dynamic financial assessment for the hybrid system over the defined lifetime.

WACC Model

To define the nominal discount rate in HOTEM, the user can provide the value of the nominal discount rate directly as an input or use the integrated weighted average cost of capital (WACC). The WACC is used when there is more than one investor like equity and dept. As each entity has its own share of capital and required return on investment, the WACC is then utilized to find the average cost for the investment capital of both equity and debt. Based upon the same approach of the developed model in M. Elkadragy [88, 89], The WACC is calculated in HOTEM model as given in Eq. (5.51). This WACC model offers detailed economical analysis allowing to include many economical case specific variables, in addition to policy and support mechanism

effects on the economical evaluation.

$$WACC = g_d \times (r_{fd} + r_{pd}) \times (1 - r_t) + g_e \times \left(R_{fe} + (\beta_{ref} \times \alpha_{sm}) \times (R_{me} - R_{fe}) \right) \quad (5.51)$$

where;

- g_d = Share of debt [%]
- r_{fd} = Risk free rate for debt [%]
- r_{pd} = Market risk premium for debt [%]
- r_t = Tax rate [%]
- g_e = Share of equity [%]
- R_{fe} = Risk free rate [%]
- β_{fe} = Equity risk measurement factor [-]
- α_{sm} = Support mechanism risk premium [-]
- R_{me} = Return in the financial market for equity [%]
- $R_{me}-R_{fe}$ = Market risk premium for equity [%]

Real discount rate

The real discount rate and the discount factor are calculated in HOTEM for the economic analysis of a project with multi year lifetime. These quantities are used in the dynamic financial assessment to determine the present costs of components over the system lifetime in HOTEM for overall system economics calculations.

The real discount rate is calculated as in equation 5.52 [51].

$$r = \frac{i - g}{1 + g} \quad (5.52)$$

- where r : real discount rate [%]
- i : nominal discount rate [%]
- g : inflation rate [%]

Based on the real discount rate, the discount factor used in the dynamic financial assessment is calculated as in equation 5.53 [51].

$$df = \frac{1}{(1 + r)^{y_r}} \quad (5.53)$$

- where df : discount factor [-]
- r : real discount rate [%]
- y_r : year of replacement [-]

5.2 HOTE M optimization targets and power dispatch strategy

This section describes the optimization goals developed in HOTE M. The model presented is based on the double target problem with minimization of Cost of Electricity (COE) and Loss of Power Supply probability (LOLP) as formulated in the original model.

5.2.1 Cost of electricity

The cost of electricity is the most famous and commonly used economic indicators of profitability for the off-grid hybrid energy system.

According to [90, 91], COE can be calculated by using the following expression:

$$COE = \frac{C_T}{\sum_{h=1}^{8640} P_{load}} \times CRF \quad (5.54)$$

where:

COE = Cost per unit of electricity [\$/kWh]

C_T = Total net present cost [\$]

P_{load} = Hourly power consumption [kWh]

$$1year = 8640hours \quad (5.55)$$

$$8640hours = 24h \times 30days \times 12months \quad (5.56)$$

Capital Recovery Factor (CRF) is a ratio to calculate the present value of the costs for a system components in given planning period taking into account an interest rate which used as a discount rate [65, 91]. It is calculated as:

$$CRF = \frac{i(1+i)^n}{(1+i)^n - 1} \quad (5.57)$$

where, i is the real interest rate and n is the system lifetime. During the economic data entry in HOTE M, user can either enter the real interest rate or follow the WACC model given in Eq. 5.51.

The battery degradation overtime is taken into consideration, so the cost associated with degradation of battery (C_d) is also included in this study. The expression to calculate (C_d) defined by [92] is given in Eq. 5.58

$$C_d = \frac{C_{bat}}{L_c \times E_s \times DOD} \quad (5.58)$$

C_{bat} = Total battery cell cost [\$]

L_c = Cycle lifetime of battery [cycles]

E_s = Energy storage capacity [kWh]

DOD = Depth of discharge of the battery [%]

$$C_T = C_i + C_m + C_{br} + \sum_{h=1}^{8640} C_d \quad (5.59)$$

All the installed capital cost is represented by C_T as: total system initial cost including installation and connection (C_i), maintenance cost of system components (C_m) and battery replacement cost (C_{br}).

5.2.2 Loss of power supply probability

Loss of power supply probability (LPSP) is a statistical parameter that represents the failure of electricity supply due to unavailability of solar and wind resources or due to technical failure. Statistical techniques and chronological simulation approaches can be used to calculate the LPSP [65]. LPSP calculation in HOTEM is based on the work described [65] and calculated as in Eq. (5.60)

$$LPSP = \frac{\sum (P_{load} - P_{pv} - P_w - P_{dch} + P_{diesel})}{\sum P_{load}} \quad (5.60)$$

where;

P_{load} = Hourly power consumption [kW]

P_{pv} = Power generated by PV [kW]

P_w = Power generated by wind generator [kW]

P_{dch} = Discharge power of the battery [kW]

P_{diesel} = Power from diesel generator [kW]

5.2.3 Renewable Factor

The renewable factor RE_{factor} is a side condition that assures that electricity is mainly generated via renewable resources within the Hybrid Micro Grid System (HMGS) [30]. The RE_{factor} of 100% represents a ideal system based on renewable resources only. However, the renewable factor of zero percent shows that the amount of power coming from a diesel generator is equivalent to the power from renewable resources, It is calculated as Eq. (5.61) [65].

$$RE_{factor} = \left(1 - \frac{\sum P_{diesel}}{\sum P_{pv} + \sum P_w} \right) \times 100 \quad (5.61)$$

where;

P_{diesel} = Power from diesel generator [kW]

P_{pv} = Power generated by PV [kW]

P_w = Power generated by wind generator [kW]

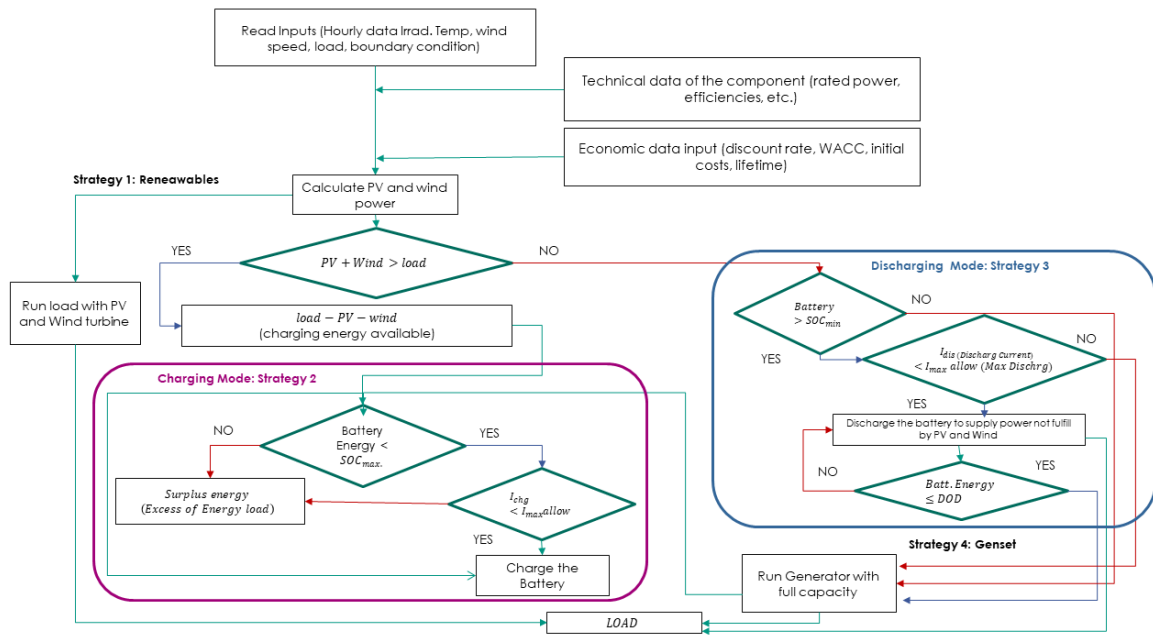


Figure 5.20: Power dispatch strategies in HOTEM.
Figure reference: Author's publication [5].

5.2.4 Power dispatch strategies

A continuous and flexible provision of electricity is crucial to meet local loads and to maintain security of supply

However, renewable energy sources have an unpredictable nature of electric generation.

Due to the limited ability of renewable to follow load, it is not possible to increase the generator capacity immediately to meet the load demand.

On the other hand, renewables may produce more than the required energy, in that case, the battery must be protected by dissipating the surplus energy to dump load.

Therefore, the power dispatch strategy is the most important criteria to model a hybrid system. Figure 5.20 shows the main strategies considered in designing the HOTEM:

Strategy 1: Energy required by load is provided by renewables and surplus energy will charge the battery bank.

Strategy 2: If energy from renewables is more than the demanded load and batteries are also fully charged, the control algorithm for our OHRES system allows excess energy to flow into the system and not be curtailed. This strategy participate in raising the utilization of the renewable resources available and the system available produced energy, where other system algorithm designs are based on power curtailment in such operation condition.

The surplus energy is utilized in an excess of energy (or dump) load, where excess energy has a productive use application. In the Canada case-study, the system is designed and the algorithm is adapted to provided surplus energy to an electrical water

heater placed in a hot water storage tank. So in case of surplus renewable energy the water in the tank is heated and stored to be used in the different hot water applications in the household.

Strategy 3: If power output of renewables is not able to cover the load, batteries kick-in to cover demand

Strategy 4: If the energy from renewables is not enough to meet the load demand and batteries are also depleted, the case diesel generator will provide energy to load and also charge the batteries.

5.2.5 C-DEEPSO optimization model overview

As mentioned earlier, C-DEEPSO optimization algorithm is adapted in HOTEEM based on the work previously developed in the C-DEEPSO algorithm development and its applications in [28], [29], [66], [67], [68], and [69]. This section gives a brief overview on the algorithm modelling fundamentals, more in depth explanation of how the optimization algorithm is developed and operating can be found in the previously mentioned references.

C-DEEPSO, which stands for Canonical Differential Evolutionary Particle Swarm Optimization, is a hybrid single objective meta-heuristic that assimilates peculiar attribute of Evolutionary Computation, Particle Swarm Optimization (PSO), and Differential Evolution (DE). In recent years C-DEEPSO emerged as one of the best solutions for corresponding optimization problems. This algorithm, which is an enhancement over EPSO (Evolutionary Particle Swarm Optimization) and Differential Evolutionary Particle Swarm Optimization (DEEPSO) [93] can be seen as an evolutionary algorithm with recombination laws taken from PSO with selection and self-adaptiveness properties proper from DE. Figure 5.21 shows the algorithm flowchart.

Like every population-based meta-heuristic, C-DEEPSO depends on the repeated application of mutation, recombination, and selection operators over a population of solutions (individuals), to create new solutions such that the overall fitness of the population is gradually improved until the desired convergence criterion is achieved. Generation of new solutions in C-DEEPSO is based on successive recombination operations applied on current and past solutions. The recombination is governed by the Movement Rule, given in Eq. (5.62) and Eq. (5.63) [29]:

$$X_t = X_{t-1} + V_t \quad (5.62)$$

$$V_t = w_I^* V_{t-1} + w_A^* (X_{st} - X_{t-1}) w_c^* C(X_g^* b - X_{t-1}) \quad (5.63)$$

where the strategy st can be expressed by means of Eq. (5.64)

$$X_{st} = X_r + F(X_{best} - X_r) + F(X_{r1} - X_{r2}) \quad (5.64)$$

where t : The current generation
 X : the Current solution
 X_{best} : The best solution ever found by the individual
 X_{gb} : The best solution ever found by the population
 X_r : An individual different from X_{t-1}
 V :The velocity of solution
 $*$:parameter is subjected to the mutation process
 C :The Diagonal matrix of random variable sampled at each iteration
 St :Bin strategy by Differential Evaluation algorithm
 $N(0, 1)$:Number sampled from standard Gaussian Distribution.
 W_1, W_a, W_c : Weights on the inertia, assimilation and communication respectively

The term t denotes the current generation, X the current position or solution, X_{best} the best solution ever found by the individual, X_{gb} the best solution ever found by the population, V the velocity of the individual, and a diagonal matrix of random variables that is sampled every iteration and follows a Bernoulli distribution with success probability P .

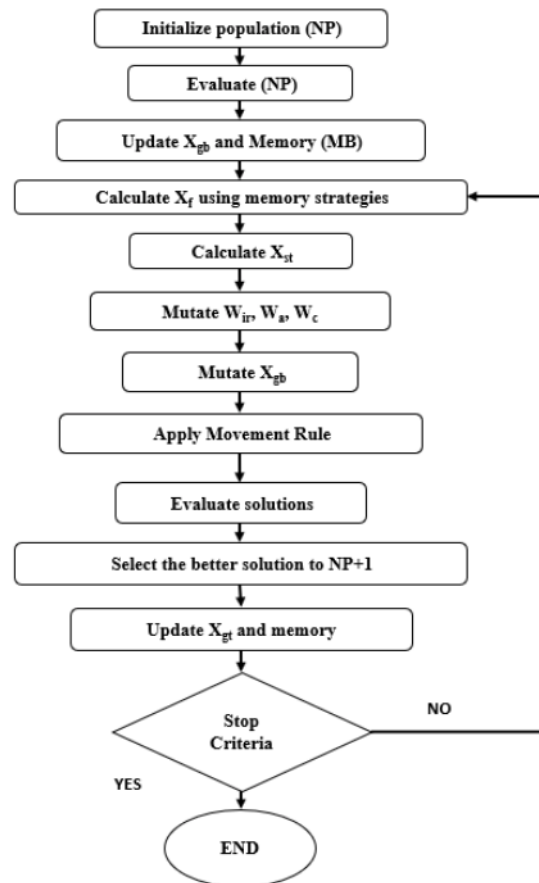


Figure 5.21: C-DEEPSO algorithm flowchart.
 Figure reference: Source [28].

The superscript $*$ indicates that the corresponding parameter/quantity undergoes evolution under a mutation process.

Typically, the mutation of a generic weight w of an individual follows a simple additive rule

$$w^* = w + \tau \times N(0; 1); \quad (5.65)$$

The mutation of X_{gb} , which is done for every particle, is according to the following equation,

$$X_{gb}^* = X_{gb}[1 + \tau \times N(0, 1)] \quad (5.66)$$

In number of the references listed in the beginning of this section, C-DEEPSO is applied and tested, and suggested as one of the most useful and promising optimization methods, through different case studies in Wind power plant management and hybrid systems optimization applications.

5.3 HOTEM case study description and system sizing results

An off-grid house in Canada is selected as a case study where a hybrid renewable energy system had already been deployed under the research work of Karlsruhe Institute of Technology (KIT). The yearly time series data for wind speed (m/s), solar irradiance (W/m^2) and load data (kW) serve as model inputs. The potential maximum load in the house is 4kW which is mostly observed at weekends while the daily average energy consumed is around 4.5kWh.

Figure 5.22 shows the observed hourly Average Connected Load (ACL) and Total Connected Load (TCL) profile of a house under case study. The ACL peak is 0.9kW while the TCL peak is around 2.13kW.

As TCL peak mostly observed on weekends so modeling based on this profile will result in oversize system components.

Therefore, the ACL profile is used in the model, replicated each day of the first month (January) and 20% day-to-day and 40% time-step-time-step variation is added to reach the peak demand of upto 2.13 kW. Then the same profile is assumed for all other months of the year. This represents a simplification, as the yearly load might vary. It is, however, a suitable simplification for our goals

Figure 5.23 shows the hourly profile of ACL and variability load with both D-t-D & Ts-t-Ts variability. The load profile with variability is used in HOTEM to stay close with realistic behavior of demand.

To maximize the PV output, Global Solar Irradiance (GHI) is transposed to plane of array (POA) irradiance using a surface tilt angle of 45° and azimuth of 0° degree i.e pure South.

Figure 5.24 shows the hourly irradiance and wind speed (NASA, 2017) for the period of one year used as models inputs.

The economic parameter used in the designing of the off-grid system are presented in table 5.4.

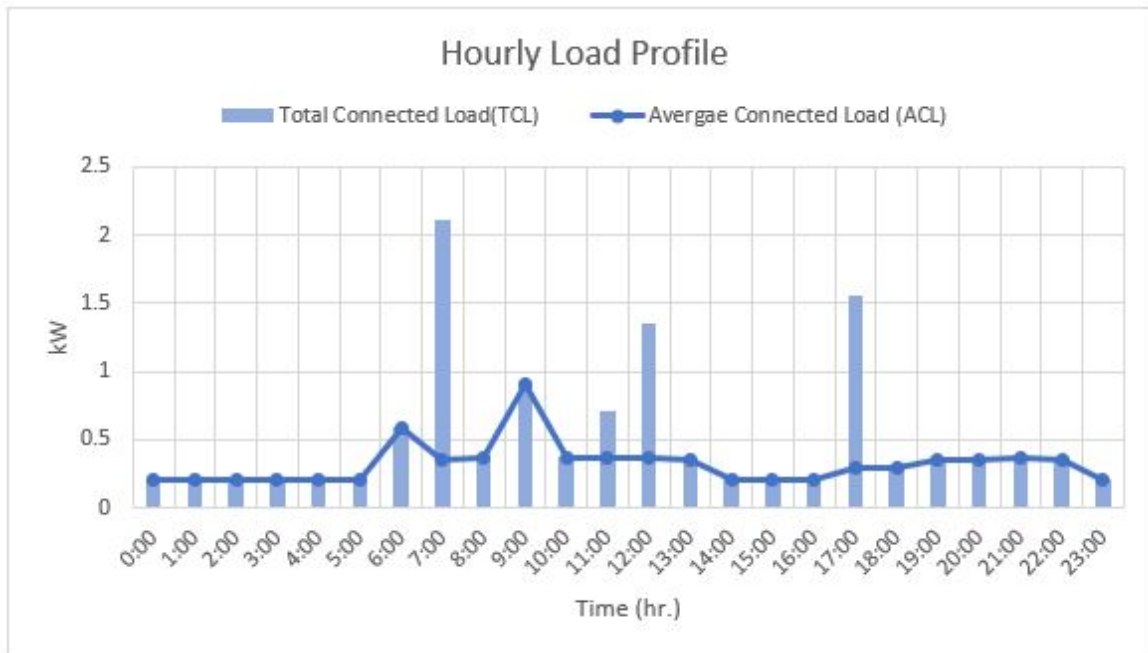


Figure 5.22: 24- hour load profile by a house under study.
 Figure reference: Author’s publication [5], and supervised work [7]

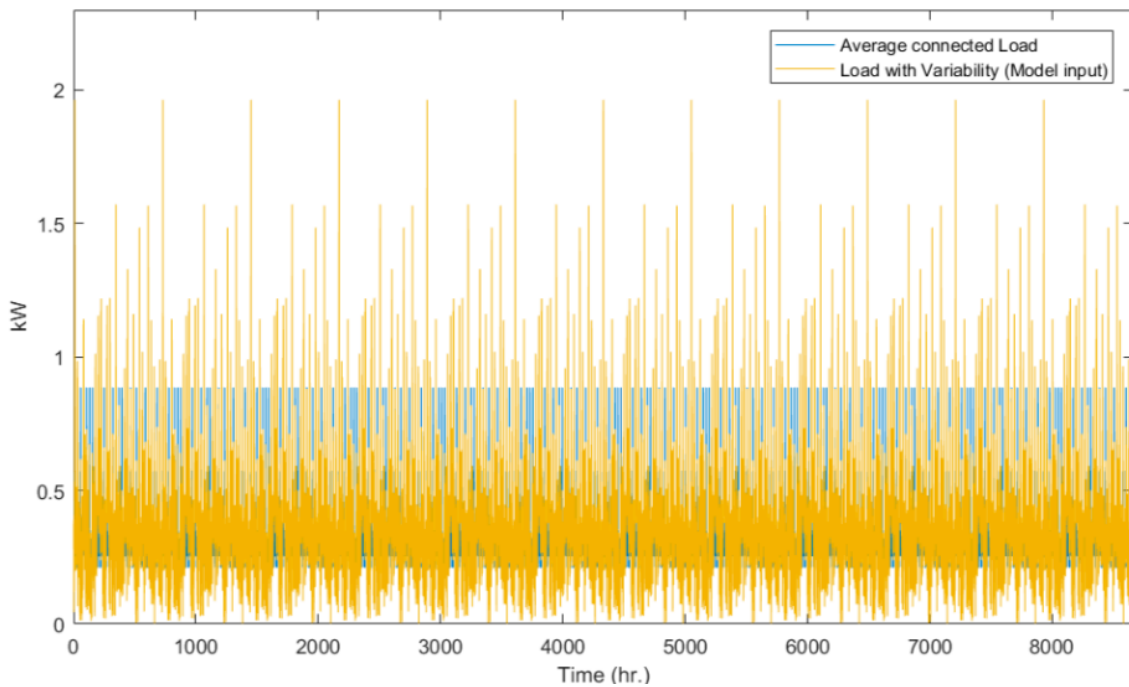


Figure 5.23: Hourly load with variability used for model input.
 Figure reference: Author’s publication [5], and supervised work [7].

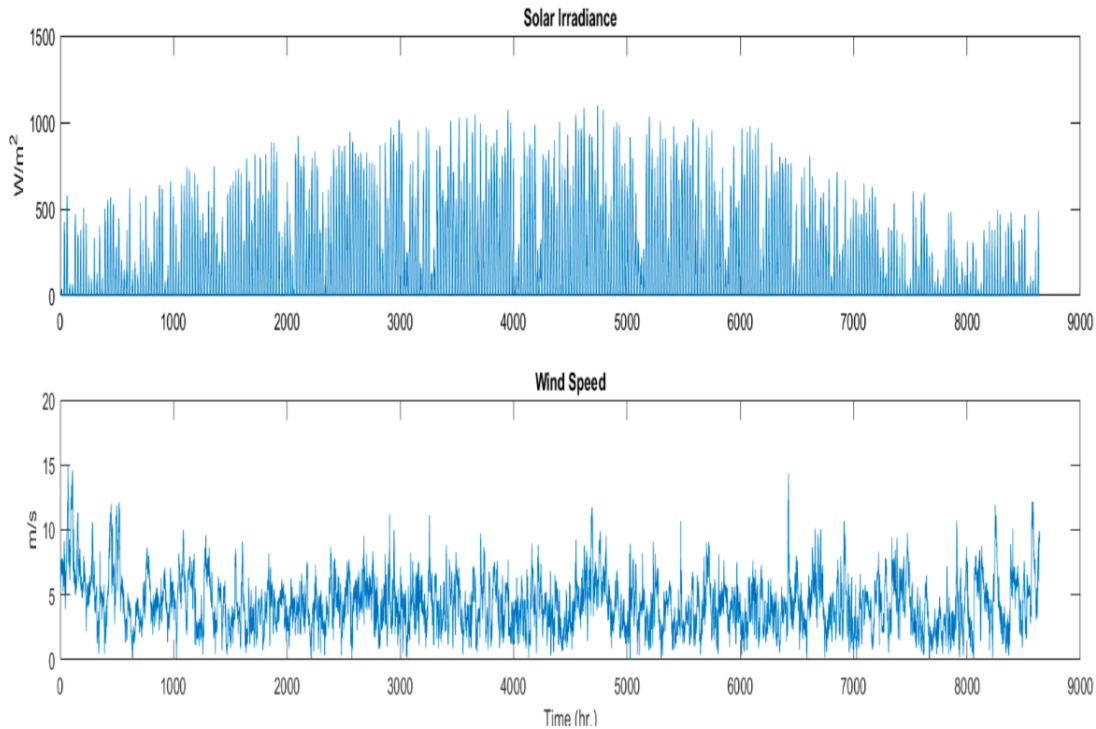


Figure 5.24: Hourly solar irradiance and wind speed served as model inputs.
Figure reference: Author’s publication [5], and supervised work [7].

The system configuration for the case study is depicted in figure 5.25. It consists of a 48 Volts DC bus with lithium-ion battery bank. The parameters selected for battery bank are; SOC_{max} 90%, SOC_{min} 15%, $I_{ch,max}$ 45 A and $I_{dsh,max}$ 65 A.

Four different dimensions are selected in the algorithm with the lower and upper boundary. These dimensions are:

- **Nominal PV power:** which predict the optimized PV system required (Eq. (5.1)) ,
- **Battery days of autonomy:** predict the optimized battery capacity (Eq. (5.29)),
- **Number of wind turbines:** represent the optimized total wind turbines required,
- **The number of houses:** refers to the load demand of the total number of houses in an off-grid location.

The population of the optimization algorithm is randomly initialized using the upper and lower bounds of each specified dimensions. These limits are PV [0 4], autonomy [1 3], wind [0 3] and houses [1 1]. As the model analyzed only one house as a case study, the boundaries for the number of houses are fixed to one.

The parameters of C-DEEPSO are empirically initialized. The value of each parameter defined in the case study are partially derived from [30] given as: communication rate 0.9, mutation rate 0.5, number of population 10, maximum number of generations 10 and dimension of search space 4.

Table 5.4: Modelling input parameters based on manufacturer data (Author’s publication [5], and supervised work [7]).

System Parameter	Unit	Values
Diesel Generator		
Life time	hours	24,000
Initial cost	\$/kW	500
Rated Power	kW	3
Inverter		
Efficiency	%	95
Life time	Years	15
Initial cost	\$/kW	500
Battery		
Efficiency	%	85
Life time	Years	15
Initial cost	\$/kWh	140
PV		
Derating factor	%	85
Life time	Years	25
Initial cost	\$/kW	140
Economic parameters		
Discount rate	%	8.5
WACC	%	8
Life time	Years	25
O&M + running cost	%	5
Fuel inflation rate	%	1
Project life time	Year	25
Wind Turbine		
Blades diameter	m	8.5
Wind turbine electric AC/DC converter Efficiency	%	95
Cut out	m/s	30
Cut in	m/s	2.5
Rated speed	m/s	9.5
Price	\$/kW	4000
Life time	Year	18

HOTEM case study sizing results:

The resulting optimum generation capacities stemming from the HOTEM are given in table 5.5.

The results shows that HOTEM provides optimum solar, wind and battery ratings within the scope of the required objectives (min. COE & LPSP, max. RE_{factor}).

The results show a total of 4kW rated PV with only one wind turbine. Moreover, the result shows the battery should be able to supply energy to the load for one day

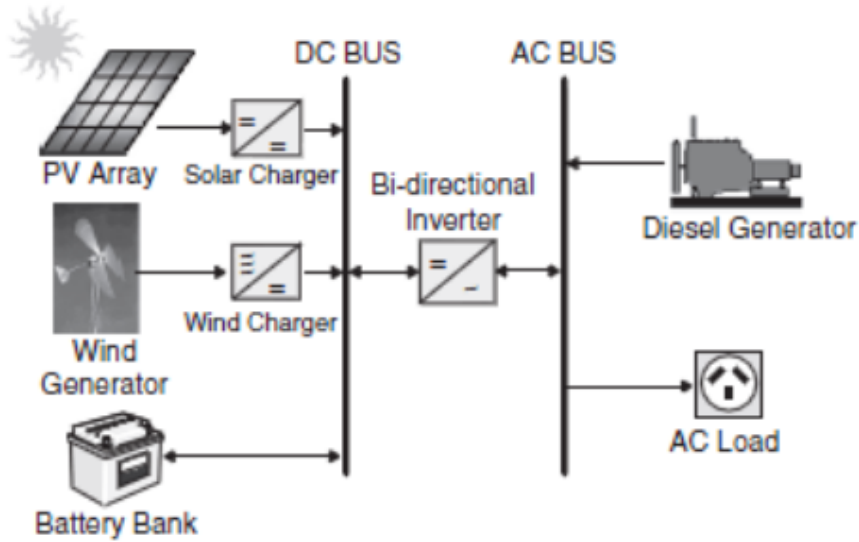


Figure 5.25: Configuration of hybrid off-grid system under case study.
Figure reference: Author's publication [5].

Table 5.5: HOTE M Simulation Results (Author's publication [5], and supervised work [7]).

Number of iteration	10
Number of particles	10
Power of PV panels (kW)	4
Battery autonomy (Days)	1
Number of wind turbines	1
LPSP (%)	1
COE (\$/kWh)	0.58
Renewable factor (%)	95

to avoid outage when no renewables are available. This leads to COE of 0.58 \$/kWh with a LPSP of 1% and renewable factor of 95%. The calculated cost of (0.58 \$/kWh) by HOTE M is in the range of the 0.42-0.70 \$/kWh for the off-grid hybrid system as stated by Energy Sector Management Assistance Program 2019 (ESMAP) [94]. A high RE_{factor} (95%) shows that area under study has high renewable resources which limit the use of diesel generator that has a major impact on the rise of the COE in off-grid locations as compared to other components, predicted by Bornanzad [65].

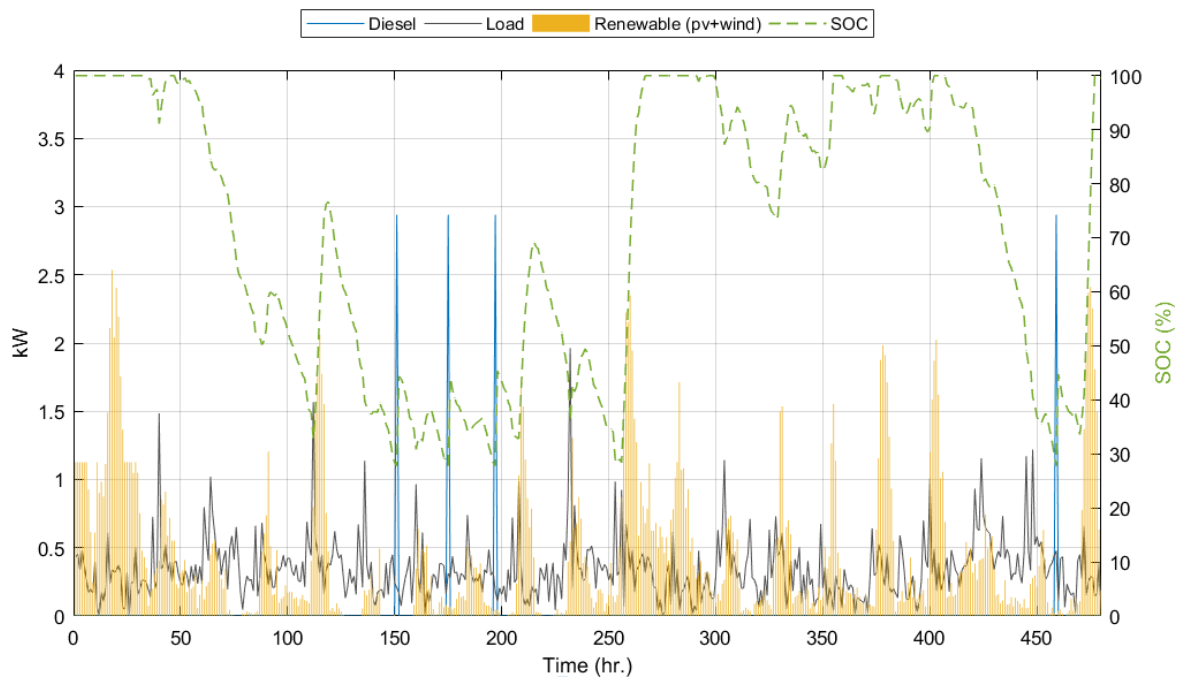


Figure 5.26: Hybrid system generation and load dynamics.
 Figure reference: Author's publication [5], and supervised work [7].

PV and Wind simulation

Figure 5.27 presents the hourly simulation of the renewable based generation for the Canada Case-study. The maximum power generated by the PV is 3.6 kW while the wind reaches a maximum of 1.1 kW. The PV produces more power in the middle of the year (summer) because of increased solar irradiance.

System power flow simulation

The HOTE M uses power from the diesel generator when there is not enough power from renewables (PV + Wind) and the batteries (in case of low SoC). In that case, the generator runs at full capacity to supply power to cover the load and also charges the batteries (cycle charging). Figure 5.26 shows an excerpt of the yearly simulation to analyse the operation modes of all components. It can be seen clearly that the model follows the four dispatch strategies and that the diesel generator only runs when renewable (PV + Wind) is less than the demand and the battery is also at minimum energy state (27% SOC). It can also be observed that the Genset always runs with full capacity (3kW x Converter efficiency) to fulfill the load demand and also charges the batteries (battery SOC increases on secondary axis).

Resulting in Generation Shares

The resulting total energy generation shares of HOTE M system components (PV, Wind, Storage, and Generator) are given in table 5.6. The result from the HOTE M simulation shows that the highest reliability (99%) with lowest cost of 0.58 \$/kWh and

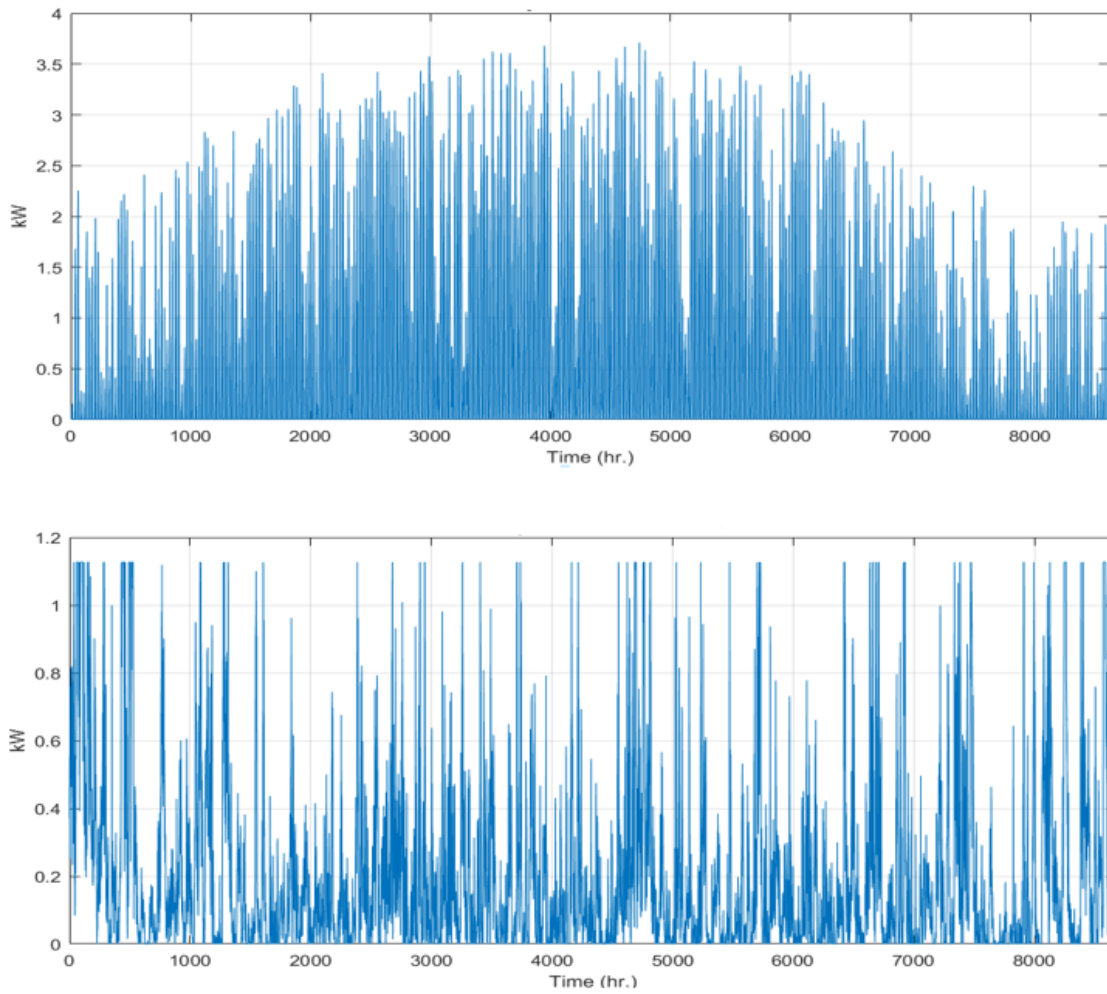


Figure 5.27: PV and Wind power generation.
 Figure reference: Author’s publication [5], and supervised work [7].

Table 5.6: Annual energy production of each hybrid component (Author’s publication [5]).

<i>Annual Production</i>	<i>kWh/Year</i>
PV array	4148.62
Wind Generator	1772.34
Battery Energy	893.91
Generator energy	313
Surplus	3080.23

high contribution of renewable energy (95%) are achieved when the PV array power production accounts for 41% (4148.62 kWh/year) of the total demand, including a 17% (1772.34 kWh/year) share of the wind, 9% (893.91 kWh/year) share of the battery. Finally, only a 3% (300 kWh/year) share is provided by the generator.

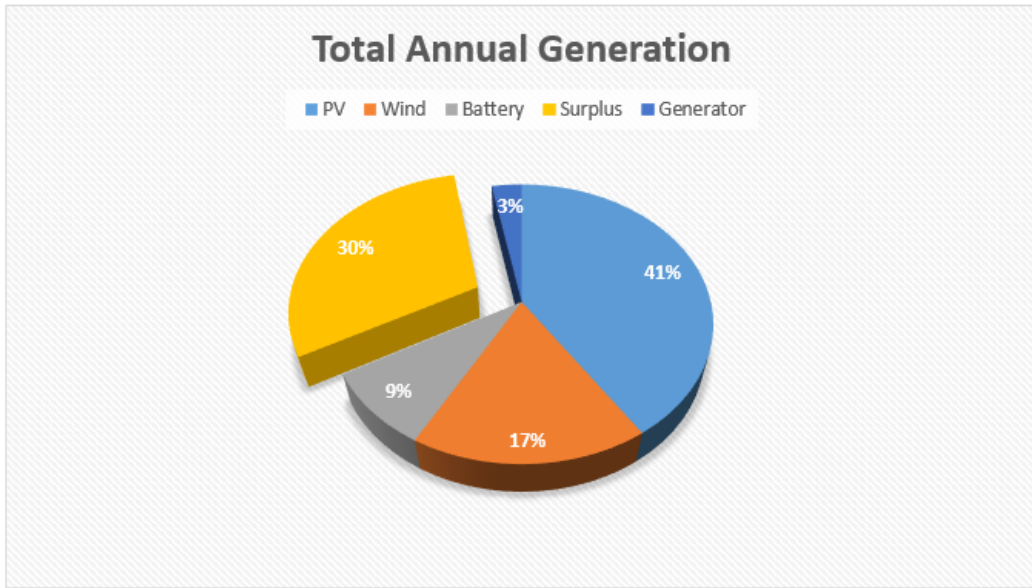


Figure 5.28: Total annual generation shares: wind, solar, battery, surplus.
 Figure reference: Author's publication [5], and supervised work [7].

The remaining 30% (3080 kWh/year) is the surplus energy which cannot be used locally (Figure 5.28). The surplus energy is generated when there is more renewable energy available than demand and batteries are also fully charged. This surplus energy is undesirable, resulting in over sizing the hybrid system component. Therefore, it is important to limit the surplus generation to avoid oversized systems. One way to limit the surplus production is the right selection of a battery energy storage (BESS) technology as mentioned by Marcelino et al [30]. Another way presented by Bornanzad [65] is to keep changing the limits of the optimization parameter after every simulation until the desired energy generation is reached.

5.4 HOTE M Benchmarking

Finally, the performance of HOTE M is benchmarked against the HOMER software which is commercially available to model the off-grid hybrid system. Figure 5.29 shows the design configuration of the hybrid system modeled in HOMER for benchmarking with HOTE M. Both HOMER and HOTE M used the same system configuration and feed in with the same PV, wind resource data (NASA,2017) and load profile (Figure 5.22). The technical and economic parameters were also set to the same level (table 5.4).

There was difficulty in perfectly matching the dispatch profiles between models, as HOMER performs optimization only for minimum COE while HOTE M follows four different power management strategies to perform optimization for minimum COE and LPSP and maximizing the renewable factor. Despite all these differences, the parameters in both models were set to equal to achieve comparable results for benchmarking. The simulation comparison between different component sizing of HOMER and HOTE M is given in the table 5.7.

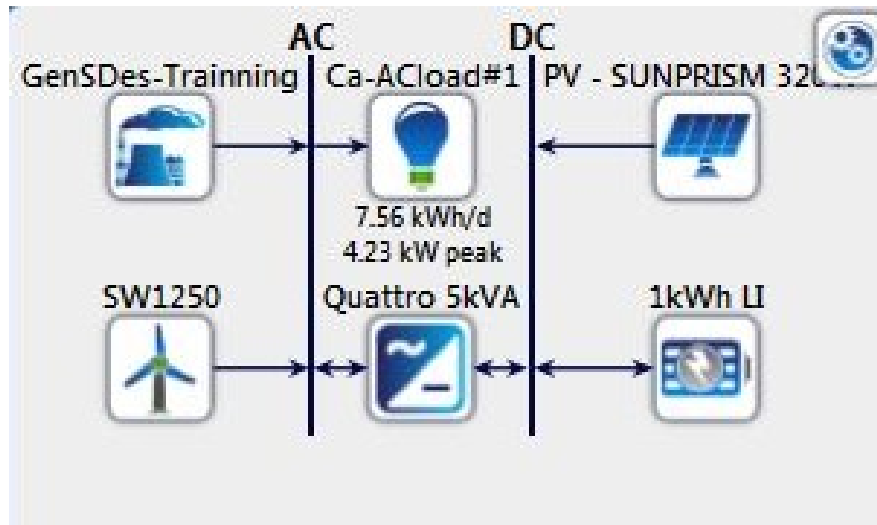


Figure 5.29: HOMER off-grid system configuration for benchmarking.
 Figure reference: Case study modelling in HOMER [50].

Table 5.7: Simulation comparison between HOMER and HOTE M (Author’s publication [5]).

Parameters	HOMER	HOTE M
PV rating(kW)	3	4
Wind turbine (kW)	1.25	1.25
Battery (kWh)	16	18
Renewable factor (%)	79	95
COE (\$/kWh)	0.52	0.58

The simulation comparison shows that HOMER required 3 kW of PV against 4 kW predicted by HOTE M while the wind power is same for both systems. Similarly the battery capacity selected by HOTE M is 2 kWh more than the HOMER. This lead to 0.58 \$/kWh of electricity from HOTE M and 0.52 \$/kWh using HOMER. The difference in per unit cost reflect the fact that HOMER optimized system only for the minimum COE while the HOTE M minimized COE and maximized the renewable factor (95%) which leads to larger renewable capacity system (PV, wind and battery) and eventually a higher cost. This has a great advantage in off-grid locations as they are meant to use maximum renewable resources and avoid the use of generators due to very limited fuel transport facilities in off-grid areas. The comparison of various parameters between HOMER and HOTE M is summarized in the table 5.8.

Table 5.8: Comparison of results from HOMER and HOTEM (Author’s publication [5]).

Parameters	HOMER	HOTEM	Description
Detailed WACC Model	NO	YES	HOTEM is design to use either direct interest rate or follow the WACC economic model (RE support mechanism implication for investment not explicitly available in HOMER).
Different battery models availability	YES	YES	HOMER offers three different battery types (idealized, kinetic and modified kinetic model) while HOTEM Offers only two battery type (idealized and Kinetic).
Modelling of Hybrid battery storage system	NO	YES	HOTEM utilize the lead-acid and Li-ion integrated models to allow modeling a Hybrid lead-acid & Li-ion storage with a certain charge and discharge strategy for each battery in the hybrid system, and hybrid storage sizing input parameters. Where in HOMER Pro including different battery technologies (as lead-acid and Li-ion) in one system model results in selecting one of the two technologies in each system architecture scenario, and such hybrid storage modeling is not explicitly available.
Multi optimization objective	NO	YES	HOTEM has 3 optimization objectives (minimize COE and LPSP, maximize RE_{factor}). HOMER optimized only for minimum net present cost.
Graphical User Interface	YES	NO	HOTEM offers the user a graphical interface to model parameters directly inside the HOMER while HOTEM does not support GUI, it reads all parameters from Excel or CSV files.
Load profiling and randomness	YES	YES	Both HOMER and HOTEM allows the user to add randomness in load for better realistic load profile.
Different genset fuels modeling	YES	NO	HOMER allow modeling of different fuel types for gensets, while HOTEM doesn’t allow so far such functionality and base the modelling on one type of fuel only .
multi-year analysis	YES	NO	Multi-year inputs can be entered in HOMER to analyses multi-year analysis. HOTEM does not support such analysis yet.

6 Off-grid and decentralized System Data Analysis Platform (OSDAP)

The first and second building blocks of the comprehensive approach used in this study was previously covered in Chapters 2, 3, 4, and 5. This chapter covers the third building block which is related to the Off-grid and decentralized System Data Analysis Platform (OSDAP) as shown in figure 6.1. Chapter 6 address stages 13 and 14 of the hybrid systems operation and monitoring phase presented before in figure 1.2.

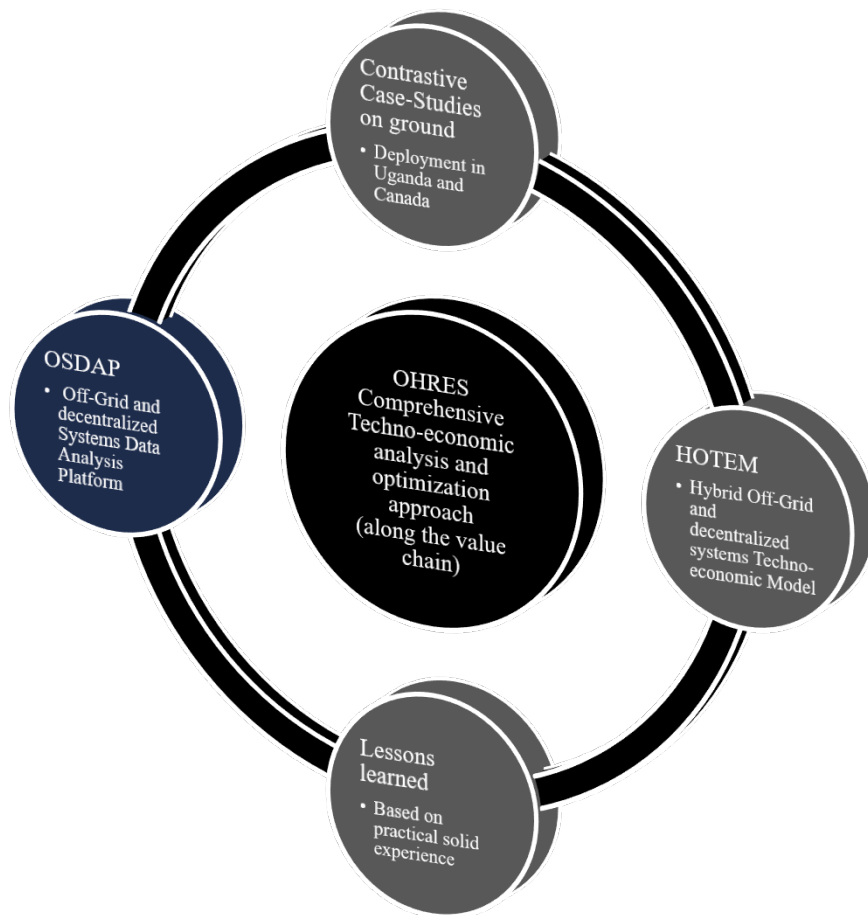


Figure 6.1: Third building block of OHRES Comprehensive Techno-economic analysis and optimization approach - OSDAP.

Figure reference: Author's illustration.

OSDAP is a developed data handling and analysis platform which is python based. The platform includes three main functionalities, which are covered in details within this chapter:

- i Data handling and visualization.
- ii Hybrid system performance analysis.
- iii Solar irradiance forecasting.

Chapter 6 includes two sections: Section 1 address OSDAP data handling and visualization development. Section 2 covers the hybrid system performance analysis and solar irradiance forecasting functionalities in OSDAP.

The content of this chapter is based on the supervised scientific work of Alsersy et al. [95], and Alici et al. [10], and part of its content is from the author's published work in Elkadragy et. al [8].

6.1 OSDAP data handling and visualization development

6.1.1 OSDAP objectives

The development objective of OSDAP is to be a tool specifically tailored for OHRES monitoring and analysis. This tool should be able to handle two types of data sets: 1) Weather and renewable resources data, whether it is satellite-based data and/or measured data available from ground-based weather stations, and 2) System operational data, whether provided from a centralized system controller or measured using installed sensors. OSDAP's core objectives include the following functionalities:

- i Providing a clear and dynamic data visualization tool for hybrid systems end-users, supporting better utilization and interaction between collected data and the system user.
- ii Standardized performance analysis indicators to support the comparison of off-grid renewable energy systems data across different geographical locations.
- iii Renewable resources forecasting based on advanced methodologies such as artificial neural networks used in OSDAP for solar irradiance forecasting.

The following sections will cover these three functionality objectives in detail.

OSDAP and Python

The energy application data is numerical which means it can be subjected to numerous ways of computations such as general, statistical and scientific, etc., which can be performed with several programming languages such as Python or R and the list goes on. Python is one of the programming languages suitable for Scientific computing and data analysis. Python can perform data mining, Big data handling, and data analysis and is compatible with desktop and web applications.

Motivational characteristics for selecting python as a base for OSDAP development:

- High level

- Open source
- Lightweight compiling
- Object-oriented
- Includes predefined functions
- Combines general, statistical and scientific computing with visualization
- Cross-platform compatible
- Active community-supported (trending)
- Combines general, statistical and scientific computing with visualization

6.1.2 OSDAP data handling and visualization

The OSDAP uses data analysis techniques to manipulate quantitative numerical data in the size of Gigabytes into useful information. Data by nature is unsorted, unstructured and complex, in common words “messy” which is known as “dirty data”. Eventually, data develop into big data with the characteristics of the 3 V’s: Volume, Velocity, Variety. When it comes to energy applications, the data type is numerical and is stored in databases and comes in a variety of sizes from Kilobytes up to Gigabytes and as fast as milliseconds “live” up to annual frequency.

Methodology

The platform reflects the backend handling data analysis into an interactive Graphical User Interface, it is designed to be specifically used for Off-grid and decentralized Hybrid Renewable Electrical Systems. However, it can be used as well (with minor modification) for other electrical energy systems.

Libraries such as “datetime” and “PYTZ” are responsible for manipulating time and date. These libraries were used for changing the time and date format from naive time to aware time and assigning a time zone. Daylight saving was also taken into account considering the actual location of the recorded data.

The HTTP library “requests” is the key library communicating between the database and the platform requesting a Uniform Resource Locator (URL) with desired data files downloading the files in bulks or chunks ensuring connection establishment without timeouts, where the “Zipfile” library extracts the requested files into their original formats.

Part of the backend engine is the visualization that includes libraries Matplotlib and PIL. The Matplotlib library is a cross-platform 2D plotting tool that generates plots and charts and saves them in certain formats where the PIL library extends the list of supported formats for giving more options to the user to save figures into more convenient formats. The front end of the platform uses the built-in library TKinter for creating a GUI that include buttons, text fields, dropdown lists, explorer, pictures and plotting canvas. The FigureCanvasTkAgg library enables embedding plots inside the GUI rather than a pop-up window, navigating through the canvas is possible and

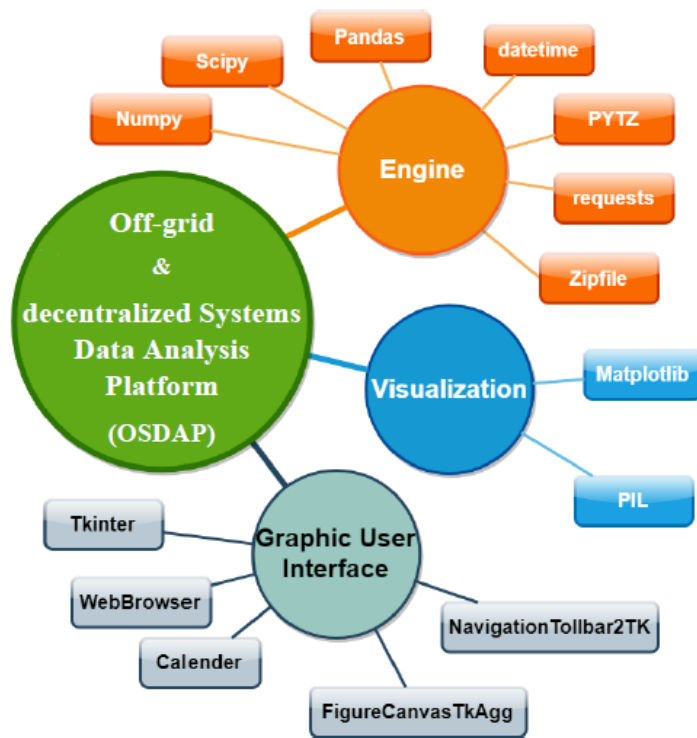


Figure 6.2: OSDAP data handling and visualization Structural chart.
 Figure reference: Author’s publication [8], and supervised work [95].

more features like zooming in/out, grabbing coordinates, saving screenshots and other are handled by the library NavigationToolbar2TK. Both libraries are critical to linking the visualization with GUI. Each widget is connected to the platform engine easing the user experience. Combining the engine, the interactive visualization and the GUI create an enhanced platform with many features which makes the user experience wider and accurate.

Structure

In the previous methodology section, OSDAP is divided into engine, visualization, and GUI. The next diagrams are a flowchart description of how the OSDAP operates in the backend and front end.

Figure 6.3 illustrates that the user has the choice to use a local database or a cloud database, either raw or sorted data to upload energy or weather data in CSV and other formats. Within selection from a database, the user has the choice to filter and sort the input data by specifying a certain system location with a certain date range. Moreover, the user can manipulate the data’s resolution and timezone. Upon selection, the data is fetched from the database and downloaded as a zipfile, extracted and unzipped into raw data files for handling process.

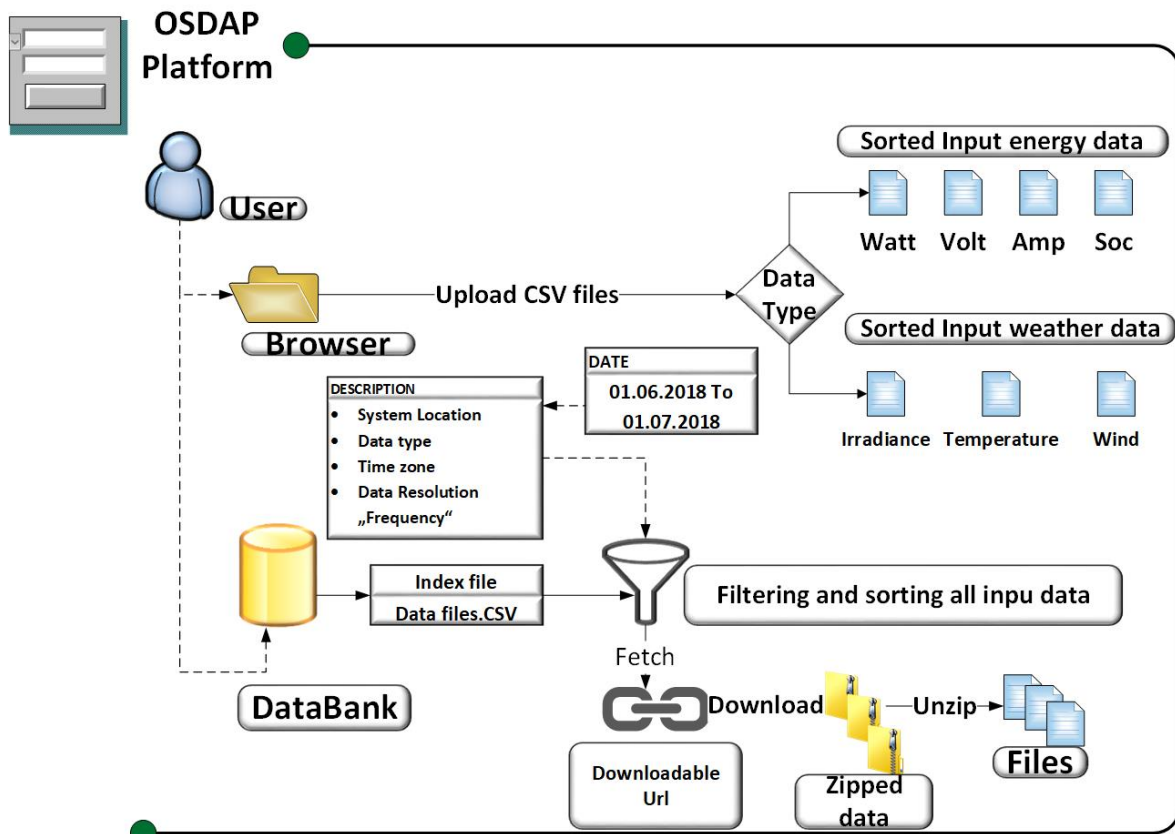


Figure 6.3: Offgrid Systems Data Analysis Platform Inputs and Analysis flow paths. Figure reference: Author's publication [8], and supervised work [95].

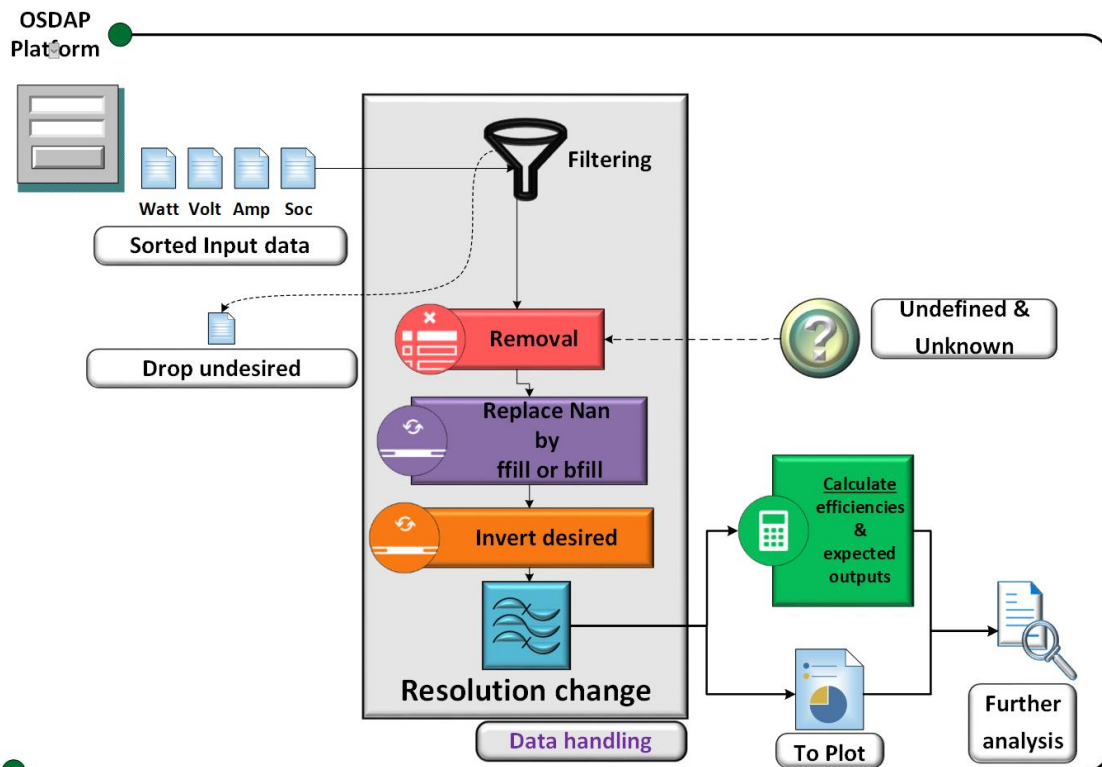


Figure 6.4: Offgrid Systems Data Analysis Platform close view on Raw data handling. Figure reference: Author's publication [8], and supervised work [95].

The handling process in figure 6.4 is only applied to raw data where it is sorted into specific files rather than scattered unsorted data. The sorted data is filtered where undesired data is excluded and then unknown and undefined values are removed. After that, the Nan values are replaced using fill forward or fill backward methods. afterward, some of the column values are subjected to inverting its values for visualization purposes.

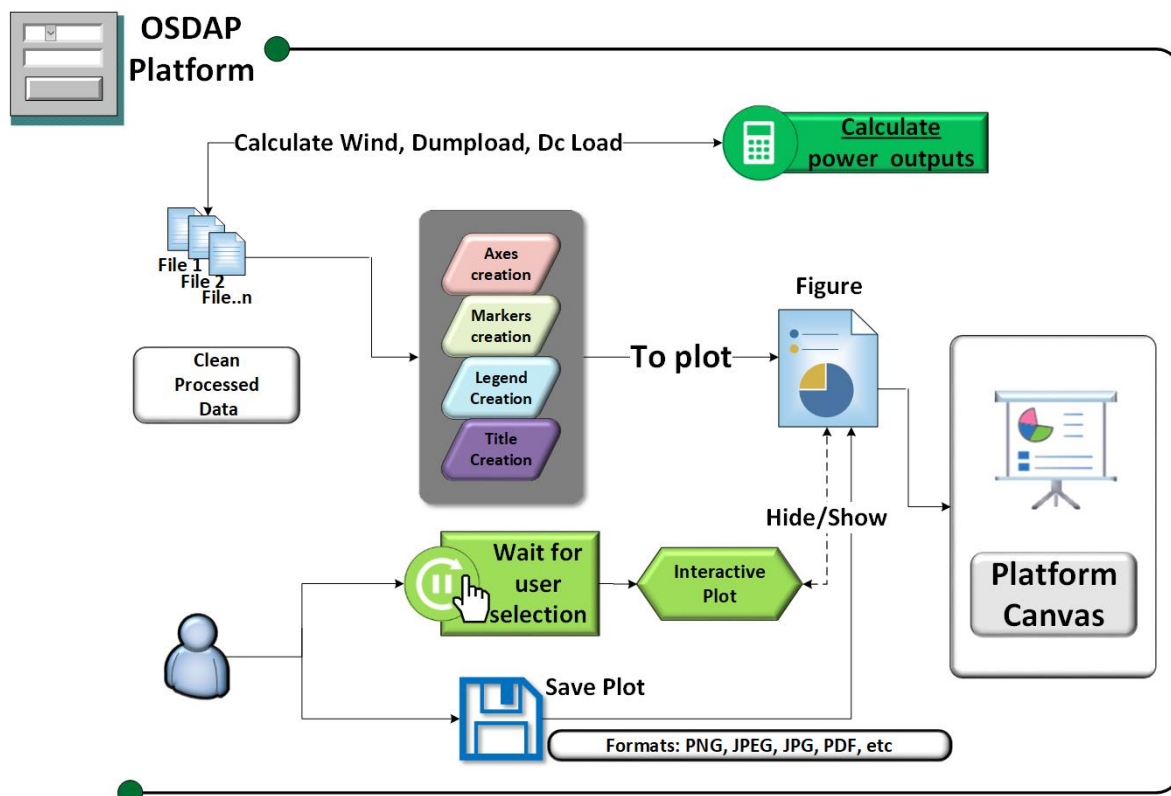


Figure 6.5: Offgrid Systems Data Analysis Platform System selected data visualization and analysis.

Figure reference: Author's publication [8], and supervised work [95].

The plotting process and visualization in figure 6.5 uses the processed (clean) data files, and creates a plot with dynamic axes and markers, which allows user interaction and selection through the plot's legend or curves for showing and hiding the curves and save plots in different formats.

6.1.3 Data preparation and visualization Graphical User Interface (GUI)

The GUI for the data preparation and visualization section of OSDAP consists of three tabs. Each tab is linked to the engine where the user can hover over each tab and select the desired one whether the user wants to fetch data or upload data directly or interact with the plot.

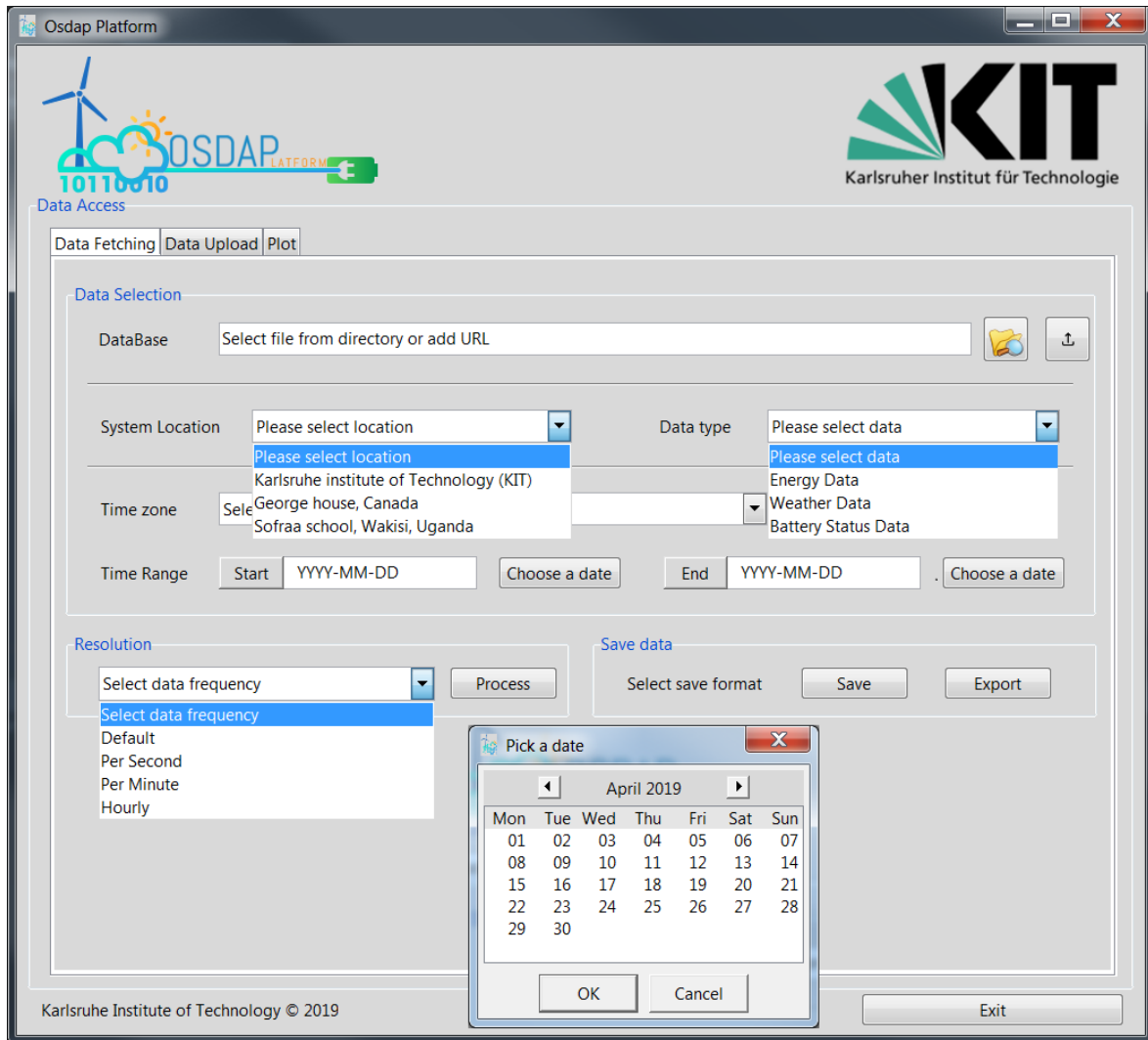


Figure 6.6: OSDAP data preparation and visualization GUI.
Figure reference: Author’s publication [8].

Data fetching tab in figure 6.6 allows the user to select the desired data type at a desired installed system location. OSDAP processes the data for a selected time range (dates), from a certain database. The data is either saved for later use or directly exported to the processed data section to be plotted according to the needed criteria.

In the second tab, the user can upload and specify a processed energy data file or weather data file. By selecting the data type, the data criteria list is enabled and changed according to the selected data type (weather data or energy data), in order to limit the user error from mixing data types. After successfully uploading the right processed files, the user can select what is needed to be visualized by selecting from the check-in boxes and then proceed with plotting by electing the “start plotting” button. The data is then dynamically visualized in the plot section where it can be also be saved.

The visualization tab contains the canvas where the plot is embedded inside for display as in figure 6.7. In the canvas, the user can interact with the plot using the mouse-triggering event to study the curves as desired. Some of the user interaction

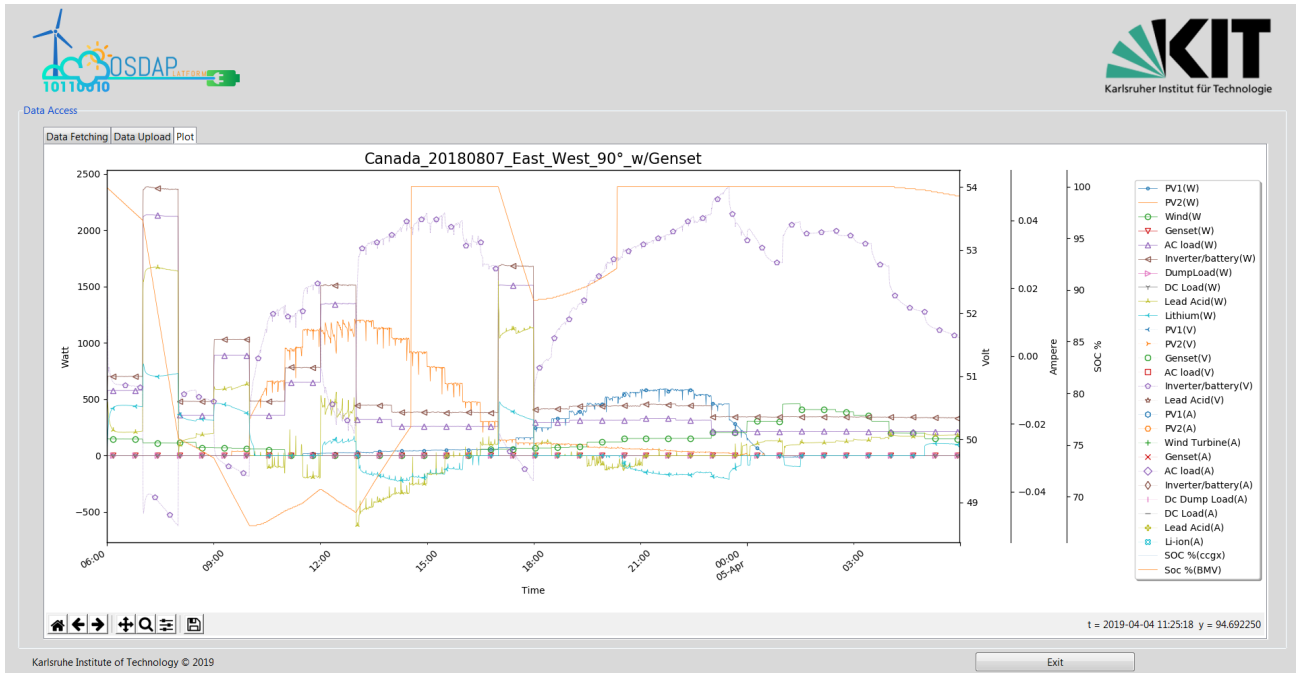


Figure 6.7: GUI: Display example of interactive plot embedded inside Canvas.
Figure reference: Author's publication [8], and supervised work [95].

features are:

- Showing and hiding curves.
- Zooming in and out.
- Extracting information of a certain point.
- Saving plot.

By showing and hiding curves, the y-axis adapts to the curve's absolute values and automatically adjusts the ratio of the curve to the y-axes as part of the adaptable visualization.

6.1.4 Hybrid system testing

OHRES and OSDAP as any newly developed system require a testing process for validation. Therefore testing scenarios need to be developed and used on a testing bench to assess both OSDAP and OHRES.

Off-grid Hybrid Systems testbench

The OHRES system is simulated in a controlled environment as well as in real environment at the Battery technical center – Karlsruhe Institute of Technology (BATEC) labs, using several simulators fully automated and remotely controlled emulating the case study such as:

- PV Simulator.
- Wind Simulator.
- DC Simulator.
- AC Simulator.
- Dumpload Simulator.

The PV simulator simulates the PV arrays providing short circuit current (I_{sc}) and open-circuit voltage (V_{oc}) of the PV module. The unit of irradiance values is W/m^2 and ambient temperature in celcius degrees to our simulated location with time intervals of 1/2 - 1 hour. As for the wind and DC simulators, both are the same in terms of using a sequence arbitrary function for programming where duration is specified in seconds based on the wind and DC load profiles, however, one is a supply and the other is a load while both use their own conditions. The wind simulator operates at the system voltage while given a projection of Nominal Current from the relationship between wind speed and power output. As for the DC simulator, it uses the Current of the existing DC appliances installed at the DC Voltage of the system.

The AC electronic load has a maximum output current of 20A, and power of 5600 watts. The load profile is programmable (using a CSV file). The electronic load is programmed to emulate the real-case load profile through specifying the load current, and the duration of consumption. Which is tracked by a sampling period to ensure that the current is following the load profile.

Test scenarios

The system including the hybrid battery system was subjected to testings using the supply and load profiles from the canada case study location, and with/without Genset using Low Voltage Disconnects (LVD) conditions in the test bench.

Figure 6.8 shows the flowchart diagram of the different scenarios used during the testing phase of the hybrid system components and performance dynamics. The scenarios developed to test both the OSDAP and the OHRES took into consideration several aspects and ignored some as well, over time other aspects were included. In the beginning, only solar, wind and load were used to come up with a scenario but with simplicity, meaning that only one orientation and one tilt angle were used to develop the initial scenario while ignoring the ambient temperature which contributes to the PV panel temperature. As for the load, DC and AC load were used from day 1 however the AC load is split into Average Connected Load (ACL) and Total Connected Load (TCL), where ACL was only considered in the beginning. The scenarios for testing were to test the extreme conditions of the OSDAP and the OHRES, therefore 6 simulation scenarios that conducted for full 24 hours considered three different orientations (South, East & West), 3 different tilt angles (15° , 45° , 90°), ambient temperature and wind speed of the day selected to emulate solar irradiance and wind profile. As for the demand side, the Total Connected Load (TCL) was used with all the scenarios and the DC load. These aspects were used on hourly bases. The last scenario was a week commissioned test that used all load such as DCL, ACL, and TCL as connected load

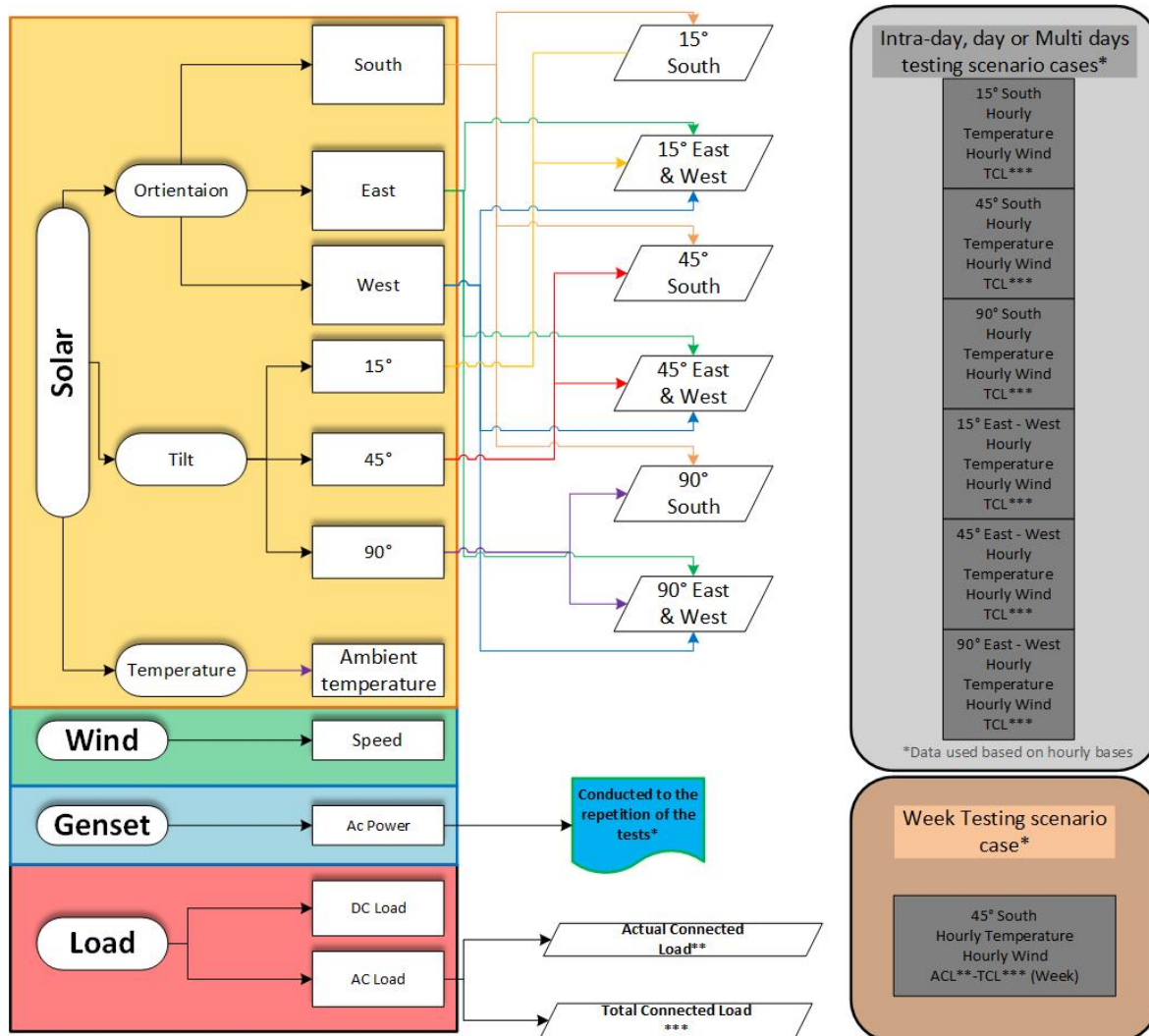


Figure 6.8: OHRES testing scenarios.

Figure reference: Author's publication [8], and supervised work [95].

however this time only considering one orientation and one tilt angle which were 45° tilt angle towards South orientation. The scenarios that were conducted were repeated for validation and were simulated again using Genset to test the Low Voltage Disconnect (LVD) occurrence and the OHRES and OSDAP response to it.

6.1.5 Canada case-study system testing and data handling

Since the testing scenarios are developed and ready to be used, a case study must be selected with the characteristics of inclusivity regarding weather conditions as energy supply and consumption as energy demand. Selecting the right case is crucial at that point since it will be either the cornerstone of the process, or it will lead back to square one. The case study should be as inclusive as possible to be able to simulate the system while imitating the caseload and the actual environment.

Load and supply profiles

The OHRES designed for the Canada (Colgate's Household) case-study was used during this system testing and data collection phase. The private residence has an off-grid system installed a total of 6 PV panels connected in 2 parallel connection with a total power of 1320 Watt and a 2000 Watt Diesel Genset supporting an Average Connected Load of 4.5 kWh/day (rated), 3.6 kWh/day (actual measured). The maximum-load scenario in this study is represented by the Total Connected Load (TCL) which can reach up to 3500 W.

The load profile for the Colgate study case was developed using the actual reading and measurements from the residence. Figure 6.9 describes the DC loads combined with self-consumption, Actual Connected Load (ACL), and Total Connected Load (TCL). The ACL has fewer peak loads and power consumption than TCL with a maximum load of 1 kW.

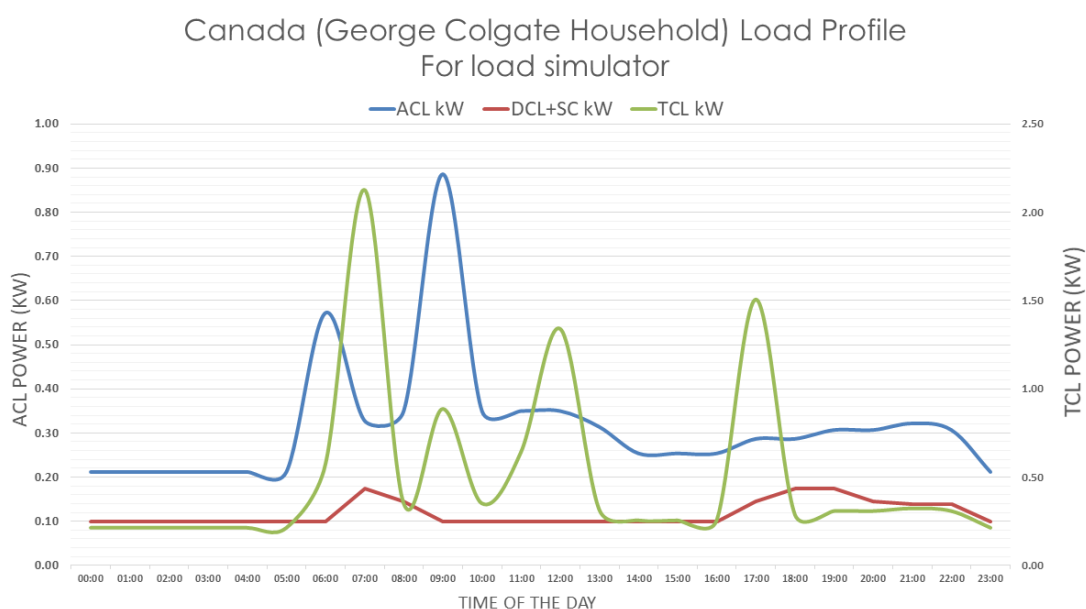


Figure 6.9: Canada Case Study (Colgate's Household): Developed Load Profile.
Figure reference: Author's publication [8], and supervised work [95].

The Solar PV and Wind profiles have been developed from meteorological data using a public satellite database. PV power and wind power were developed using the data from the day 08 of June 2006 to be used with the day load profile available from the Canada case study load survey done in earlier stage of our study as explained previously in chapter 2. The PV irradiance data was gathered from the nearest available location to the Canada (Colgate's Household) case study for reasons of availability and PV power curves were developed with 3 orientations, south, east and west and 3 tilt angles 15°, 45° and 90° from the database [96]. The coordinates were longitude 51 and latitude -56.

The wind data was gathered from the Canadian database [97] of the exact location. Combining the wind power and PV power production curves for the previously men-

tioned day, resulted in none overlapping power generation from both resources. As Wind power generation was available during night time, where Solar PV power during day time.

Orientation and tilt angle effect

The plots seen in this section are a representation of the results generated from running the scenarios discussed in 6.1.4 and illustrated in figure 6.8, the results include the power, the current, the voltage, and the state of charge curves.

Two examples are presented here, the first figure 6.10 is the current state of the installed system at the Canada (Colgate's Household) case study, it shows the plot of running 24 hours test with setting both PV arrays to south orientation at 45° tilt angle.

While the second figure 6.11 is the plot of running 24 hours test with east and west orientations where array 1 is oriented towards the west and array 2 is oriented towards the east and both are tilted at 45° tilt angle.

Findings

Figures 6.10 and 6.11 are different than other test scenarios shown in figure 6.8 in terms of tilt angles, the change in tilt angles resulted in lower power supply , thus draining the battery much faster and reaching 50% SOC which eventually triggers the LVD condition and turns on the Genset. Unlike other test conditions, the tilt angle set to the PV arrays in figures 6.10 and 6.11 manages to supply the system and maintains the batteries state of charge above the LVD condition, eliminating the use of the Genset and saving fuel costs.

However, the main difference between both figures is partial overlapping in supply PV power where PV array 1 oriented towards the east at 45° tilt angle starts supplying power in the early morning and followed up by PV array 2 oriented towards the west at 45° tilt angle which partially shares power generation with PV array 1 and continuing alone afterward until sunset. The phenomena of partial overlapping power generation results in:

- Stable battery discharge and charging behavior.
- A dramatic decrease in depth of discharge DOD.
- Increase the battery charge/discharge cycles.
- Increase the expected battery life.

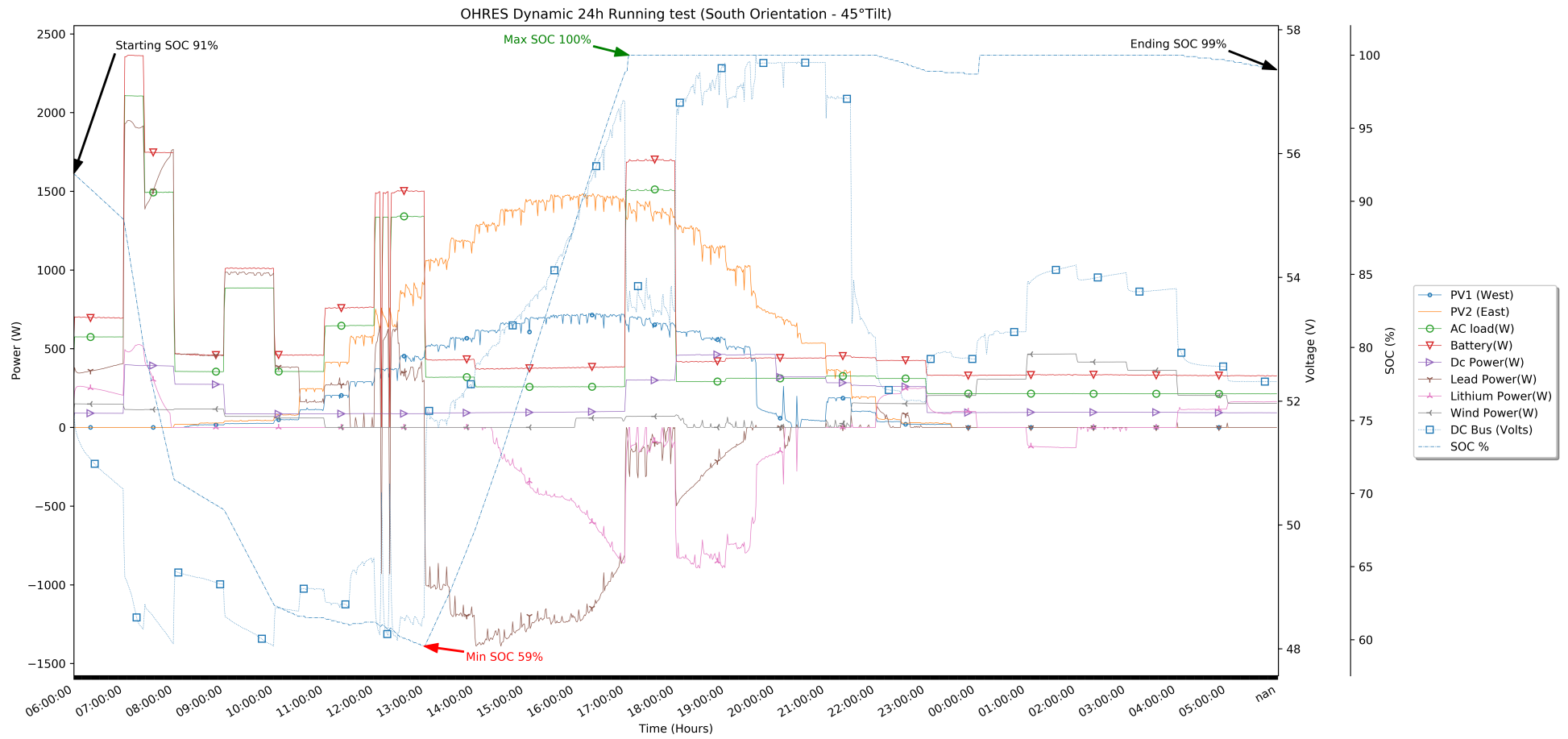


Figure 6.10: 24H Running test South orientation - 45° tilt angle.
 Figure reference: Author's publication [8], and supervised work [95].

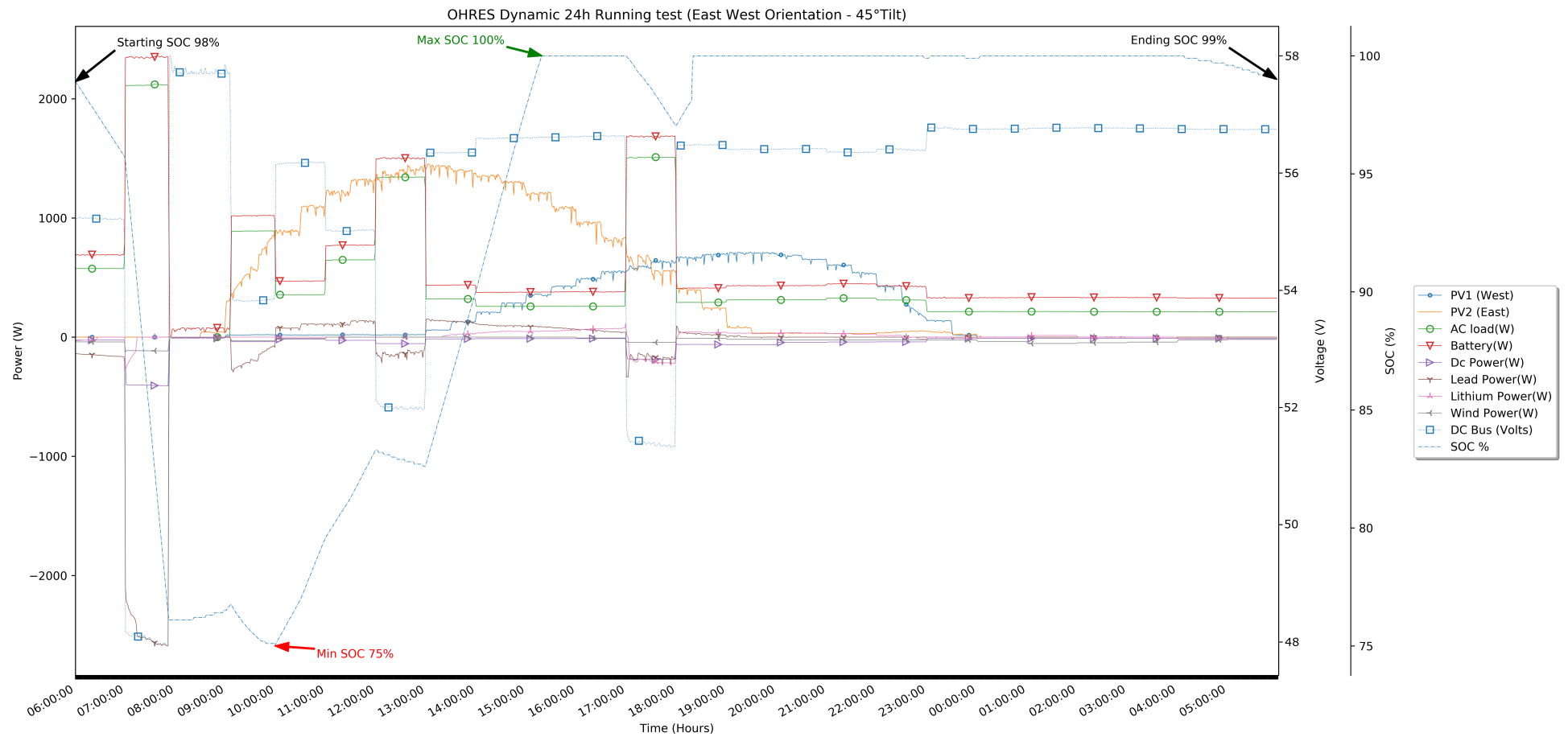


Figure 6.11: 24H Running test East West orientation - 45° tilt angle.
Figure reference: Author's publication [8], and supervised work [95].

Important to mention that even that the east-west PV configuration has a potential for better performance, but as seen before in chapter 4, and shown in figure 4.17 in the Canada case study south orientation is used. This is due to the fact that the current system includes only one PV array, which makes it not possible to use an east-west PV orientation configuration where two separate PV arrays are needed to realized such configuration in practice. However, this was taken into consideration as an outcome from our analysis and a second PV array modules have been supplied and shipped to the Canada case study location to build up the second PV array beside the existing one. Also this have been taken into consideration in the very early stage of the project in the system hardware architecture where two separate MPPT's for two PV arrays are already included in the system control cabinet as shown before in chapter 4, figure 4.1. However due to the global pandemic (started early 2020) and highly limited outdoor installation time window in the Canada case study very remote location, which is one or two month per year during summer period due to harsh weather conditions most of the year in this north remote area, the installation couldn't be realized in the period of this study. It is planned to for the installation to be done as soon as the global and outdoor installation conditions allows for that.

6.2 OSDAP Performance Analysis and Solar Irradiance Forecasting

According to the IRENA off-grid status report (2015), nearly 26 million households are served through off-grid energy systems, 5 million households through renewables-based mini-grids and 0.8 million households through small wind turbines [98]. In short to medium term, the off-grid hybrid renewable systems market is expected to grow. One of the main challenges slowing down the acceleration of the OHRES market lies in the absence of standardization in technical and economic factors. The OHRES market suffers from a lack of reliable performance data combined with economic aspects of the systems. This section presents an OHRES performance analysis tool which is used to analyze OHRES' performances in case study locations. However, the presented tool can be applied to any other OHRESs as well. Also, to give OHRES owners one-day ahead and one-hour ahead solar irradiance forecasts, development of a 24-hour ahead and one-hour ahead irradiance forecasting models were included in the scope of this work. An accurate irradiance forecasting would bring advantages such as operational control and optimization of the energy system [33].

6.2.1 Performance Analysis Tool Development Methodology

Performance analysis tool is a computer program developed in Python to carry out performance analysis tasks on the OHRES operation data. This tool has been developed for one day or long term performance analysis of PV array, energy storage unit and overall system performance. It has been only applied to the OHRES installed in Canada as it is the only operating OHRES in our study so far. However, the tool has been developed in a generic architecture so that it can also perform the performance analysis on the Uganda OHRES, once it is deployed and starts operating, or on any hy-

brid system around the globe. The OHRES operation data consist of voltage, current and power measurement from the sensors placed within the OHRES. A python based tool "Off-grid and Decentralized Systems Data Analysis Platform" (OSDAP) is used to acquire energy data as well as weather and battery energy storage data from our sensor-measurements database. The operation methodology of OSDAP can be found in section 6.1. Figure 6.12 is a screenshot of the latest version of OSDAP.

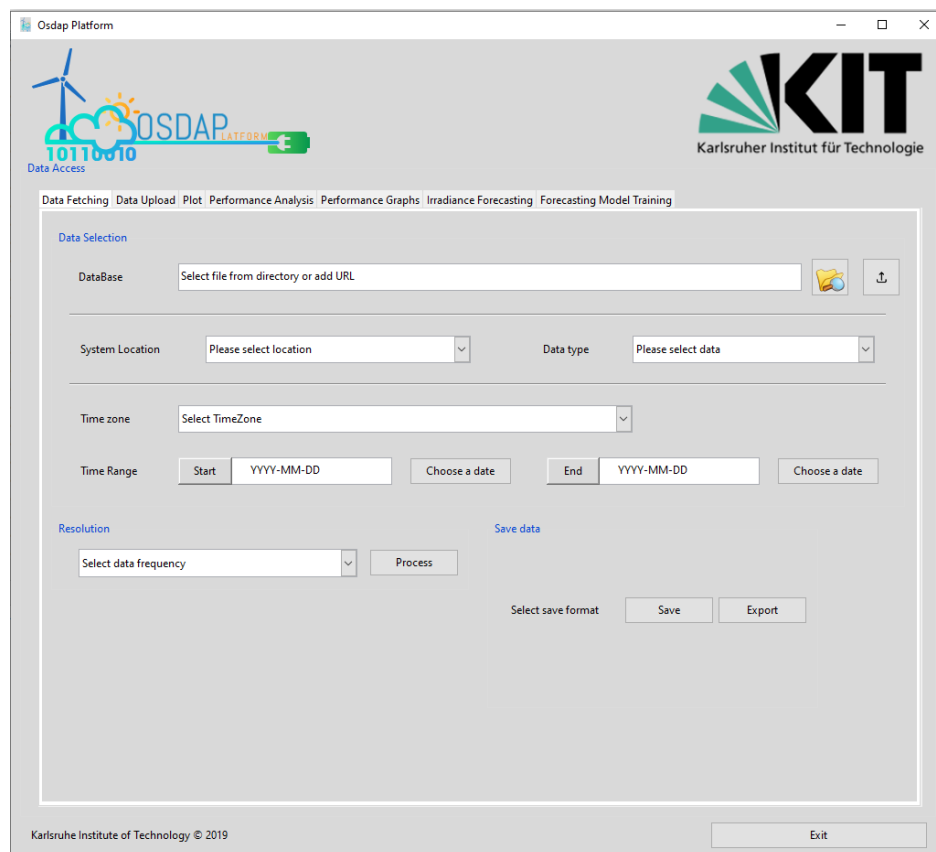


Figure 6.12: The Off-grid and Decentralized Systems Data Analysis Platform (OSDAP).

Figure reference: Author's publication [8].

Data preparation for performance analysis starts with downloading energy data, weather data, and battery SOC data via OSDAP. The OHRES system in Canada was commissioned on 13.08.2019 and the on-site testing procedures were completed on 19.08.2019. Therefore, the data starting from 20.08.2019 were used for performance analysis purposes. Table 6.1 lists all the accessible data from OHRES.

The table 6.2 shows a list of derived parameters that are suggested by IEC 61724 standards [9]. The original version of the derived parameters list also includes parameters such as net energy to utility grid, net energy from utility grid. However, the utility grid-related parameters are not considered in the scope of this work as the OHRES systems subject to this study do not have utility grid connections.

Battery round trip efficiency is calculated, as shown in equation 6.1 [99], to evaluate the performance of the energy storage unit. It provides important insights on battery health and life span, as well as the operational cost of storage systems [99]. This

Table 6.1: Measured parameters from OHRES (Author’s publication [8], and supervised work [10]).

Energy Data	Weather Data	Battery SOC Data
PV Array (W)	Global horizontal irradiance	State-of-charge (%)
PV Array (I)	Plane-of-array irradiance	
PV Array (V)	Ambient temperature	
Generator (W)	Back of the module temperature 1	
Generator (I)	Back of the module temperature 2	
Generator (V)	Wind speed	
Inverter/Battery (W)		
Inverter/Battery (I)		
Inverter/Battery (V)		
Dumpload (W)*		
Dumpload (I)		
Lead Acid Battery (W)		
Lead Acid Battery (I)		
Lead Acid Battery (V)		
Li-ion Battery (W)*		
Li-ion Battery (I)		
AC Load (W)		
AC Load (I)		
AC Load (V)		
DC Load (W)*		
DC Load (I)		

*Calculated values.

efficiency parameter essentially represents the proportion of energy input to the storage and the energy recovered from the storage. There are inevitable energy losses due to electrochemical energy conversion operation inside the battery. Therefore, there will be a difference between the energy that goes into an empty battery to fully charge it and the energy taken out from the battery to completely discharge it.

$$\eta_{Batt,rt} = \frac{\sum_{\tau_{SOC,initial}}^{\tau_{SOC,final}} E_{battout,\tau_r}}{\sum_{\tau_{SOC,initial}}^{\tau_{SOC,final}} E_{battin,\tau_r}} \quad (6.1)$$

where SOC initial = SOC final and τ_r is recording interval, expressed in hours. Therefore, $\sum_{\tau_{SOC,initial}}^{\tau_{SOC,final}}$ represents the time range between charging from a certain SOC level and discharging back to the same SOC level. The battery round trip efficiency evaluation is carried out between two time steps where the energy storage unit’s SOC starts increasing from a certain level and then decrease back to the same level. If the energy storage unit’s SOC starts increasing from 70% at a time step τ_{start} and discharge back to 70% SOC at a time step τ_{end} , $\sum_{\tau_{SOC,initial}}^{\tau_{SOC,final}}$ represents the time range between τ_{start} and τ_{end} .

Table 6.2: Derived performance parameters suggested by IEC 61724 [9] standards (Author’s publication [8], , and supervised work [10]).

Parameter	Symbol	Unit
Meteorology		
Daily global irradiation in the plane of the array	$H_{I,d}$	$kWhm^{-2}.d^{-1}$
Electrical energy quantities		
Net energy from array	$E_{A,\tau}$	kWh
Net energy from wind turbine**	$E_{W,\tau}$	kWh
Net energy to load	$E_{L,\tau}$	kWh
Net energy to storage	$E_{TSN,\tau}$	kWh
Net energy from storage	$E_{FSN,\tau}$	kWh
Net energy from back-up	$E_{BU,\tau}$	kWh
Total system input energy	$E_{in,\tau}$	kWh
Total system output energy	$E_{use,\tau}$	Dimensionless
Fraction of total system input contributed by PV array	$F_{A,\tau}$	Dimensionless
Fraction of energy input contributed by generator**	$F_{G,\tau}$	Dimensionless
Fraction of energy input contributed by wind turbine**	$F_{W,\tau}$	Dimensionless
System efficiency	η_f	Dimensionless
System performance indices		
Array yield*	Y_A	$h.d^{-1}$
Final PV system yield*	Y_f	$h.d^{-1}$
Reference yield*	Y_r	$h.d^{-1}$
Array capture losses*	L_c	$h.d^{-1}$
Performance ratio	R_P	$h.d^{-1}$
Mean array efficiency	$\eta_{Amean,\tau}$	Dimensionless

*Calculated values, **Not covered by the standard.

6.2.2 Solar Irradiance Forecasting Methodology

Related Work

Based on the previous related work and literature presented beforehand in section 1.3.1 of different ANN methods, we implemented the Long-Short Term Memory (LSTM) method for our solar irradiance forecasting application. One-hour ahead and 24-hour ahead irradiance forecasting models have been developed using two different datasets. An overview of the process flow can be seen in figure 6.13.

Dataset Description

The weather station installed at the case study location in Canada started to provide global horizontal irradiance, in-plane irradiance, temperature, relative humidity, pressure, precipitation, wind speed data from 16.12.2018. On hour-ahead, the irradiance forecasting model was trained and tested with an hourly weather dataset between 12.08.2019 and 30.06.2019.

HelioClim-3 datasets provide satellite-derived solar irradiance data and other meteorological data as well as clear-sky conditions. The solar irradiance data include global

horizontal irradiance and in-plane irradiance for multiple angles, irradiation at the top of the atmosphere irradiance and clear-sky irradiation which indicates the irradiance if the sky were clear. However, to match cases with our weather station data and considering practical use cases, features like clear-sky condition and top of the atmosphere irradiance were disregarded. HelioClim serves data from 01.02.2004 up to 31.12.2006 free of charge while limiting both longitude and latitude between -66° and 66° . A free-version dataset from 01.02.2004 to 31.12.2006 was downloaded for latitude 48° longitude 7.8° . HelioClim-3 data is used for the 24-hour ahead irradiance forecasting.

Data Preparation

The irradiance forecasting models were designed to make a univariate prediction out of multivariate input. In a multivariate model, the input features must be correlated so that the model builds a relation among the features and make a prediction considering changes in input features and their effects on the output vector [100]. Therefore, determining the correlation between features in the data was an important step to decide whether a feature will take part in the input vector or be discarded. Figure 6.14 depicts a correlation matrix in a color-map form. After inspecting the figure, weakly correlated features were discarded from the dataset. Hence, only the following features were selected: solar irradiance, temperature, relative humidity, day of the year, time of the day. The rest of the features had been dropped from the dataset.

Once the input features are selected, the next step is to prepare output vectors so that the output would represent 24-ahead solar irradiance. One point to note is that irradiance values in the input vector and the output vector are essentially the same. However, the output vector is shifted by 24-hours. If we consider input vector and output vector as columns of a table, one row would contain t_0 value of irradiation in the corresponding input vector column and the same row would contain t_{20} value of irradiation in the corresponding output vector column. The model would try to predict the corresponding output value for each input vector. This would give us a 24-hour ahead prediction. Since the output vector is shifted by 24 hours to represent 24-hour ahead irradiation values, the last 24 hours dropped the input vector because there are no corresponding output values for the last 24 hours. The same process was done for the one-hour ahead prediction model by shifting the data for only one hour.

Data Split

After deciding on the input vector features and making the time shift adjustments, the data set needs to be split into three before going into the ANN model. All datasets are split into three subsets, training set (70%), validation set (20%) and test set (10%). Data splitting points are carefully adjusted to take place at the end of the day. We avoided splitting data at different hours of a day, to keep the consistency of data splitting operation.

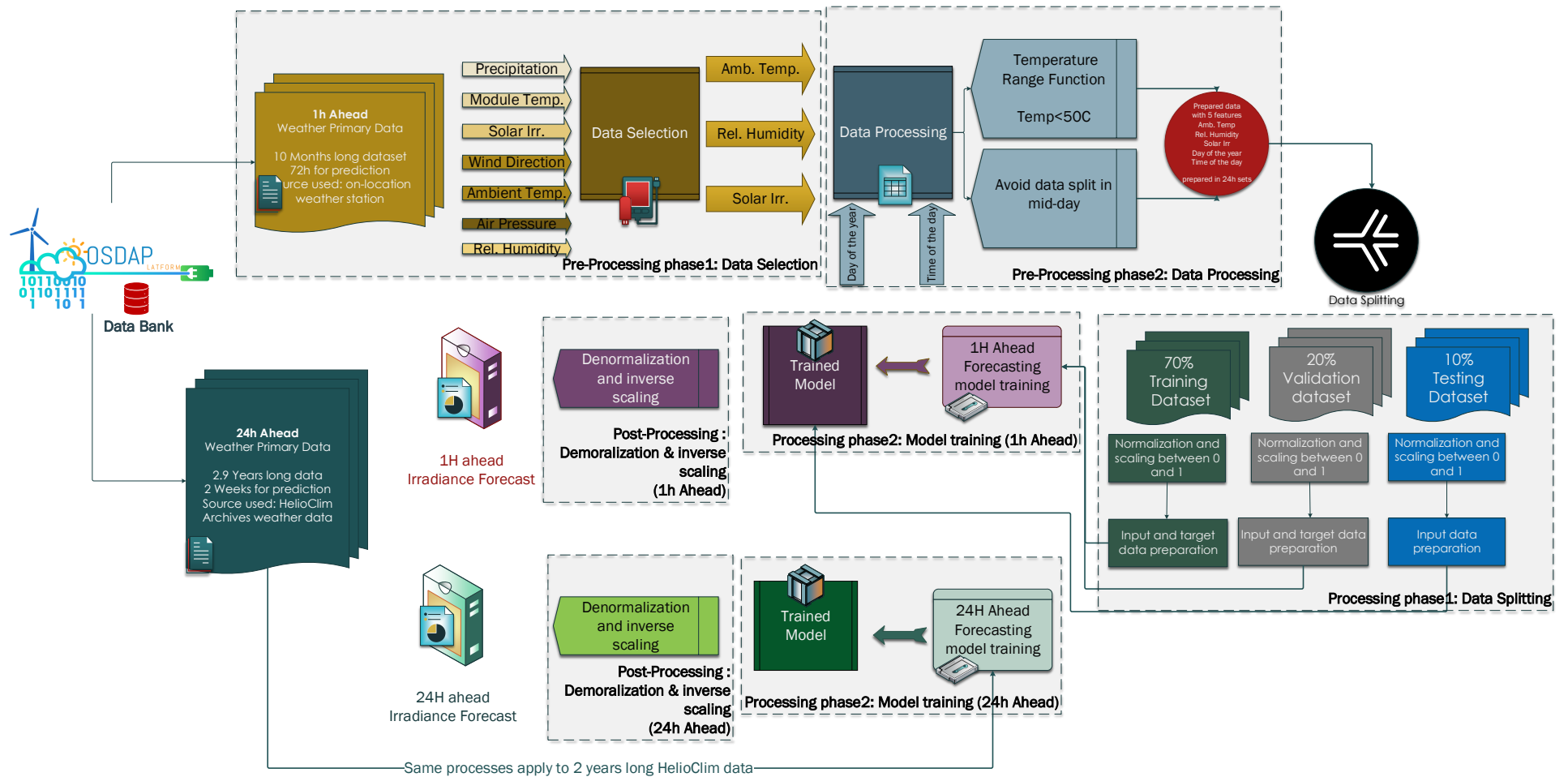


Figure 6.13: Operation flow diagram of solar irradiance forecasting models.
Figure reference: Author's publication [8].

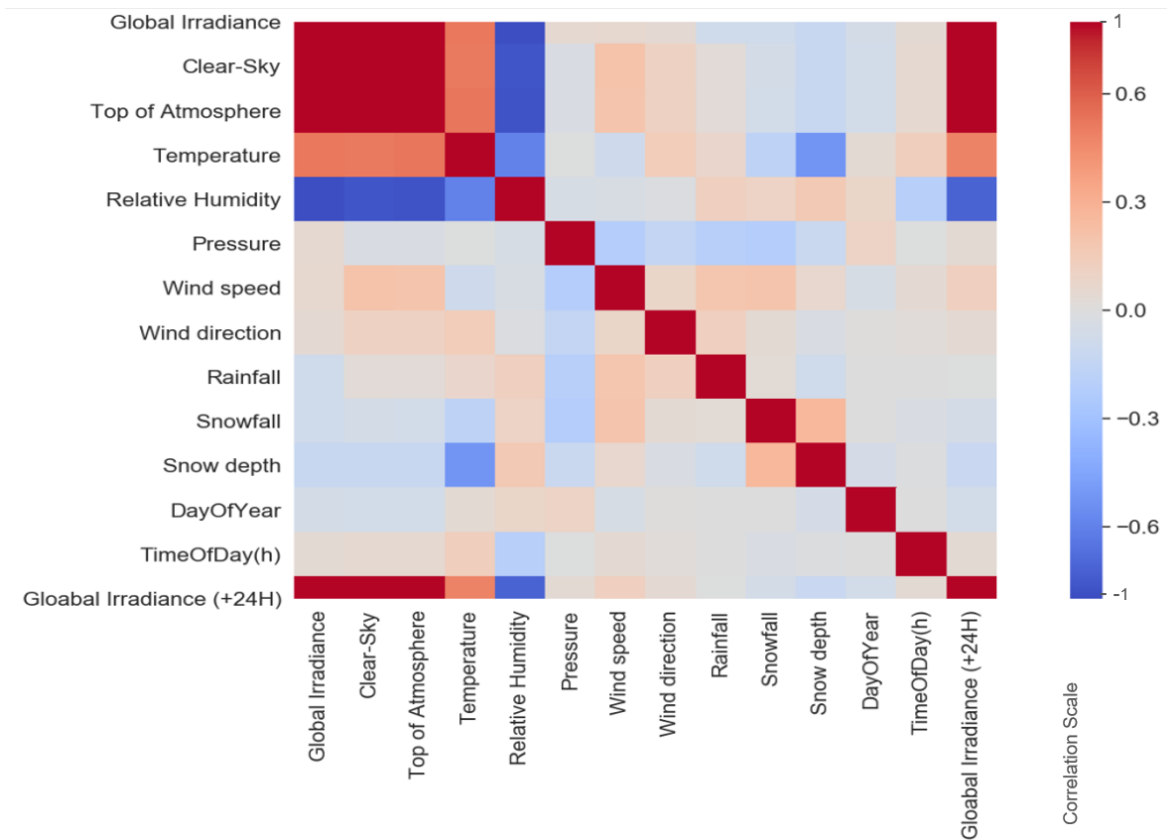


Figure 6.14: Color-map depicting correlation between features of HelioClim-3 dataset. Figure reference: Author’s publication [8], and supervised work [10].

Building sequences

LSTM accepts input vectors in 3-dimensional form. Therefore, input vectors of training, validation and test sets are transformed into 3D vectors. Sequence length has been set as 336 hours which accounts for 2 weeks of length (24x7x2). On the other hand, the sliding window slip rate set as one hour. Each one-hour slide of the window creates a sequence that consists of 336-hour time-steps. Considering these two facts, samples, 336 hours long and containing 5 features, are created.

Figure 6.15 depicts the sliding window effect and sequence structure for the 24-hour ahead irradiance forecasting model. This model takes an input sequence of 336-hour time-steps and 5 features to predict an output sequence of 24-hour time-steps and one feature which is irradiance. The input sequence is highlighted in the turquoise box and the output sequence is highlighted in the orange box. Each one-hour slide of the window generates 24-hour ahead irradiance prediction.

Figure 6.16 depicts the sliding window effect and sequence structure for the one-hour ahead irradiance forecasting model. Notation D represents days, notation h represents hours of the day and notation F represents features. This model takes an input sequence of 72-hour time-steps and 5 features to predict an output sequence of one-hour time-step and one feature which is irradiance. The input sequence is highlighted in the turquoise

Sliding Window

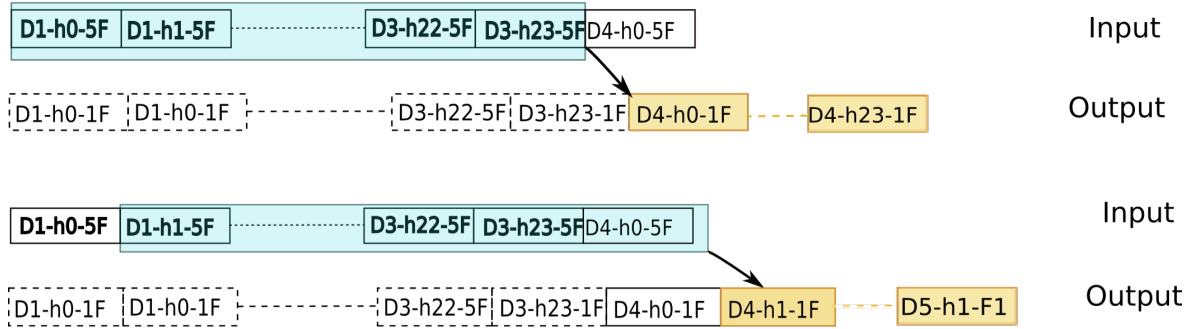


Figure 6.15: Sliding window effect for 24-hour ahead predictions. Figure reference: Author’s publication [8], and supervised work [10].

box and the output sequence is highlighted in the orange box. Each one-hour slide of the window generates one-hour ahead irradiance prediction.

Sliding Window

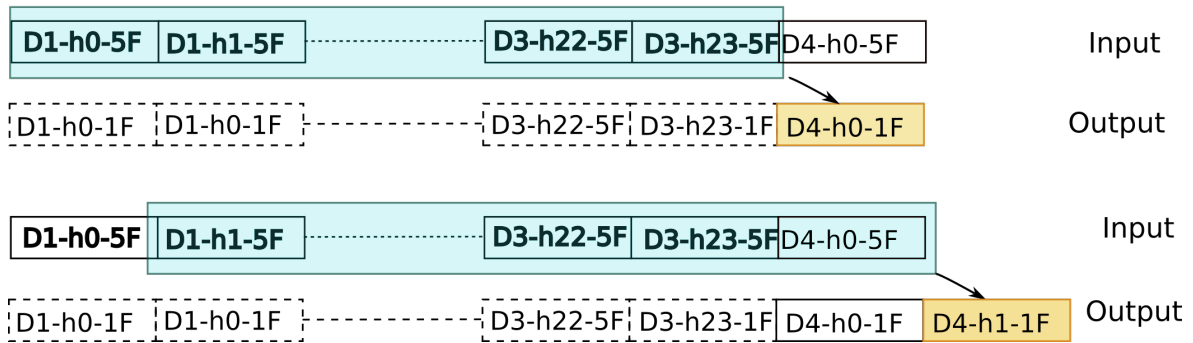


Figure 6.16: Sliding window effect for one-hour ahead prediction. Figure reference: Author’s publication [8], and supervised work [10].

Model Structure

This section describes architectures of the 24-hour ahead and the one-hour ahead irradiance forecasting models. Hyperparameters of each model were presented in detail together with their explanations.

24-hour Ahead Irradiance Forecasting

The forecasting model structure consists of six layers. Layer types and number of neurons in each layer are given in table 6.3.

An LSTM layer expects a 3-dimensional input vector. Depending on the Return_Sequence parameter, it can return either a 3D vector or a 2D vector. The Return_Sequence parameter is set to True for the LSTM1 layer. Hence, the LSTM1 returns a 3D vector

Table 6.3: 24-hour ahead irradiance forecasting model structure (Author’s publication [8], and supervised work [10]).

Layer Type	Number of Neurons	Notes
LSTM1	110	Return Sequence = True
Dropout(0.2)	N/A	
LSTM2	110	Return Sequence = False Bias Initialization = zero matrix Kernel Initializer = glorot_uniform
Dropout(0.2)	N/A	
Dense1	48	Activation = Tanh
Dense2	24	Output layer Activation = Relu

which is appropriate to be an input vector for the LSTM2 layer. Since a dense layer expects a 2D input vector, the LSTM2 layer’s Return.Sequence parameter is set to False. Bias initialization parameter of the LSTM2 layer indicates that the initial values of the bias matrix will be equal to zero matrices. Kernel’s initializer is set to be uniform so that the initial weights of the LSTM2 layer will have a uniform distribution. The LSTM2 layer returns a 2D vector which is appropriate to be an input vector for the Dense1 layer. Finally, the Dense2 layer returns a 2D vector of 24 time-steps and one feature. Dropout layers are seen in table 6.3 are used to avoid over-fitting.

Before running the model, batch size has been set to 128 and the maximum number of epochs is 500. Adam optimizer was used for backpropagation optimization. If training loss did not decrease in two consecutive epochs, the ReduceLRonPlateau function decreases the learning rate by a factor of 0.1. The training operation has two termination conditions which are: a) completing 500 epochs, b) early stopping if the validation loss doesn’t decrease for 5 consecutive epochs.

One-hour Ahead Irradiance Forecasting

One-hour ahead irradiance forecasting model has been designed to make an accurate short-term prediction with fewer data. One hour ahead irradiance forecasting is influenced by recent weather activities. Therefore, the input sequence length was set as 72 hours. Shorter input sequence length enabled us to use fewer neurons in each layer compared to the 24-hour ahead forecasting model. The model structure of the one hour ahead irradiance forecasting model is given in the table 6.4.

The model structure consists of six layers, two of which are LSTM layers. 32 neurons are placed into each LSTM layer. On the other hand, the Dense1 layer includes only one neuron which behaves as a non-linear transition layer between LSTM2 and Dense2 output layer. Since the model was expected to make one prediction for each input sample, only one neuron took place in the Dense2 output layer. A linear activation function was used as an activation function of the output layer.

Mean square error function is used as a loss calculation function during training. Net-

Table 6.4: One-hour ahead irradiance forecasting model structure (Author’s publication [8], and supervised work [10]).

Layer Type	Number of Neurons	Notes
LSTM1	60	Return Sequence = True
Dropout(0.2)	N/A	
LSTM2	60	Return Sequence = False Bias Initialization = zero matrix Kernel Initializer = glorot_uniform
Dropout(0.2)	N/A	
Dense1	10	Activation = Tanh Kernel Initializer = glorot_uniform
Dense2	1	Output layer Activation = linear

work weights are adjusted by Adam optimizer during backpropagation operation. The training operation has two termination conditions which are: a) completing 200 epochs, b) early stopping if the validation loss doesn’t decrease for 5 consecutive epochs.

Model Evaluation

The solar irradiance forecasting models’ performances were evaluated with the following metrics: MAE, MSE, RMSE, nRMSE, and coefficient of determination [36] [101]. Error and coefficient of determination calculations were performed on the test set. Test set input vectors were entered into the models to derive predictions. Error and correlation calculations were carried on the predicted irradiance values and observed irradiance values. During the model development phase, modifications on the models were judged according to these metrics. However, it would be difficult to compare the performance of different models that perform irradiance forecasting on different locations because of various reasons such as forecasted time horizon, data resolution, variations on the weather conditions from one site to another [36].

Mean Absolute Error (MAE): denotes the average distance between the predicted and observed irradiation values over the forecasted time horizon.

$$MAE = \frac{1}{N} \times \sum_{i=1}^N |\hat{y}(i) - y(i)| \quad (6.2)$$

Mean Square Error (MSE): denotes the average squared difference between the predicted and observed irradiation values over the forecasted time horizon.

$$MSE = \frac{1}{N} \times \sum_{i=1}^N (\hat{y}(i) - y(i))^2 \quad (6.3)$$

Mean Root Square Error (RMSE): is a square rooted version of the MSE. RMSE is sensitive to big forecast errors. It is appropriate to apply where small errors are

tolerable. Hence, RMSE was also chosen as the training loss calculation function in our irradiance forecasting models. Therefore, the objectives of the irradiation forecasting models are to minimize RMSE between predicted irradiance values and the observed irradiance values. The RMSE was also used to evaluate forecasting results.

$$RMSE = \sqrt{\frac{1}{N} \times \sum_{i=1}^N (\hat{y}(i) - y(i))^2} \quad (6.4)$$

Normalized Mean Root Square Error (nRMSE): is a normalized version of RMSE by the mean observed irradiance value over the forecasted time horizon. nRMSE has and advantages to compare the forecasting performance over different times of the year. Since mean daily irradiance varies over different seasons of the year, evaluating the forecasting performance by only RMSE may be misleading. Mean daily irradiation is lower in the winter season than in the summer season. This may lead the winter forecasting performance to have lower RMSE value than summer forecasting, even though summer forecasting performs better. On the other hand, nRMSE would yield easily interpretable results as it is normalized by the mean irradiation value over the forecasted time horizon.

$$nRMSE = \frac{\sqrt{\frac{1}{N} \times \sum_{i=1}^N (\hat{y}(i) - y(i))^2}}{\bar{y}} \quad (6.5)$$

Coefficient of Determination (R^2): denotes squared of the correlation coefficient between predicted and observed irradiation values over the forecasted time horizon. It represents how well the model predicts future values.

$$R^2 = 1 - \frac{\sum_{i=1}^N (\hat{y}_i - y_i)^2}{\sum_{i=1}^N (\hat{y}_i - \bar{y})^2} \quad (6.6)$$

where: \hat{y} represents predicted solar irradiance values, y represents observed solar irradiance values.

6.2.3 OHRES Performance Analysis Results

OHRES-Canada performance has been analyzed from 20.08.2019 to 30.09.2019. PV array supplied 178.67 kWh of electrical energy over this period. Figure 6.17 compares daily nominal PV energy yield and daily measured PV energy yield. The nominal PV energy yield represents the energy yield of PV array if it was operating at its rated power during given the measured solar irradiance conditions. The nominal energy yield was calculated within the performance analysis tools at standard test conditions. Measured PV energy yield is measured by sensors and it represents the actual energy yield of the PV array. The highest gap between the two energy values occurred on August 29th where the nominal energy yield is 10 kWh and the measured energy yield is 5.83 kWh. On September 9th, the nominal energy output is 1.65 kWh while the measured energy output is 1.7 kWh. The highest measured PV energy yield was observed as 7.6 kWh on September 16th and the lowest energy yield was observed as 465 Wh on September 27th. August 31st was left blank because a data registration problem a data

inconsistency occurred on 31.08.2019. Therefore, the data on that date removed from the graph and further performance calculations. The further performance parameter calculations were carried out as if August consisted of 30 days instead of 31 days.

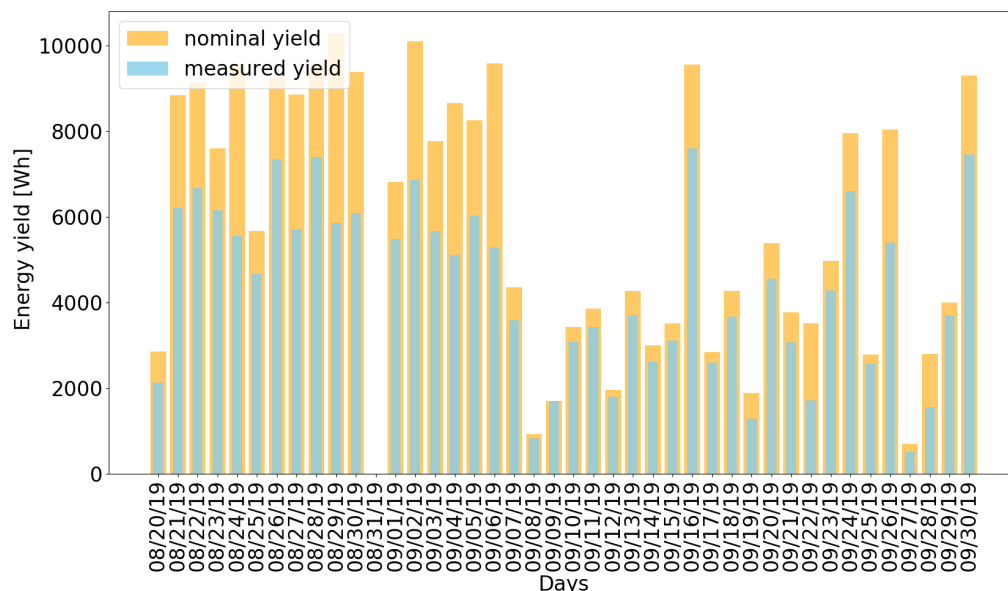


Figure 6.17: Nominal PV energy yield vs measured PV energy yield between 20.08.2019 and 30.09.2019.

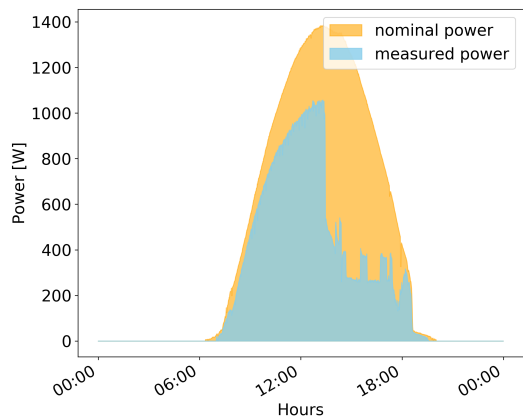
Figure reference: Author’s publication [8], and supervised work [10].

Nominal and measured energy yield differences from August 29th and September 9th are presented in figure 6.18 with minute-based data resolution. On August 29th, the measured power of the PV array decreased sharply after 1 pm while the pyranometer was still measuring above 1.3 kWh/m^2 . On September 9th, measured power is slightly higher than the nominal energy power between 9 a.m. and 4 p.m. Module temperature was $18 \text{ }^\circ\text{C}$ during peak irradiance hours on that day. However, nominal energy yield was calculated with rated power which is determined in standard test conditions (STC) at $25 \text{ }^\circ\text{C}$. The PV array has slightly higher efficiency at $18 \text{ }^\circ\text{C}$ than it has at STC. This could result in measured yield to be slightly higher than nominal energy yield if the system losses are negligibly small.

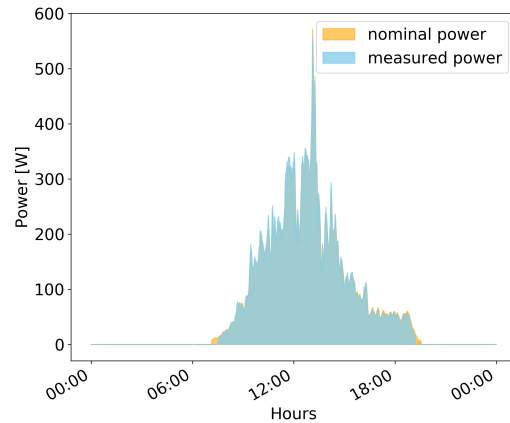
The close relationship between solar irradiance and DC PV output can be seen in figure 6.19. The figures 6.19a and 6.19b depict minutely distribution of the solar irradiance and the PV array output power per watt peak on 26 August 2019 and 9 September 2019. Regression graphs in figure 6.20 more clearly show linear dependence between solar irradiance and PV array DC output power on the given days. The coefficient of determination value of above 99% was observed which indicates the PV array’s ability to instantaneously react to changes in solar irradiance.

Battery Bank Performance Analysis

Figure 6.21 shows the battery bank’s voltage levels in September. The maximum battery voltage is about 58 V and this level indicates that both lead-acid and lithium-ion batteries are full. Battery voltage had reached the maximum level multiple times,

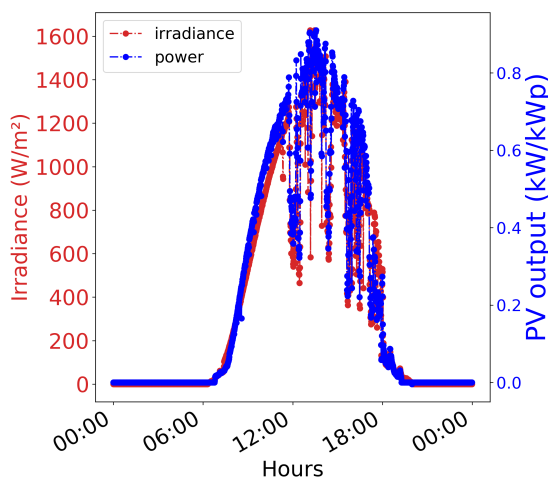


(a) 29 August 2019

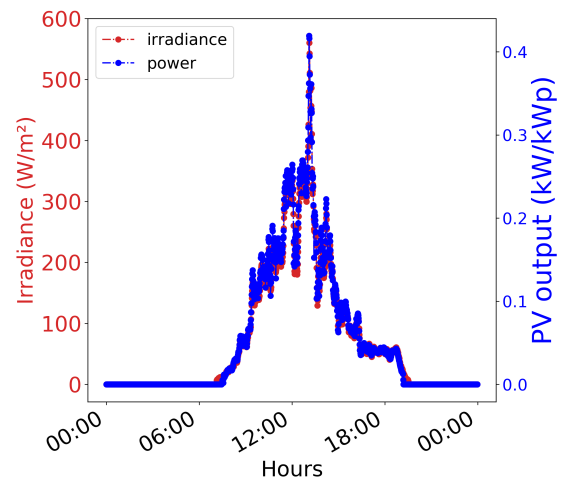


(b) 9 September 2019

Figure 6.18: Nominal power vs measured PV DC power outputs on two days.
Figure reference: Author's publication [8], and supervised work [10].



(a) 26 August 2019



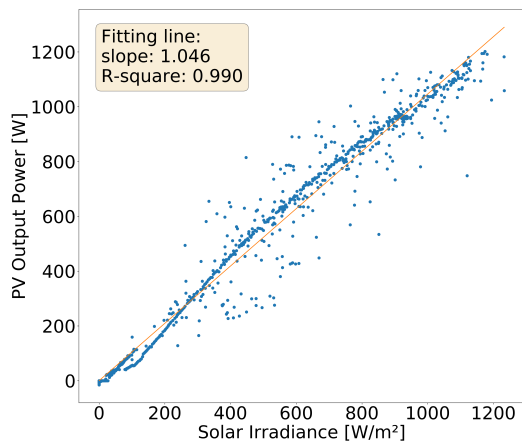
(b) 9 September 2019

Figure 6.19: Solar irradiance versus PV array DC output power per watt peak on two days.

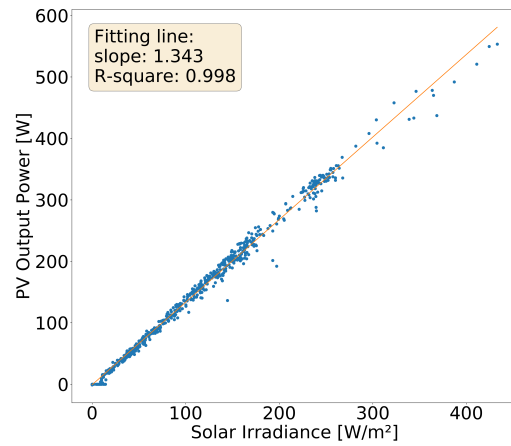
Figure reference: Author's publication [8], and supervised work [10].

especially during the first seven days of September it reached maximum voltage six times. The battery bank experienced deepest discharge between September 10th and September 13th.

Figure 6.22 represents PV array DC power generation, generator's AC power output and AC load in September 2019. The figure was plotted according to data that were derived from the power sensors of the OHRES. The figure shows that the diesel generator engages if the battery bank and instantaneous PV array yield are not able to supply the load. On 9th of September, PV array generated only 300 W at the peak



(a) 26 August 2019



(b) 9 September 2019

Figure 6.20: Solar irradiance versus PV array DC power output on two days.
Figure reference: Author's publication [8], and supervised work [10].

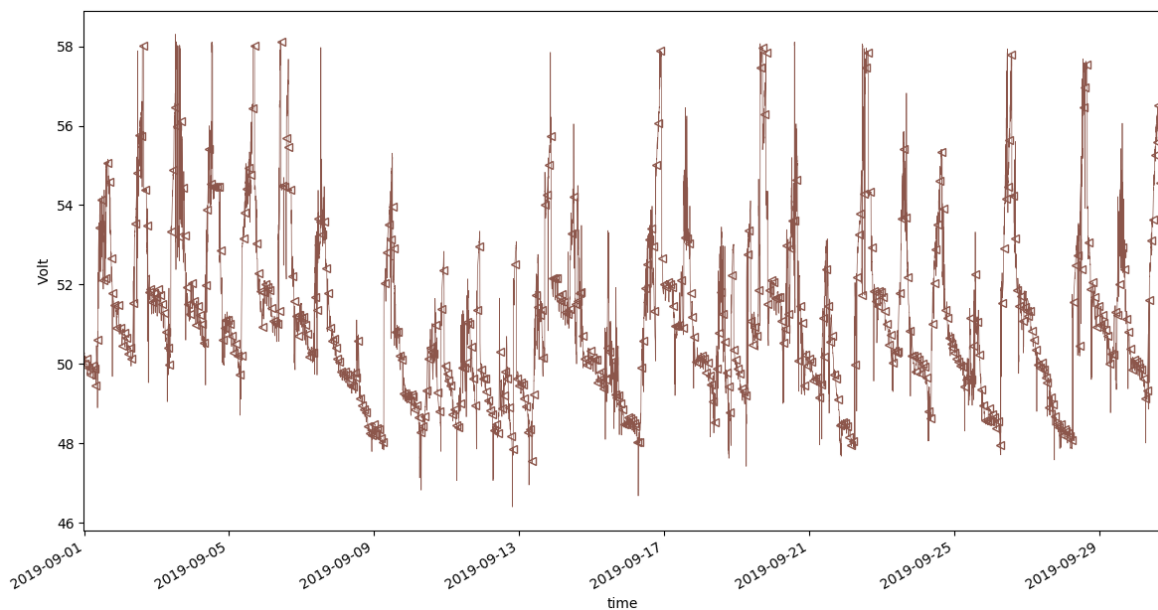


Figure 6.21: Battery voltage between 01.09.2019 and 30.09.2019
Figure reference: Author's publication [8], and supervised work [10].

solar irradiation of the day. By looking back to figure 6.21, we can see that most of the load was supplied by the battery bank on September 9th. Solar irradiation was still poor on September 10th and the AC load started to increase during the day. Since the battery bank was drained from the day before, the battery bank did not have enough energy to supply the load. Hence, the diesel generator engaged to supply the load and the surplus energy charged the battery bank. The sudden increase in battery voltage on September 10th was caused by diesel generator's surplus energy.

The battery bank's round trip efficiency calculations were carried out between two

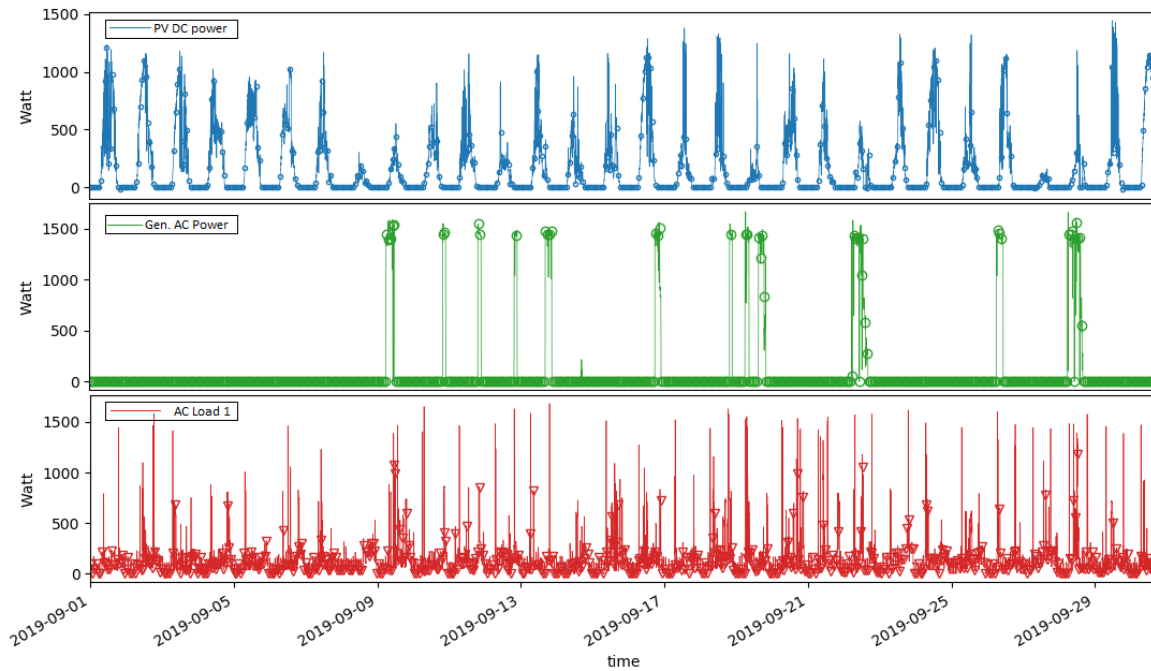


Figure 6.22: PV DC power, generator AC power and AC load 1 between 01.09.2019 and 30.09.2019.

Figure reference: Author's publication [8], and supervised work [10].

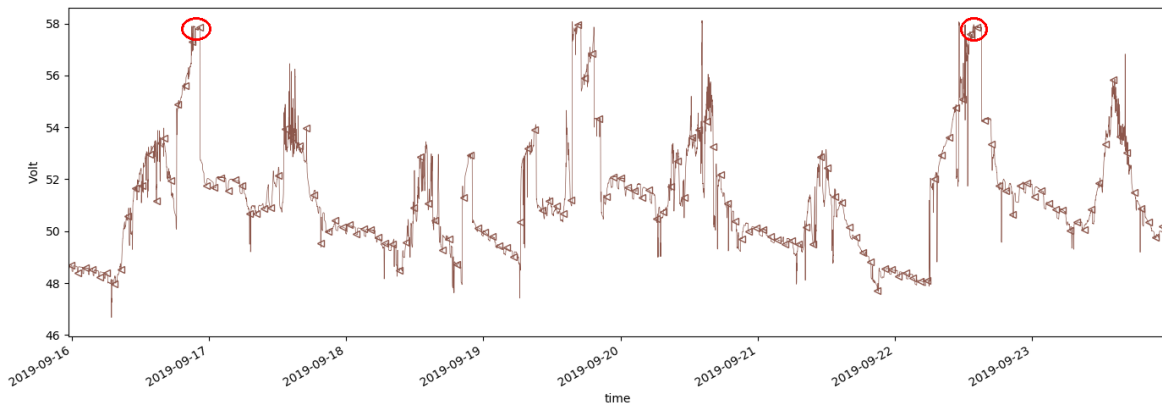


Figure 6.23: Battery voltage between 16.09.2019 and 24.09.2019.

Figure reference: Author's publication [8], and supervised work [10].

timestamps where battery bank voltages are the same. Battery voltage was taken as a reference instead of SOC because the SOC value is an estimation of the battery management system and it was found out that voltage value was more accurate to be a reference. Figure 6.23 shows two timestamps, indicated with red circles, where the battery voltage is 57.8 V for both timestamps. Total energy that went to the battery bank and total energy that went from the battery bank were calculated between the two indicated timestamps. When the power sensors were used to calculate the energy values, battery round trip efficiency was found to be 194 %. An efficiency value of above

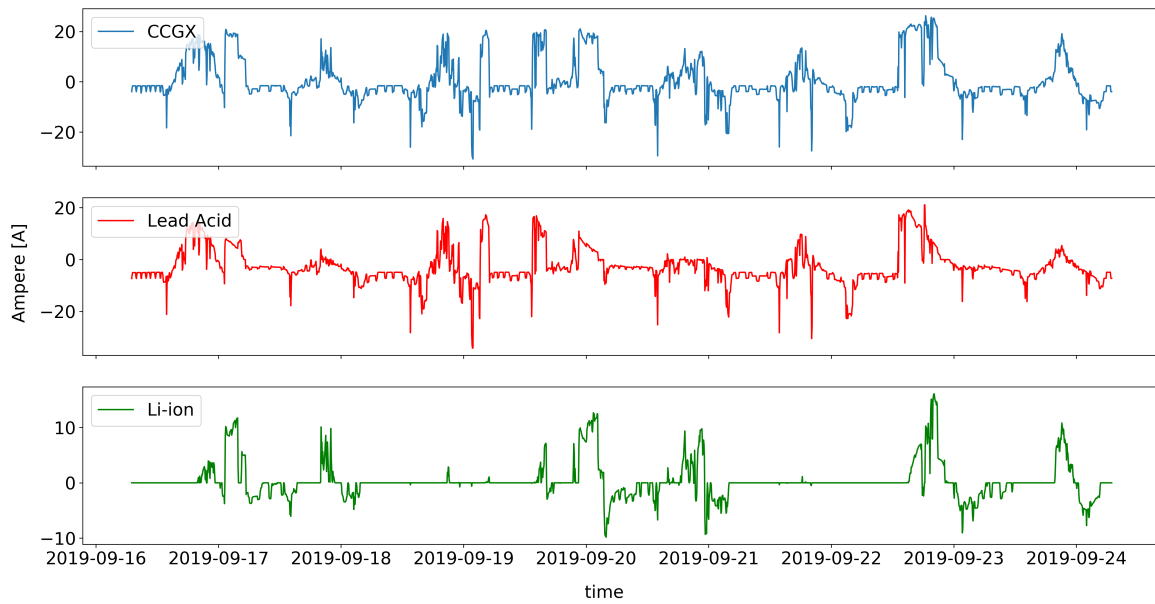


Figure 6.24: Comparison of sensor measured individual battery currents and CCGX derived battery bank current.

Figure reference: Author's publication [8], and supervised work [10].

100% is illogical because it indicates that the battery discharges more energy than it has charged. When the sensor measurements were inspected to understand the battery behaviors individually, it was seen that lead-acid battery discharged 10.6 kWh and discharged 30.5 kWh between the two timestamps, whereas Li-ion battery charged 6.94 kWh and discharged 3.6 kWh.

Since battery round trip efficiency calculations based on sensor measurements yielded illogical results, it raised a question about the reliability of the sensor measurements of the battery bank. Therefore, another battery round trip efficiency calculation was performed based on the data received from the Color Control GX (CCGX) component in the system. As illustrated before in chapter 4, and shown in figure 4.5a, all system components such as inverter/chargers, solar chargers, and batteries are connected to CCGX which provide a communication central point as a main system controller allowing the visualization of all these components timely behavior, and also adjustment of the control actions and algorithms included in each of these components and also for the whole hybrid system [57]. CCGX does not monitor lead-acid and Li-ion batteries individually but it monitors the battery bank as a whole, through getting the battery bank measurements from the battery-monitoring device (BMV) (shown before in chapter 4, figure 4.22), which uses a shunt resistance sensor installed on the battery bank main terminal, and integrated calculation algorithm for providing the battery bank parameters such as voltage, current, Power and SOC on three seconds resolution (averaged to one minute) for our remote monitoring platform (as shown before in chapter 4, figure 4.8). Figure 6.24 shows the comparison of current measurements from CCGX and sensors. According to CCGX data, the battery bank was charged by 422.2 Ah and discharged by 384.7 Ah between two timestamps. According to sensor measurements, the lead-acid battery was charged and discharged by 197.3 Ah and

611.7 Ah, respectively and li-ion battery was charged and discharged by 124.9 Ah and 70.1 Ah, respectively. Battery round trip efficiency calculation based on CCGX data resulted in an efficiency value of 84% for the whole battery bank.

Overall System Performance Analysis

Table 6.5 shows OHRES performance calculations that were carried out according to IEC 61724 standards [9] formulations. The OHRES performance was analyzed for September and the results are presented in two columns. Sensor measurement data were used for battery energy values in the first column and CCGX data was used for battery bank energy in the second column. The rest of the input values were kept the same for both columns. Daily global irradiation in the plane of the array ($H_{I,d}$) was found as $3.67 \text{ kWhm}^{-2} \cdot \text{d}^{-1}$. Array yield and reference yield values are 2.81 h/d and 3.67 h/d, respectively. The difference of array yield and reference yield would give array capture loss which is 0.86 h/d for the calculation period. The array capture loss value indicates that the PV array under-performing 0.86 hours times its rated power capacity every day. Dividing array yield to reference yield would be another way to compare measured PV energy yield to nominal PV energy yield. Division of Y_A to Y_r would give us 76.56% and this ratio can be roughly validated by revisiting figure 6.17 where measured and nominal PV energy yields are compared over the whole reporting period. Mean PV array efficiency ($\eta_{Amean,\tau}$) represents mean efficiency which the PV array was operating at over the reporting period. Net energy generation ($E_{A,\tau}$) of the PV array was 107.43 kWh during and net energy input from the diesel generator ($E_{BU,\tau}$) was 71.93 kWh during the reporting period.

Battery energy values show the difference between two columns. In the first column, net energy from storage ($E_{FSN,\tau}$) value is 91.03 kWh while net energy to the storage ($E_{TSN,\tau}$) value is zero. This indicates that the battery bank discharged net 91.03 kWh of energy during the reporting period. Having such a high discharge reading from sensors affects total system input energy ($E_{in,\tau}$). $E_{in,\tau}$ was found as 270.4 kWh while the total system output ($E_{use,\tau}$) was only 158.3 kWh. The gap between the two values caused the system efficiency (η_f) to be low. Since the final yield is a product of system efficiency and array yield, a low system efficiency value causes final yield value to be low as well. Hence, the system's performance ratio (R_P) calculation also yielded a poor result of 47.7% due to low final yield value. The difference between the array yield and the final yield values indicate that system losses were occurring during the reporting period. In this case, the system losses seemed very significant due to the high net discharge value from the battery bank. PV output energy fraction in $E_{in,\tau}$ was found as 39.7%. The same calculations were done by using CCGX data for battery energy values. The performance parameters in the second column show that $E_{TSN,\tau}$ was 11.5 kWh which indicates that the battery had net charge as opposed to the first column's indication of net discharge. The gap between $E_{in,\tau}$ and $E_{use,\tau}$ had dropped to 12.96 kWh after introducing 11.5 kWh of net charge to the calculations. The reduced gap between $E_{in,\tau}$ and $E_{use,\tau}$ led to an increase in η_f from 58.5% to 92.8%. The increase in η_f also led Y_f and R_P values to increase to 2.66 h/d and 70.9% respectively. PV fraction within $E_{in,\tau}$ has also increased in the second column to 60%.

Such comparison is done as part of our objective to understand and evaluate if de-

Table 6.5: OHRES performance parameters (Author’s publication [8], and supervised work [10]).

Parameters	Description	01.09.2019 30.09.2019	-	01.09.2019 30.09.2019	-
				*CCGX	
$H_{I,d}$	Daily global irradiation in the plane of the array	3.67 $kWhm^{-2}.d^{-1}$		3.67 $kWhm^{-2}.d^{-1}$	
Y_A	Array yield*	2.81 h/d		2.81 h/d	
Y_r	Reference yield*	3.67 h/d		3.67 h/d	
Y_f	Final PV system yield*	1.64 h/d		2.66 h/d	
L_c	Array capture losses*	0.86 h/d		0.86 h/d	
R_P	Performance ratio	47.7%		70.9%	
$\eta_{Amean,\tau}$	Mean array efficiency	11.5%		11.5%	
$E_{in,\tau}$	Total system input energy	270.4 kWh		179.36 kWh	
$E_{use,\tau}$	Total system output energy	158.3 kWh		166.40 kWh	
η_f	System efficiency	58.5%		92.8%	
$E_{A,\tau}$	Net energy from array	107.43 kWh		107.43 kWh	
$E_{L,\tau}$	Net energy to load	157.82 kWh		157.82 kWh	
$E_{TSN,\tau}$	Net energy to storage	0 kWh		11.58 kWh	
$E_{FSN,\tau}$	Net energy from storage	91.03 kWh		0 kWh	
$E_{BU,\tau}$	Net energy from back-up	71.93 kWh		71.93 kWh	
$F_{A,\tau}$	Fraction of total system input contributed by PV array	39.7%		59.9%	
	*Calculated Values				

pending on the system components measurements in an OHRES is reliable, or extra sensors are always needed for having an accurate system components measurements and primary data. Such The comparison presented here is only done as an example for how such evaluation can take place in future studies which shall utilize our study infrastructure, as such evaluation require a long time period (yearly or multi-years) time series values comparison which can be realized in future studies.

6.2.4 Solar Irradiance Forecasting Results

24-hour Ahead Irradiance Forecasting

Choosing an appropriate RNN architecture and deciding on the number of hidden neurons are mainly carried out by trial and error methods in artificial neural networks project. Determining a suitable number of neurons is difficult and could be very a time-consuming task depending on training duration of a network. For the 24-hour ahead irradiance forecasting model, more than 20 different architectural combinations were tested and only the best performing model is presented in this section. Training duration of models varied between 3 hours and 3 days depending on the number of layers, the number of neurons in the layers, sequence length, batch size, and computer performance. Training operation of the presented 24-hour ahead irradiance forecasting model took 11 hours on a computer with Intel i7-7700K 4.20 GHz CPU, 16-gigabyte

memory and 64-bit Windows 10 operating system. Figure 6.25 shows training and validation loss graph of the model. We see a steady decrease in loss during the first two epochs. Then, the validation loss makes a small peak while the training loss keeps decreasing. The validation loss becomes fairly stable after the 8th epoch while the training loss keeps decreasing slowly. Since the validation loss did not decrease for five consecutive epochs, early stopping function engaged and stopped the training after 13th epoch to avoid overfitting.

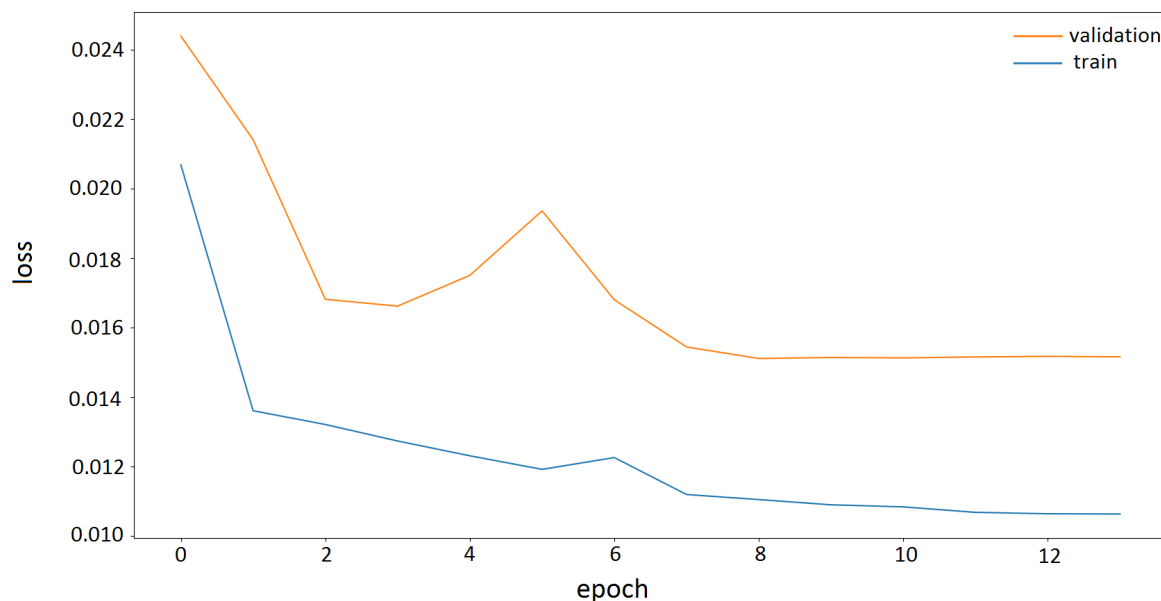


Figure 6.25: Training and validation loss graph of 24-hour ahead irradiance forecasting model.

Figure reference: Author’s publication [8], and supervised work [10].

The 24-hour ahead irradiance forecasting model was trained with 745 days long hourly weather data which was derived from HelioClim-3 online archives. A training dataset and a validation dataset were used during the model training. After the training was complete, a test dataset of 151 days was entered into the model to generate predictions. Figure 6.26 presents 24-hour ahead irradiance prediction output of the test set between 20.08.2006 and 25.08.2006. These dates were chosen to evaluate the model performance in the summer season. At first glance on the figure, we can see that the model predicts the sunrise and sunset hours very well. Also, the model predicts a steady rise and fall on the irradiance level quite well during the presented prediction period. However, the model generated rather smooth predictions that it does not predict instantaneous irradiance drops and rises. There could be a cloud passing at noon on August 24th but the model could not predict this weather activity. Root mean square error of this prediction period was 114.7 which indicates that the mean distance between predicted irradiance values and the true irradiance values was 114.7 W/m². Normalizing the RMSE value relative to the peak irradiance value of the prediction period resulted in nRMSE value of 15%. The mean absolute error value of 65 indicates that the mean absolute difference between the predicted irradiance values and true irradiance values was 65 W/m².

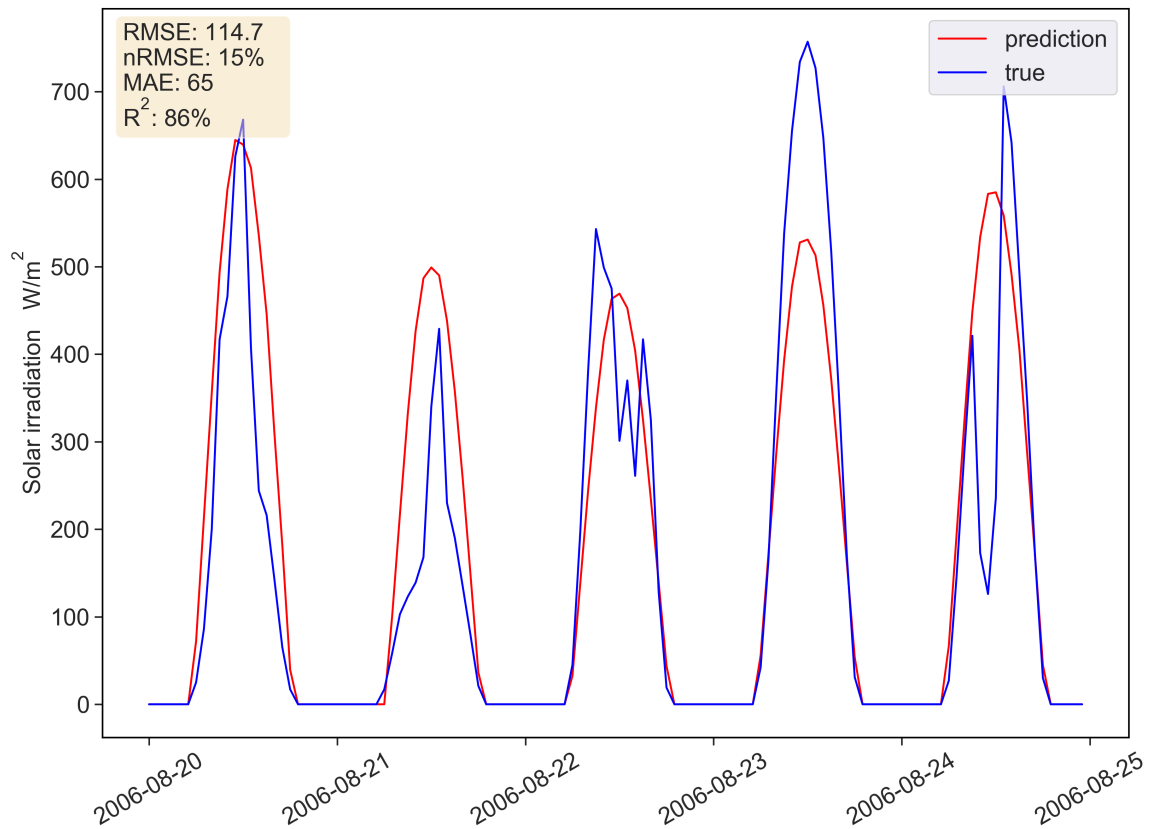


Figure 6.26: 24-hour ahead irradiance predictions between 20.08.2006 and 25.08.2006. Figure reference: Author’s publication [8], and supervised work [10].

Five days were chosen from November to evaluate 24-hour ahead irradiance forecasting model’s performance under low solar irradiation conditions. Figure 6.27 presents solar irradiance prediction between 09.11.2006 and 14.11.2006. Error metrics of this prediction period show that prediction inaccuracies observed in the figure have a low impact on the error metrics. RMSE value of 30.7 indicates that the mean distance between predicted values and the true values was 30.7 W/m². Mean absolute error is 14 W/m² and R² value is 92%.

One-hour Ahead Irradiance Forecasting

40 different architectural combinations were tested during the fine-tuning step of the one-hour ahead irradiance forecasting model. The training duration of each model ranged between 10 minutes to 3 hours. The results of the best performing model are presented in this section. The best performing one-hour ahead irradiance forecasting model was trained with 32 days of weather data which were measured by the OHRES weather station in Canada case study location. Since we were only interested in one-hour ahead irradiance forecasting, a relatively short sequence length of 72 hours was chosen. It was found that having longer sequence lengths caused more noise in predictions. It was also realized that, when all else is the same, introducing more neurons caused a higher gap between training loss and validation loss. Training operation of

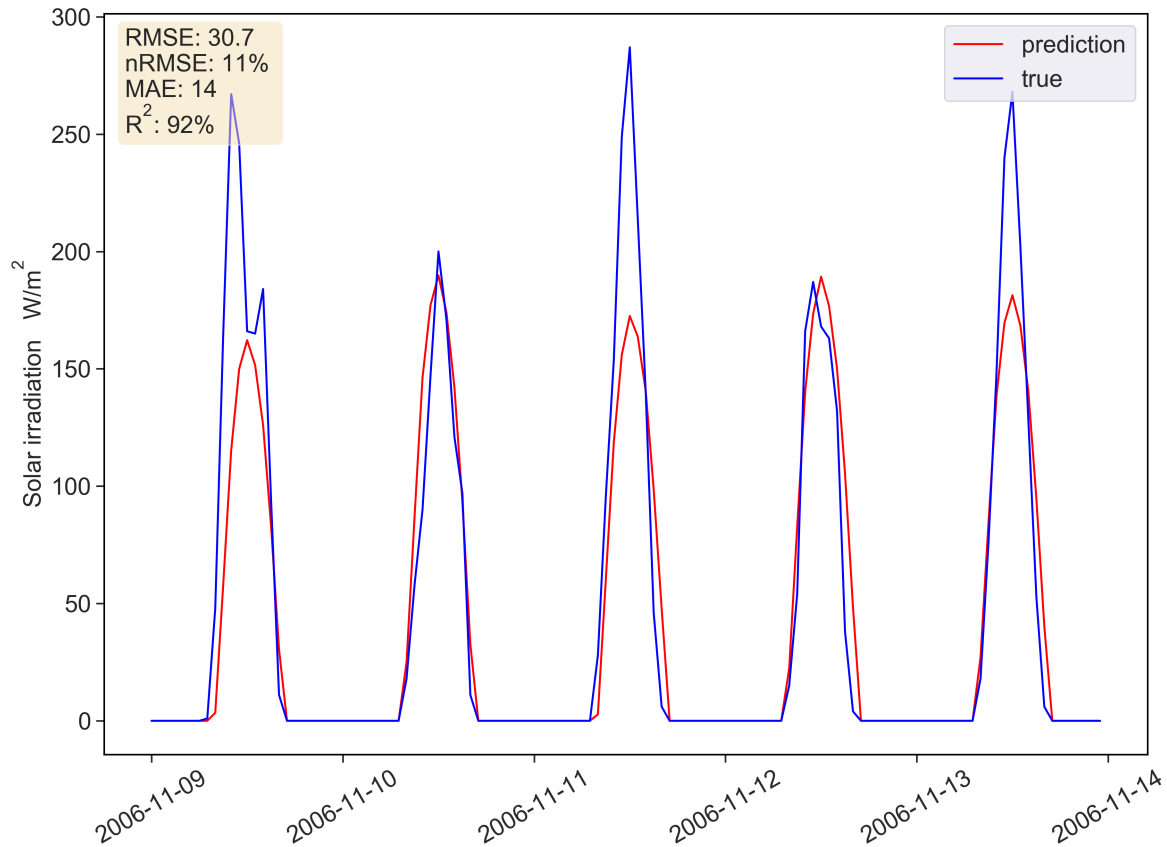


Figure 6.27: 24-hour ahead irradiance predictions between 09.11.2006 and 14.11.2006. Figure reference: Author’s publication [8], and supervised work [10].

the model was 15 minutes which was much faster than 24-hour ahead irradiance forecasting model due to less training data, shorter sequence length and fewer neurons in the layers.

Figure 6.28 shows the training and validation loss graph of the one-hour ahead irradiance forecasting model. Validation loss is lower than training loss after the first epoch which can also be interpreted as a warming-up period of the training operation. During the second epoch, the model recalculates the weights and validation loss becomes higher than the training loss. Then the validation loss keeps decreasing rather smoothly while the validation loss shows small ups and downs on a slightly linear basis. Since the validation loss did not decrease for five consecutive epochs from 12th epoch, early stopping function engaged and stopped the training after 17th epoch to avoid overfitting.

Figure 6.29 shows the prediction output of the test set between 10.06.2019 and 26.06.2019. The model did not see the test set during training. The input introduced to the model for the first time and one hour ahead irradiance predictions received as an output. The blue line on the figure represents true irradiance values and the red line represents the predicted values which were predicted one-hour in advance. RMSE value of this prediction period is 107 which indicates the mean distance between predicted irradiance values and true irradiance values is 107 W/m². nRMSE value is 10% which is

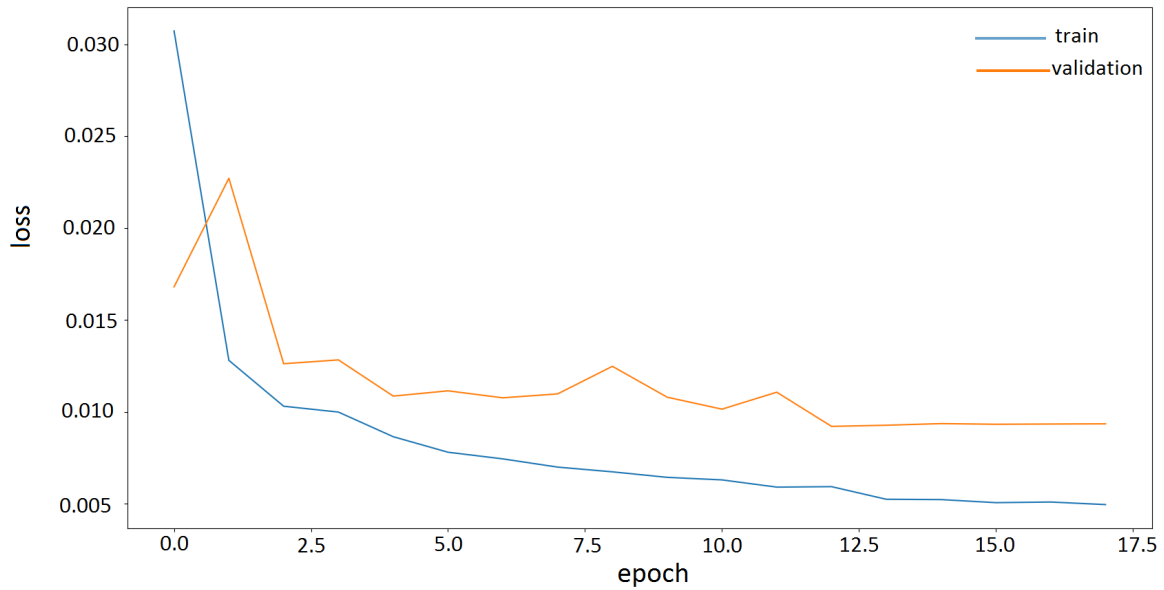


Figure 6.28: Training and validation loss graph of one-hour ahead irradiance forecasting model.

Figure reference: Author’s publication [8], and supervised work [10].

the normalized version of RMSE by the highest irradiance value within this prediction period. R^2 value is 91.8% which indicates the performance of the model while reacting to irradiance drops and raises. MAE value is 57.7 which indicates the mean absolute difference between predicted and true values was 57.7 W/m^2 . It is found that the model predicted small negative irradiance values at some of the sunrise and sunset hours. These negative values must be neglected. At first glance, one can see that the prediction performance on June 15th was quite good while it was relatively poor on June 16th.

Figure 6.30 presents a closer look into the two days where the model performed quite well and poorly. In figure 6.30a, the R^2 value of 99.2% indicates that the model was able to predict the steady irradiance raise and drop quite well. RMSE value of 50.6 indicates that the mean distance between predicted and true irradiance values was 50.6 W/m^2 and this value corresponds to 5% relative to the peak true irradiance. In figure 6.30b, we see that the model was able to predict the sunrise and sunset hours but did not predict the sudden irradiance drops very well. Therefore, R^2 calculation resulted in a value of 84%. The mean distance between predicted and true irradiance values was 105 W/m^2 and this value corresponds to 31% relative to the peak true irradiance. MAE value of 64.86 indicates that the mean absolute difference between predicted and true values was 64.86 W/m^2 .

The one-hour ahead irradiance forecasting model was tested with more recent weather data from September 10th - September 27th. This dataset was not a part of the initial test split and it was prepared after the aforementioned initial testing. Figure 6.31 represents the model’s performance with the weather data from September. At first glance, it can be seen that there are some peak mismatches along the prediction period. RMSE value of 105 indicates that the mean distance between predicted and the

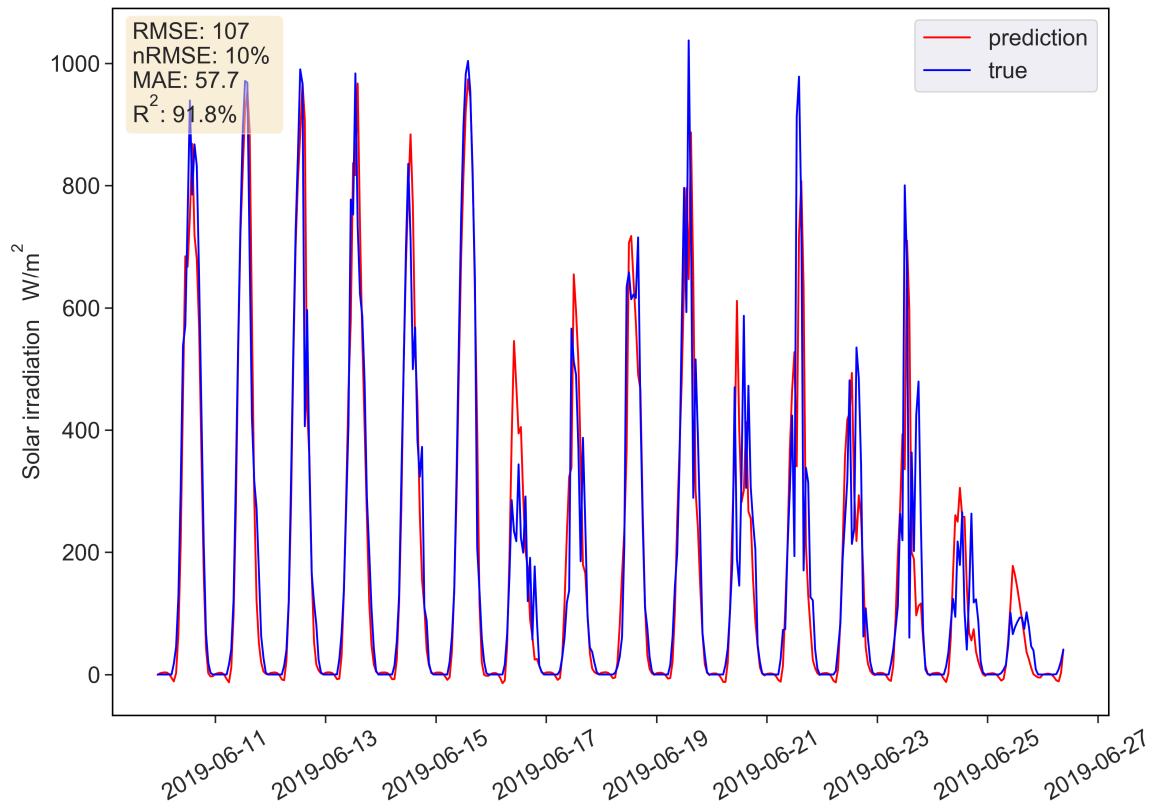


Figure 6.29: One-hour ahead irradiance predictions between 10.06.2019 and 26.06.2019. Figure reference: Author’s publication [8], and supervised work [10].

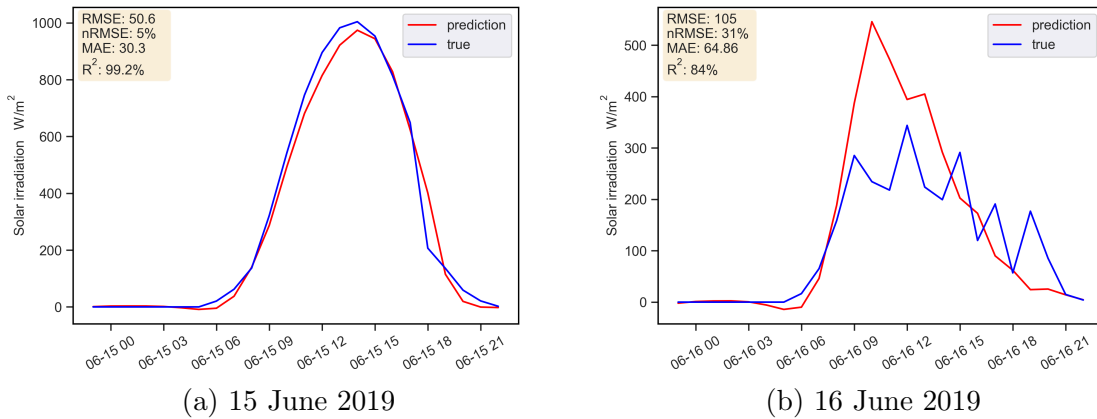


Figure 6.30: Comparison of good and poor predictions in June 2019. Figure reference: Author’s publication [8], and supervised work [10].

true irradiance values are 105 W/m^2 which corresponds to 10% relative to the peak irradiance value of the prediction period. Mean absolute difference between predicted and true irradiance values is 59 W/m^2 and the R^2 value is 89.7%. We can see from the figure that the prediction model yielded good predictions on September 26th where the peak irradiance reached slightly above 1000 W/m^2 . However, the model struggled in

adapting to the low irradiance on the next day.

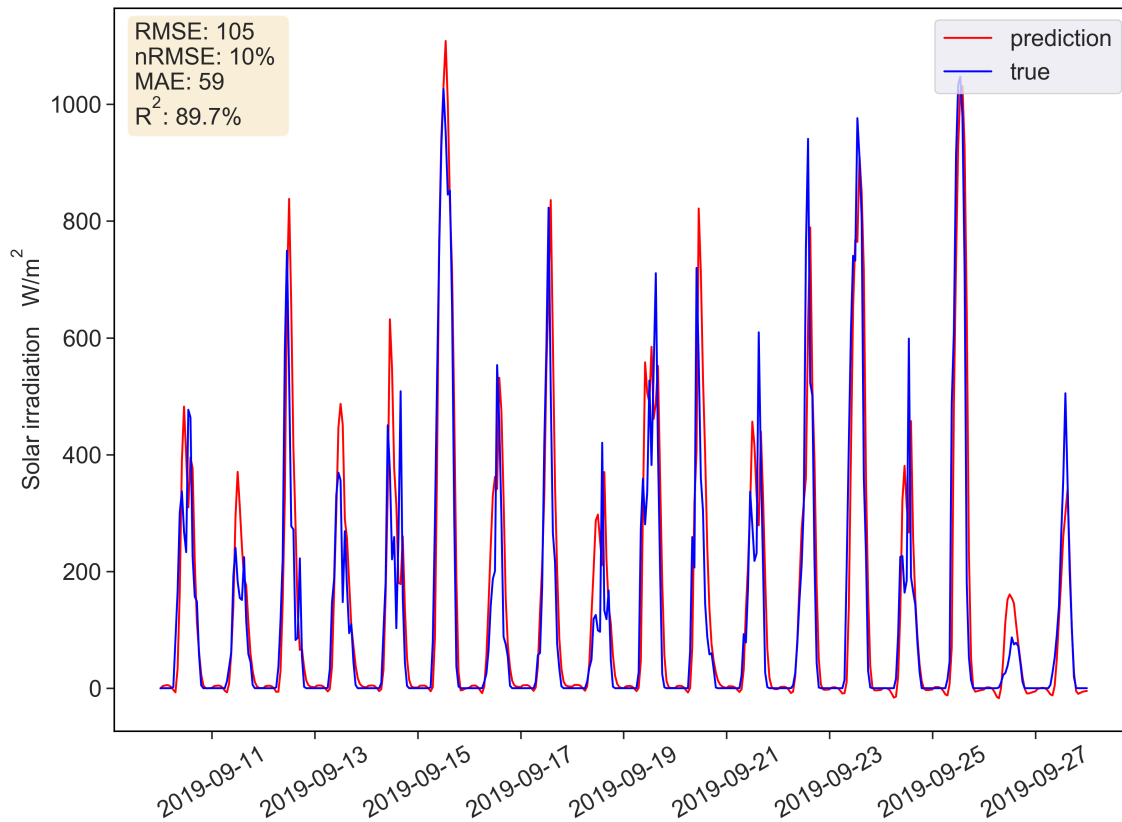
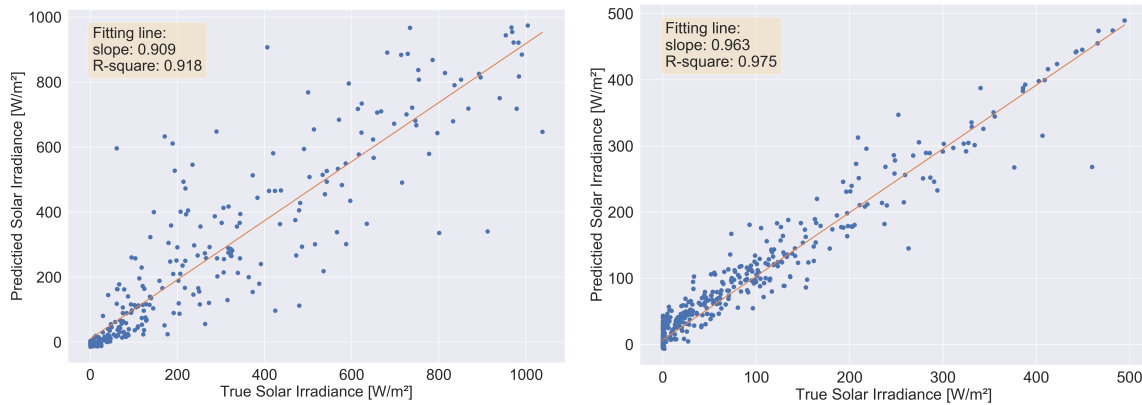


Figure 6.31: One-hour ahead irradiance predictions between 10.09.2019 and 27.06.2019. Figure reference: Author’s publication [8], and supervised work [10].

As mentioned before, the one-hour ahead irradiance forecasting model was trained with 137 days of hourly weather data which did not cover a whole year. Since the model had not seen more than half of a year, the model’s prediction performance for unseen seasons of a year may be misleading. Therefore, the same model architecture was also trained with one year-long hourly weather data which was downloaded from HelioClim-3 Archive. Figure 6.32 presents a comparative regression analysis between the model’s prediction performance with our measured weather data and HelioClim-3 Archive data. Both graphs show the model’s performance with test sets which were not introduced to the model during the training operation. It was found that R² value of figure 6.32b is significantly higher than the figure 6.32a. Therefore, this analysis stresses the impact of data size on the model’s performance.

The Off-grid and decentralized System Data Analysis Platfom(OSDAP) represents a significant and unique contribution to off grid renewable energy access as it provides big data handling, remote monitoring capabilities, standardized performance analysis, and data collection and visualization platform that provides valuable information to the system user. OSDAP represents a significant and unique contribution to off grid renewable energy access as it provides remote monitoring capabilities, standardized performance analysis, and data collection and visualization platform that



(a) Regression analysis of test set predictions of measured weather data (b) Regression analysis of test set predictions of Helioclim-3 Archive weather data.

Figure 6.32: Regression analysis of the model on measured weather data and Helioclim-3 Archive weather data

Figure reference: Author’s publication [8], and supervised work [10].

provides valuable information to the system user. OSDAP can be used to compare the performance of off grid renewable electricity systems across the globe. Through testing, it was determined that the one-hour ahead irradiance prediction model performs better than the 24-hour ahead model given that it has sufficient training data. The one-hour ahead irradiance prediction model was trained and tested with weather data from the weather station installed at the Canada case study location. The model’s performance was evaluated with June and September test data. Prediction evaluations resulted in a normalized mean root mean square error value of 10% for prediction periods in both months. The same model was then trained with one year-long weather data derived from Helioclim-3 archives to understand how the model would perform if it was trained with a larger dataset. R^2 values of test dataset predictions from the initial model and Helioclim-3 model were compared. The initial model yielded R^2 value of 91.8% and the Helioclim-3 model yielded a R^2 of 97.5%. This comparison indicated that the one-hour ahead irradiance prediction model is likely to perform better if it is trained again with a larger dataset of measured weather data. The 24-hour ahead solar irradiance forecasting model was evaluated with August and November data. Normalized mean root mean square error values were found as 15% for August predictions and 11% in November predictions. The Integrated ANN irradiance forecasting models can provide also an accurate one-hour and 24-hours ahead irradiance forecasting, which can be utilized for many use cases as power yield prediction and action based early alarms for the end user.

7 Final remarks, conclusion and outlook

Chapter 7 includes two sections¹: Section 1 presents the major learned lessons and key consideration factors for offgrid and decentralized systems, which have been gathered along this study scope of work from practical on-ground activities in Canada and Uganda, to hybrid system modelling and data analysis platform development. Section 2 represents the conclusion and outlook for the study.

7.1 Highlight on major lessons learned and key consideration factors for off grid and decentralized systems

Some of the challenges and lessons learned which have been gathered based on the experience gain during the commissioning activities in the Canada and Uganda, and are shared before in chapter 4 (section 4.4). In this section major lessons learned and key consideration factors are shared related to the whole study scope. The shared learned lessons and key consideration factors are very useful for both scientific (research) and practical (commercial business) areas, as they are gathered based on a practical research study nature which targets bridging the gap between both sides as mentioned before in chapter 1 (Section 1.3).

The lessons learned and best practices presented are sorted under three main categories:

- Techno-economic related
- Offgrid and decentralized systems modelling and sizing tools related.
- Project handling and management related.

Points related to each of these three categories are presents in the following section.

Techno-economic related

- Plug and play commissioning philosophy.

Having a plug and play commissioning process was the core philosophy used in the hybrid system preparation for shipment and on-site installation. Most of the complex connection and component integration were pre-prepared before the

¹Part of the content of this chapter is based on author's published work in Elkadragy et. al [1] [5] [8].

system shipment to its final destination. Only interconnections between different cabinets such as between the main control cabinet and the batteries cabinets were left to be done on-site. Also, the different system inputs and outputs for energy sources, batteries, and load connections were all gathered on one cabinet so the user interface and connection work is done in one location, and in a clear plug and play manner.

- Test as much as possible prior to shipment.

An important pre-requisite to conduct, when possible, pre-commissioning and cold-run tests for different OHRES parts in a controlled environment (lab test, factory test or local prototypes) before sending it to the final off-grid location. This minimizes both the magnitude and likelihood of system failure in the final remote location where there is almost no technical support or room for complicated troubleshooting.

- Some components would still represent a technical challenge.

For some of the OHRES parts, it is not possible to perform pre-commissioning and testing before sending them off-grid. Even some of the pre-tested components can represent a challenge for commissioning them on-site. For example, in our case such components included the Global System for Mobile (GSM) modem that provides the internet connection for the remote data stream flow from our remote location in Uganda to the database in Germany. Such components present high risks to the success of the overall initiative. Unfortunately, there are no clear risk mitigation strategies available for such risk sources due to the general lack of standardization in the off-grid sector, in addition to the lack of sufficient publicly shared practical field experience.

- Having the right local main project partner.

One of the most critical lessons learned is having a reliable local partner who represents the main access point to the targeted local community. Such a partner plays most of the local coordination roles and conducts support activities on the ground. One of the common partner types in developing countries is Non-Governmental Organizations (NGOs). Most active local NGOs in developing countries know most of the local real needs and have a solid foundation of trust and contacts in their service areas. A selection of a reliable and trustworthy NGO is not as easy as it sounds. If the NGO does not share the same general vision of the project and has a real need for the type of development proposed within the project scope, it will not be possible to establish a productive partnership. On the other hand, if the project represents one of the core needs or activities of the NGO the reflection on results will be remarkable.

- Local community involvement

In remote areas, local communities are either a support or a risk source for off-grid projects. The involvement of the local community in early stages of the project (even in the project planning stages if possible) increases the chances of gaining their full support during the project life-cycle and even can be the only guarantee

of the project sustainability in some cases. What we learned also is that the involvement of the local community should be done while respecting hierarchy. In our case, this was achieved through project information gatherings arranged by our local main NGO partner, through the local village mayor who addressed the invitation for the local community and the local government responsible.

- Even experienced end users can cause critical failures.

Some of the end users of the off grid systems have already been living on similar systems for years as was the case for our Canada case study, and have a very solid experience with the technical aspects related to hybrid off grid systems components. However, one of the lessons learned was that even for experienced users, dealing with new technologies for the first time might lead to some critical installation failures.

An example is with the Canada case study weather station installation. The end user's technical experience provided motivation to use remote guidance and detailed installation instructions with the Canada end user for installing the weather station in his location. After the installation the end user did confirm everything was installed according to the installation instructions, however we collected detailed photos for the weather station installation. A critical installation failure was reconfigured for the irradiance sensor, which could have affected the quality of our data collection to the extent of making it completely unusable for the purpose we need it for.

This raised the value of detailed checking of any remote guided installation regardless of the users' experience, and the level of clarity or simplicity of the installation and commissioning instructions given. Also, it was clear for us that there must be on site physical support for the hybrid system installation and commissioning.

Offgrid and decentralized systems software tools related

- Market availability gap for open source tools for off-grid and decentralized systems.

There is a clear gap in the open source tool availability for off grid and decentralized systems for techno-economic assessment and system sizing. Although there are a few available tools targeting such work scope, they are not comparable to a commercial tool like HOMER that has a high amount of modelling details, inputs and results. There is also a gap for generic tools used for system remote monitoring and data analysis. The software tools developed in our study scope (HOTEM and OSDAP) represents a step toward filling such gaps.

- Modelling of some of the state-of-the-art technologies could be challenging, even in developed commercial software tools.

Modelling of some of the state-of-the-art components was not possible using existing software, which forced the requirement of high effort and extra involved costs in order to model such components . An example from our study was the

modelling of our hybrid lead-acid and Li-ion battery storage in HOMER. Although HOMER has a very broad library, a direct model for a hybrid battery is not included (even though there is already some state-of-the-art commercial products available for hybrid battery storage). This led to the need for deep understanding of the software tool functionalities, and coming up with a new approach to include the hybrid battery model in our HOMER system modelling. This would not be doable for the majority of other system sizing end users, especially for those in a fast market development and introducing new products or solutions in the market on a short time basis. More efforts are needed to include newly introduced technologies and solutions into existing modelling tools, to enable end users to use these tools in an effective way and have more optimized assessments and system sizing results.

More open source optimized tools are needed for the off grid market needs, and the tool developed within the scope of this study (HOTEM) is a step toward providing one of them. HOTEM is developed with taking into account overcoming some identified gaps in the commercially available tools as HOMER, as described in details before in chapter 5. These advantage features in HOTEM includes a detailed Weighted Average Cost of Capital (WACC) calculation model, which can model policy and support schemes implications on the dynamic economical indicators. Also modelling different battery technologies through using different generic battery models is included in HOTEM, with the advantage of direct modelling hybrid battery energy storage systems (HBESS) utilizing lead-acid and Li-ion battery technologies which was identified as a gap while using HOMER for the modelling of our OHRES systems for the case-studies in Canada and Uganda. HOTEM also has the advantage of using multi-objective optimization criteria for selecting the optimum system design (minimize COE and LPSP, maximize RE_{factor}), where HOMER optimize for one objective (minimize COE). On the other hand, HOMER as a well established tool developed over a 25 years period [50] also has other advantages over HOTEM as described before in chapter 5, and summarized in table 5.8.

- Availability of hybrid system products required technical data for modelling.

One of the challenges we experienced in the system components modelling, is the availability of some products' technical data required for completing the modelling parameters. An example was the modelling of the lead acid battery used in our system (as part of the hybrid battery storage) in HOMER. Not all required technical parameters for completing the required battery model in HOMER were available in the manufacturer's user manual or data sheet. It was also not easy to get the required detailed battery data through contacting the manufacturer directly. To overcome such challenges, the development of calculation models for estimating the required parameters and set points based on the manufacturer provided data was required for completing the modelling required data.

- Techno-economic analysis and system sizing tools track of record validation.

For the sizing tool in our study (HOMER) there was no clear track record for the validation of the modelling results as compared to the final system's techno-

economic aspects. Few shared cases are available in such a context, and from our perspective more efforts in a proven track record for the used sizing tools through more case studies is required for optimizing the modelling approach used and creating credibility for the dependency of the outcome results.

Project handling and management related

- Early site visits for the case studies locations.

Having an early site visit to the case study locations is a very important factor, which dramatically affects the identification of challenges along the value chain of the hybrid system's deployment. Many local challenges would have never been identified and taken into consideration in our system design and planning unless this step was taken (especially in the Uganda case study) and local experience and surveys were gathered and carried out.

- Close involvement of the case study end-users along with the different phases.

One of the key factors we based our methodology on is the involvement of the end-user along the different system planning and implementation phases. Especially to overcome the international logistics and transportation challenges, close involvement of the end-user was highly required to realize realistic planning and overcome many local obstacles.

- Timeline planning need to be carefully considered due to local resources availability and culture differences.

A major lesson learned from the Uganda case study was related to the timeline planning approach, which differed completely before and after the first site visit. The timeline planning approach before the first site visit to the Uganda case study location was based on adding some self-estimated safety margins to the business as usual timeline planning as for carrying out the same project required activities in Germany. However, two factors changed this perspective after the first site visit to the case study location: 1) The facts collected regarding difficulties in both human and material resources required locally. 2) The major work and cultural differences. Both these factors had high effects on extending the required timeline planned for all on site activities in Uganda. On the other hand this made our future timeline planning process more realistic, and left us with a greater understanding of the need for the end users perspectives to be involved more closely in the planning process.

- Early identification of local resources and local capacity building.

Another major advantage of having an early site visit was the identification of locally available resources from both human and required materials sides. Local technical partners and selected human resources were identified for providing the local technical support needed for the system deployment and operation. Local capacity building was another a key factor, which helped create technically qualified local human resources needed for overcoming the lack of specialized technical support during the system implementation stages.

- Handling logistics in an effective way.

System logistics could be an under-estimated aspect in theoretical evaluations for off-grid electrical systems, due to the lack of practical experience in most of the research work done in this area so far. In practice, logistics play a major role in the system deployment feasibility and represents a major influence on the economics of the off-grid system.

7.2 Conclusion and outlook

Off grid and decentralized hybrid renewable electricity systems are a proven and crucial technology for alleviating energy poverty and catalyzing rural electrification. Several issues hinder the progress and scalability of these systems around the world such as lack of standardization for performance analysis across varying geographic contexts, techno-economic feasibility, and a lack of hybrid systems sizing models, as well as operation data analysis and forecasting tools. This study uses a novel applied research approach to bridge several of these gaps, with the ultimate goal of improving global energy access.

This study aims to participate in the global vision of ending energy poverty through increasing electrical energy access levels. The methodological approach presented in this study, aiming to address specific challenges related to off grid and decentralized systems is not properly covered in the existing literature to our knowledge. Especially applied research involving not only theoretical assessment but also practical contrastive case-study on-ground work using such a comprehensive methodological approach along the value chain from system development to deployment and operation & monitoring as described before. This study contributes to filling an existing knowledge gap in the off grid and decentralized systems techno-economic context.

The first building block of our study is the OHRES deployment in the selected case-study locations within Canada and Uganda. A detailed contrastive case studies selection criteria based on multi- criteria analysis method is also developed in the scope of this study as presented before, which can be adapted for further studies targeting contrastive case studies analysis. Related information to each case study was presented, as well as the techno-economic analysis and system sizing for each case study. The study also provided an overview of the OHRES design, including an integrated 48V DC Hybrid lead-acid & lithium-ion Battery Storage System (HBSS), system monitoring, and data analysis applications. The OHRES system's remote Monitoring and Weather Station (SMWS), including the allocation of remote monitoring devices, as well as system monitoring infrastructure, are described explicitly.

Our first OHRES system is already installed and in operation since August 2019 in Nemaiah Valley, British Columbia, Canada. One of the major techno-economic aspects related to OHRES presented in this study is the dynamic economic assessment for three battery storage systems which can be used for the presented hybrid system's residential application. The investigated three battery systems were based on three storage configurations: lead-acid (AGM) based storage, lithium-ion (LiFePO₄) based

storage, and hybrid lead-acid and lithium-ion battery storage. Based on the assumptions given, the hybrid battery storage represents the most economical solution for our OHRES residential application over its lifetime. Major differences experienced between the case studies were also illustrated.

The second building block of our study is HOTEEM development and optimization. HOTEEM is developed to be utilized as an OHRES sizing and techno-economic assessment tool. The model can perform feasibility analysis for electrical energy hybrid systems to obtain the best configuration and sizing of the hybrid system at the off grid or decentralized location. HOTEEM addresses the challenge of scarcity in the available tools addressing the techno-economic analysis and system sizing for off grid and decentralized systems. Due to this scarcity, the engineering and techno-economic assessment process of such systems are based on whether on very simple calculations, which in most cases end in the system over-sizing and poor economic feasibility. The other approach is using a commercial (paid) tool, which is for the end-user a black-box where a lot of the optimization and model operational functionalities are not shared due to intellectual property protection. Also which could be an expensive and complicated to use option for some of the end-users and stockholders in the context of the off grid and decentralized system. The unique approach used in HOTEEM development is basing the optimization and functionality objectives integrated into the model on the on-ground experience gained from the deployment of our hybrid systems in Canada and Uganda. This approach allowed HOTEEM to be a practical tool, reflecting the market needs experienced through end-users and different stakeholder interaction along with the hybrid system's different implementation phases. The presented model has major enhancements and optimizations as compared to the based model which HOTEEM were further developed up on, including detailed solar PV modeling, Solar irradiance transposition models, a user-friendly interface in data input and output reports, Developed and integrated battery storage models, different integrated power dispatch methods, and additional detailed economic and Weighted Average Cost of Capital (WACC) Modelling. The only part left without changes from the base model which HOTEEM is developed further based on, is the optimization algorithm called C-DEEPSO. This optimization algorithm was programmed to find optimal system sizing and configuration for three objectives: Minimum Cost of Electricity (COE), Minimum Loss of Power Supply Probability (LPSP), and Maximum Renewable Factor (RE_{factor}).

The performance of HOTEEM was analyzed via the case study in Canada. The outcomes presented from the HOTEEM simulation were based on the Canada case-study inputs. The results predicted by HOTEEM were then benchmarked using HOMER software, which showed satisfactory results that reflect that the HOTEEM could be utilized in the planning and optimization of the off grid hybrid system. There is good potential for HOTEEM development to overcome its shortcomings. A solid example is the large surplus energy which shows the need for another objective inside the model to limit the generation of excess energy to avoid over-sizing of the systems. In addition, all different technical and economic models used have the potential for further optimization.

The third building block of this study focused on the development and functionalities of the Off grid and decentralized hybrid renewable electricity Systems Data Analysis Platform (OSDAP). OSDAP Graphical User Interface (GUI) allows the utilizing of the sophisticated algorithms, and artificial intelligence, and machine learning-based functionalities used in OSDAP in a user friendly, and visual manner. The OSDAP data handling and visualization functionality objectives are providing a clear and dynamic data visualization tool for hybrid systems end-users, supporting better utilization and interaction between collected data and the system user. Dynamic data handling methodology and functionality development were explained in detail based on the data provided from the Canada case study OHRES. The OSDAP performance analysis tool was developed using the IEC 61724 standard along with a battery round trip efficiency parameter. The OSDAP tool was validated through evaluating the performance of an off grid hybrid renewable electricity system installed in British Columbia, Canada. The performance analysis method and calculations were validated for the system operation data generated between 01.09.2019 and 30.09.2019. It was found that the Color Controller (CCGX) data provided for the battery system resulted in acceptable performance calculations. On the other hand, the same calculations based on the data received from the installed battery hall effect sensors were not in the same acceptable range. Such differences in the performance indicators results indicate that on-site investigation needed to be done for both the data transmission infrastructure and the installed battery sensors, even though all sensors and data transmission infrastructure were calibrated and validated during the system testing period before the shipment to the final installation location in Canada. Within OSDAP, two Artificial Neural Networks (ANN) based irradiance forecasting models were developed. Through testing, it was determined that the one-hour ahead irradiance prediction model performs better than the 24-hour ahead model given that it has sufficient training data. OSDAP represents a significant and unique contribution to off grid renewable energy access as it provides remote monitoring capabilities, standardized performance analysis, and data collection and visualization platform that provides valuable information to the system user. OSDAP can be used to compare the performance of off grid renewable electricity systems across the globe.

A major future development aspect for OSDAP is the utilization of the solar forecasting models for generating action based alarms for the hybrid system end-users. These action alarms will support helping off grid system users to adapt to weather conditions. Also giving an early alarm in case preparation for backup Genset fuel is required to avoid loss of power supply based on the system energy production forecast. Developing the forecast results to estimate the future energy yield production can also support optimizing the use of renewable energy resources, and improve the efficiency and lifespan of the battery storage system. Another development potential is the establishment of a direct link between OSDAP and HOTEEM. Where the data handled and prepared from OSDAP for a certain off grid or decentralized location, for example locally measured solar irradiance, wind energy measurements, and temperature can be directly utilized in HOTEEM for the techno-economic assessment and system sizing optimization.

The fourth building block of our study was the lessons learned and key contributing factors for off grid and decentralized hybrid systems, where major technical, economic, managerial, and modeling tools related factors were presented which can be utilized for both scientific research and practical business.

This study contributes to the goal of ending global energy poverty. Primary data generated and gathered from the hybrid system in Canada and weather station in Uganda will stimulate and support further research and business activities aiming for the same purpose. Tools such as HOTEEM represent a solid step toward enabling the deployment of off grid and decentralized hybrid systems and participating in the big vision of ending energy poverty on a global scale. Also, OSDAP's different functionalities will improve the techno-economic feasibility of off grid and decentralized hybrid renewable energy systems around the world. This study has a very high potential to be developed further with the advancement of the off grid renewable energy system case studies in Canada and Uganda, besides the developed tools HOTEEM and OSDAP. The study is complemented by further work supporting the understanding of technical and economic factors affecting the feasibility, sustainability, and reliability of off grid systems along the value chain. It also can be utilized to help understand the effect of other factors such as social, political, and business models on off grid and hybrid systems. Such applied research presents a novel contribution to off grid energy literature and a tangible contribution to energy access practitioners.

References

- [1] Mohamed Mamdouh Elkadragy, Manuel Baumann, Nigel Moore, Marcel Weil, Nicolaus Lemmert, and Marc Hiller. Contrastive Techno-Economic Analysis Concept for Off-Grid Hybrid Renewable Electricity Systems Based on comparative case studies within Canada and Uganda. In *3rd International Hybrid Power Systems Workshop*, number May, 2018. URL http://www.hybridpowersystems.org/wp-content/uploads/sites/9/2018/05/5A.4_TENE18_012_paper_Elkadragy_MohamedM.pdf.
- [2] D. L. King, J. A. Kratochvil, and W. E. Boyson. Measuring solar spectral and angle-of-incidence effects on photovoltaic modules and solar irradiance sensors. In *Conference Record of the Twenty Sixth IEEE Photovoltaic Specialists Conference - 1997*, pages 1113–1116, Sep. 1997. doi: 10.1109/PVSC.1997.654283.
- [3] Joseph H. McIntyre. Community-scale assessment of rooftop-mounted solar energy potential with meteorological, atlas, and GIS data: A case study of Guelph, Ontario (Canada). *Energy, Sustainability and Society*, 2(1):1–19, 2012. ISSN 21920567. doi: 10.1186/2192-0567-2-23.
- [4] Nian Liu, Hui Wu, Matthew T. McDowell, Yan Yao, Chongmin Wang, and Yi Cui. A yolk-shell design for stabilized and scalable Li-ion battery alloy anodes. *Nano Letters*, 12(6):3315–3321, 2012. ISSN 15306984. doi: 10.1021/nl3014814. URL <https://pubs.acs.org/doi/abs/10.1021/nl3014814>.
- [5] Mohamed M Elkadragy, Mughees Iqbal, Mohammed Labib Awad, Manuel Baumann, Ambika Opal, Marc Hiller, Jatin Nathwani, and Joachim Knebel. Hybrid Off-grid and decentralized renewable electricity systems Techno-Economic Model (HOTEM). A building block of a comprehensive techno-economic approach based on contrastive case studies in Sub-Saharan Africa and Canada. In *10th Solar and Storage Integration Workshop*, page 25, Germany, 2020. energynautics. URL https://ae4h.org/download/documents/projects/hotem_ae4hpdf;v1?attachment=1.
- [6] Mohamed Labib Awad, Carsten Agert, Hans Holtorf, and Mohamed M. Elkadragy. *Development and Analysis of a Hybrid Battery Energy Storage System in the Hybrid Off-grid Techno-Economic Model*. Master thesis, Univeristy of Oldenburg, 2020.
- [7] Muhammad Mughees Iqbal, Anke Weidlich, Marc Hiller, and Mohamed M. Elkadragy. *Development and Optimization of Hybrid Off-Grid Techno- Economic Model for System Design and Analysis*. Master thesis, University of Freiburg, 2019.

- [8] Mohamed M Elkadragy, Mert Alici, Ahmed Alersy, Ambika Opal, Jatin Nathwani, Joachim Knebel, and Marc Hiller. Off-grid and decentralized hybrid renewable electricity systems data analysis platform (OSDAP) A building block of a comprehensive techno-economic approach based on contrastive case studies in Sub-Saharan Africa and Canada. *Journal of Energy Storage*, (November): 101965, 2020. ISSN 2352-152X. doi: 10.1016/j.est.2020.101965. URL <https://doi.org/10.1016/j.est.2020.101965>.
- [9] International Electrotechnical Commission (IEC). International electrotechnical commission (iec), iec standard 61724, photovoltaic system performance - part 1: Monitoring, 2017.
- [10] Mert Alici, Anke Weidlich, Marc Hiller, and Mohamed M. Elkadragy. *Design and Performance Analysis of Off-Grid Hybrid Renewable Electricity Systems Using Two Case Studies in Uganda and Canada*. Master thesis, University of Freiburg, 2019.
- [11] Affordable Energy For Humanity (AE4H), global initiative. URL www.ae4h.org.
- [12] UN, Sustainable Development Goal 7-sdg7, 2020. URL <https://sustainabledevelopment.un.org/sdg7>.
- [13] IEA. IEA (2019), SDG7: Data and Projections. Technical report, international Energy Agency (IEA), Paris, 2019. URL <https://www.iea.org/reports/sdg7-data-and-projections>.
- [14] Michael Brooks, Nigel Moore, Hayley Rutherford, Julie Wright, and Dana Bowman. OpenAccess Energy Blueprint. Technical report, 2017. URL http://wgisi.org/sites/wgisi-live.pi.local/files/OpenAccess_Energy_Blueprint_WGSI_2017.pdf.
- [15] UN, Sustainable development goals, 2020. URL <https://sustainabledevelopment.un.org/sdgs>.
- [16] World Bank. Access to Electricity (% of Population), 2020. ISSN 1098-6596. URL <https://data.worldbank.org/indicator/eg.elc.accs.zs>.
- [17] James Knowles. Power Shift: Electricity for Canada's Remote Communities. Technical report, The conference board of canada, 2016. URL <http://www.conferenceboard.ca/e-library/abstract.aspx?did=6231>.
- [18] IRENA, Ruud Kempener, Olivier Lavagne, Deger Saygin, Jeffrey Skeer, Salvatore Vinci, and Dolf Gielen. IRENA, Off-Grid Renewable Energy Systems: Status and Methodological Issues. Technical report, IRENA, 2015. URL http://www.irena.org/DocumentDownloads/Publications/IRENA_Off-grid_Renewable_Systems_WP_2015.pdf.
- [19] Off grid Renewable Energy Solutions Global, regional status, and trends. IRENA, OFF-GRID RENEWABLE ENERGY SOLUTIONS. Technical report, 2018. URL <https://www.irena.org/publications/2018/Jul/Off-grid-Renewable-Energy-Solutions>.

- [20] Hans Holtorf, Tania Urmee, Martina Calais, and Trevor Pryor. A model to evaluate the success of Solar Home Systems. *Renewable and Sustainable Energy Reviews*, 50:245–255, 2015. ISSN 18790690. doi: 10.1016/j.rser.2015.05.015.
- [21] AE4h. Off-grid Hybrid Systems Techno-Economic Study, 2020. URL <https://ae4h.org/projects/ohres>.
- [22] Ghada Merei, Cornelius Berger, and Dirk Uwe Sauer. Optimization of an off-grid hybrid PV-Wind-Diesel system with different battery technologies using genetic algorithm. *Solar Energy*, 2013. ISSN 0038092X. doi: 10.1016/j.solener.2013.08.016.
- [23] Lee Wai Chong, Yee Wan Wong, Rajprasad Kumar Rajkumar, and Dino Isa. Modelling and Simulation of Standalone PV Systems with Battery-supercapacitor Hybrid Energy Storage System for a Rural Household. *Energy Procedia*, 107(September 2016):232–236, 2017. ISSN 18766102. doi: 10.1016/j.egypro.2016.12.135. URL <http://dx.doi.org/10.1016/j.egypro.2016.12.135>.
- [24] Steven Chung and Steven Chung. Hybrid Lead-Acid / Lithium-Ion Energy Storage System with Power-Mix Control for Light Electric Vehicles by A thesis submitted in conformity with the requirements Graduate Department of Electrical and Computer Engineering. 2016.
- [25] Jeanette Munderlein, Gerrit Ipers, Marc Steinhoff, Sebastian Zurmühlen, and Dirk Uwe Sauer. Optimization of a hybrid storage system and evaluation of operation strategies. *International Journal of Electrical Power and Energy Systems*, 119(October 2019):105887, 2020. ISSN 01420615. doi: 10.1016/j.ijepes.2020.105887. URL <https://doi.org/10.1016/j.ijepes.2020.105887>.
- [26] Christiane Rahe. Lead-acid Batteries and Lithium-ion Batteries in parallel Strings for an Energy Storage System for a Clinic in Africa. pages 1–7, 2016. URL https://juser.fz-juelich.de/record/829025/files/PE_{ }070_{ }Christiane.pdf.
- [27] Thilo Bocklisch. Hybrid energy storage systems for renewable energy applications. In *Energy Procedia*, 2015. doi: 10.1016/j.egypro.2015.07.582.
- [28] Carolina G. Marcelino, Paulo E.M. Almeida, Elizabeth F. Wanner, Leonel M. Carvalho, and Vladimiro Miranda. Fundamentals of the C-DEEPSO algorithm and its application to the reactive power optimization of wind farms. *2016 IEEE Congress on Evolutionary Computation, CEC 2016*, pages 1547–1554, 2016. doi: 10.1109/CEC.2016.7743973. URL <https://ieeexplore.ieee.org/abstract/document/7743973>.
- [29] Carolina Marcelino, Paulo Almeida, Carlos Pedreira, Leonel Caroaalha, and Elizabeth Wanner. Applying C-DEEPSO to Solve Large Scale Global Optimization Problems. *2018 IEEE Congress on Evolutionary Computation, CEC 2018 - Proceedings*, 2018. doi: 10.1109/CEC.2018.8477854. URL <https://ieeexplore.ieee.org/abstract/document/8477854>.

- [30] Carolina Marcelino, Manuel Baumann, Leonel Carvalho, Nelson Chibeles-Martins, Marcel Weil, Paulo Almeida, and Elizabeth Wanner. A combined optimisation and decision-making approach for battery-supported HMGS. *Journal of the Operational Research Society*, 0(0):1–13, 2019. ISSN 14769360. doi: 10.1080/01605682.2019.1582590. URL <https://doi.org/10.1080/01605682.2019.1582590>.
- [31] A. T.D. Perera, R. A. Attalage, K. K.C.K. Perera, and V. P.C. Dassanayake. A hybrid tool to combine multi-objective optimization and multi-criterion decision making in designing standalone hybrid energy systems. *Applied Energy*, 107:412–425, 2013. ISSN 03062619. doi: 10.1016/j.apenergy.2013.02.049. URL <http://dx.doi.org/10.1016/j.apenergy.2013.02.049>.
- [32] Stanley K.H. Chow, Eric W.M. Lee, and Danny H.W. Li. Short-term prediction of photovoltaic energy generation by intelligent approach. *Energy and Buildings*, 55:660–667, 12 2012. ISSN 0378-7788. doi: 10.1016/J.ENBUILD.2012.08.011. URL <https://www.sciencedirect.com/science/article/pii/S037877881200415X>.
- [33] Adel Mellit and Alessandro Massi Pavan. A 24-h forecast of solar irradiance using artificial neural network: Application for performance prediction of a grid-connected PV plant at Trieste, Italy. *Solar Energy*, 84(5):807–821, 5 2010. ISSN 0038092X. doi: 10.1016/j.solener.2010.02.006.
- [34] Xiangyun Qing and Yugang Niu. Hourly day-ahead solar irradiance prediction using weather forecasts by lstm. *Energy*, 148:461 – 468, 2018. ISSN 0360-5442. doi: <https://doi.org/10.1016/j.energy.2018.01.177>. URL <http://www.sciencedirect.com/science/article/pii/S0360544218302056>.
- [35] E. Lorenz and D. Heinemann. Prediction of solar irradiance and photovoltaic power. In *Comprehensive Renewable Energy*. 2012. ISBN 9780080878737. doi: 10.1016/B978-0-08-087872-0.00114-1.
- [36] Cyril Voyant, Gilles Notton, Soteris Kalogirou, Marie Laure Nivet, Christophe Paoli, Fabrice Motte, and Alexis Fouilloy. Machine learning methods for solar radiation forecasting: A review. *Renewable Energy*, 105:569–582, 2017. ISSN 18790682. doi: 10.1016/j.renene.2016.12.095. URL <http://dx.doi.org/10.1016/j.renene.2016.12.095>.
- [37] Y. Yu, J. Cao, and J. Zhu. An lstm short-term solar irradiance forecasting under complicated weather conditions. *IEEE Access*, 7:145651–145666, 2019. ISSN 2169-3536. doi: 10.1109/ACCESS.2019.2946057. URL <https://ieeexplore.ieee.org/document/8864021>.
- [38] Shikhar Srivastava and Stefan Lessmann. A comparative study of lstm neural networks in forecasting day-ahead global horizontal irradiance with satellite data. *Solar Energy*, 162:232 – 247, 2018. ISSN 0038-092X. doi: <https://doi.org/10.1016/j.solener.2018.01.005>. URL <http://www.sciencedirect.com/science/article/pii/S0038092X18300173>.

- [39] Francesco Fuso Nerini, Oliver Broad, Dimitris Mentis, Manuel Welsch, Morgan Bazilian, and Mark Howells. A cost comparison of technology approaches for improving access to electricity services. *Energy*, 95:255–265, 2016. ISSN 03605442. doi: 10.1016/j.energy.2015.11.068. URL <http://dx.doi.org/10.1016/j.energy.2015.11.068>.
- [40] Regulatory Indicators for Sustainable Energy(RISE), Uganda country profile, . URL <http://rise.esmap.org/country/uganda>. Accessed December 2020.
- [41] Natural Resources Canada, photovoltaic and solar resource maps, . URL www.nrcan.gc.ca/18366. Accessed December 2020.
- [42] The Africa-EU Renewable Energy Cooperation Programme (RECP), Uganda renewable energy potential, . URL www.africa-eu-renewables.org/market-information/uganda/renewable-energy-potential. Accessed December 2020.
- [43] Natural Resources Canada, Financial incentives by province, . URL www.nrcan.gc.ca/energy/funding/efficiency/4947. Accessed December 2020.
- [44] The Africa-EU Renewable Energy Cooperation Programme (RECP), Uganda governmental framework, . URL www.africa-eu-renewables.org/market-information/uganda/governmental-framework. Accessed December 2020.
- [45] UN. World Economic Situation Prospects 2016. page 231, 2016.
- [46] M Elkadragy, M Baumann, A Alsersy, N Moore, N Lemmertz, and M Hiller. Off-Grid Hybrid Renewable Electricity System (OHRES) techno-economic assessment, system size optimization and design. 2nd International Conference on Solar Technologies & Hybrid Mini Grids to improve energy access, Poster presentation, Palma de Mallorca, Spanien, 17.–18. Oktober 2018, 2018. URL www.energy-access-conferences.com/33167/detail/3rd-international-conference-on-solar-technologies-and-hybrid-mini-grids-to-improve-energy-access.html.
- [47] Mohamed M Elkadragy. Off-Grid Hybrid Renewable Energy Systems, A techno-economic analysis of the concept. *Windtech international*, 14:22–25, 2018. ISSN 1547-2415. URL <https://www.windtech-international.com/editorial-features/off-grid-hybrid-renewable-energy-systems>.
- [48] Hoppecke. *sun — powerpack VR M*, June 2018. URL <https://www.hoppecke.com/en/product/sun-power-vr-m/>.
- [49] BOS-ag. *LITHIUM EXTENSION BATTERY LE300*. BOS Balance of Storage Systems AG, version no. 98803201 edition, January 2018. URL <https://www.bos-ag.com/products/le300/>.
- [50] Hybrid Optimization of Multiple Energy Resources (HOMER Energy). URL www.homerenergy.com.

- [51] Homer Energy. HOMER PRO HELP, 2020. URL https://www.homerenergy.com/products/pro/docs/latest/levelized_{_}cost_{_}of_{_}energy.html.
- [52] Homer Energy. HOMER Pro database, 2020. URL https://www.homerenergy.com/products/pro/docs/latest/finding_{_}data_{_}to_{_}run_{_}homer.html.
- [53] World Bank. The World Bank - Real interest rate (%) - Canada, 2020. URL <https://data.worldbank.org/indicator/FR.INR.RINR?end=2017{&}locations=CA{&}start=1972>.
- [54] World Bank. The World Bank - Inflation, consumer prices (annual %) - Canada, 2020. URL <https://data.worldbank.org/indicator/FP.CPI.TOTL.ZG?locations=CA>.
- [55] World Bank. The World Bank - Real interest rate (%) - Uganda, 2020. URL https://data.worldbank.org/indicator/FR.INR.RINR?locations=UG{&}year_{_}high_{_}desc=false.
- [56] World Bank. The World Bank - Inflation, consumer prices (annual %) - Uganda, 2020. URL <https://data.worldbank.org/indicator/FP.CPI.TOTL.ZG?locations=UG>.
- [57] Color control gx manual, 2019. URL <https://www.victronenergy.com/live/ccgx:start>.
- [58] Victron Energy, VRM Portal online, 2020. URL www.vrm.victronenergy.com/landingpage.
- [59] Rainwise Inc. URL <https://www.rainwise.com>. Accessed December 2020.
- [60] FERNTTECH, Monitor & Control Off-Grid Power Systems. URL <https://fernttech.io/>. Accessed December 2020.
- [61] International Electrotechnical Commission (IEC). IEC TS 62257 - Recommendations for renewable energy and hybrid systems for rural electrification, 2020. URL <https://webstore.iec.ch/publication/23502>.
- [62] Solar radiation Data SoDa. Solar radiation Data (SoDa)-HelioClim-1. URL <http://www.soda-pro.com/es/web-services/radiation/helioclim-1>.
- [63] IATA. International Air Transport Association (IATA) - Lithium Batteries, 2020. URL <https://www.iata.org/en/programs/cargo/dgr/lithium-batteries/>.
- [64] Sofraa Worldwide Organization. URL www.sofraa.org. Accessed December 2020.
- [65] Hanieh Borhanazad, Saad Mekhilef, Velappa Gounder Ganapathy, Mostafa Modiri-Delshad, and Ali Mirtaheri. Optimization of micro-grid system using MOPSO. *Renewable Energy*, 71:295–306, 2014. ISSN 09601481. doi: 10.1016/j.renene.2014.05.006. URL <http://dx.doi.org/10.1016/j.renene.2014.05.006>.

- [66] Carolina G. Marcelino, Paulo E M Almeida, Elizabeth F Wanner, Leonel M. Carvalho, and Vladimiro Miranda. Fundamentals of the C-DEEPSO algorithm and its application to the reactive power optimization of wind farms. In *2016 IEEE Congress on Evolutionary Computation (CEC)*, pages 1547–1554, 2016. ISBN 978-1-5090-0623-6. doi: 10.1109/CEC.2016.7743973. URL <http://ieeexplore.ieee.org/document/7743973/>.
- [67] C Marcelino, M Baumann, et al. Battery storage for hybrid smart grids: Optimization and decision making analysis using c-deepso and ahp+ topsis. *IEEE Transactions on Smart Grid*.
- [68] M. Baumann, J. Peters, M. Weil, C. Marcelino, P. Almeida, and E. Wanner. Environmental impacts of different battery technologies in renewable hybrid microgrids. In *2017 IEEE PES Innovative Smart Grid Technologies Conference Europe (ISGT-Europe)*, pages 1–6, Sept 2017. doi: 10.1109/ISGTEurope.2017.8260137.
- [69] P. Almeida C. Marcelino and E. Wanner. Solving security constrained optimal power flow problems: a hybrid evolutionary approach,” appl. intell. March 2018.
- [70] S. Diaf, D. Diaf, M. Belhamel, M. Haddadi, and A. Louche. A methodology for optimal sizing of autonomous hybrid pv/wind system. *Energy Policy*, 35(11):5708–5718, 2007. ISSN 0301-4215. doi: <https://doi.org/10.1016/j.enpol.2007.06.020>. URL <https://www.sciencedirect.com/science/article/pii/S0301421507002893>.
- [71] Ina Neher, Tina Buchmann, Susanne Crewell, Bernd Evers-Dietze, Klaus Pfeilsticker, Bernhard Pospichal, Christopher Schirrmeyer, and Stefanie Meilinger. Impact of atmospheric aerosols on photovoltaic energy production scenario for the sahel zone. *Energy Procedia*, 125:170–179, 2017.
- [72] PVSyst Photovoltaic Software, . URL <https://www.pvsyst.com/>. Accessed December 2020.
- [73] Samer Yassin Alsadi and Yasser Fathi Nassar. Estimation of solar irradiance on solar fields: An analytical approach and experimental results. *IEEE Transactions on Sustainable Energy*, 8(4):1601–1608, 2017. doi: 10.1109/TSTE.2017.2697913.
- [74] Michael Gostein, Bill Stueve, Kendra Passow, and Alex Panchula. Evaluating a model to estimate ghi, dni, dhi from poa irradiance. In *2016 IEEE 43rd Photovoltaic Specialists Conference (PVSC)*, pages 0943–0946, 2016. doi: 10.1109/PVSC.2016.7749749.
- [75] Matthew Lave, William Hayes, Andrew Pohl, and Clifford W Hansen. Evaluation of global horizontal irradiance to plane-of-array irradiance models at locations across the united states. *IEEE journal of Photovoltaics*, 5(2):597–606, 2015.
- [76] Nelson A Kelly and Thomas L Gibson. Improved photovoltaic energy output for cloudy conditions with a solar tracking system. *Solar Energy*, 83(11):2092–2102, 2009.

- [77] P. G. Loutzenhiser, H. Manz, C. Felsmann, P. A. Strachan, T. Frank, and G. M. Maxwell. Empirical validation of models to compute solar irradiance on inclined surfaces for building energy simulation. *Solar Energy*, 81(2):254–267, 2007. ISSN 0038092X. doi: 10.1016/j.solener.2006.03.009.
- [78] Richard Perez, Robert Seals, Pierre Ineichen, Ronald Stewart, and David Menicucci. A new simplified version of the perez diffuse irradiance model for tilted surfaces. *Solar Energy*, 39(3):221–231, 1987. ISSN 0038092X. doi: 10.1016/S0038-092X(87)80031-2.
- [79] Richard Perez, Ronald Stewart, Robert Seals, and Ted Guertin. CONTRACTORREPORT SAND88-7030 Unlimited Release The Development and Verification of the Perez Diffuse Radiation Model. (October), 1988. URL <http://prod.sandia.gov/techlib/access-control.cgi/1988/887030.pdf>.
- [80] Lingfeng Wang and Chanan Singh. Pso-based multi-criteria optimum design of a grid-connected hybrid power system with multiple renewable sources of energy. pages 250–257, 2007.
- [81] J. F. Manwell and J. G. McGowan. Lead acid battery storage model for hybrid energy systems. 50:399–405. URL [https://doi.org/10.1016/0038-092X\(93\)90060-2](https://doi.org/10.1016/0038-092X(93)90060-2).
- [82] S. D. Downing and D. F. Socie. Simple rainflow counting algorithms. 4:31–40. URL [https://doi.org/10.1016/0142-1123\(82\)90018-4](https://doi.org/10.1016/0142-1123(82)90018-4).
- [83] J. F. Manwell, A. Rogers, G. Hayman, C. T. Avelar, J. G. McGowan, U. Abdulwahid, and K. Wu. Hybrid2: A hybrid system simulation model: Theory manual. pages 151–153. URL <http://citeseerx.ist.psu.edu/viewdoc/download?doi=10.1.1.466.731&rep=rep1&type=pdf>.
- [84] Olivier Tremblay and Louis A. Dessaint. Experimental validation of a battery dynamic model for EV applications. *World Electric Vehicle Journal*, 3(2):289–298, 2009. ISSN 20326653. doi: 10.3390/wevj3020289.
- [85] Olivier Tremblay, Louis A. Dessaint, and Abdel Illah Dekkiche. A generic battery model for the dynamic simulation of hybrid electric vehicles. *VPPC 2007 - Proceedings of the 2007 IEEE Vehicle Power and Propulsion Conference*, (October): 284–289, 2007. doi: 10.1109/VPPC.2007.4544139.
- [86] Nicholas Diorio, Aron Dobos, Steven Janzou, Austin Nelson, Blake Lundstrom, Nicholas Diorio, Aron Dobos, Steven Janzou, Austin Nelson, and Blake Lundstrom. Technoeconomic Modeling of Battery Energy Storage in SAM (<http://www.nrel.gov/docs/fy15osti/64641.pdf>). *NREL Technical Report NREL/TP-6A20-64641*, (September), 2015. URL <http://www.nrel.gov/docs/fy15osti/64641.pdf>.
- [87] MK Deshmukh and SS Deshmukh. Modeling of hybrid renewable energy systems. *Renewable and sustainable energy reviews*, 12(1):235–249, 2008.

- [88] Mohamed Mamdouh Elkadragy. Renewable Electricity (RES-E) Policy Implications On Market Actors In Germany Modelling. Modelling and Analysis focusing on Onshore Wind and PV Plant Operation and Investment., 2014. URL <http://elib.dlr.de/93851/>.
- [89] M Reeg and M M Elkadragy. Changed risk premiums and equity debt requirements due to different RES-E policy instruments for market integration of renewable energies in Germany. In *Sustainable Energy Policy Strategies for Europe 14th IAAE European Energy Conference.*, pages 28.–31, Rome, Italy., 2014. URL <https://elib.dlr.de/89678/>.
- [90] A. Kaabeche, M. Belhamel, and R. Ibtouen. Sizing optimization of grid-independent hybrid photovoltaic/wind power generation system. *Energy*, 36(2):1214–1222, 2011. ISSN 03605442. doi: 10.1016/j.energy.2010.11.024. URL <http://dx.doi.org/10.1016/j.energy.2010.11.024>.
- [91] Abdelhamid Kaabeche and Rachid Belhamel. Techno-economic valuation and optimization of integrated photovoltaic/wind energy conversion system. *Solar Energy*, 85(10):2407–2420, 2011. ISSN 0038092X. doi: 10.1016/j.solener.2011.06.032. URL <https://www.sciencedirect.com/science/article/pii/S0038092X11002635>.
- [92] Willett Kempton and Jasna Tomić. Vehicle-to-grid power fundamentals: Calculating capacity and net revenue. *Journal of power sources*, 144(1):268–279, 2005.
- [93] V. Miranda and R. Alves. Differential evolutionary particle swarm optimization (deepso): A successful hybrid. pages 368–374, 2013. ISSN 2377-0597. doi: 10.1109/BRICS-CCI-CBIC.2013.68.
- [94] Energy Sector Management Assistance Program. Mini Grids for Half a Billion People: Market Outlook and Handbook for Decision Makers. ESMAP Technical Report;014/19. 2019. URL <https://openknowledge.worldbank.org/handle/10986/31926>.
- [95] Ahmed Alsersy, George Tsatsaronis, and Mohamed M. Elkadragy. *Developing a data analysis platform for the monitoring of off-grid hybrid energy storage system*. Master thesis, Technical University of Berlin (TUB), 2019.
- [96] HelioClim. Helioclim-3 Overview. URL <http://www.soda-pro.com/help/helioclim/helioclim-3-overview>.
- [97] Government of Canada. Government of Canada, Historical Climate Data., 2020. URL <http://climate.weather.gc.ca/>.
- [98] International Renewable Energy Agency. Off-grid renewable energy systems: status and methodological issues. 2 2015. ISSN 978-92-95111-62-2. URL <https://www.irena.org/publications/2015/Feb/Off-grid-renewable-energy-systems-Status-and-methodological-issues>.

- [99] C. M. Colson, M. H. Nehrir, R. K. Sharma, and B. Asghari. Improving sustainability of hybrid energy systems part i: Incorporating battery round-trip efficiency and operational cost factors. *IEEE Transactions on Sustainable Energy*, 5(1):37–45, Jan 2014. ISSN 1949-3037. doi: 10.1109/TSTE.2013.2269318.
- [100] Ethem Alpaydin. *Introduction to Machine Learning*. Adaptive Computation and Machine Learning. MIT Press, Cambridge, MA, 3 edition, 2014. ISBN 978-0-262-02818-9. URL <https://mitpress.mit.edu/books/introduction-machine-learning-third-edition>.
- [101] Mostafa Ezziyyani. *Advanced Intelligent Systems for Sustainable Development (AI2SD'2018)*, volume 912 of *Advances in Intelligent Systems and Computing*. Springer International Publishing, Cham, 2019. ISBN 978-3-030-11883-9. doi: 10.1007/978-3-030-11884-6. URL <http://link.springer.com/10.1007/978-3-030-11884-6>.

Appendix A

Publications, conferences and research related activities during study period

Appointed international roles

- **Senior research fellow, the Waterloo Institute for Sustainable Energy (WISE), University of Waterloo, Canada.**

Appointment year (starting from): 2020

Institute: Waterloo Institute for Sustainable Energy (WISE)

Link [accessed April 2021]: <https://wise.uwaterloo.ca/>

- **International visiting scientist at University of Waterloo, Canada.**

Period: June - August 2019

Institute: Waterloo Institute for Sustainable Energy (WISE)

Location: Waterloo, Canada

- **European Energy Research Alliance (EERA)- Sub-Program(6) Energy storage.**

Role: Work package coordinator (Technical, Costs & Economic Viability), under SP6 Energy Storage.

Year: 2019

Link [accessed April 2021]: <https://www.eera-energystorage.eu/about/sub-programmes/es-tes.html>

- **PRE-LEAP Long-Term EU-AU Research and Innovation Partnership on Renewable Energy.**

Role: Selected expert for representing the battery storage sub program

Year: 2018

Location: Brussels, Belgin

Link [accessed April 2021]: <http://www.leap-re.eu/>

Author's scientific publications within the scope of the presented study

- **Off-grid and decentralized hybrid renewable electricity systems data analysis platform (OSDAP). A building block of a comprehensive techno-economic approach based on contrastive case studies in Sub-Saharan Africa and Canada.**

Publication type: Paper

Published in: Journal of Energy Storage - Elsevier

Publication reference: Volume 34, **February 2021**, 101965

Authors: **Mohamed M. Elkadragy**, Mert Alici, Ahmed Alsersy, Ambika Opal, Jatin Nathwani, Joachim Knebel, Marc Hiller.

Institutions: Karlsruhe Institute of Technology(KIT) & University of Waterloo, Waterloo Institute for Sustainable Energy (WISE).

Available online [accessed April 2021]: www.sciencedirect.com/science/article/abs/pii/S2352152X20318004

Reference: [8].

- **Hybrid Off-grid and decentralized renewable electricity systems Techno-Economic Model (HOTEM). A building block of a comprehensive techno-economic approach based on contrastive case studies in Sub-Saharan Africa and Canada.**

Awards: **Selected best paper** (beside another paper from a different author) in the 10th Solar and Storage Integration Workshop, Grid Integration Week 2020, and eligible for the manuscript submission process of the "IET Renewable Power Generation" Journal.

Award Announcement Web-page (accessed April 2021): Click link best papers announcement

Publication type: Paper

Published in: 10th Solar and Storage Integration Workshop

Publication date: 5 November 2020

Authors: **Mohamed M. Elkadragy**, Mughees Iqbal, Mohammed L. Awad, Manuel Baumann, Ambika Opal, Marc Hiller, Jatin Nathwani, Joachim Knebel.

Institutions: Karlsruhe Institute of Technology(KIT) & University of Waterloo, Waterloo Institute for Sustainable Energy (WISE).

Available online [accessed April 2021]: <https://ae4h.org/projects/ohres>

Direct download link [accessed April 2021]: https://ae4h.org/download/documents/projects/hotem_ae4hpdf;v1?attachment=1

Reference: [5]

- **Contrastive Techno-Economic Analysis Concept for Off-Grid Hybrid Renewable Electricity Systems Based on comparative case studies within Canada and Uganda.**

Publication type: Paper

Published in: 3rd International Hybrid Power Systems Workshop

Publication date: 08 May 2018

Authors: **Mohamed M. Elkadragy**, Manuel Baumann, Nigel Moore, Marcel Weil, Nicolaus Lemmertz, Marc Hiller.

Available online [accessed April 2021]: <https://ae4h.org/projects/ohres>

Direct download link [accessed April 2021]: www.hybridpowersystems.org/wp-content/uploads/sites/9/2018/05/5A_4_TENE18_012_paper_Elkadragy_MohamedM.pdf

Reference: [1].
- **Off-Grid Hybrid Renewable Electricity System (OHRES) techno-economic assessment, system size optimization and design.**

Publication type: Scientific poster

Published in: 2nd International Conference on Solar Technologies & Hybrid Mini Grids to improve energy access.

Publication date: 17 October 2018

Authors: **Mohamed M. Elkadragy**, Manuel Baumann, Ahmed Alsersy, Nicolaus Lemmertz, Marc Hiller.

Available Online [accessed April 2021]: <https://ae4h.org/projects/ohres>

Direct download link [accessed April 2021]: https://ae4h.org/download/documents/181017_me_accessposter_revdpdf?attachment=1

Reference: [46].
- **Off-Grid Hybrid Renewable Energy Systems, A techno-economic analysis of the concept.**

Publication type: Article

Published in: Windtech international

Publication date: 29 August 2018

Authors: **Mohamed M. Elkadragy**

Available online [accessed April 2021]: www.windtech-international.com/editorial-features/off-grid-hybrid-renewable-energy-systems

Reference: [47].

Other author's scientific publications used in the scope of this study

- **Renewable Electricity (RES-E) Policy Implications On Market Actors In Germany Modelling. Modelling and Analysis focusing on Onshore Wind and PV Plant Operation and Investment, Master thesis, 2014.**

Authors: **Mohamed M. Elkadragy**

Available online [accessed April 2021]: <https://elib.dlr.de/93851/>

- **Changed risk premiums and equity debt requirements due to different RES-E policy instruments for market integration of renewable energies in Germany, 2014.**

Authors: M Reeg and **M M Elkadragy**

Paper published in: Sustainable Energy Policy Strategies for Europe 14th IAEE European Energy Conference., pages 28.-31, Rome, Italy., 2014.

Available online [accessed April 2021]: <https://elib.dlr.de/89678/>.

Presentation, talks and events

- **The Road to Reliable and Economically Feasible Electricity for Remote Communities in Developing and Developed Economies.**

Participation type: International public lecture

Location: University of Waterloo, Canada

Date: 26 June 2019

Presented: **Mohamed M. Elkadragy**

International Public Lecture announcement [accessed April 2021]: [Click Link](#)

International Public Lecture available online [accessed April 2021]: <https://www.youtube.com/watch?v=V-r1nexe0E&list=PLV3MaCeB6SEnJ60aGZYecfoNeNKu2kasg>

- **Li-ion and Hybrid Battery Storage Systems - Using Case studies within Africa and North America.**

Participation type: International public lecture

Location: University of Waterloo, Canada

Date: 25 July 2019

Presented: **Mohamed M. Elkadragy**

International Public Lecture announcement [accessed April 2021]: [Click link](#)

- **10th Solar & Storage Integration Workshop.**

Activity: Accepted paper presentation

Presenter: **Mohamed M. Elkadragy**

Link [accessed April 2021]: www.solarintegrationworkshop.org/

- **3rd International Hybrid Power Systems Workshop**

Activity: Accepted paper presentation

Presenter: **Mohamed M. Elkadragy**

Link [accessed April 2021]: <https://hybridpowersystems.org/tenerife2018/>
- **2rd International Conference on Solar Technologies & Hybrid Mini Grids to improve energy access.**

Activity: Accepted poster presentation

Presenter: **Mohamed M. Elkadragy**

Link [accessed April 2021]: <http://www.energy-access-conferences.com/33167/section/19245/3rd-international-conference-on-solar-technologies-and-hybrid-mini-grids-to-improve-energy-access.html>
- **European Energy Research Alliance (EERA)- Members Meeting, and Workshop on Hybrid Energy and Energy Storage Systems.**

Event type: Steering committee and Sub-Program(6) Energy storage members meeting, plus a workshop.

Participation: Presenter, Experts panel member: Techno-economic and environmental assessment of materials for energy storage technologies, and Work package coordinator.

Year: 2019

Location: Rome,Italy.

Link [accessed April 2021]: <https://www.eera-energystorage.eu/about/sub-programmes/es-tes.html>
- **Off-Grid Hybrid Systems (OHRES) for contrastive remote communities in Uganda and Canada ”Techno-economic modelling, remote data analysis and hands-on lessons learned”.**

Participation type: Presentation

Event: Off-Grid Power Conference – Intesolar.

Year: 2019

Location: Munich, Germany.

Presented: **Mohamed M. Elkadragy**

Link [accessed April 2021]: <https://www.ruralelec.org/event-calendar/intersolar-europe-grid-power-forum-conference-exhibition-0>
- **Off-grid Experts international workshop.**

Activity: participant

Location: Germany

Link [accessed April 2021]: <https://www.ruralelec.org/event-calendar/grid-experts-workshop-enhancing-end-users-grid-technology-experience-training>

- **AE4H 2017 International Affordable Energy for Humanity innovation lab.**

Activity: Participant

Location: Germany

Link [accessed April 2021]: https://ae4h.org/projects/innovation_lab_current/innovation_lab_2017

- **AE4H 2019 International Affordable Energy for Humanity innovation lab.**

Activity: Participant, and working group presenter

Location: Waterloo, Canada

Link [accessed April 2021]: https://ae4h.org/projects/innovation_lab_current/innovation_lab_2019

Appendix B

Supervised Studies and activities during the study period

Table 7.1: Studies and activities supervision during thesis and study period

Type	Period	Title and details	Student University
Master thesis	01.02.2019 to 16.09.2019	Developing a data analysis platform for the monitoring of off-grid hybrid energy storage system [95]	Technical University of Berlin (TUB)
Internship	15.03.2019 to 15.05.2019	Practical internship on the hybrid system techno-economic modeling	University of Freiburg
Master thesis	15.05.2019 to 15.11.2019	Development and Optimization of Hybrid Off-Grid Techno-Economic Model for System Design and Analysis [7]	University of Freiburg
Master thesis	01.06.2019 to 01.12.2019	Design and Performance Analysis of Off-Grid Hybrid Renewable Electricity Systems Using Two Case Studies in Uganda and Canada [10]	University of Freiburg
Internship	01.12.2019 to 01.04.2020	Off-grid systems data and performance analysis	University of Freiburg
Master thesis	01.06.2020 to 31.12.2020	Development and Analysis of a Hybrid Battery Energy Storage System in the Hybrid Off-grid Techno-Economic Model [6]	University of Oldenburg

